

Targeting Hepatocytes via the Asialoglycoprotein-Receptor

Inauguraldissertation

zur Erlangung der Würde eines Doktors der Philosophie vorgelegt der Philosophisch-
Naturwissenschaftlichen Fakultät der Universität Basel

von

Daniela Stokmaier
aus Langwies GR, Schweiz

Referent: Prof. Dr. Beat Ernst

Koreferent: Prof. Dr. Dario Neri

Basel, 14 December 2010

Originaldokument gespeichert auf dem Dokumentenserver der Universität Basel
edoc.unibas.ch



Dieses Werk ist unter dem Vertrag „Creative Commons Namensnennung-Keine kommerzielle Nutzung-
Keine Bearbeitung 2.5 Schweiz“ lizenziert. Die vollständige Lizenz kann unter
creativecommons.org/licences/by-nc-nd/2.5/ch
eingesehen werden.



Namensnennung-Keine kommerzielle Nutzung-Keine Bearbeitung 2.5 Schweiz

Sie dürfen:



das Werk vervielfältigen, verbreiten und öffentlich zugänglich machen

Zu den folgenden Bedingungen:



Namensnennung. Sie müssen den Namen des Autors/Rechteinhabers in der von ihm festgelegten Weise nennen (wodurch aber nicht der Eindruck entstehen darf, Sie oder die Nutzung des Werkes durch Sie würden entlohnt).



Keine kommerzielle Nutzung. Dieses Werk darf nicht für kommerzielle Zwecke verwendet werden.



Keine Bearbeitung. Dieses Werk darf nicht bearbeitet oder in anderer Weise verändert werden.

- Im Falle einer Verbreitung müssen Sie anderen die Lizenzbedingungen, unter welche dieses Werk fällt, mitteilen. Am Einfachsten ist es, einen Link auf diese Seite einzubinden.
- Jede der vorgenannten Bedingungen kann aufgehoben werden, sofern Sie die Einwilligung des Rechteinhabers dazu erhalten.
- Diese Lizenz lässt die Urheberpersönlichkeitsrechte unberührt.

Die gesetzlichen Schranken des Urheberrechts bleiben hiervon unberührt.

Die Commons Deed ist eine Zusammenfassung des Lizenzvertrags in allgemeinverständlicher Sprache: <http://creativecommons.org/licenses/by-nc-nd/2.5/ch/legalcode.de>

Haftungsausschluss:

Die Commons Deed ist kein Lizenzvertrag. Sie ist lediglich ein Referenztext, der den zugrundeliegenden Lizenzvertrag übersichtlich und in allgemeinverständlicher Sprache wiedergibt. Die Deed selbst entfaltet keine juristische Wirkung und erscheint im eigentlichen Lizenzvertrag nicht. Creative Commons ist keine Rechtsanwaltsgesellschaft und leistet keine Rechtsberatung. Die Weitergabe und Verlinkung des Commons Deeds führt zu keinem Mandatsverhältnis.

Genehmigt von der Philosophisch-Naturwissenschaftlichen Fakultät auf Antrag von:

Prof. Dr. Beat Ernst, Institut für Molekulare Pharmazie, Universität Basel

Prof. Dr. Dario Neri, Institute für Pharmazeutische Wissenschaften, ETH Zürich

Basel, den 9. Dezember 2008

Prof. Dr. E. Parlow

Dekan

Lieber auf neuen Wegen stolpern,
als in den alten Bahnen auf der Stelle treten

Jochen Mariss, (*1955)

It is better to stumble on new paths than to make no
headway on the old tracks

Table of Contents

1. INTRODUCTION	1-1
1.1 General Overview - The Liver	1-1
1.2 Chronic Liver Disease.....	1-3
1.3 The ASGP-R.....	1-7
1.3.1 Structure of the Asialoglycoprotein Receptor	1-9
1.3.2 Receptor Mediated Endocytosis	1-10
1.3.3 Physiological Function	1-11
1.3.4 Structure of the H1-CRD	1-14
1.3.5 Ligand Specificity and Affinity	1-15
1.3.6 Drug Delivery via the ASGP-R	1-17
1.4 Antibodies	1-18
1.4.1.1 The Genetic Basis of Antibody Diversity	1-19
1.4.1.2 Antibody Structure	1-20
1.4.2 Antibodies as Therapeutics	1-21
1.4.3 Antibody Fragments	1-23
1.4.4 Recombinant Antibodies	1-24
1.4.4.1 Expression of Recombinant Antibodies in <i>E.coli</i>	1-25
1.4.5 Generation of Murine scFv from Hybridoma	1-26
1.4.6 Antibody Phage Display	1-28
1.4.6.1 Types of Phage Display Libraries	1-30
1.4.6.2 The ETH-2-Gold Library	1-31
1.5 Receptor-ligand Interaction Measurement Technologies	1-32
1.5.1 Solid-phase Binding Assays	1-34
1.5.2 Fluorescence Microscopy and Flow Cytometry	1-34
1.5.3 Surface Plasmon Resonance (SPR)	1-37
2. MATERIALS AND METHODS.....	2-41
2.1 Expression and Purification of ASGP-R H1-CRD	2-41
2.1.1 Solubilization and Renaturation of H1-CRD	2-42
2.1.2 Purification by Affinity Chromatography	2-42
2.1.3 Separation of H1-CRD Monomers and Dimers by IEC	2-43

2.1.4	Concentration by HPLC Affinity Chromatography	2-44
2.1.5	Final Buffer Exchange and Concentration	2-44
2.1.6	SDS-polyacrylamide Gelelectrophoresis (SDS-PAGE)	2-45
2.1.6.1	Enhanced Coomassie-blue staining	2-45
2.1.7	Western Blotting (WB)	2-46
2.1.8	Bradford Estimation of Protein Concentration	2-47
2.2	Competitive Solid Phase Binding Assay	2-48
2.2.1	Evaluation of Small Molecules	2-48
2.3	General Methods for Mammalian Cells.....	2-50
2.3.1	Standard Protocol for Freezing of Mammalian Cells	2-50
2.3.2	Production of Mouse anti-human H1-CRD Antibodies	2-51
2.3.2.1	Adaptation of Hybridoma Cells to low Serum Conditions	2-51
2.3.3	Purification of Murine Monoclonal Antibodies	2-51
2.3.4	Isotyping of anti-H1-CRD Antibodies	2-52
2.3.5	Hepatoma Cell-lines Culture Conditions	2-53
2.3.6	Propagation of Hepatoma Cells	2-53
2.3.7	Preparation of Cover Slips for Microscopy	2-53
2.4	Immunohistochemistry (IHC)	2-55
2.5	Immunocytochemistry	2-56
2.5.1	Immunofluorescence Staining	2-56
2.5.1.1	Indirect Staining of Cells	2-56
2.5.1.2	Direct Staining of Cells	2-57
2.5.2	Receptor Specific Uptake of Ligands into HepG2 Cells	2-58
2.5.3	Extracellular Staining of Hepatic Cells by Flow Cytometry	2-60
2.6	Triantenary Gal/GalNAc Ligand Binding and Internalization	2-61
2.6.1	Fluorescence Microscopy	2-61
2.6.2	Flow Cytometry	2-62
2.7	Molecular Cloning of Single Chain Antibodies.....	2-64
2.7.1	Vector Plasmids	2-64
2.7.1.1	The pAK Vector System	2-64
2.7.1.2	The pHEN1Phagemid Vector	2-66
2.7.1.3	VCSM13 Helper Phage	2-66
2.7.2	Synthetic Oligonucleotides	2-67

2.7.2.1 Degenerate Primers for the Amplification of scFv	2-67
2.7.2.2 Primers for Sequencing	2-71
2.7.3 Construction of Murine scFv Expression Plasmids	2-71
2.7.3.1 mRNA Isolation from Hybridoma Cells	2-71
2.7.4 PCR Reactions	2-72
2.7.4.1 First Strand cDNA Synthesis by RT-PCR	2-72
2.7.4.2 Amplification of the Variable Antibody Domains V_H and V_L	2-73
2.7.4.3 Assembly of the Variable Antibody Domains V_H and V_L	2-74
2.7.5 Digestion and Cloning of murine scFv Genes	2-75
2.7.5.1 <i>Sfi</i> I Digest of the Vector and the scFv-DNA	2-75
2.7.5.2 Ligation of scFv-DNA into pAK300-Vector	2-76
2.7.5.3 Analytical Digest of Ligation Product	2-77
2.7.6 DNA Sequencing	2-77
2.7.6.1 Purification of the Extension Products	2-78
2.7.7 Sequence Analysis	2-78
2.7.8 Agarose Gel Electrophoresis	2-78
2.7.9 UV-Quantitation of DNA	2-79
2.8 General Methods for Bacteria.....	2-80
2.8.1 Material	2-80
2.8.2 <i>E.coli</i> Strains	2-80
2.8.3 Bacterial Culture Media and Buffers	2-81
2.8.3.1 Media and Buffer for Electro-competent Cells	2-81
2.8.3.2 Media and Buffer for Chemo-competent Cells	2-81
2.8.3.3 Expression Media	2-82
2.8.3.4 Agar Plates	2-83
2.8.3.5 Antibiotics for Selection	2-83
2.8.4 Preparation of Competent Cells	2-84
2.8.4.1 Rubidium Chloride Method for Chemo-competent <i>E.coli</i>	2-84
2.8.4.2 Cells for Electroporation	2-85
2.8.5 Transformation of <i>E.coli</i>	2-85
2.8.5.1 Heat-shock Transformation	2-85
2.8.5.2 Electroporation	2-86
2.8.6 Preparing Glycerol Stocks of Bacteria	2-86
2.8.7 Clone Picking and Plasmid Isolation (Mini-prep)	2-87
2.9 Antibody Phage Display.....	2-88

2.9.1.1 Exponential Growing Bacterial Cultures for Infection with Phage	2-88
2.9.1.2 Preparation of Helper Phage	2-88
2.9.2 Biopanning using Immunotubes	2-88
2.9.3 Phage Amplification	2-89
2.9.4 PEG precipitation of Phage	2-89
2.9.5 scFv Expression Screening ELISA	2-90
2.9.5.1 Preparation of ELISA Plate for scFv Expression Screening	2-90
2.9.6 Screening for murine scFv Clones by Colony Blotting	2-91
2.9.7 Expression of soluble scFv in <i>E.coli</i>	2-92
2.9.8 Purification of murine scFv via His-tag	2-92
2.9.8.1 Periplasmic extraction	2-92
2.9.8.2 Downstream Protein Purification	2-93
2.9.9 Purification of human scFv	2-93
2.9.9.1 Buffer Exchange and Sample Concentration	2-94
2.9.10 Analysis of Binding Properties of murine scFv in ELISA	2-94
2.9.11 Affinity Measurements	2-95
2.9.12 Activity Testing of H1-CRD in SPR	2-95
2.9.13 Affinity Testing of scFv	2-96
3. RESULTS AND DISCUSSION	3-97
3.1 H1-CRD Production	3-97
3.1.1 Production of a Big Batch of H1-CRD	3-101
3.1.1.1 Stability of the Protein	3-102
3.2 Heterogeneous Competitive Solid-phase Binding Assay	3-104
3.2.1 Selection of the Competitive Ligand and Buffer System	3-104
3.2.2 Receptor / Ligand Probe Concentrations	3-105
3.2.3 Specificity of the Assay System	3-106
3.2.4 Variability of the Assay	3-108
3.2.4.1 Probing pH Dependence of Ligand Binding to H1-CRD	3-109
3.2.4.2 Amount of Calcium in Buffer	3-110
3.2.4.3 Incubation Temperature	3-111
3.2.4.4 DMSO Tolerance	3-112
3.2.5 Sensitivity of the Assay System, Testing of H1-CRD Ligands	3-114
3.2.6 Analysis of the Data	3-115
3.2.7 Adaptation of the Assay to the H2-CRD	3-116

3.3	Evaluation of new Glycomimetic Ligands for the ASGP-R	3-118
3.4	Murine anti-H1-CRD Antibodies.....	3-127
3.4.1	Antibody Production	3-127
3.4.2	Immunohistochemistry (IHC)	3-130
3.5	Ligand Uptake in Hepatoma Cells	3-132
3.6	Internalization Experiments.....	3-133
3.6.1	Immunofluorescence (IF)	3-134
3.7	Flow Cytometry with murine Antibodies.....	3-136
3.8	Endocytosis of Triantennary Galactose Compounds.....	3-140
3.8.1	Method Development	3-150
3.8.2	Uptake of Ligands in Living Cells	3-151
3.9	Adaptation of mouse Antibodies to scFv.....	3-155
3.9.1	Source of mRNA	3-155
3.9.1.1	Selection of Antibodies for Adaption	3-155
3.9.1.2	Isotyping	3-156
3.9.1.3	mRNA Purification and First Strand cDNA Synthesis	3-156
3.9.1.4	Amplification of V _L and V _H - First Step in Assembly	3-157
3.9.1.5	Assembly of the Heavy and Light Chains	3-159
3.10	Cloning of the scFv Genes into pAK300	3-160
3.10.1	Digestion of pAK300 and the scFv Constructs	3-160
3.10.1.1	Ligation of the scFv Constructs into pAK300	3-161
3.10.2	pAK300-scFv Plasmid Amplification	3-161
3.10.3	Production and Purification of murine scFv	3-163
3.10.3.1	Transformation of pAK300scFv into BI21(DE3) for Expression	3-163
3.10.4	Expression and Purification of murine scFv	3-164
3.11	Phage Display of murine scFvs	3-169
3.11.1	Cloning of murine scFvs into Phagemid Vector pAK100	3-169
3.11.2	Preparation of mouse scFv Phage Libraries	3-169
3.11.2.1	First Round of Phage Panning on Immunotubes	3-170
3.11.2.2	Soluble scFv ELISA	3-170
3.12	Phage Display human scFv	3-172
3.12.1.1	ETH-2-Gold Phage Sub-library Rescue after First Panning	3-172

3.12.1.2 Biopanning using Immunotubes	3-172
3.12.1.3 Screening scFv Expression by ELISA	3-173
3.12.1.4 Small Scale Production of human scFv	3-176
3.13 Affinity Evaluation of scFvs	3-179
3.13.1 Activity Testing of H1-CRD	3-179
3.13.2 Screening of human scFv in SPR	3-180
3.13.3 Affinity Determinations of human scFv	3-181
4. GENERAL DISCUSSION AND OUTLOOK	4-182
4.1 ASGP-R Carbohydrate Recognition Domains H1- and H2-CRD	4-182
4.2 Competitive Solid-phase Binding Assay	4-182
4.3 New Glycomimetic Ligands for the human H1-CRD	4-183
4.4 Antibodies against the ASGP-R for Drug Targeting	4-183
4.4.1 Mouse anti-human H1-CRD Antibodies	4-184
4.4.2 Murine scFv Adaptation	4-184
4.4.3 Selection of human scFv against the H1-CRD	4-185
5. APPENDICES	5-189
5.1 Sequences of scFv	5-189
5.2 Curriculum Vitae	5-191
6. BIBLIOGRAPHY	194

Tables

Table 1. Buffer gradient for the separation of monomers and dimers by HPLC IEC.....	2-44
Table 2. Buffer gradient for the concentration of H1-CRD monomers by HPLC affinity chromatography	2-44
Table 3. V _L BACK-Primer mix.....	2-67
Table 4. V _L FOR-Primer mix.....	2-68
Table 5. V _H BACK-Primer mix	2-69
Table 6. V _H FOR-Primer mix	2-70
Table 7. SOE-PCR Primers.....	2-70
Table 8. Primers for sequencing pAK300scFv	2-71
Table 9. Primers for sequencing pHEN1scFv	2-71
Table 10. Reaction batch for variable antibody domain amplification	2-73
Table 11. Cycling protocol for variable antibody domain amplification.....	2-73
Table 12. Reaction batch for SOE-PCR.....	2-74
Table 13. Cycling protocol for SOE-PCR	2-75
Table 14. Reaction batch used for scFv digest	2-76
Table 15. Reaction batch used for vector digest	2-76
Table 16. Ligation mixture	2-76
Table 17. Reaction batch for analytical digest.....	2-77
Table 18. Reaction batch for sequencing PCR	2-77
Table 19. Cycling protocol for sequencing	2-78
Table 20. Ethanol precipitation of PCR-products	2-78
Table 21. Variability measurements	3-108
Table 22. Comparison of results of a panel of carbohydrate analytes	3-114
Table 23. Summary of the competitive binding assay results for the directed library compounds	3-124
Table 24. Productivity of hybridoma clones.....	3-129
Table 25. Characteristics of selected H1-CRD antibodies	3-155
Table 26. Size of plasmid and insert (in bp)	3-162

Figures

Figure 1. Liver cells	1-1
Figure 2. Localization of the ASGP-R in the liver	1-8
Figure 3. Scheme of the H1 subunit of the ASGP-R	1-10
Figure 4. Receptor-mediated internalization of ligands by the ASGP-R	1-11
Figure 5. Ribbon diagram of the human H1-CRD	1-14
Figure 6. A model of GalNAc docked into the sugar-binding site of the H1-CRD	1-15
Figure 7. Carbohydrate ligands for the ASGP-R	1-16
Figure 8. Binding model for ASGP-R ligands	1-17
Figure 9. Antibody structure (IgG)	1-21
Figure 10. Antibody fragments	1-24
Figure 11. Production of soluble, folded scFv in <i>E.coli</i>	1-26
Figure 12. The general strategy used for the adaption of murine IgG to the scFv format	1-28
Figure 13. Antibody phage display cycle	1-30
Figure 14. ETH-2 Gold library: Positions of introduced diversity	1-32
Figure 15. Jablonski diagram	1-35
Figure 16. Basic principles of flow cytometry measurements.....	1-36
Figure 17. Quantitative flow cytometry measurement principle.....	1-37
Figure 18. The basic outline of a SPR measurement.....	1-38
Figure 19. H1-CRD immobilized on CM5 sensor chip via amine coupling.....	1-40
Figure 20. Indirect detection of antibody binding to the receptor	2-57
Figure 21. Indirect detection of internalized antibody	2-59
Figure 22. Direct detection of internalized antibody or ligand	2-59
Figure 23. pAK100 phagemid vector map	2-64
Figure 24. pAK300 expression vector map	2-65
Figure 25. pHEN1 phagemid vector map	2-66
Figure 26. DNA Markers.....	2-79
Figure 27. Simplified overview of the production cycle of H1-CRD	3-98
Figure 28. Affinity chromatography H1-CRD	3-99

Figure 29. Analysis of collected affinity chromatography fractions of H1-CRD	3-99
Figure 30. Separation of H1-CRD monomers and dimers by HPLC	3-100
Figure 31. Analysis of fractions collected during HPLC IEC.....	3-100
Figure 32. Final preparation of monomeric H1-CRD	3-101
Figure 33. Purified H1-CRD monomers after 1 year of storage	3-102
Figure 34. Constitution of a biotin labeled glyco-PAA-polymer	3-104
Figure 35. Setup of the competitive solid-phase binding assay	3-105
Figure 36. Optimization of H1-CRD and polymer concentrations.....	3-106
Figure 37. Calcium dependency of polymer binding	3-107
Figure 38. Binding of different glycopolymers to the H1-CRD.....	3-107
Figure 39. Washing steps after polymer incubation	3-109
Figure 40. pH dependency of ligand binding to the H1-CRD	3-110
Figure 41. Influence of calcium concentration in the buffer on the IC ₅₀ of galactose	3-111
Figure 42. Influence of incubation temperature during the polymer-binding step	3-112
Figure 43. DMSO Tolerance of the competitive solid-phase binding assay	3-113
Figure 44. Structures of carbohydrate analytes.....	3-115
Figure 45. Adaptation of the assay to H2-CRD	3-116
Figure 46. Comparison of the binding activity of H2-CRD (0-50 µg/ml)	3-117
Figure 47. Comparison of Gal- and GalNAc-PAA-polymer (0.5 µg/ml) binding to H2-CRD	3-118
Figure 48. Lead compound <i>N</i> -acetylgalactosamine (GalNAc)	3-119
Figure 49. Summary on the 4 directed libraries produced by C.Riva	3-120
Figure 50. Starting point for the design of new glycomimetic ligands for the H1-CRD	3-121
Figure 51. Docking study of hypothetical Ligand into H1-CRD	3-122
Figure 52. Compound 56 represents a general structure of the compounds.....	3-123
Figure 53. Relative IC ₅₀ values measured in the competitive solid-phase H1-CRD assay	3-125
Figure 54. A comparison of the structures of the best binding drug-like ligands	3-126

Figure 55. A hypothetical trivalent ligand (1) for the ASGP-R featuring a GalNAc mimic	3-126
Figure 56. Western Blot analysis with hybridoma cell supernatants	3-128
Figure 57. Immunohistochemistry staining of H1-CRD in human liver tissue.....	3-130
Table 58. Visual interpretation of tissue staining (by Prof. Terracciano)	3-131
Figure 59. Internalization of Texas Red labeled Asialofetuin	3-133
Figure 60. Internalization of ant human H1-CRD antibodies via the ASGP-R	3-135
Figure 61. Storage of ASGP-R in fixed and permeabilized HepG2, stained with antibody C18.1	3-136
Figure 62. Titration of mouse anti-human H1-CRD antibodies.....	3-137
Figure 63. Mouse anti-human H1-CRD mAb binding to different hepatoma cell lines 1	3-137
Figure 64. Mouse anti-human H1-CRD mAb binding to different hepatoma cell lines 2	3-138
Figure 65. Triantennary compounds for the ASGP-R.....	3-141
Figure 66. Summarized features of the trivalent drug carrier	3-142
Figure 67. Fluorescent, trivalent compounds 6 , 7 , and control 8 ;	3-143
Figure 68, Fluorescent microscopy images depicting the ASGP-R-specific uptake of Alexa Fluor [®] 488-labeled compounds.	3-145
Figure 69. Example of flow cytometry analysis showing uptake of compound 7 into HepG2 cells.	3-146
Figure 70. Titration of compound 7	3-147
Figure 71. Time dependency of uptake of compound 7	3-147
Figure 72. Competitive uptake of compound 7 at a concentration of 10 μ M	3-148
Figure 73. Uptake of compound 6 in HepG2 cells (live image)	3-152
Figure 74. Uptake of compound 6 in SK-Hep1 cells (live image).....	3-152
Figure 75. Autofluorescence of untreated HepG2 cells (Live image).....	3-153
Figure 76. Uptake of compound 7 in single HepG2 cells after 10 min of internalization	3-154
Figure 77. Uptake of compound 8 in (A) HepG2 and (B) in SK-Hep1 after 10 min of internalization.....	3-154
Figure 78. Antibody isotyping ELISA	3-156

Figure 79. V _L and V _H amplification	3-158
Figure 80. Assembly of scFv (V _L -linker (Gly ₄ Ser) ₄ -V _H).....	3-159
Figure 81. pAK300 digestion	3-161
Figure 82. Digested scFv fragments.....	3-161
Figure 83. Agarose gel of selected pAKscFvs.....	3-162
Figure 84. Colony blotting of transformed BL21(D3) pAk300scfv	3-164
Figure 85. Growth of C11.1scFv, 500ml culture	3-165
Figure 86. SDS-PAGE analysis of C11.1scFv purification via IMAC.....	3-166
Figure 87. Example chromatogram of IMAC purification for B01.4scFv from periplasmic extract.....	3-167
Figure 88. Sensorgram obtained from the screening of C11.1scFv in SPR.	3-168
Figure 89. purified C11.1scFv tested for binding to H1-CRD	3-168
Figure 90. Analytical digest of pAK100scfv constructs.....	3-169
Figure 91. Soluble scFv ELISA of murine antibodies after the first panning round	3-171
Figure 92. Titer after panning rounds on immunotubes.....	3-173
Figure 93. Soluble scFv ELISA from ETH-2-Gold clones.....	3-175
Figure 94. Chromatograms of the affinity purification of selected scFvs 2D3, 2D8, 2E8 and 5B8 from 100ml of supernatant of each clone using a Protein A column.....	3-176
Figure 95. Growth curve of clone 5B8, 500ml culture	3-177
Figure 96. Chromatogram of the affinity purification of scFv 5B8 from 500 ml supernatant.....	3-177
Figure 97. Analysis of scFv 5B8 purified from supernatant over Protein A..	3-178
Figure 98. 5B8 scFv sample for SPR analysis	3-178
Figure 99. Immobilization of H1-CRD on a CM5 sensor chip.....	3-179
Figure 100. Sensorgram of H1-CRD activity testing with GalNAc.....	3-180
Figure 101. Screening of human ETH-2-Gold derived scFvs.....	3-180
Figure 102. Preliminary affinity measurements of human scFv 5B8 and 2E8.....	3-181

Acknowledgments

First of all I would like to thank Professor Beat Ernst for giving me the opportunity to work on this interesting and challenging project and for selecting so many interesting personalities to build up a group of people with whom working with is a pleasure.

I would also like to thank:

The former ASGP-R team for the constructive discussions and fruitful collaborations: Dr. Rita Born, Dr. Daniel Ricklin, Dr. Claudia Riva-Mahler, Dr. Oleg Khorev, Dr. Brian Cutting and Dr. Karin Johansson.

Stefanie Mesch not only for her help with the Biacore experiments and Morena Spreafico, Céline Weckerle, Matthias Wittwer, Maike Scharenberg, Katrin Lemme and Florian Binder and all the other members of the IMP-team for being exceptionally good coworkers and friends, for all the coffee breaks and lunches and IMP and extra-IMP traveling, hiking, skiing and cooking events and, of course, Cargo-bar nights that we shared. I will miss you guys a lot.

Adrian Ensner, Dr. Andreas Stöckli, Dr. Matthias Studer and Jonas Egger for spending their time helping me whenever I had a computer related problem and for being on top of that very good friends.

My diploma students Katrin Schwingruber, Maria Kubinkova and Francina Purchert for the work they shared with me and for their friendship.

Dr. Stefan Ewert for his tips and help in finding protocols to start the scFv project. Rosmarie Sütterlin and Dr. Markus Dürrenberger for their helpful hints on how to use the fluorescence microscopes. Marco Cavallari for his instructions on the flow cytometer. Prof. L. Terrachiano and Dr. Tornillo for their contributions with the IHC experiments. Prof. D.Neri for providing the ETH-2-Gold library.

My 'longtime and nearly family' friends Bernhard Straubhaar, Sarah Limonta and Jochen Wyss, whom I met during my apprenticeship and who are since then always here for me when I need them.

My friends Haike Süring, and Tina Pfeiffer-Unkrich, who are the best friends a girl can ask for, for their constant support and friendship.

Matthias Hoch, for his love and support during the last stressful part of my thesis, who brought sunshine in my life and successfully convinced me that it's up to oneself to make every day a happy day.

And last but not least my mum Rosmarie Stokmaier who always believed in and cared for me. Thank you for passing on your stamina to me, I needed it.

Publications arising from this thesis

Trivalent, Gal/GalNAc-containing Ligands Designed for the Asialoglycoprotein Receptor

Oleg Khorev, Daniela Stokmaier, Oliver Schwardt, Brian Cutting, Beat Ernst
Bioorg Med Chem (2008) May 1;16(9):5216-31

Abstract:

A series of novel, fluorescent ligands designed to bind with high affinity and specificity to the asialoglycoprotein receptor (ASGP-R) has been synthesized and tested on human liver cells. The compounds bear three non-reducing, beta-linked Gal or GalNAc moieties linked to flexible spacers for an optimal spatial interaction with the binding site of the ASGP-R. The final constructs were selectively endocytosed by HepG2 cells derived from parenchymal liver cells—the major human liver cell type—in a process that was visualized with the aid of fluorescence microscopy. Furthermore, the internalization was analyzed with flow cytometry, which showed the process to be receptor-mediated and selective. The compounds described in this work could serve as valuable tools for studying hepatic endocytosis, and are suited as carriers for site-specific drug delivery to the liver.

Design, synthesis and evaluation of monovalent ligands for the asialoglycoprotein receptor (ASGP-R)

Stokmaier D, Khorev O, Cutting B, Born R, Ricklin D, Ernst TO, Böni F, Schwingruber K, Gentner M, Wittwer M, Spreafico M, Vedani A, Rabhani S, Schwardt O, Ernst B. *Bioorg Med Chem*. 2009 Oct 15;17(20):7254-64.

Abstract:

A series of novel aryl-substituted triazolyl D-galactosamine derivatives was synthesized as ligands for the carbohydrate recognition domain of the major subunit H1 (H1-CRD) of the human asialoglycoprotein receptor (ASGP-R). The compounds were biologically evaluated with a newly developed competitive binding assay, surface plasmon resonance and by a competitive NMR binding experiment. With compound 1b, a new ligand with a twofold improved affinity to the best so far known D-GalNAc was identified. This small, drug-like ligand can be used as targeting device for drug delivery to hepatocytes.

In preparation:

Production and Characterization of Antibodies against the human ASPG-R H1 Subunit Carbohydrate Recognition Domain (H1-CRD)

pH Dependence of Ligand binding to the H1-CRD of the human Asialoglycoprotein-receptor

Thesis abstract

The asialoglycoprotein-receptor (ASGP-R) is a C-type lectin predominantly expressed on the sinusoidal surface of mammalian hepatocytes and is responsible for the blood-clearance of desialylated glycoproteins by receptor-mediated endocytosis. The human receptor consists of two homologous subunits, H1 and H2, whose carbohydrate recognition domains (CRDs) specifically bind non-reducing galactose- and *N*-acetylgalactosamine-residues. The presence of this specific receptor in high numbers on human hepatocytes attracts scientists all over the world to evaluate its potential as a mediator for the targeting of therapeutic agents and foreign genes to the liver.

Although the ASGP-receptor has been intensively investigated, numerous questions remain unanswered; e.g., what are the specific functions of the receptor subunits H1 and H2? What is the mechanism leading to an increased rate of endocytosis upon ligand binding? Is there a difference in specificity of ASGP-receptors on hepatocytes, peritoneal blood macrophages and Kupffer-cells? Can monovalent high affinity ligands be designed which specifically bind to the hepatic receptor. Can antibodies or antibody fragments be developed as specific drug carriers to the liver?

Thesis aims

The aims aspired in the scope of this thesis, were the implementation of new tools for the further elucidation of some of the questions above and the development of new targeting moieties to deliver drugs specifically to the liver via the ASGP-R.

- In order to generate glycomimetics with improved affinity towards the ASGPR, the availability of suitable assay systems is crucial. To date the only competitive *in vitro* binding assays for ASGP-R ligands described in literature use radioactive-labeled ligands. Within the scope of this thesis a new cell-free competitive binding assay was developed to confirm the basic approach of new rationally designed ligands and to compare their affinities to the receptor with known galactose-derived compounds. In this assay, the purified human H1-CRD of the ASGP-R expressed in *E.coli* was coated

onto 96-well plates and the competition in binding of galactose-derivates with a biotin-labeled polyacrylamide-carrier bearing *N*-acetyl-galactosamine-residues to the H1-CRD was measured. The features of the assay were characterized and the IC₅₀ values of galactose-derivates evaluated. In the same assay the binding activities of cysteine mutants of the H1-CRD were tested.

- On cellular level, methods for visualization of binding and internalization of synthetic drug carriers and antibodies raised against the receptor and the study of their receptor specificity (hepatic ASGP receptor versus galactose-specific receptors on the surfaces of other cells) were established.

Although there is much interest in the use of the ASGP-R for hepatotropic drug delivery, no attempt has been made to address the receptor using an antibody instead of the usual sugar-based delivery systems. However, as carbohydrate-protein interactions are exceptionally weak, higher affinity glycomimetics or antibodies would be of great advantage for targeted therapy.

- For proof of principle drug targeting into hepatocytes or as a diagnostic tool for liver diseases in Immunohistochemistry (IHC), The adaptation of high affinity murine anti-human H1-CRD IgG antibodies, previously developed in our institute, to a single chain format (scFv) was attempted.
- In order to develop a biopharmaceutical drug, phage display technology was used to select a human scFv antibody with high affinity to the H1-CRD of the ASGP-receptor that could be applied as carrier in the form of an immuno-conjugate for the hepatotropic targeting of drugs and genes (e.g. siRNA).

Abbreviations

aa	amino acids
Ab	antibody
ABTS	2, 2'-azino-di-[3- ethylbenzthiazoline-6-sulfonic acid]
AIH	auto immune hepatitis
Amp	ampicillin
ASF	asialofetuin
ASGP-R	asialoglycoprotein receptor
ASOR	asialoorosomuroid
AU	absorbance units
BCR	B-cell receptor
bp	base pairs
BSA	bovine serum albumin
Cam	chloramphenicol
cDNA	complementary DNA
CLSM	confocal laser scanning microscopy
CRD	carbohydrate recognition domain
CV	column volume
DEPC	diethyl pyrocarbonate
DMEM	Dublecco's modified Eagle medium
DMSO	dimethyl sulfoxide
DPBS	Dulbecco's PBS, Ca ²⁺ /Mg ²⁺ -free
DTT	dithiothreitol
FBS	fetal bovine serum
FC	flow cytometry

FPLC	fast protein liquid chromatography
Gal	D-Galactose
GalNAc	N-acetyl-galactosamine
Glc	D-Glucose
HI	asialoglycoprotein receptor subunit 1
HI-CRD	carbohydrate recognition domain of the major subunit HI of the human Asialoglycoprotein receptor
H2	asialoglycoprotein receptor subunit 2
HBS	HEPES buffered saline
HBV	hepatitis B virus
HCC	hepatocellular carcinoma
HCV	hepatitis C virus
HEPES	4-(2-Hydroxyethyl) piperazine-1-ethanesulfonic acid
HPLC	high performance liquid chromatography
IEC	ion exchange chromatography
IHC	immunohistochemistry
IMAC	immobilized metal affinity chromatography
IUB	International Union of Biochemistry
IUPAC	International Union of Pure and Applied Chemistry
Kan	kanamycin
K_D	equilibrium dissociation constant
kDa	kilo Dalton
k_{off}	dissociation rate constant
k_{on}	association rate constant
mAb	monoclonal antibody
MFI	median fluorescence intensity
mRNA	messenger RNA

MW	molecular weight
Ni-NTA	nickel-nitrilotriacetic acid
OD	optical density
OPD	O-phenyldiamine
PAGE	polyacrylamide gel electrophoresis
PBS	phosphate buffered saline
PCR	polymerase chain reaction
RME	receptor mediated endocytosis
RT	room temperature
RU	resonance units
SD	standard deviation
SDS	sodium dodecylsulfate
SEC	size exclusion chromatography
siRNA	short interfering RNA
SPR	surface plasmon resonance
TBS	Tris buffered saline
Tet	tetracycline
TR	Texas Red
Tris	Tris(hydroxymethyl)-aminomethan

1. Introduction

1.1 General Overview - The Liver

The liver, weighing about 1.5 kg, is the largest gland in the body and the main metabolic organ responsible for clearing the blood from undesired endo- and exogenous compounds. Its main functions are: the storage of carbohydrates, proteins, fats, certain vitamins and iron, to control the production and removal of cholesterol, the production of bile and blood clotting factors, the removal and detoxification of waste products, drugs and other noxious substances, the production of immune factors, and removal of bacteria from the bloodstream to combat infections.

The liver is divided into two main lobes that are further subdivided into approximately 100,000 lobules. Two-thirds of the liver is the *parenchyma*, which contains the hepatocytes (Figure 1), and the remainder is the biliary tract. It receives its blood supply via the hepatic artery and portal vein.

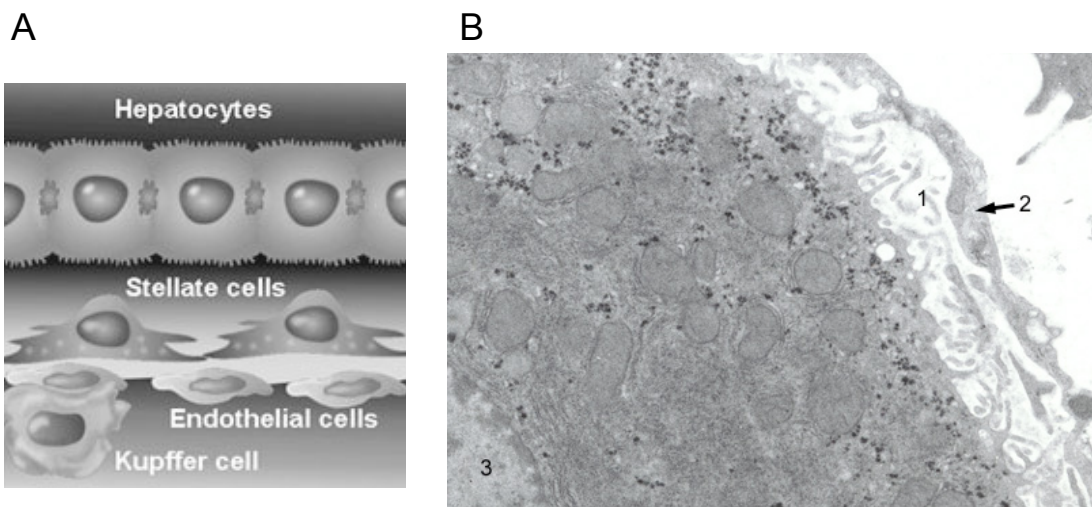


Figure 1. Liver cells

(A) Liver cells ¹ **(B)** Electron microscopy picture of a hepatocyte: the space of Disse (1) is lying between the sinusoidal endothelium (2) and the cell surface. Microvilli on the hepatocyte surface protrude into the space of Disse. Within the hepatocyte cytoplasm high numbers of mitochondria, rough ER, polyribosomes, glycogen particles and the nucleus (3) are visible ².

The sinusoids

The sinusoids are low-pressure vascular channels that receive blood from terminal branches of the hepatic artery and portal vein at the periphery of lobules and deliver it into central veins. They are composed of a layer of highly fenestrated endothelial cells that are separated from the underlying hepatocytes by a subendothelial space known as the space of Disse or perisinusoidal space. Plasma from the sinusoidal blood flows nearly unhindered through the endothelial wall fenestrae, which are about 100 nm in diameter and are grouped into clusters called sieve plates, into the space of Disse. There the plasma gets in close contact with the hepatocytes' microvilli, which increases their perisinusoidal surface by about 6-fold to allow absorptive processes.

Hepatocytes

About 60-80% of the cytoplasmic mass of the liver is made up by hepatocytes. Hepatocytes are organized into plates one or two cells thick and have an average lifespan of 150 days. To achieve their role as the chief functional cells of the liver, they are highly differentiated and produce a plethora of enzymes and receptors and are specialized in metabolizing and excreting different classes of molecules. With up to 500,000 receptors/hepatocyte, the asialoglycoprotein receptor is one of the most abundant receptors on hepatocytes³.

Kupffer cells

Kupffer cells, the resident macrophages of the liver, are located along the sinusoids, account for 80 to 90% of resident macrophages in the body and they constitute about 15% of the liver cells. The principal role of Kupffer cells is phagocytosis of particulate and soluble components from the blood and mediation of the innate immune response in the liver.

Stellate cells

A third type of cells, hepatic stellate cells also known as Ito cells, is found in the perisinusoidal space. The stellate cell is the major cell type involved in liver fibrosis, which is the formation of scar tissue in response to liver damage.

In normal liver, stellate cells are in a quiescent state and represent 5-8% of the total number of liver cells ⁴.

1.2 Chronic Liver Disease

The liver as the center of metabolism can be affected by genetic disorders, intoxication, viral infection and tumor growth. Due to the great importance of a fully functioning liver, such diseases often dramatically reduce a patient's quality or even expectance of life.

Chronic liver disease damages hepatocytes, which are responsible for the hundreds of critical metabolic functions performed by the liver. Damage to these cells and the surrounding tissue establishes a state of inflammation in the liver called hepatitis. Inflammation further exacerbates damage to the liver and initiates a process of wound healing to cope with the ongoing damage. This process involves the production of a number of extracellular matrix proteins, which maintain the structural integrity of the liver. In the case of chronic liver disease, in which the inflammation is persistent, mechanisms that would normally terminate the wound healing process are overridden. Over time, the loss of hepatocytes and ongoing fibrogenesis results in cirrhosis.

The liver diseases described in the following paragraphs are those responsible for chronic liver disease. The severity of these diseases puts an emphasis on the importance of research aiming at the development of new hepatotopic drug-delivery approaches. First of all, hepatic targeting will allow to achieve higher and more efficient concentrations of drugs in the liver. It will also enable administration of more powerful drugs whose use without being directed to the site of action might otherwise be prevented by extrahepatic side effects.

Viral Hepatitis

Viral hepatitis is an inflammation of the liver caused by several different viruses, namely the hepatitis A, B, C, D, and E viruses. All of these viruses cause acute viral hepatitis. The hepatitis B, C, and D viruses can also cause chronic hepatitis, in which the infection is prolonged, sometimes lifelong. Chronic hepatitis can lead to cirrhosis, liver failure, and liver cancer.

Hepatitis B (HVB)

Hepatitis B is caused by the hepatitis B virus (HVB), which belongs to the family of *Hepadnaviridae*. The symptoms of the disease range in severity from a mild illness, lasting a few weeks with full remission in about 90% of the cases, to a serious chronic form that can lead to liver disease or liver cancer. Transmission of the virus occurs via contact with infectious blood, semen, and other body fluids, sharing contaminated needles, or from an infected mother to her newborn (infants born to infected mothers usually receive hepatitis B immune globulin and hepatitis B vaccine within 12 hours of birth to prevent infection) ⁵.

Drugs approved for the treatment of chronic hepatitis B include peginterferon, which slows the replication of the virus in the body and also boost the immune system, and the antiviral drugs lamivudine, adefovir dipivoxil, entecavir, and telbivudine ⁶.

Hepatitis C (HCV)

Hepatitis C is caused by the hepatitis C virus (HCV). HCV is a small (40 to 60 nm in diameter), enveloped, single-stranded RNA virus of the *Flaviviridae* family. Because the virus mutates rapidly, changes in the envelope proteins allow it to evade the immune system. There are at least six major genotypes and more than 50 subtypes of HCV. The different genotypes have different geographic distributions. HCV infection sometimes results in an acute illness, but more often becomes a chronic condition. Chronic hepatitis C varies greatly in its course and outcome. The hepatitis C virus (HCV) is one of the most important causes of chronic liver disease. It accounts for about 15 percent of acute viral hepatitis, 60 to 70 percent of chronic hepatitis, and up to 50 percent of cirrhosis, end-stage liver disease, and liver cancer ⁷. The virus is transmitted via contact with the blood of an infected person, primarily through sharing contaminated needles. Maternal-infant transmission is not common, less than 5 percent of infants born to HCV-infected mothers become infected. Up to date, no vaccination is available.

Standard therapy for HVC- patients are peginterferon as monotherapy or in combination with ribavirin ⁸. Ribavirin is an oral antiviral agent that has activity

against a broad range of viruses. By itself, ribavirin has little effect on HCV, but in combination with interferon it increases the sustained response rate by two- to three-fold.

Autoimmune Hepatitis (AIH)

Autoimmune hepatitis is a disease that mainly affects young women (70% of the patients are female)⁹. In AIH the body's immune system attacks liver cells and this immune response causes hepatitis. The usual presentation is with fatigue, pain in the right upper quadrant of the abdomen, and polymyalgia or arthralgia associated with abnormal results of liver function tests. AIH is classified as type 1 or type 2¹⁰. Type 1 is the most common form. It can occur at any age but most often starts in adolescence or young adulthood. Other autoimmune diseases are present in 17% of patients with AIH type 1, predominantly thyroid disease, rheumatoid arthritis, and ulcerative colitis. AIH type 2 is less common; typically affecting girls aged 2 to 14.

The diagnosis of AIH is important, as immunosuppressive drugs (e.g., prednisolone and azathioprine) produce lasting remission and an excellent prognosis. Although AIH can produce transient jaundice, the inflammation process can continue at a sub-clinical level, leading to cirrhosis and liver failure. The diagnosis is based on detection of autoantibodies (anti-nuclear antibodies (60% positive), anti-smooth muscle antibodies (70% positive), anti-ASGP-R antibodies (88% positive)) and high titers of immunoglobulins (present in almost all patients, usually IgG).

Hepatocellular carcinoma (HCC)

Hepatocellular carcinoma (HCC) is currently the fifth most common solid tumor worldwide, and the fourth leading cause of cancer-related death, involving more than a half million new cases yearly¹¹. In some areas of Asia and the Middle East, HCC ranks as the leading cause of cancer-related death. The major risk factor for HCC development is the presence of liver cirrhosis, mostly related to chronic infection with the hepatitis B or C virus, alcohol intake, and iron deposition¹². The incidence of HCC is increasing in Europe and the United States¹³ and it is currently the leading cause of death among cirrhotic patients¹⁴. Not all cirrhotic patients develop HCC, and factors that

define those at high risk are male sex, age older than 50 years, increased alpha-fetoprotein (AFP) concentration, and intense inflammation and hepatocyte proliferation ¹⁵.

In general, therapies for HCC can be divided into those that are potentially curative and those that are palliative only. Survival of untreated individuals is poor. Despite the implementation of screening programs in cirrhotic patients through biannual abdominal ultrasound examination, only 30% of HCC are diagnosed at an early stage when potentially curative therapies, including surgical resection, liver transplantation and percutaneous ablation, are possible. Several therapies have been proposed for patients who cannot benefit from this approaches, but up to now only transarterial chemoembolization has demonstrated survival benefits ¹⁶. However, it can only be performed in patients with preserved liver function, absence of extrahepatic spread/vascular invasion, and no significant cancer-related symptoms. Therefore, no more than 20% of the patients affected by HCC can benefit from this therapy.

Ideally, treatment of the tumor should target the specific mechanisms that are dysregulated. In this way, therapeutic action would be selective and targeted at correcting the specific defect that facilitates cancer progression. Improvements in the understanding of the molecular pathogenesis underlying HCC ¹⁷ have led to the testing of cytostatic agents that affect some of these disrupted pathways. New non-surgical therapies are currently evaluated, for example chemoprevention with retinoids. Retinoids are important candidates for cancer chemoprevention because cancer is characterized by abnormal growth with a lack of differentiation, and the dysfunction of retinoid nuclear receptors is closely related to the carcinogenic process. Chemoprevention of de novo HCC with acyclic retinoids has been effectively tested in a single positive randomized controlled trial after surgical resection ¹⁸. And phase I/II studies are currently under way to investigate whether epidermal growth factor receptor inhibitors, platelet-derived growth factor receptor inhibitors, and antibodies against VEGF (vascular endothelial growth factor) may have a role in the treatment of HCC ^{19, 20}. In chemotherapy, new agents have emerged during the last several years and are currently tested in large

cohorts of patients. But until now, none of these agents has resulted in a proven advantage in terms of survival.

However, some strategies provide objective response rates greater than 20%, as is the case with internal radiation with ^{131}I -labeled lipiodol (iodinated, radio-opaque contrast poppyseed oil) or arterial lipiodolization (chemotherapeutic agents and lipiodol) ²¹⁻²³. Systemic chemotherapy has been tested in 9 randomized controlled trials. One of the most active drugs in this setting *in vitro* and *in vivo* is doxorubicin ²¹. Systemic doxorubicin administration provides partial responses in approximately 10% of cases, without evidence of survival advantage, and has well-known treatment-related adverse effects. Given that the currently available anticancer drugs have limited effectiveness in the treatment of HCC at conventional doses, and the fact that dose escalation is impeded by unacceptable high associated toxicity, the efficacy of these drugs might be enhanced by coupling them to a drug-carrier taken up by the Asialoglyco-protein receptor (ASGP-R). The ASGP-R is present in 20% of poorly differentiated HCCs and in up to 80% of well-differentiated tumors ²⁴. The work of Fiume and colleagues ²⁵⁻²⁹ helped to establish the rationale for a liver selective delivery of high concentrations of doxorubicin coupled to lactosaminated human albumin (L-HAS; a galactosyl-terminating neoglycoprotein), selectively taken up by the ASGP-R. When administered to rats in an experimental model of diethylnitrosamine-induced HCC, L-HSA-doxorubicin was associated with a significant decrease in the number of nodules compared with that found in sham-treated animals. Unexpectedly, they could also show that the L-HSA-doxorubicin conjugate targeting the ASGP-R enhanced the uptake of doxorubicin in all forms of HCCs, independently of their differentiation grade. These results further corroborate the eligibility of the ASGP-R as an interesting research topic for hepatotropic drug targeting in the treatment of HCC.

1.3 The ASGP-R

The human Asialoglycoprotein Receptor (ASGP-R) is a membrane-bound Ca^{2+} dependent (C-type) lectin, a carbohydrate-binding protein, found abundantly on the surface of hepatocytes. Ashwell and Morell were the first to

describe the receptor, after they discovered that removal of the sialic acid residues of N-linked oligosaccharides on glycoproteins resulted in their rapid clearance from the blood and degradation in the liver³⁰⁻³³.

The ASGP-R mediates the endocytosis and degradation of a wide variety of desialylated glycoproteins (Asialoglycoproteins) that contain terminal galactose (Gal) or *N*-acetylgalactosamine (GalNAc) on their N-linked carbohydrate chain³⁴. The endocytosis of receptor-bound asialoglycoproteins via coated pits and vesicles and the routing of these ligands to lysosomes where they are degraded have been intensely investigated³⁵.

The ASGP-R is located on the basolateral membrane of parenchymal liver cells facing the sinusoids and is therefore in direct contact with the blood passing the liver (Figure 2). It is estimated that there are up to 500'000 receptor subunits presented per cell. This high abundance, its localization and the efficient internalization of its ligands make the receptor an intriguing target for the development of high affinity ligands to be used as homing devices to specifically target drugs or genes to parenchymal liver cells³⁶.

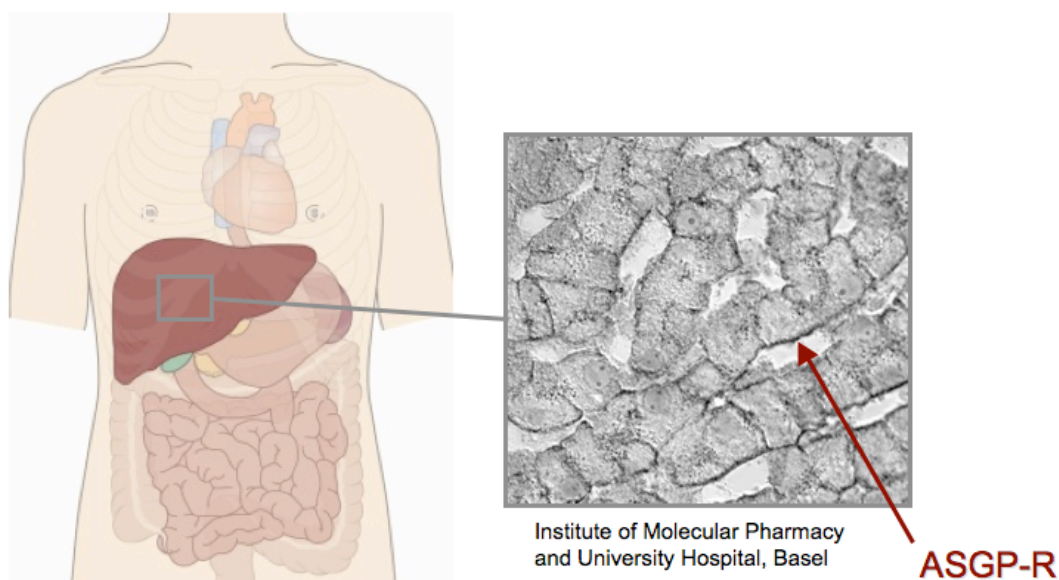


Figure 2. Localization of the ASGP-R in the liver
Normal liver tissue (University Hospital Basel) stained with the anti-human H1-CRD antibody C14.6 developed at the Institute of Molecular Pharmacy.

1.3.1 Structure of the Asialoglycoprotein Receptor

In humans, the functional receptor is a hetero-oligomer consisting of two homologous subunits sharing 58% sequence homology, designated H1 for the major and H2 for the minor subunit (M_r 45 kD and 50 kDa respectively) ³⁷. They belong to the superfamily of C-type lectins and, in particular, to the long-form subfamily that contains three conserved intramolecular disulfide bonds in their carbohydrate recognition domain (CRD) ³⁸. Both subunits contain a single transmembrane domain with extracellular carboxyl terminus and with cytoplasmic amino terminus (type II transmembrane orientation) (Figure 3). The CRD is located at the extracellular carboxyl terminus and for H1 a consensus tyrosine amino acid motif (YQDL) is responsible for the association with clathrin-coated vesicles within its cytoplasmic domain ³⁹. The subunits form a noncovalent oligomeric complex by a coiled-coil stalk segment interaction ⁴⁰.

Although it is agreed that the functional ASGP-R is a hetero-oligomeric complex composed of two types of subunits, the subunit stoichiometry and size of the native ASGP-receptor in hepatocytes is still debated ⁴¹. Henis ⁴² reported a H1/H2 ratio of 3:1, whereas Bider ⁴⁰ suggested the formation of non-functional H1 homo-trimers and functional 2:2 H1/H2 hetero-tetramers. Literature data suggest a dominant biological role of the H1 subunit of the ASGP-receptor ⁴³.

Both H1 and H2 are required to reach full functionality of the receptor. Mice lacking the minor mouse subunit (MHL-2), due to disruption of the corresponding gene, showed significantly reduced expression of the major mouse subunit (MHL-1) in their livers and were unable to clear asialoorosmucoid (ASOR) from their circulation. In addition, mice deficient of MHL-1 showed no detectable expression of MHL-2 and an incapability of clearing ASOR from the circulation ⁵⁰. Interestingly, in both, MHL-1 and MHL-2 deficient mice, even though the clearance of ASOR by the ASGP-R was severely impaired, neither accumulation of desialylated glycoproteins in the circulation nor any phenotype abnormalities could be observed.

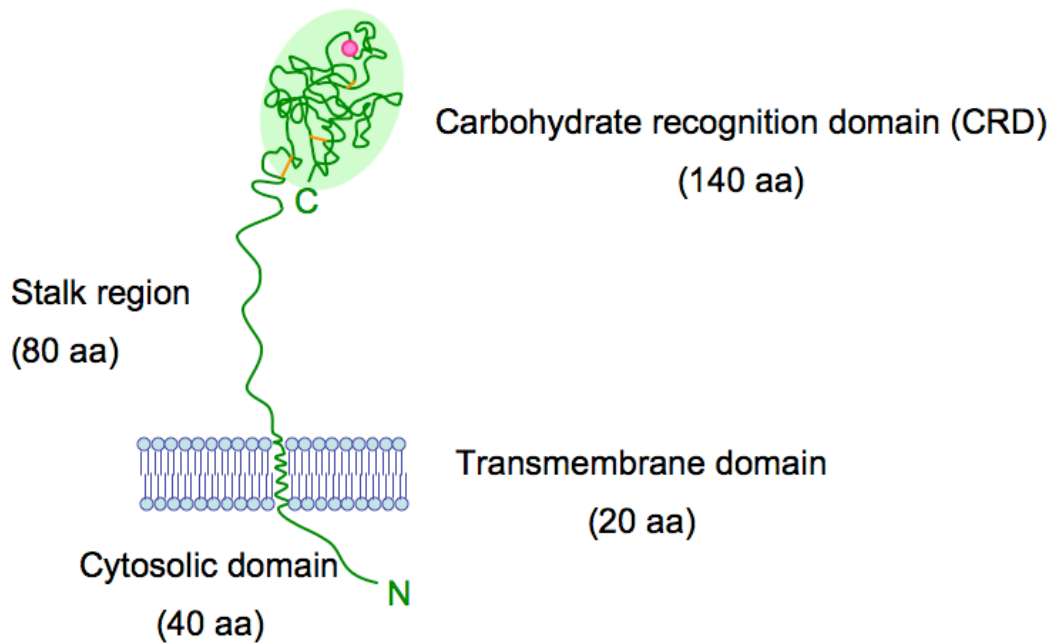


Figure 3. Scheme of the H1 subunit of the ASGP-R

The general structure of the two ASGP-R subunits is illustrated by H1, which consists of 291 amino acids (aa). H1 is a type II integral membrane protein, which contains a 40-amino acid N-terminal cytoplasmic domain, a 20-amino acid single-pass transmembrane domain, an 80-amino acid extracellular stalk region, and a 140-amino acid carbohydrate recognition domain (CRD) containing 3 calcium-ions. Picture by courtesy of Dr.D.Ricklin⁷³.

1.3.2 Receptor Mediated Endocytosis

Receptor mediated endocytosis (RME) is a common mechanism for the uptake of macromolecules by cells and the ASGP-R is one of the best-explored model of an endocytic transport receptor³. After ligand binding to ASGP-R, the receptor-ligand complex migrates along the plane of the plasma membrane to a site of active internalization, the clathrin-coated pit (Figure 4). Shortly after the coated-pits pinch off from the plasma membrane, the clathrin coat dissociates and the uncoated vesicles fuse to form larger early endosomes. Those endosomes are then delivered to and fuse with an organelle designated compartment for the uncoupling of receptors and ligands (CURL)⁴⁴. The endosomes are segregated into receptor-containing and ligand-containing vesicles that are then routed along different intracellular pathways⁴⁵. The ASGP-receptors are recycled to the cell membrane, whereas the ligands are shuttled to lysosomes where they are degraded⁴⁶. Bananis⁴⁷ showed that the ligand-containing vesicles associate with cytoplasmic kinesins; this motor molecules mediate the movement of the

vesicles along microtubules in direction of the centrosome near the nucleus of the cells ⁴⁸. The ASGP-receptor is continuously internalized and recycled even in the absence of ligands. Thus, at steady-state, only 40–60% of the total cellular ASGP-receptors are on the cell surface and the rest is distributed intracellularly throughout the endocytic compartments traversed by the receptor during its cycle ⁴⁹. The rate of endocytosis is, however, increased upon ligand binding to its extracellular domain.

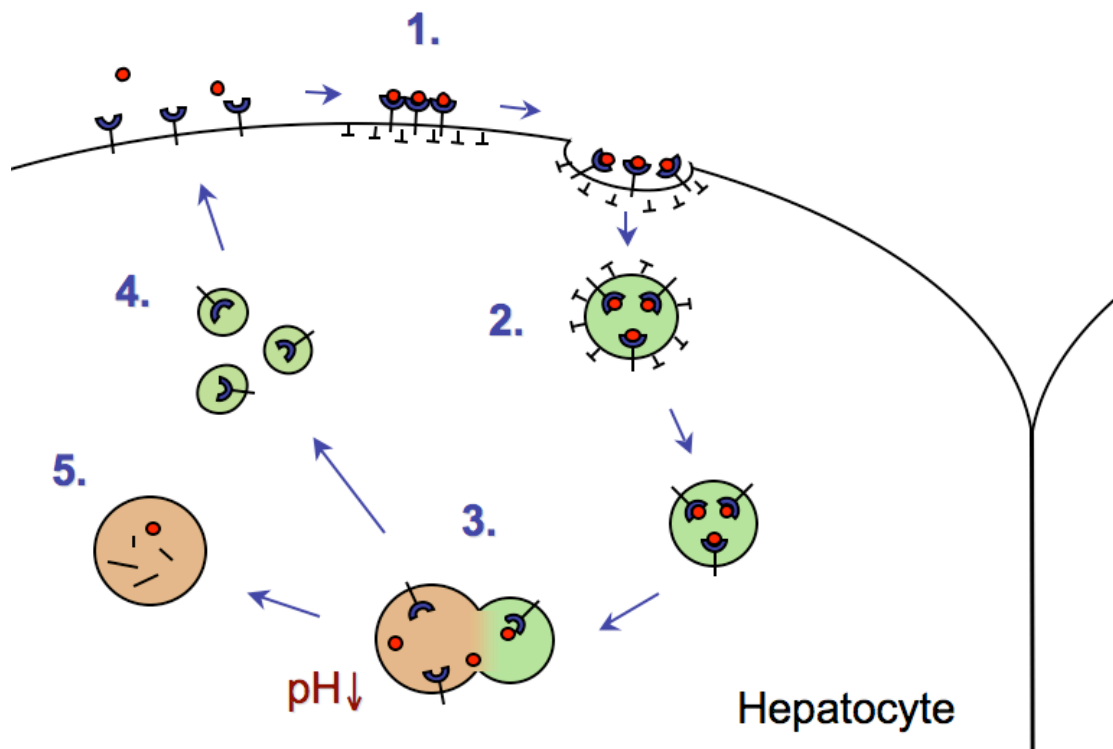


Figure 4. Receptor-mediated internalization of ligands by the ASGP-R
Upon ligand binding, the receptor clusters into coated pits (1.), and is then internalized in clathrin-coated vesicles (2.) The receptor and ligands dissociate due to a drop in the vesicular pH (3.). The receptor is recycled to the basolateral membrane of the hepatocyte (4.), and the ligand is shuffled to lysosomes for degradation (5.).

1.3.3 Physiological Function

The full physiological role of the ASGP-R has still not been elucidated. Although it was initially presumed that its major function was restricted to the physiologic turnover of 'aged' plasma glycoproteins, repeated attempts over a period of years have failed to provide convincing evidence to support that view. For example, receptor-deficient mice did not show significantly elevated plasma level of asialoglycoproteins nor was their life span influenced in any

way ⁵⁰ Dozens of plasma glycoproteins, when desialylated, are suitable ligands for the ASGP-R. Low-density lipoproteins, chylomicron remnants ⁵¹, fibronectin ⁵² and IgA ⁵³ have all been proposed as candidate *in vivo* ligands for the ASGP-R.

The potential role of ASGP-R in the phagocytosis of dying cells was evidenced by the ability of receptor-specific antibody and known ASGP-R ligands to block the uptake of the apoptotic bodies ⁵⁴. The receptor seems to recognize Asialooligosaccharide-chains on the surface of apoptotic cells.

Hardy ⁵⁵ proposed that clusters of ASGP-receptors on the cell surface might present a lattice of sugar-binding sites that could recognize a wide variety of oligosaccharide structures containing different numbers of branches and different spatial organizations of their terminal sugars. Such a lattice-like arrangement would provide great flexibility to bind and internalize a variety of endogenous ligands.

Asialoglycoprotein-receptors of extra hepatic origin

Other Gal/GalNAc binding proteins sharing extensive amino acid sequence homology to the hepatic ASGP-R were found in various tissues or cell types, such as macrophages ⁵⁶, intestinal epithelial cells ⁵⁷, testis ⁵⁸, thyroid glands ⁵⁹, renal tubular epithelial cells ⁶⁰ and on some tumor cells of non-hepatic origin ⁶¹.

These extra-hepatic ASGP-receptors likely have functions different from that of the hepatic ASGP-R, reflected, for example, in the different binding affinities of GalNAc and Gal to the macrophage-receptor compared with the hepatic receptor ⁶².

The role of the ASGP-R in liver disease

The ASGP-R is not only an important target for site-specific drug targeting, but it may play also a role in the genesis and diagnosis of certain liver diseases as it has been shown to represent a common target for humoral and cellular autoimmune responses in chronic hepatitis, probably contributing to disease perpetuation. For example, anti-ASGP-R autoantibodies are detected in 88% of patients with AIH (both types ^{63,64}). These autoantibodies are also

found in some patients with PBC (primary biliary cirrhosis), chronic viral hepatitis B and C and alcoholic liver disease although at lower frequency and lower titers^{65,66}. The ASGP-R is preferentially expressed on the surface of periportal liver cells where piecemeal necrosis is found as a marker of severe inflammatory activity in patients with AIH⁶⁷. This finding may suggest a possible immuno-pathogenetic involvement of anti-ASGP-R autoantibodies in AIH. The general presumption is that the target of potentially tissue-damaging autoreactions in AIH must be liver-specific and available to the immune system *in vivo* (e.g. expression on the surface of hepatocytes). So far, the ASGP-R is the only target-autoantigen that fulfils these criteria. Additional support to this findings emerged from the determinations of anti-ASGP-R autoantibodies in consecutive AIH patients. The levels of anti-ASGP-R autoantibodies vary according to the inflammatory activity of the disease. In addition, anti-ASGP-R antibody titers decreased significantly in response to immunosuppression, while they reappear when the disease has relapsed^{63,68}. The detection of ASGP-R autoantibodies is therefore diagnostically helpful when other autoantibodies are not detected and AIH is suspected⁶⁹.

Some enveloped viruses are known to work as 'opportunistic endocytic ligands' and catch a ride on membrane proteins capable of endocytosis to enter the cell. Inside the endosome specific viral membrane proteins undergo conformational change in the low pH surrounding and promote their insertion into and fusion with the organelle membrane. This places the nucleocapsid into the cytoplasm where it has access to the cells synthetic machinery to replicate itself. In the case of the ASGP-R, the receptor is thought to be involved in the uptake of hepatitis B virus⁷⁰ and Marburg virus⁷¹ during infection. The role of ASGP-R as putative receptor in hepatitis C virus infection is controversially discussed⁷².

1.3.4 Structure of the H1-CRD

The X-ray crystal structure of the carbohydrate recognition domain of the human major subunit H1, the H1-CRD, has been published ⁷³. The CRD of H1 is the first reported structure that contains three Ca^{2+} ions as an integral part of the structure with the calcium ions coordinating several loops within the structure, including the sugar-binding site from residues Arg236 to Cys268. When a Gal or GalNAc monosaccharide is bound to the sugar-binding site, the 3-hydroxyl and 4-hydroxyl groups of the sugar interact directly with the Ca^{2+} in position 2 and the hydrophobic ring surface of the pyranose-ring is stacked against the planar indole-side chain of Trp243. The monosaccharide also forms four hydrogen bonds with residues Gln239, Asp241, Gln252, and Asn264. In addition to the primary binding site there is a shallow hydrophobic pocket on the surface of the CRD providing a binding subsite for the N-acetyl substituent of GalNAc. This interaction likely accounts for the higher affinity of the receptor for GalNAc compared to Gal ^{62,74}.

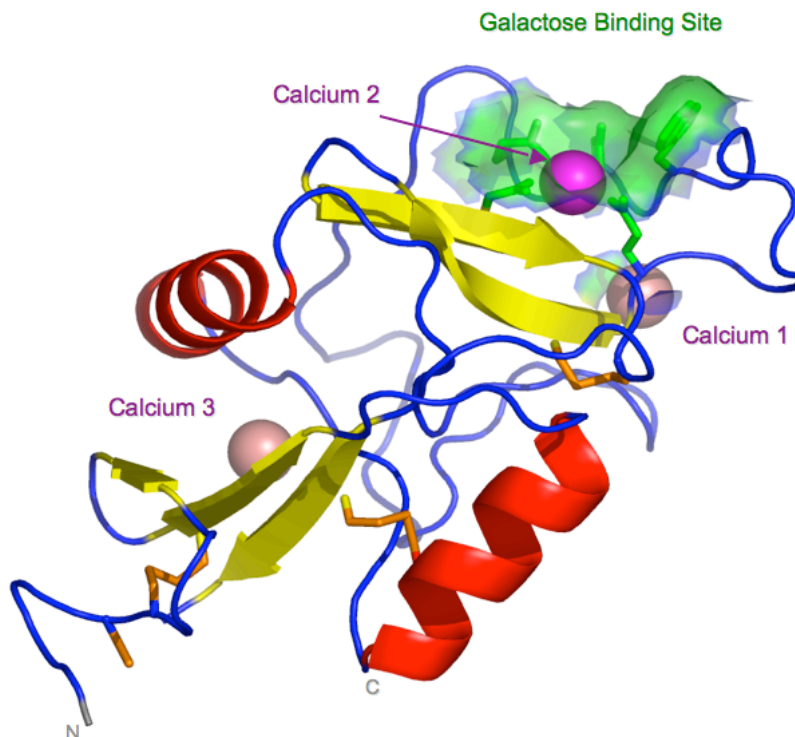


Figure 5. Ribbon diagram of the human H1-CRD

The two β -helices are shown in red, the α -strands in blue, the calcium ions in pink and magenta, and the three disulphide bridges in yellow. Both the N and the C terminus are on the bottom of the image. The sugar binds to calcium ion 2 in front of the glycine-rich loop in the upper part of the picture. Adapted from Meier et al. ⁷³ by Ricklin ⁷⁵

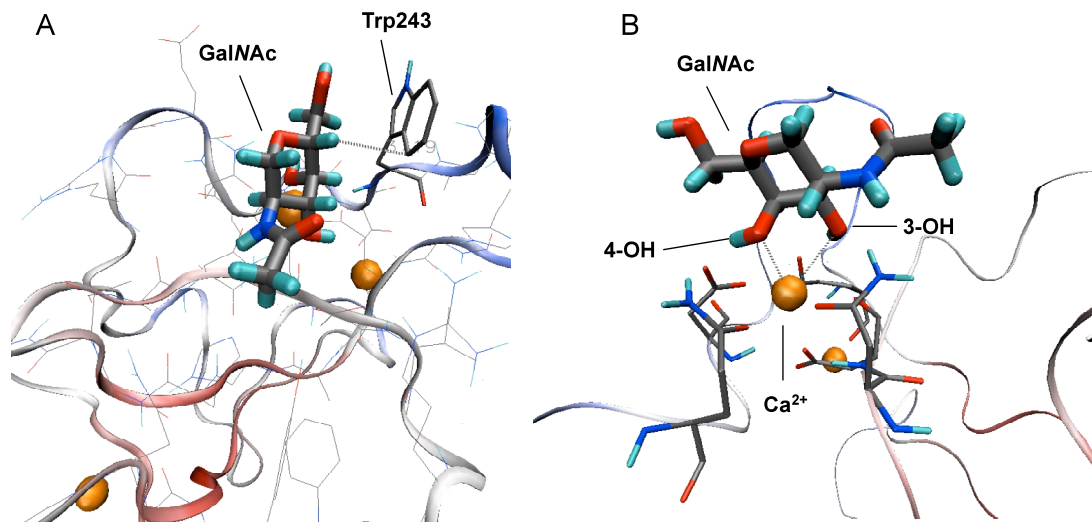


Figure 6. A model of GalNAc docked into the sugar-binding site of the H1-CRD
(A) Illustration of the hydrophobic interaction between Trp243 and α -face of GalNAc. (B) Illustration of the 3- and 4-OH groups coordinating to the calcium ion. Picture courtesy of M.Spreafico, manual-docking trial, MacYeti 7.05.

1.3.5 Ligand Specificity and Affinity

Binding to and internalization of ligands by the hepatic ASGP-R depend on the ligand type (GalNAc > Gal), the valency (binding hierarchy of polyvalent ligands tetra- > tri- >> di- >> mono-antennary)⁷⁶, the spacing of the carbohydrate ligands⁷⁷ and the size of glycosylated particles (limited by the perisinusoidal space to a diameter of ≤ 70 nm *in vivo*)⁷⁸. The affinity and specificity of the ASGP-R is a consequence of oligovalent interactions with its physiological ligands, a process termed 'cluster glycoside effect' by Lee *et al.*⁷⁶.

Many studies have been performed with both natural and synthetic carbohydrates to establish the structure-affinity relationship for the ASGP-R. Baenzinger *et al.*⁷⁹ have shown that the mammalian receptor exhibits specificity for terminal Gal and GalNAc (with an up to 50-fold higher affinity for the latter) on desialylated glycoproteins.

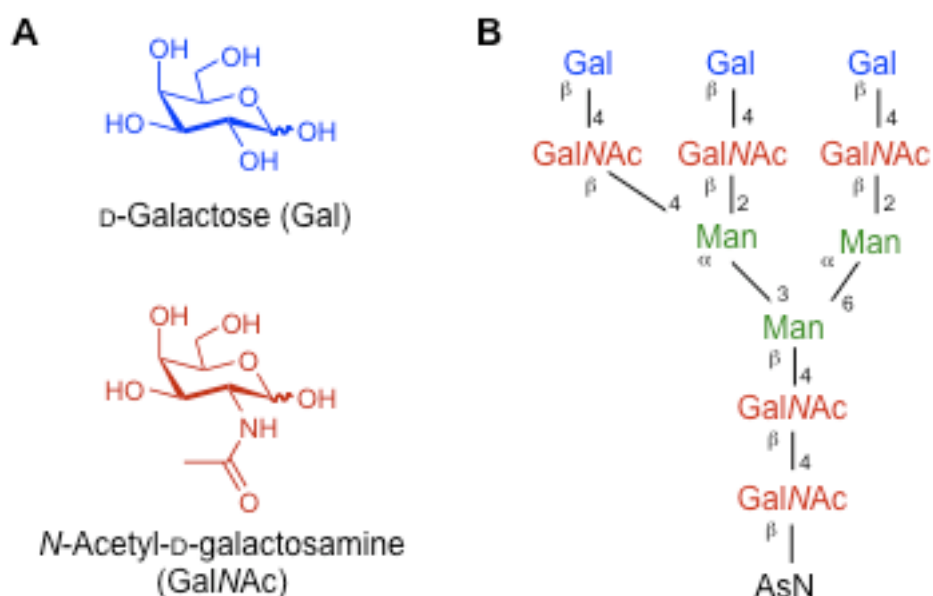


Figure 7. Carbohydrate ligands for the ASGP-R
(A) Monosaccharide ligands galactose and *N*-acetylgalactosamine, **(B)** Natural triantennary ligand TRI-GP⁷⁶

The binding of a single galactose residue to one individual receptor subunit is of low affinity with dissociation constants in the order of 1 mM. In contrast, oligovalent galactose ligands, such as natural bi-, tri- and tetra-antennary desialylated *N*-linked oligosaccharides or glycoproteins, exhibit binding with dissociation constants of approximately 1 mM, 300 nM and 20 nM, respectively ⁷⁶. In other words, although the number of Gal residues/mol of ligand increased only 4-fold, the inhibitory potency increased 10⁶-fold. Because the fourth Gal moiety present in the tetraantennary ligand does not markedly enhance the affinity, it was assumed that the binding requirements of the cell-surface receptor are largely satisfied by the triantennary structure ⁸⁰.

The optimal distance of the Gal moieties in these oligosaccharides was determined by binding assays with synthetic carbohydrates representing partial structures of *N*-linked glycans ⁸¹, high-resolution NMR and molecular modeling studies ⁸². Based on these results, Lee *et al.* ^{76,81} proposed a model for the optimal spatial arrangement of the terminal sugar residues (Figure 8).

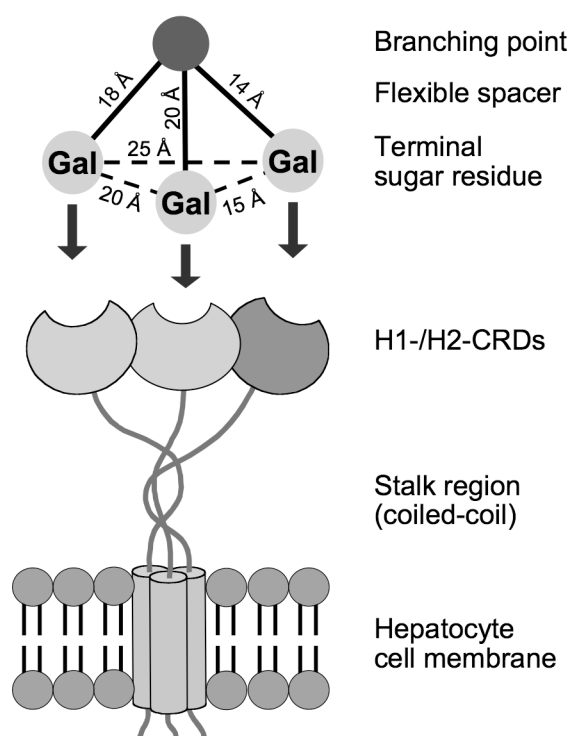


Figure 8. Binding model for ASGP-R ligands in an optimal conformation to the heterooligomeric receptor consisting of H1 and H2 subunits. Dashed line indicates the distance between the C-4 of each Gal moiety; filled line represents approximate distance between branching point and C-6 of Gal (14-20 Å). Adapted from Lee *et al.*⁷⁶ by O.Khorev¹⁵⁸.

Furthermore, the studies led to the conclusion that only the terminal residues are necessary for specific recognition, and that the binding process proceeds through a simultaneous interaction of 2 to 3 sugar residues with 2 to 3 binding sites of the heterooligomeric receptor. On the native receptor on the hepatocyte surface these binding sites are 25-30 Å apart.

1.3.6 Drug Delivery via the ASGP-R

Drug and gene targeting to specific organs is a promising approach for the development of highly effective therapies while reducing side effects. Carbohydrate-lectin interactions between transport receptors in the liver and their physiological (or synthetic) ligands have been described as an efficient method showing high specificity. Due to its specificity, predominant expression on hepatocytes and high capacity for receptor-mediated endocytosis, the ASGP-R has been intensely validated as potential target for drug and gene delivery to the liver^{36,83}. As an alternative to *ex vivo* gene

transfer to the liver, which requires invasive surgery⁸⁴, there is much interest in *in vivo* protocols: (i) Wu *et al.*⁸⁵ demonstrated successful *in vivo* gene transfer to hepatocytes with poly-L-lysine linked asialoorosomuroid, (ii) Hara *et al.*⁸⁶ showed that asialofetuin-labeled liposomes that encapsulate plasmid DNA cause gene expression and (iii) successful gene transfer to hepatocytes using liposomal gene carriers that possess synthetic galactose residues as a targetable ligand for parenchymal liver cells has been reported by Kawakami *et al.*⁸⁷

1.4 Antibodies

Antibodies are part of the body's natural defense system against virus and bacterial infections. They bind to the pathogenic antigens and flag them for destruction by complement and cells of the immune system.

A variety of more than a billion different sequences encoding for antibodies can be achieved in the mammalian immune system by combining a set of variant gene cassettes with unique mutation mechanisms. The genetic material for this huge 'library' of different antibodies is stored in the B-cell pool of the lymphatic tissue, which is the source to generate versatility of antibodies *in vivo*.

After immunization there is usually a progressive increase in the affinity of the antibodies produced against the immunizing antigen. The high-affinity antibodies to a specific antigen are naturally selected by the immune system in a process called affinity maturation. This phenomenon is unique to antibodies and is due to the accumulation of point mutations specifically in both heavy- and light-chain variable region coding sequences⁸⁸. These mutations occur long after the coding regions have been assembled, when B-cells are stimulated by antigen and helper T-cells to generate memory cells in the germinal center of a lymphoid follicle in the secondary lymphoid organs. The point mutations occur at a rate of about one mutation per variable region coding sequence and per cell generation, which is about a million times greater than the spontaneous mutation rate in other genes⁸⁹

Only a small minority of these point mutations result in antigen receptors that have an increased affinity for the antigen. The few B-cells expressing these

high-affinity receptors are able to survive and proliferate, while the other B-cells will undergo apoptosis when the B-cells are stimulated by the presence of an antigen, as explained by the clonal selection theory proposed by the Nobel Prize winners Jerne and Burnet^{90,91}. B-cells within a selected clone begin their antibody-synthesizing lives by making IgM molecules and inserting them into the plasma membrane as B-cell antigen receptor (BCR). Upon stimulation by antigen, some of these cells are activated to secrete IgM antibodies, which dominate the primary antibody response referred to as primary class of antibody⁹². Other antigen-stimulated cells switch to make IgG, IgE, or IgA antibodies⁹³; memory B-cells express one of these three classes of molecules on the surface, while activated B-cells, the so called plasma cells, secrete them. The IgG, IgE, and IgA molecules dominate the secondary antibody response.

1.4.1.1 The Genetic Basis of Antibody Diversity

The human genome is thought to contain less than 10^5 genes, but antibody molecules with different specificities are approximately 10^{6-8} in a given individual. Therefore, antibody diversity raises a special genetic question: how can humans / animals make more antibodies than there are genes in their genome? Antibody gene rearrangements during lymphocyte differentiation, discovered by Tonegawa⁹⁴, provide the answer to the above question. Briefly, both somatic recombination and mutation contribute greatly to an increase in the diversity of antibodies^{88,94}. Antibody genes can move and rearrange themselves within the genome of a differentiating cell^{95,96}. A variable (V) gene located in one position in the DNA of an inherited chromosome (the germline), can move to another position on the chromosome during lymphocyte differentiation. This genetic recombination is promoted by transposases, enzymes that snip pieces of DNA out of one location in a chromosome and transpose these pieces elsewhere⁹⁷. This process of rearrangement during differentiation brings together an appropriate set of genes for the variable and constant regions. The variable domains are created by the combinatorial rearrangement of a relatively small number of gene segments, variable (V_H), diversity (D) and joining (J_H) segments for the

V_H domain, and variable (V_L) and joining (J_L) segments for the V_L domain^{95,98}. Together with deletion and insertion of nucleotides at the segment junction and association of different heavy chains and light chains, this generates a diverse primary repertoire of antibodies with huge number of antigen binding specificities⁹⁹.

1.4.1.2 Antibody Structure

All antibodies have a common structure (Figure 9) consisting of two identical heavy (H) chain polypeptides (about 55–70 kDa / 440 amino acids) and two identical light (L) chain polypeptides (about 24 kDa / 220 amino acids) held together by disulphide bridges and non-covalent bonds.

The four chains contain defined variable (V), diversity (D) (heavy chain only), joining (J), and constant (C) domains. The constant domain amino acid sequences, which determine effector functions of antibodies, are relatively conserved among immunoglobulins of a given animal species, while the variable domains of an antibody are highly heterogeneous; they endow the antibody's binding specificity and affinity¹⁰⁰.

Pairing of the heavy and light chain V domains creates an antigen-binding site (paratope), which recognizes a single antigenic determinant (epitope). The V domains can be further subdivided into different regions, the framework regions (FR) and the complementarity determining regions (CDRs). CDRs are divided into CDR1, CDR2, and CDR3. The framework regions form a scaffold structure, referred to as a β -pleated sheet, from which the CDRs loop out. The amino acid sequences of the CDRs have been shown to be 'hypervariable' and are largely responsible for interacting with the targeted antigen¹⁰⁰. To engineer a small recombinant antibody with the unique specificity and affinity of the parent antibody it is important not to disrupt the tertiary structure and orientation of the CDRs residues.

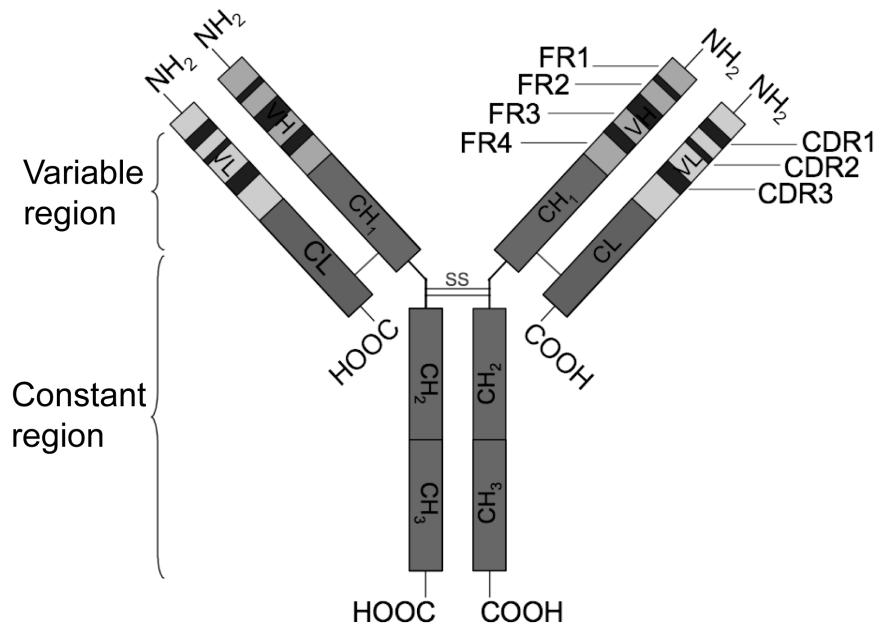


Figure 9. Antibody structure (IgG)

IgG, the main serum antibody is a Y-shaped multidomain protein with two antigen-binding sites located at the variable region. The stem Fc domain of the constant region mediates recruitment and cytotoxic effector functions through complement interaction and binding to γ Fc-receptors.

1.4.2 Antibodies as Therapeutics

Antibodies were discovered more than 100 years ago. In the 1890s horse anti-serum was used to treat tetanus and diphtheria, and is still used today to treat snakebites. However, the human immune system recognizes horse anti-serum as foreign and reacts by producing antibodies against it, especially on repeat doses, which leads to serum sickness and, in the worst case, anaphylactic shock ¹⁰¹.

An important first step towards the development of antibodies as useful therapeutics came from the invention of monoclonal antibodies by Köhler and Milstein in 1975 ¹⁰³. By immunizing rodents, and fusing the antibody-producing B-cells from the spleen with a myeloma, Köhler and Milstein made hybrid cells (hybridomas) that were immortal and secreted murine monoclonal antibodies (mAbs). These cells could be grown in fermenters for large-scale antibody production. The technology also allowed an antibody response directed against a complex mixture of antigens (such as on the surface of a cancer cell) to be dissected into its components. Hence, it became possible to

distinguish between normal and cancer cells on the basis of reactivity with individual mAbs, and thereby many new molecular targets and markers of disease were discovered.

Murine antibodies still have two major drawbacks. One is that murine antibodies are glycosylated differently than human antibodies, which often leaves them with a poor ability to trigger human effector functions. Secondly and most important, their suitability as therapeutics is limited because the human immunosystem recognizes them as foreign proteins and mounts an immune response against them by producing human anti-mouse antibodies (HAMA)¹⁰⁴. These not only cause the therapeutic antibodies to be quickly eliminated from the body, but also form immune-complexes that cause damage to the kidneys. Therefore, murine monoclonal antibodies can usually only be administered once.

These difficulties prompted the use of genetic engineering to convert murine mAbs into human-like mAbs. Recombinant DNA technologies, include chimerization, (meaning the transplantation of variable domains from a murine antibody in place of the corresponding domains of a human antibody, these antibodies, two-thirds human, have the binding activity of the parental murine antibody and the effector functions of human antibodies^{105, 106, 107}), and humanization (the transplantation of just the antigen contact surfaces, the complementarity determining regions or CDRs, from the murine mAb leads to antibody molecules that are about 95% human¹⁰⁸). Both techniques have lead to enhanced clinical efficiency of murine mAbs and their regulatory approvals as treatment of cancer and inflammatory disease.

In theory it is possible to produce human monoclonal antibodies, for example by immortalization of human B-lymphocytes with the Epstein-Barr virus (EBV)¹⁰⁹, or with the generation of transgenic mice having a human antibody repertoire¹¹⁰, but to date there exist no effective methods of production to meet the needs for therapeutic antibodies in the long run. Also the generation of stable human hybridoma cell-lines, which is difficult due to the lack of a matching myeloma-cell fusion partner, did not lead to the desired breakthrough¹¹¹⁻¹¹³.

1.4.3 Antibody Fragments

Antibody fragments were first produced in the late 1950's when Porter isolated Fab (fragment antigen binding) and Fc (fragment crystallizable) fragments from proteolytically (with papain or pepsin) cleaved rabbit gamma globulins (IgG) ¹¹⁴. Recent advances in understanding of immunoglobulin structure through three-dimensional studies, using NMR and X-ray crystallography and increased computer-assisted molecular modeling capabilities in combination with novel selection methods have led to the evolution of a new class of antibody-like molecules, the recombinant antibody fragments.

Recombinant antibodies are an indispensable part of the development of new proteogenic therapeutics. New methods of *in vitro* selection ¹¹⁵ and generation of specific binders outside a living organism allowed the production of clinically effective antibodies. The most important of these methods is Phage-display ¹¹⁶. Fusion of the recombinant antibodies with other proteins or protein-domains generates recombinant antibodies with new properties that nature is not able to provide. Moreover, production in microorganisms allows easier scale-up and reduces costs of production.

In some clinical applications small recombinant antibody fragments have an advantage over whole immunoglobulins, such as good penetration of solid tumors and rapid clearance ^{117,118}.

The smallest portion of an antibody containing an antigen-binding site is the variable fragment (Fv) assembled from V_H and V_L. Because there is no covalent link between the variable heavy and light chain ($K_D = \text{ca. } 10^{-6} \text{ M to } 10^{-9} \text{ M}$) ¹¹⁹ it is necessary to provide a linker between the two domains to prevent their dissociation. To stabilize the association of recombinant Fv fragments, they are joined with a short peptide linker and expressed as a single peptide, the scFv. A variety of linker peptides were tested and did not disturb the proper folding of the V_H and V_L domains ¹²⁰. The most frequently used linker today for scFv antibodies is (Gly₄Ser)₃, a flexible 15 aa-peptide that bridges the 4.5 nm gap between the C terminus of one domain and the N terminus of the other.

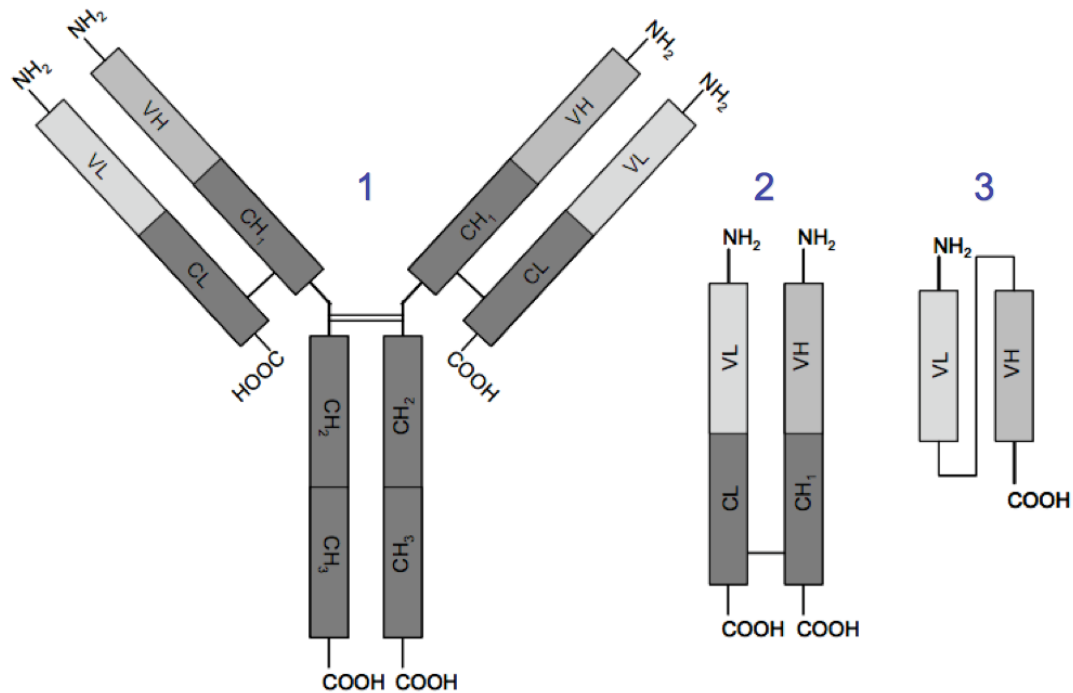


Figure 10. Antibody fragments
 (1) Full IgG, (2) Fab (antigen binding fragment), (3) scFv (single chain variable fragment)

1.4.4 Recombinant Antibodies

Recombinant antibody is the general term for either heterologously produced Fab or scFv fragments of an antibody. Elucidation of the molecular structure of immunoglobulins and sequence data allowed to develop immunoglobulin-specific oligonucleotide primers and to use them in conjunction with polymerase chain reaction (PCR) techniques to clone antibody fragments for the generation of recombinant antibodies. Recombinant antibodies have a variety of uses, ranging from simple research tools as diagnostic reagents to highly refined biopharmaceutical drugs. Their exquisite selectivity and the increasing ease of manipulation have facilitated their use as delivery vehicles for drugs and genes. Recently, recombinant antibodies have been dissected into minimal binding fragments (single domain antibodies) and rebuilt into multivalent high-avidity reagents (di- to tetra-bodies) and fused with a broad range of molecules including enzymes for prodrug therapy, toxins and radionuclides for cancer treatment, liposomes for enhanced drug delivery, viruses for gene therapy and cationic tails for DNA and siRNA delivery^{121, 122}.

1.4.4.1 Expression of Recombinant Antibodies in *E.coli*

Production of stable, high affinity antibody fragments in high yield for preclinical and clinical trials can be a serious bottleneck in the product pipeline. Recombinant antibody fragments have been produced in various expression systems such as bacteria¹²³, mammalian¹²⁴, insect¹²⁵, yeast¹²⁶, plant¹²⁷, and *in vitro*-translation systems¹²⁸. The yields and biological activity of recombinant proteins differ greatly and depend on a large number of factors, such as solubility, stability, and size of the protein.

Bacteria are the favored system for expression of small non-glycosylated Fab and scFv fragments. Advantages are the systems ability to produce protein in large quantities, being faster and cheaper than other expression methods. Most production studies favor scFv over Fab fragments due to their superior expression levels in bacteria (to over 1g/l using fermentors). Nevertheless several strategies have been developed to improve recombinant expression. Terminal polypeptides as C-myc, His and the FLAG tag have been appended for affinity purification after expression. Whether these have to be removed due to immunogenicity and related concerns from drug regulatory agencies is still under investigation.

The expression of recombinant antibody fragments in the reducing environment of the cytoplasm leads to the formation and accumulation of insoluble inclusion bodies, which contain unfolded protein. This necessitates the development of refolding protocols, as one of the major problems that need to be overcome during the refolding process is the formation of aggregates. Another approach is to use leader sequences such as pelB¹²³ to direct secretion of the antibody to the periplasmic space of the bacteria. The periplasmic space lies between the inner and outer membrane of gram-negative bacteria and is an oxidizing environment. The leader sequence is cleaved by signal peptidases inside the periplasm¹²⁹. Depending on the antibody sequence sometimes leaking from the periplasm occurs. This can help to simplify screening and purification of the scFvs from the bacterial supernatant.

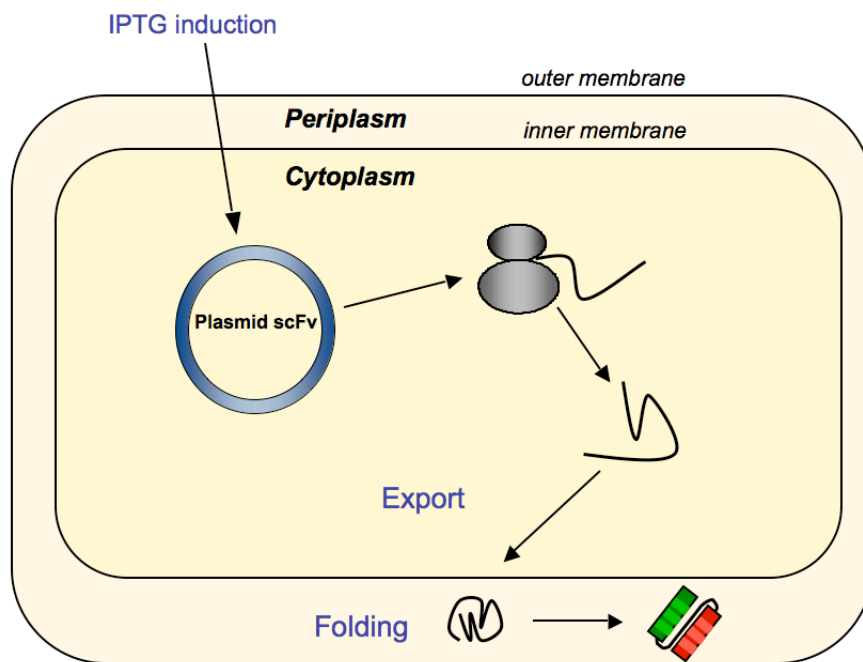


Figure 11. Production of soluble, folded scFv in *E. coli*

1.4.5 Generation of Murine scFv from Hybridoma

Although today human antibodies can be obtained by phage display from native repertoires^{130, 131} or libraries of fully synthetic genes¹³², still many mouse antibodies with interesting properties are generated by the hybridoma method of Köhler and Milstein¹⁰³. Cloning of antibody fragments from hybridoma retains the unique properties of the antibodies, which can be exploited for the rescue of interesting antibodies from unstable hybridoma clones.

Cloning and sequencing of antibody variable domains is the basis of antibody modeling¹³³ antibody engineering¹³⁴, experimental structure determination by NMR or x-ray crystallography at high resolution¹³⁵. Moreover, once cloned from the parental hybridoma clone, the antibody domains can be further engineered in a multitude of ways to produce variants with lower immunogenicity, higher affinity^{136, 137}, enhanced stability^{138, 139}. They can also be genetically fused to effector proteins and toxins¹²⁹.

In the mouse, there are five classes of constant heavy (C_H) chain genes (α , δ , ϵ , γ and μ) and two classes of constant light (C_L) chain genes (κ and λ). DNA

and amino acid sequences are relatively conserved within each class. Antibodies are grouped into five major classes according to their C_H-region: IgA, IgD, IgE, IgG and IgM and further distinguished by the class of their light chains (κ or λ). The class of each chain can be isotyped with commercially available kits, which are animal-species-specific.

The V region consists of alternating framework (FR) and hypervariable, or complementarity-determining regions (CDRs). The greatest sequence diversity occurs in the CDRs, while the FR region sequences are more conserved. The J region (heavy and light chains) and the D region (heavy chain only) lie immediately upstream from the C region. The CDRs, and to some extent the FR regions, interact with the antigen to form the core of an antigen-binding site. Because the DNA sequences within the first FR and the carboxy-terminal portion of the J region are relatively conserved for all classes of antibodies in a given animal, amplification schemes for antibody V genes can be devised using a collection of primers that hybridize to these conserved sequences¹⁴⁰.

The general strategy used in this work to adapt murine monoclonal antibodies to the scFv format is depicted in Figure 12.

There are two orientations possible to link the V_L and V_H in the scFv, either V_L-linker-V_H or V_H-linker-V_L. The length of the chosen polypeptide linker depends on the orientation of the fragments. The distance between the C terminus of V_L and the N terminus of V_H is about 39 - 42 Å, whereas the distance in the other direction between the C terminus of V_H and the N terminus of V_L is slightly shorter (32 - 34 Å).

As already mentioned, the most commonly used peptide linker consists of 15 aa, (Gly₄Ser)₃, independent from the orientation of the two variable domain genes in the resulting scFv. The linker used in this work is 20 aa long (Gly₄Ser)₄ and accommodates the longer distance between the V gene fragments in the V_H-linker-V_L orientation. The use of the longer linker minimizes fragment dimerization and therefore formation of diabodies that often occurs when shorter linkers are used¹⁴⁰.

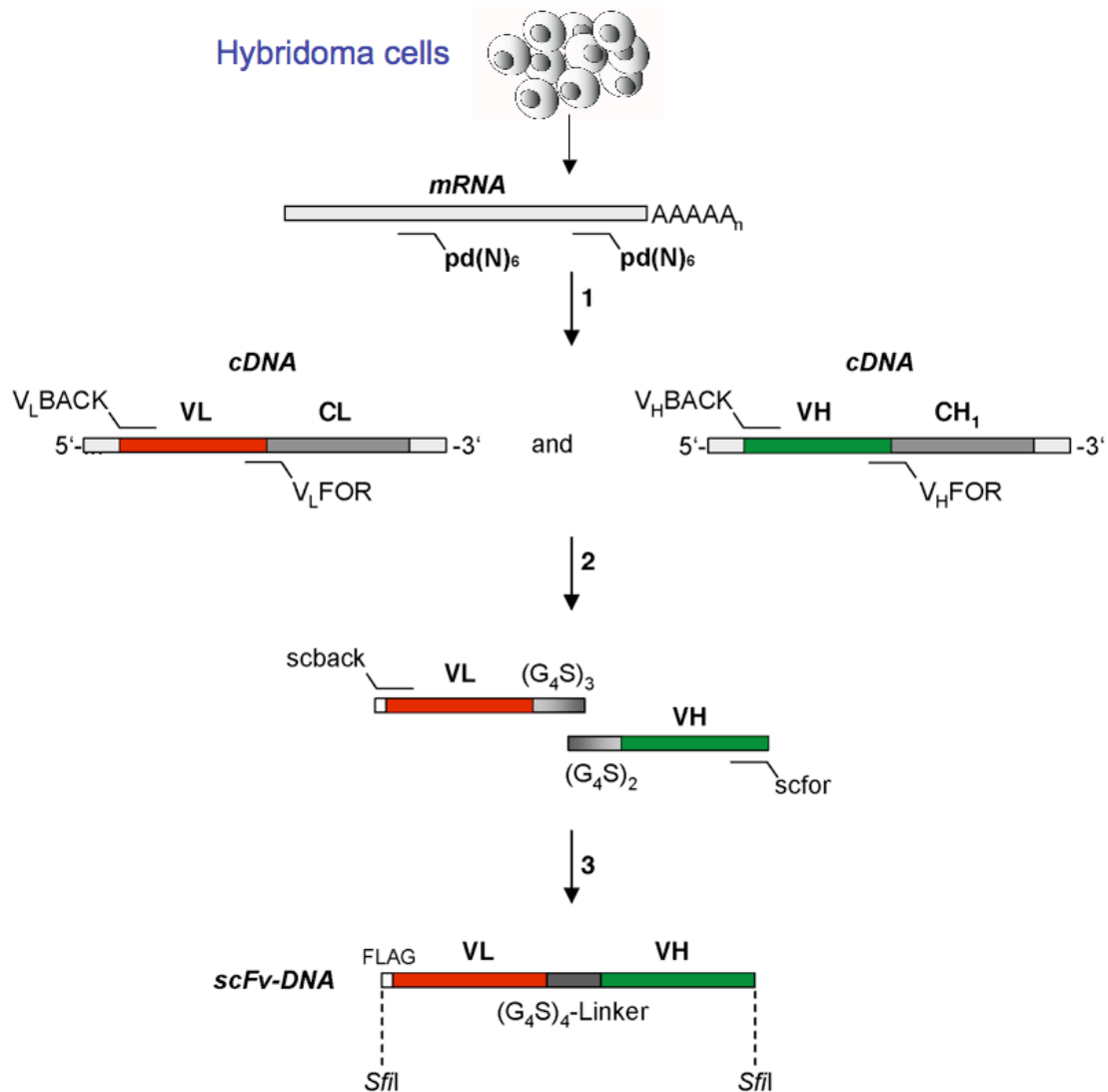


Figure 12. The general strategy used for the adaptation of murine IgG to the scFv format (1) The mRNA from hybridoma cells and a random hexamer primer mixture $pd(N)_6$ is used for the PCR amplification of V_L and V_H domains, (2) which are assembled into the scFv format by the outer primer pair scback and scfor. (3) For directional cloning of the scFv gene fragment into the expression vector, a single restriction enzyme is used (*SfiI*). Self-ligation of the insert or the plasmid is prevented by the asymmetry of the overhang.

1.4.6 Antibody Phage Display

Phage display can be used to generate antibodies to virtually any antigen. This requires a number of crucial steps that are common to all molecular diversity technologies: the creation of diversity, coupling of phenotype (antibody protein) to genotype (antibody gene), selection, amplification, and analysis of the binding properties.

Since the generation of the first human antibodies by phage display^{129, 141, 142}, technology has evolved to allow the creation of large, fully human scFv

repertoires that yield antibody fragments with comparable affinities to those obtained using classical hybridoma technology¹⁴². Using a variety of selection and screening strategies, the same library can be used to derive many high-affinity antibody fragments with different specificities. Antibody fragments isolated from such fully human scFv repertoires have a multitude of applications, e.g. as immunological reagents for ELISA, immunocytochemistry, western blotting, or epitope mapping, and as they show low immunogenicity in humans they are especially interesting for therapeutic application.

Furthermore, phage-display technology also provides a means by which a selected recombinant antibody can, if necessary, be affinity-matured for improved affinity and binding kinetics¹³⁷.

Recombinant antibody libraries have been constructed from a wide range of B-lymphocyte sources using a number of different approaches. Sizes of the libraries that have been produced vary considerably, from small libraries of 10^6 different clones up to large libraries ($>10^{10}$ clones). Often an antibody with the desired specificity exists at low frequencies in the recombinant antibody repertoire. It is therefore necessary to have an effective technique for the enrichment and identification of a desired antibody from a heterogeneous repertoire. The process for the selection of specific antibodies is referred to as 'panning', and in principle involves the selection of antibodies on the basis of their affinity. The phage libraries can be selected using antigen immobilized to immunotubes, biotinylated antigen immobilized to streptavidin-beads (if available amounts of antigen are low), or by affinity chromatography on antigen-coupled Sepharose columns.

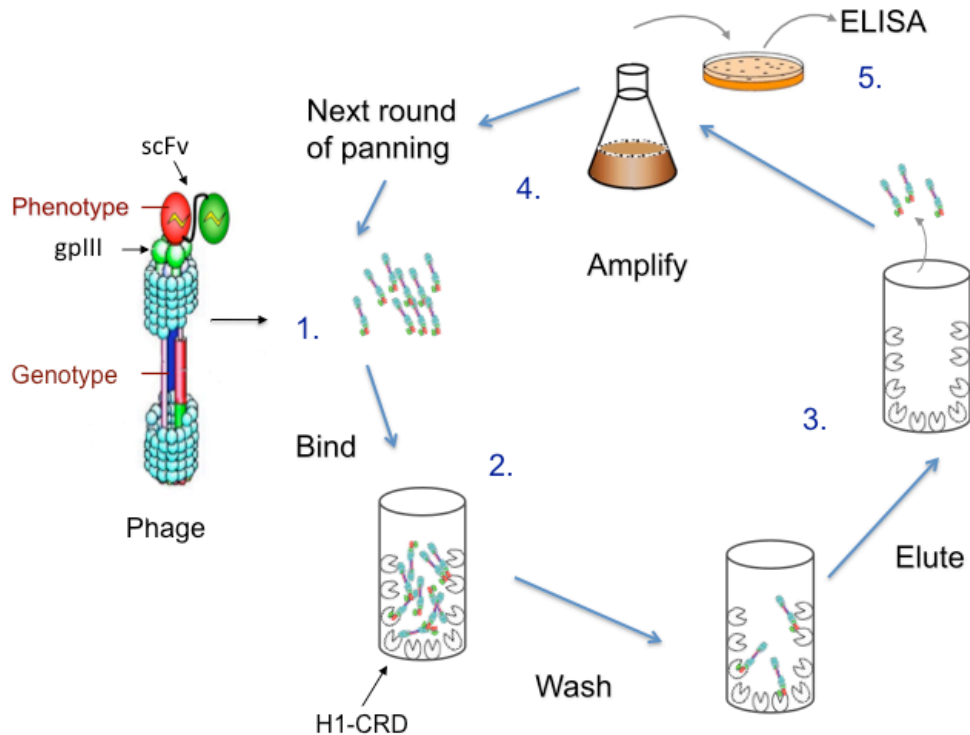


Figure 13. Antibody phage display cycle

Libraries of antibodies are displayed on the surfaces of bacteriophage as fusions to the coat protein (usually gpIII). (1.) Each phage particle displays a unique antibody (Phenotype) and also encapsulates the vector that contains the encoding DNA (Genotype). (2.) Highly diverse libraries can be constructed and represented as phage pools, which can then be used in selections for binding to immobilized antigen (panning). (3.) The immobilized antigen retains antigen-binding phage, whereas the nonbinding ones are removed by washing. (4.) The retained phage pool can be amplified by infection of an *E. coli* host and submitted for further rounds of panning, and after several cycles (6.) be used in a an ELISA for selection of productive clones.

The isolation of a desired antibody fragment generally involves repeated rounds of panning, with each successive round resulting in the enrichment of the desired antibody. Each round of antibody selection can be divided into panning, removal of nonspecific phage, and the elution and amplification of phage for the next round (Figure 13). In this way, antigen-specific antibody that occur at low frequencies in a library can be enriched by over a million-fold

129

1.4.6.1 Types of Phage Display Libraries

The libraries available can be divided into natural immune antibody libraries, containing fragments from immunized donors (biased towards certain

antigens), non-immune or naïve libraries (derived from non-immunized natural donors or semi-synthetic sources), and synthetic libraries. With the latter having the advantage to be a source of antibodies against a large number of antigens, including self, non-immunogenic and toxic antigens.

Synthetic libraries are constructed entirely *in vitro* using oligonucleotides that introduce areas of complete or tailored degeneracy into the CDRs of one or more V genes. The first reports of synthetic antibody libraries were made in 1992^{143,144}. Later on, libraries with improved quality and/or downstream characteristics were developed by choosing CDRs for randomization based on the relatively high mutation frequency of these positions in natural antibody repertoires and then randomizing them in a set of frequently used V germline segments^{145, 146}.

1.4.6.2 The ETH-2-Gold Library

The ETH-2-Gold library employed in this work is a synthetic 'single-pot' library that was developed in the labs of Prof. D. Neri at the ETH in Zurich¹⁴⁵.

The library was constructed based on the knowledge that human antibodies are assembled from approximately 50 different V_H and 70 V_L germline genes of which only a few dominate the functional repertoire. Three of this dominating antibody germline gene segments (DP-47 for the heavy chain, and DPK-22 for the light chain V_κ and DPL-16 for V_λ) were chosen as scaffold, which represent 12%, 25%, and 16%, respectively, of the antibody repertoire in humans¹⁴⁷. To produce a large repertoire, random loops of 4, 5 or 6 amino acids were appended at position 95¹⁴⁸ to the CDR3 of V_H , the largest and most diverse loop of the antigen recognition site. Similarly, diversity was introduced in six amino acid positions in the CDR3 of V_L assembled with DPL-16 or DPK-22 germline genes (Figure 14).

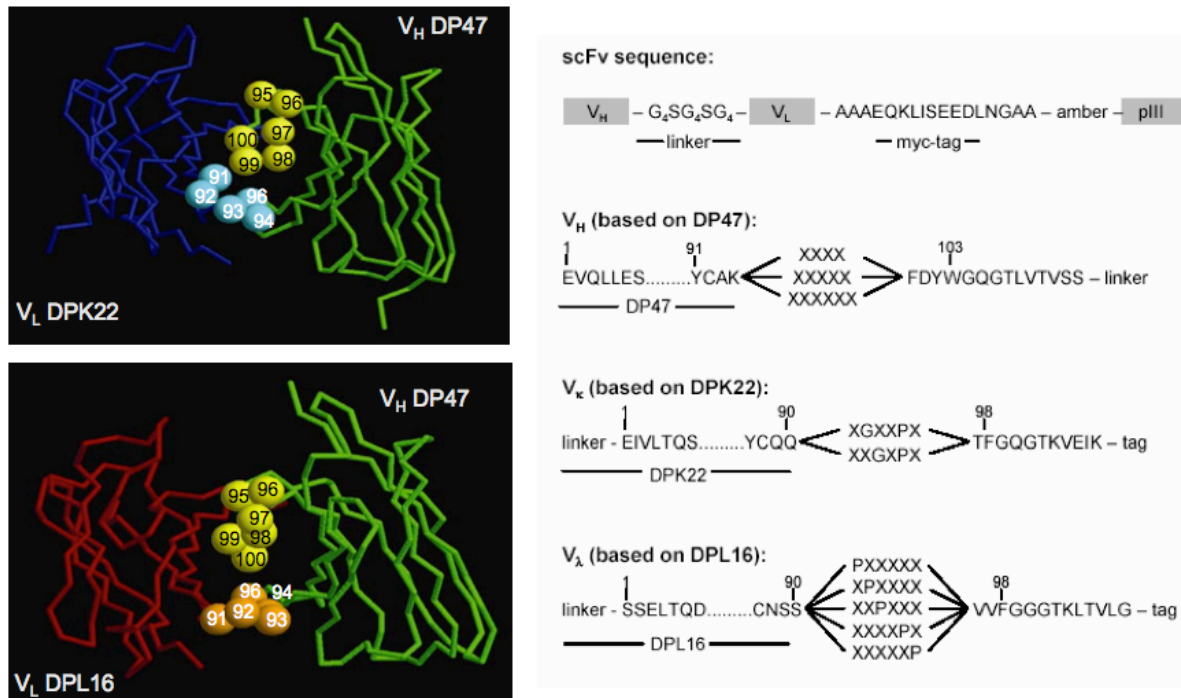


Figure 14. ETH-2 Gold library: Positions of introduced diversity
Picture from Silacci et al.¹⁴⁵

The use of only the DP47 V_H germline segment for library construction has the advantage of a high thermodynamic stability¹⁴⁹ and the possibility to purify the resulting scFv fragments by Protein A affinity chromatography.

The scFvs from this library contain a 14 aa long (Gly₄SerGly₄Ser Gly₄) peptide linker and are encoded in the pHEN1 phagemid vector¹⁵⁰ which also codes for a C-myc tag for the detection of expressed fragments e.g. in ELISA or western blots. This library, which has already been successfully used to generate scFv antibodies against more than 80 antigens¹⁵¹, was employed to select human scFvs against the H1-CRD.

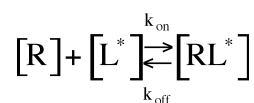
1.5 Receptor-ligand Interaction Measurement Technologies

Receptor–ligand interactions play a crucial role in biological systems and their measurement forms an important part of modern pharmaceutical development.

While receptor-ligand assays based on radioactive labeled ligand binding are usually fast, easy to use and reproducible, their major disadvantage is that they are hazardous to human health, produce radioactive waste, require

special laboratory conditions and are thus rather expensive on a large scale. This has led to the development of non-radioactive assays based on colorimetric or fluorescence detection, or label-free optical methods such as surface plasmon resonance.

Receptor binding assays have their origin in the competition between an analyte [A] and a labeled ligand [L*] for binding to a certain receptor [R]. The relationship between the labeled ligand, the receptor and its complex is given by Eq. (1) and follows the law of mass action assuming reversible binding.



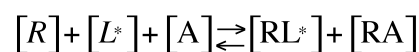
Equation 1

The ratio $k_{\text{off}}/k_{\text{on}}$ refers to the dissociation constant K_D , which is inversely proportional to the ligand affinity towards the receptor. At equilibrium, the K_D can be determined as shown in Eq. 2, and represents the amount of ligand that saturates 50% of the binding sites.

$$K_D = \frac{k_{\text{off}}}{k_{\text{on}}} = \frac{[R] \times [L^*]}{[RL^*]}$$

Equation 2

Introducing a competing analyte leads to the formation of two receptor complexes (see Eq. 3). The analyte will displace a certain amount of labeled ligand, which depends on both the concentration and the affinity of the analyte.



Equation 3

If the analyte concentration is varied and both the receptor concentration and labeled ligand concentration are kept constant, inhibition curves can be constructed. From these curves, the IC_{50} -value, which represents the analyte concentration that displaces 50% of the bound labeled ligand, can be determined.

1.5.1 Solid-phase Binding Assays

Receptor–ligand binding assays are often used in the screening of new chemical entities. Despite the fact that receptor–ligand binding assays do not predict the intrinsic activity (agonistic or antagonistic, blocking) of the tested compounds, the discovery of new endogenous ligands is also facilitated¹⁵². Most of the assay technologies described to date require labeling of either the ligand or the receptor. For example radio-isotopic labels such as ³H, ¹²⁵I and ³²P can be used to label ligands without having an effect on the affinity of the ligand towards the receptor. Albeit their sensitivity, the use of competitive radioassays has several drawbacks, disposal of radioactive waste, relatively long measuring times, costs, health hazards, the requirement for special licences, etc. Therefore the development of new assay technologies based on either colorimetric, fluorescence or (chemo-/bio-) luminescence detection has been intensively supported by the pharmaceutical industry.

A crucial factor for evaluating binding affinities of new compounds is the availability of a suitable assay system. In regard to the ASGP-R, there is no competitive *in vitro* binding assay for ASGP-R ligands described to date, which does not make use of radioactive-labeled competitors (i.e. ¹²⁵I-Gal-BSA)^{31, 153-156}. The design of assays for lectins is especially hindered by their tendency to bind only weakly to monovalent carbohydrate ligands (with K_D 's in the millimolar range). To overcome this problem, a multivalent competitive ligand combined with a colorimetric detection system was used to develop a competitive solid-phase assay for the H1-CRD (See chapter 2.2).

1.5.2 Fluorescence Microscopy and Flow Cytometry

Fluorophores can be introduced to examine ASGP-R localization and internalization in cells.

Fluorescence is the result of a three-stage process that occurs in certain molecules (generally polyaromatic hydrocarbons or heterocycles) called fluorophores or fluorescent dyes. The single electronic-state diagram (Figure 15) illustrates the process responsible for the fluorescence of fluorophores.

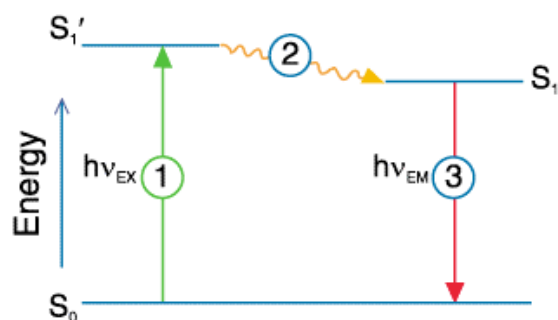


Figure 15. Jablonski diagram

1. Excitation: A photon of energy $h\nu_{EX}$ is supplied by an external source such as an incandescent lamp or a laser and absorbed by the fluorophore, creating an excited electronic singlet state (S_1'). **2. Excited-State Lifetime:** The excited state exists for a finite time (typically 1–10 nanoseconds). During this time, the fluorophore undergoes conformational changes. **3. Fluorescence Emission:** A photon of energy $h\nu_{EM}$ is emitted, returning the fluorophore to its ground state S_0 . Due to energy dissipation during the excited-state lifetime, the energy of this photon is lower, and therefore of longer wavelength than the excitation photon $h\nu_{EX}$.¹⁵⁷

The entire fluorescence process is cyclical. Unless the fluorophore is irreversibly destroyed in the excited state (known as photo bleaching) the same fluorophore can be repeatedly excited and detected. The fact that a single fluorophore can generate many thousands of detectable photons is fundamental to the high sensitivity of fluorescence detection techniques. Fluorophores can often provide well-defined images at such low concentrations that living cells are unaffected by their presence.

Fluorescence Microscopy

Fluorescence microscopy allows visualization of only the fluorescent probe. Light from an excitation lamp such as a mercury lamp or laser is used to illuminate the fluorescent-labeled sample. An excitation filter eliminates all but the desired wavelengths of light for exciting the fluorophore, those are then reflected by a dichroic mirror onto the sample, where they excite the fluorescent molecules.

Flow Cytometry

A flow cytometer works basically as an automated fluorescent microscope, analyzing single cells of a population for their size, granularity, and fluorescent content. The principle of hydrodynamic focusing arranges the cells in a cuvette like pearls on a string before they arrive at the laser interception point for analysis. Hydrodynamic focusing cannot separate cell aggregates,

therefore flow cytometry is a technique that requires single cell suspensions. Cells in suspension flow in single-file through an illuminated volume where they scatter light and emit fluorescence that is collected, filtered and converted to digital values.

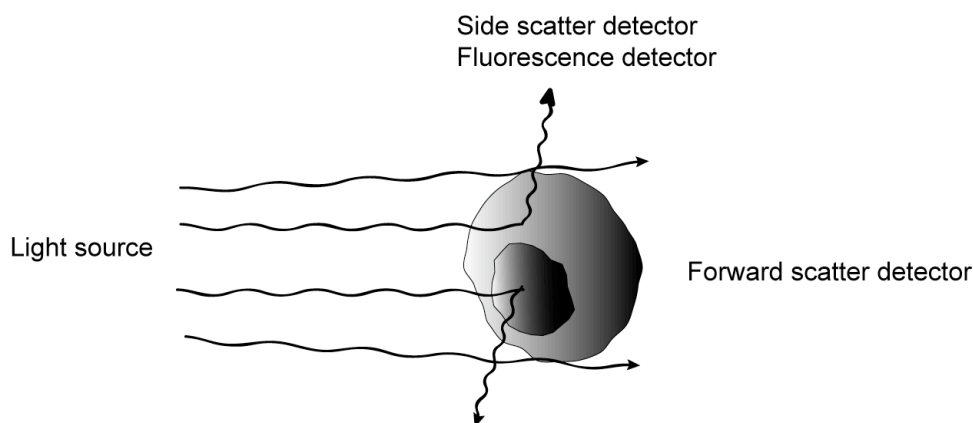


Figure 16. Basic principles of flow cytometry measurements

When the laser beam strikes the stream, the majority of the photons pass through undisturbed. When the photons get in contact with the cell membrane, light diffraction occurs (Figure 16). The diverging photons detected by the forward scatter (FSC) detector give information about cell size (the bigger the cell, the more light is scattered). On the other hand, if the photons strike cell organelles, wide-angle light scattering occurs. The so-called side scatter (SSC) of light is proportional to the cell complexity. This allows sorting cells by their morphology. The application of specific antibodies or receptor-ligands coupled with a fluorescent label enables the measurement of the staining intensity of cells via fluorescence.

In this work flow cytometry was applied to characterize the binding of mouse anti-human H1-CRD antibodies to the surface of different hepatocytes and to evaluate the extent of internalization of fluorescent triantennary galactosyl-compounds. For this purpose the fluorescence intensity of staining between untreated and treated cells, expressed as the shift in median fluorescence intensity (MFI), was compared, as illustrated in Figure 17.

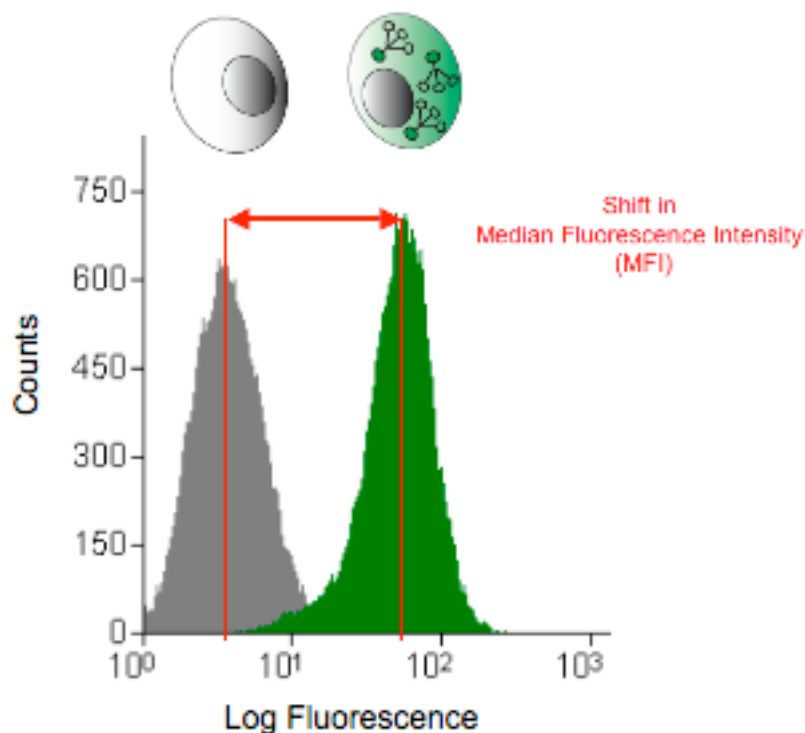


Figure 17. Quantitative flow cytometry measurement principle

Example evaluation of the shift in median fluorescence intensity (MFI) between a population of untreated cells (depicted in grey) and cells with an internalized fluorochrome-labeled triantennary galactosyl compound (in green)¹⁵⁸.

1.5.3 Surface Plasmon Resonance (SPR)

Surface plasmon resonance (SPR) is a label free technique that allows the direct analysis of interactions between analytes in solution and a ligand attached to a sensor chip surface, providing a continuous readout of complex formation and dissociation¹⁵⁹. In principle, the signal is directly proportional to the increase in molecular mass on the sensor surface. SPR technology can thus be generally applied to affinity and kinetic analysis of protein-protein, protein-peptide, protein-DNA, and protein-small molecule interactions. The information gathered from a few binding curves is sufficient for the determination of the association- and dissociation-rate constants, k_a and k_d . The K_D (equilibrium dissociation constant) describing the affinity of binding is derived from the ratio between k_{off} and k_{on} . Affinity constants can be determined from the millimolar to picomolar range; association-rate constants from 10^3 to 10^8 $M^{-1}s^{-1}$; and dissociation-range constants, from 10^{-5} to 1 s^{-1}

160

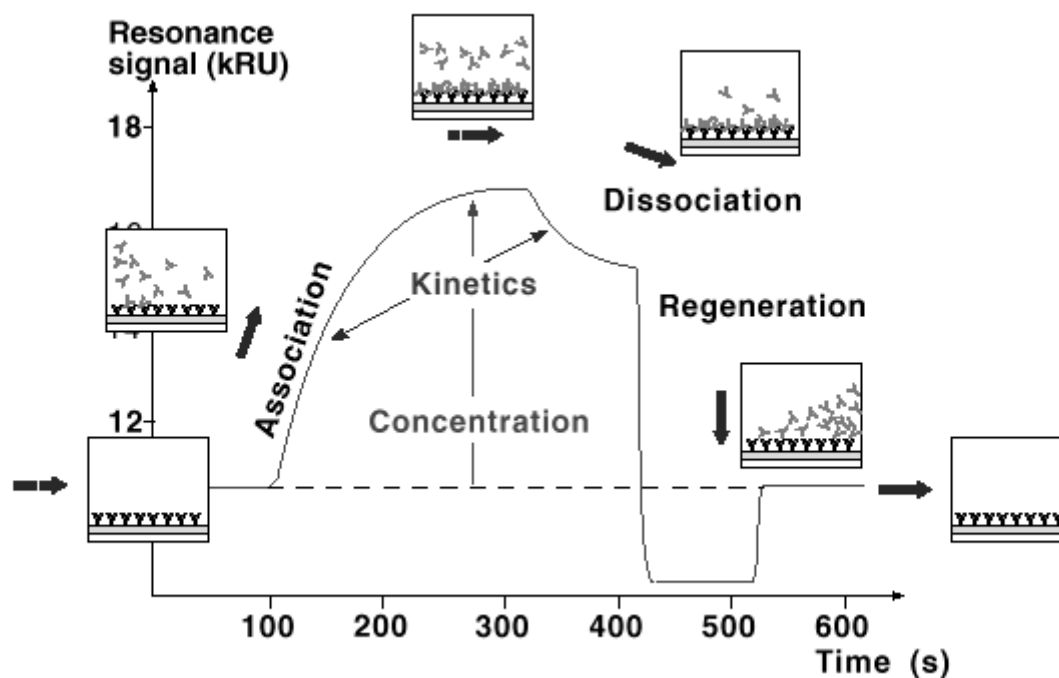


Figure 18. The basic outline of a SPR measurement
 Picture from Cooper ¹⁶¹.

Figure 18 shows a typical binding cycle observed in an SPR measurement. A binding protein (e.g. a receptor or antibody) is immobilized on the sensor surface with appropriate chemistry. A solution of an analyte is passed over the protein. As the analyte binds to the surface, the refractive index in the medium adjacent to the sensor surface increases, leading to an increase in the resonance signal. At equilibrium, by definition, the amount of analyte associating or dissociating from the receptor is equal. The response level at equilibrium is related to the concentration of active analyte in the sample. During the Dissociation phase, the analyte solution is replaced by running buffer and the analyte-receptor complex is allowed to dissociate. The half-lives of some biological complexes can be considerably long, thus a pulse of a suitable regeneration solution (e.g. high salt, EDTA, or low pH) is used to disrupt binding and regenerate the free receptor. The entire binding cycle is normally repeated several times with varying concentrations of analyte to generate a robust data set for global fitting to an appropriate binding algorithm. The affinity of the interaction can either be calculated from the ratio of the rate constants ($K_D = k_{off} / k_{on}$) or by linear or nonlinear fitting of the response at equilibrium versus varying concentrations of analyte.

In the Biacore system, samples are delivered to the sensor surface using a micro-fluidic system. This ensures reproducible sample delivery and low sample consumption. The sensor surface is a glass slide coated with a thin 50 nm gold film mounted in a plastic carrier. The gold surface is derivatized to allow covalent attachment of molecules using well-defined chemistry ¹⁶². Changes in the refractive index at the sensor surface are measured. The sensor surface is divided into several sensing areas or flow cells, and a signal can be obtained from each cell. In the same injection, a sample can therefore pass over both active and reference cell.

SPR technology has many practical advantages: detection is instantaneous, allowing continuous real-time monitoring of molecular binding, no labels are required on any of the molecules involved, and the light used in detection is reflected from the back of the sensor surface and does not penetrate the sample. During sample injection, any change in the refractive index is detected. A change can either be caused by a binding event or by a difference in refractive index between sample solution and running buffer. The signal related to the ligand binding alone is obtained by subtracting the signal obtained on the reference cell from that obtained on the ligand cell. When the injection is terminated, running buffer flows again over the surface, and dissociation of the analyte-ligand complex can be observed. The output from the SPR detector is called a sensorgram, and is a plot of the SPR response versus time. The SPR response is expressed in resonance units (RU), where one RU corresponds to 10^{-6} refractive index units.

Amine Coupling

Amine coupling is routinely applied for immobilization of proteins. Nearly all proteins and peptides possess multiple primary amine groups, which are often surface-exposed due to their hydrophilicity. In the case of proteins, lysines are often randomly distributed over the surface and amine coupling will result in a random and non-predictable immobilization of the protein. This sometimes leads to a massive decrease of surface activity, e.g. more than 80% loss is reported for some antibodies, and this might also influence binding affinity and kinetics ¹⁶³. Analysis of the amino acid sequence, crystal structure and especially the binding site are recommended to avoid interference ⁷⁵. Another

drawback is the usage of acidic conditions for surface attraction. Acid labile proteins will result in inactive surfaces. Additionally, several popular buffer systems like Tris, bearing primary amines, are not suitable.

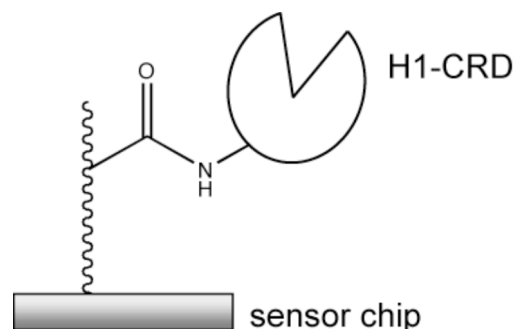


Figure 19. H1-CRD immobilized on CM5 sensor chip via amine coupling

Even though there are several drawbacks, amine coupling is still the most frequently used immobilization technique. A direct reaction of amine groups with active esters generated by N-hydroxysuccinimide (NHS)/ 1-ethyl-3-(3-dimethylaminopropyl)carbodiimide (EDC) is the chemical basis. In order to increase efficiency of the reaction, proteins are concentrated in the dextrane matrix. By lowering the pH of the immobilization buffer just below the pI of the protein, surface attraction is optimized. Amine groups become positively charged and get attracted by the negatively charged carboxyl groups of the matrix (Figure 19). A careful evaluation of pH and protein concentration is needed to optimize the attraction (pH scouting) ¹⁶⁴.

In case of the H1-CRD, the immobilization conditions were extensively evaluated and optimized by D.Ricklin ⁷⁵.

2. Materials and Methods

All buffers and solutions were prepared with double distilled water (ddH₂O).

2.1 Expression and Purification of ASGP-R H1-CRD

Material for H1-CRD production

The expression vector pET3b (Novagen) containing the cDNA of the human ASGP-R H1-CRD, designated pET3H1C⁷³ was kindly provided by Prof. M. Spiess (Biocenter, University of Basel, Switzerland). *E.coli* AD494 (DE3) was from Novagen. Bacto-Yeast extract, Bacto-Agar and Bacto-Tryptone were purchased from Becton Dickinson and were used for LB (Luria-Bertani) and TB (Terrific Broth) culture media¹⁶⁵. Sepharose 4B column material, ampicillin, kanamycin, chloramphenicol, carbenicillin and protein standard BSA solution were obtained from Sigma. Dialysis tubes were from Roth.

Expression

AD494(DE3) cells, carrying the construct pET3bH1C, were grown in 500 ml TB medium supplemented with 1% glucose, 50 µg/ml carbenicillin and 15 µg/ml kanamycin at 300 rpm and 37°C. The culture was inoculated with cells grown over night under the same conditions, aiming at an OD₆₀₀ of 0.1 to start growth. Expression was induced at OD₆₀₀ of 0.8 by addition of IPTG to a final concentration of 0.4 mM, and lasted five hours. Cells were harvested by centrifugation at 4°C and 5000 rpm for 10 minutes. The cell pellets were stored either at 4°C over night, or at -20°C in case the purification of H1-CRD from inclusion bodies was carried out later.

Dialysis tubes preparation

Dialysis tubes ZelluTrans 6.0 with a cutoff of 10 kDa were from Roth. The tubes, 20 cm long, were gently stirred in 500 ml 10 mM NaHCO₃ (pH 8.0), 1 mM EDTA, preheated to 80°C, during 30 minutes. The buffer was exchanged with water, decreasing the temperature stepwise to 60°C, 40°C and 25°C every 10 minutes. The tubes were transferred into 1 mM EDTA and stored at 4°C with the addition of 0.01% NaN₃. Before use, tubes were washed out extensively

with water and preincubated for 10 min in dialysis buffer.

2.1.1 Solubilization and Renaturation of H1-CRD

Resuspension buffer: 20 mM Tris, pH 8

Dilution buffer: 20 mM Tris, 0.5 M NaCl, 25 mM CaCl₂, pH 8

Dialysis buffer: 20 mM Tris, 0.5 M NaCl, 25 mM CaCl₂, pH 7.5

A cell pellet originating from 500 ml expression culture was resuspended in 25 ml resuspension buffer with addition of 8 M urea and 0.1% β-mercaptoethanol. Complete cell lysis was achieved by ultrasonication on ice, in intervals of 20 seconds sonication and 10 seconds stop, for a total of 30 minutes. The protein suspension was centrifuged at 4°C and 19000 rpm for 20 minutes to separate soluble proteins from cell debris. The supernatant containing solubilized proteins was collected and stored on ice. The cell debris pellet was resuspended once more in 5 ml resuspension buffer with addition of 8 M urea and 0.1% β-mercaptoethanol, followed by 4 minutes ultrasonication and centrifugation as described above. The two supernatants were combined and resuspension buffer added to reach a final volume of 50 ml with addition of 0.5 M NaCl, 25 mM CaCl₂ and 0.3% β-mercaptoethanol. The protein suspension was incubated 1 hour on ice under light shaking followed by dilution with 25 ml dilution buffer and centrifugation at 4°C and 22'000 rpm for 20 minutes. The supernatant was collected and partitioned into three dialysis tubes holding 25 ml protein suspension each. The dialysis tubes were immersed in 400 ml precooled (4°C) dialysis buffer and allowed to equilibrate for 8-12 hours under light stirring. Five to six buffer changes were made in total, each step lasting 8-12 hours, to ensure complete refolding. The refolded protein solution was collected and centrifuged at 4°C and 22'000 rpm for 1 hour to remove any precipitates prior to purification by affinity chromatography.

2.1.2 Purification by Affinity Chromatography

A 20 ml Galactose-Sepharose column was prepared as described in ¹⁶⁶. The column was stored in 20% methanol at 4°C.

Wash buffer: 20 mM Tris, 0.5 M NaCl, 25 mM CaCl₂, pH 7.8

Elution buffer: 20 mM Tris, 0.5 M NaCl, 2 mM EDTA, pH 7.8

Affinity chromatography was used to purify H1-CRD on an FPLC-system at a flow rate of 1 ml/min. First, 100-200 ml of the refolded and dialyzed protein solution were loaded onto a 20 ml Galactose-Sepharose column, followed by washing with 2.5 CV of wash buffer to remove non-bound proteins. Elution of H1-CRD was carried out with 3 CV of elution buffer. The eluted fractions were stored at 4°C.

2.1.3 Separation of H1-CRD Monomers and Dimers by IEC

All buffers used for HPLC were prepared with gradient-grade water G Chromasolv from Sigma and filtered before use (0.22 µm).

Ion exchange chromatography (IEC) was used to separate monomers and dimers of H1-CRD on a HPLC system (Agilent). A DEAE column (Shodex), a weak positively charged anion exchanger, was employed for the separation.

Buffer A: 25 mM Tris pH 8.0

Buffer B: 25 mM Tris, 250 mM CaCl₂, pH 8.0

The column was preconditioned with running buffer A and B. The buffers were run at 0.5 ml/min in a ratio of 85:15 (The pressure was set to max. 55 bar ⁷⁵.) Separation of monomers and dimers was achieved by slowly increasing the percentage of running buffer B. By changing the gradient, the concentration of CaCl₂ increases which gradually displaced the proteins from the column. Monomers, which are less charged than the dimers, will elute at a lower CaCl₂ concentration. Therefore, an initially low salt content of the samples is crucial as the elution is ion concentration dependent. Since the H1-CRD samples contained a high salt concentration (0.5 M NaCl) as a result of the previous purification step, a buffer change was necessary prior to IEC separation. Desalting was accomplished either by loading 1.5 ml sample onto a HiTrap desalting column (Amersham) followed by elution with 2 ml running buffer A or by ultrafiltration and buffer exchange by centrifugation using Icon concentrators (Pierce) with cutoff 9 kDa and 3 washing steps with buffer A.

The protein samples were injected, typically 1.4 ml at a time, on the DEAE column and separation was carried out according to Table 1.

Table 1. Buffer gradient for the separation of monomers and dimers by HPLC IEC

Time (min)	% Buffer B
2	15
25	40
27	40
29	15
32	Stop

The elution of monomers started after 15 min and that of dimers at around 23 min. Fraction collection was peak based with the lower threshold set to ca. 100 mAu. While the column was kept at 20°C, both samples and collected fractions were cooled (5°C) during the run.

2.1.4 Concentration by HPLC Affinity Chromatography

The Monomers purified by HPLC IEC were further run on a 2 ml GalNAc-Sepharose column (Bio- scale MT2 column) on HPLC, both to reconfirm the binding activity of the protein and to concentrate the samples. The column was preconditioned with running buffer containing 10 mM HEPES (pH 7.4), 10 mM CaCl₂ and kept at a constant flow-rate of 1 ml/min. The samples were loaded onto the column by repeated injections of 1.4 ml, and eluted with a gradient of buffer B (10 mM HEPES pH 7.4, 2 mM EDTA) as described in Table 2.

Table 2. Buffer gradient for the concentration of H1-CRD monomers by HPLC affinity chromatography

Time (min)	% Buffer B
2	0
25	100
27	100
29	15
32	Stop

Monomer and dimer fraction collection was peak-based and the collected fractions were stored at 4°C for further analysis.

2.1.5 Final Buffer Exchange and Concentration

H1-CRD monomer fractions (and dimer fractions) were finally concentrated and the buffer was changed to storage buffer using Icon concentrators centrifugal filter devices with cutoff 9 kDa (Pierce).

Storage buffer: 10 mM HEPES, 150 mM NaCl, 10 mM CaCl₂, pH 7.4

2.1.6 SDS-polyacrylamide Gelelectrophoresis (SDS-PAGE)

SDS-PAGE is used to separate proteins depending on their molecular weight. The anionic detergent SDS denatures secondary and non-disulfide-linked tertiary structures, and applies a negative charge to each protein, non-covalent bonds, while mercaptoethanol reduces disulfide bonds. The molecular mass can be estimated by using a molecular marker.

The gels were casted and run according to the method of Lämmler¹⁶⁷ on a Miniprotean II apparatus (Bio-Rad). Acrylamid 4k solution (30%) was from Applichem. If not otherwise stated, the gels contained 15% Acrylamid. Low molecular weight marker (LMW) was from Sigma, precision marker, SDS, and bromphenol blue were from Bio-Rad. All other chemicals were obtained from Fluka BioChemika.

Stacking buffer: 1.25 M Tris, pH 6.8

Separating buffer: 1.9 M Tris, pH 8.8

Non-reducing SDS-PAGE sample buffer (5x) : 200 mM Tris, 37.5% (v/v) glycerol, 5% SDS, 1 dip bromphenol blue, pH 6.8

Reducing SDS-PAGE sample buffer is Non-reducing sample buffer containing 2 M β -mercaptoethanol

Running buffer (10 x) : 0.25 M Tris, 2 M glycine, 1% SDS, pH 8.3

2.1.6.1 Enhanced Coomassie-blue staining

Coomassie Brilliant Blue G-250 (CBB G-250) was from Bio-Rad, aluminum sulfate from Siegfried, phosphoric acid (85%) from Sigma, and ethanol 98% from Fluka.

Fixation solution: Ethanol 10%, phosphoric acid 2.35% (w/v)

Enhanced Coomassie staining solution: CBB G-250 0.02%, ethanol 10%, phosphoric acid 2.35% (w/v), aluminium sulfate 5%

Coomassie blue was dissolved in ethanol before adding the rest of the ingredients.

The enhanced Coomassie solution¹⁶⁸ was prepared freshly.

The SDS-PAGE-gels were fixed for 30 min, kept in water for 5 min, and then incubated for 1-2 h in enhanced Coomassie solution. The gels were briefly washed with water or kept in water over night before documentation.

2.1.7 Western Blotting (WB)

The blotting ¹⁶⁹ was performed using the Trans-blot SD semi-dry transfer cell (Bio-Rad). The nitrocellulose (NC) membrane and the whatman filter paper were also from Bio-Rad. Mouse anti-human H1-CRD and polyclonal chicken IgY ¹⁶⁶ were produced at our institute, HisDetector Ni-AP kit was from KPL, mouse anti-c-myc antibody was a kind gift of Prof. Michael Halls group. The secondary antibody anti-mouse IgG (Fc specific)-alkaline phosphatase and Ponceau S red solution were obtained from Sigma. The alkaline phosphatase substrate- mixture 5-bromo-4-chloro-3-indolyl phosphate dipotassium (BCIP) / nitrotetrazolium blue chloride (NBT) was from Fluka.

Transfer buffer: 25 mM Tris, 150 mM glycine, 20% (v/v) methanol)

TBS: 10 mM Tris, 150 mM NaCl, pH 7.5

TBST: TBS with 0.05% Tween[®]20

Substrate buffer: 100 mM Tris (pH 8.8), 100 mM NaCl, 5 mM MgCl₂

Substrate solution: 0.4% NBT/BCIP in substrate buffer (always prepared freshly)

For blotting, 10 pieces of whatman paper and one NC membrane were incubated in transfer buffer. First, 5 Whatman papers were placed on the anode followed by the NC-membrane, the SDS-PAGE gel, additional 5 papers and the cathode. Transfer was carried out for 1 h applying 15 V. After the transfer the membrane was stained with Ponceau S solution to visualize the marker and verify the transfer. Afterwards, the membrane was washed with TBS for 10 min. Then the membrane was blocked for 15 min. with blocking buffer (2% BSA in TBS). After 3 washing steps (2x TBST, 1x TBS for 10 min each), the membrane was incubated with the primary antibody (in TBS, 1% BSA, 0.02% sodium azide) for either 1-2 h at RT or over night at 4°C. Additional 3 washing steps as described above were carried out before incubation with the secondary alkaline phosphatase coupled antibody (1:5'000 in TBS, 1% BSA, 0.1% sodium azide)

for 1 h at RT. After additional 3 washing steps the complex was visualized with BCIP/NBT.

If using the HisDetector Ni-AP kit for murine scFv displaying a His-tag, the NC membranes after blotting were treated as described in chapter 2.9.6.

2.1.8 Bradford Estimation of Protein Concentration

The Bradford assay is a common procedure for determining microgram quantities of protein¹⁷⁰. The Coomassie Blue G-250 dye in phosphoric acid and ethanol has an absorbance maximum of 465 nm. When mixed with protein, the absorbance maximum of the dye shifts to 595 nm. The protein stabilizes the anionic form of the dye by hydrophobic and ionic interactions principally with arginine residues, and to a lesser extent histidine, lysine, tyrosine, tryptophan and phenylalanine residues.

Sigma BSA Protein standard 1 mg/ml was from Sigma. Untreated 96-well plates were from Nunc.

Bradford dye solution: 0.01% Coomassie Blue G-250, 10% (v/v) phosphoric acid (85%), 5% (v/v) ethanol, filtered.

BSA standard was diluted from 1mg to 0.8, 0.6, 0.4, 0.2, and 0.1 mg in PBS. The protein to quantify was diluted if necessary. 10 μ l of the samples were pipetted into a 96-well plate and 200 μ l of Bradford dye solution was added, all samples were measured in triplicates. The OD was measured after 15 min at $\lambda=595$ nm on the Spectramax 190 plate reader (Molecular Devices) and analyzed using the program for Bradford assay.

2.2 Competitive Solid Phase Binding Assay

Material

Biotinylated polyacrylamide-type glycoconjugate with 20%mol of β -*N*-acetyl-D-galactosamine and 5%mol of biotin (biotinylated GalNAc-PAA) was obtained from Lectinity. HEPES (4-(2-Hydroxyethyl) piperazine-1-ethanesulfonic acid), oxalic acid, CaCl_2 and Methyl- β -glucopyranoside were from Fluka, Methyl α - and β -galactopyranoside and bovine serum albumin (BSA) was from Sigma. Lactose, *N*-acetyl-D-galactosamine and Galactosamine were obtained from Pfanstiehl Laboratories. D(+)-Galactose was purchased from Senn Chemicals. NaCl was from Merck. Streptavidin-peroxidase (POD) conjugate was from Roche Applied Science. Fetal bovine serum (FBS) was from Invitrogen. The Peroxidase substrate kit ABTS (2, 2'-azino-di-[3- ethylbenzthiazoline-6-sulfonic acid]) was obtained from BioRad and MaxiSorp 96-well microtiter plates were from Nunc. H2-CRD was produced by Dr.S.Rabbani, Methyl-acetylglucosamine was from Dr. Parday.

Precomplexation of biotinylated PAA-polymer with Streptavidin-POD

20 μl biotinylated β -GalNAc-PAA-polymer (1 mg/ml) were mixed with 80 μl of Streptavidin-POD-conjugate (500 U/ml), 20 μl FBS, and 80 μl of HBS+1mM CaCl_2 to give 200 μl complex containing 100 $\mu\text{g/ml}$ biot. β -GalNAc-PAA-polymer and 200 U/ml Streptavidin-POD-conjugate. The complex was formed at 37°C for 2 h on a thermomixer.

Precomplexed PAA-polymer was stable for several weeks when stored at 4°C.

2.2.1 Evaluation of Small Molecules

Compounds that were not soluble in HBS + Ca^{2+} alone, were first dissolved at 200 mM in DMSO before dilution with the buffer. The final DMSO-concentration in the assay did not exceed 5%.

Flat-bottom Nunc MaxiSorb 96 well Immunoplates were coated over night at 4°C with a volume of 100 μl per well of a 3 $\mu\text{g/ml}$ solution of recombinant human H1-CRD in 20 mM HEPES, 150 mM NaCl, 1 mM CaCl_2 , pH 7.4 (Ca^{2+} -containing HEPES-buffered saline, HBS + Ca^{2+}). The coating solution was

discarded and the wells were blocked with 150 μl /well of 1% BSA in HBS+Ca²⁺ for a minimum of 2 h at 4°C. Then the plates were washed 3 times with 150 μl /well of HBS + Ca²⁺ and tapped dry on tissue paper to remove excess liquid. Immediately followed by the addition of 50 μl /well of the compound-dilutions and 50 μl of a preformed complex of biotinylated GalNAc–PAA-polymer with streptavidin-POD, diluted to give a final concentration of 0.5 $\mu\text{g}/\text{ml}$ of PAA-polymer and 1U/ml of streptavidin-peroxidase. The plates were incubated for 2 hours at room temperature in a humid chamber on a laboratory shaker at 100 rpm. After the incubation, the plates were carefully washed twice with HBS + Ca²⁺ followed by the addition of ABTS–substrate (100 μl /well). Color was allowed to develop for 2 min and then the reaction was stopped with 100 μl /well of oxalic acid (2%) in H₂O. Bound GalNAc-PAA-complex was measured by determining the optical density (O.D.) of the occurring blue-green color at $\lambda = 415\text{nm}$ with a Spectramax 190 plate-reader (Molecular Devices).

2.3 General Methods for Mammalian Cells

Material for mammalian cell-culture

All cell culture media, supplements, and phosphate-buffered saline (PBS) were purchased from Invitrogen, except Trypsin/EDTA (1x) in HBSS was from Sigma, and Collagen type S from rat's tail was from Roche Applied Science. HepG2 (human hepatocellular carcinoma) and SK-Hep1 (human liver adenocarcinoma) cell lines were obtained from DSMZ (Deutsche Sammlung für Mikroorganismen und Zellkulturen). Huh7 (human hepatocellular carcinoma) was a kind gift of the group of Prof. M.H. Heim from the research department at the University Hospital Basel. Cell culture flasks, plates, cryo-tubes and plastic pipettes were from TPP, Falcon, Nunc, and BD Bioscience. Asialofetuin from fetal calf serum Type I, NaN_3 , Triton X-100 (polyethylene glycol tert-octylphenyl ether), Paraformaldehyde, *N*-propyl gallate, and sodium borohydride (NaBH_4) were obtained from Fluka. Bovine serum albumin (BSA), DMSO (Hybridoma grade), and Mowiol 4-88 were from Sigma. Cover glasses (20 mm x 20 mm) and round (d =18 mm) were from Menzel-Gläser. Monoclonal mouse anti-human ASGP-R (30201) was from Calbiochem, mouse anti- β -tubulin from Boehringer-Mannheim, R-Phycoerythrin (R-PE)-conjugated and Fluorescein-5-isothiocyanate (FITC)-coupled goat anti-mouse IgM/G/A from Southern Biotechnology, and Alexa Fluor[®] 488-conjugated goat anti-mouse IgG (H+L) from Molecular Probes.

2.3.1 Standard Protocol for Freezing of Mammalian Cells

Mammalian cells freeze most efficiently at concentrations of between 1 and $10 \cdot 10^6$ cells/ml (= final suspension in freezing medium).

Freezing medium: The cells' regular growth medium containing in minimum 10% FBS was supplemented with 10% DMSO. The amount of serum in the medium was increased up to 20% if the cells were sensitive (e.g. Hybridoma). The freezing medium was prepared freshly and chilled on ice.

Adherent cells were harvested using their standard protocol (e.g. washing with $\text{Ca}^{2+}/\text{Mg}^{2+}$ -free buffer, harvesting with Trypsin/EDTA solution, and quenching with complete medium containing FBS). The resuspended cells were counted.

The cells were pelleted by centrifugation for 5-10 minutes at 1000 rpm and 4°C. The supernatant was discarded and the cells carefully resuspended in ice-cold freezing medium. Aliquots of 1ml of the cell suspension were dispensed into prepared cryovials on ice. The vials were immediately transferred to a Styrofoam-box in the -80°C-freezer. Within 24 h of freezing, the vials were transferred to the liquid nitrogen storage.

2.3.2 Production of Mouse anti-human H1-CRD Antibodies

Murine hybridoma cells producing anti human H1-CRD antibodies were established by Rita Born¹⁶⁶.

2.3.2.1 Adaptation of Hybridoma Cells to low Serum Conditions

Complete hybridoma medium with serum:

RPMI 1640 or IMDM, 15% FBS, 2 mM L-glutamine, 1% MEM non-essential amino acids (NEAA), 100 U/ml Penicillin and 100 µg/ml Streptomycin.

Once the growth performance of the cells grown in complete medium with serum was stable, the serum reduction process was started. Therefore, complete medium with serum was gradually replaced by 50% of complete medium already incubated with the cells for about 2 days (so called conditioned medium) and 50% of fresh, serum-free complete medium. The cells tend to detach and start growing in suspension while growing under serum-reduced conditions, which is ideal for the production of antibodies in roller bottles, as higher cell densities can be achieved during production. Cells used for antibody production were maintained in medium supplemented with 1.5 or 3% of low IgG FBS in order to avoid co-purification of bovine antibodies from the serum during affinity chromatography.

2.3.3 Purification of Murine Monoclonal Antibodies

Murine IgG usually show better binding to protein G than to protein A, but have to be eluted at lower pH, which sometimes causes loss of binding activity or aggregation of the eluted protein.

Hybridoma were grown in roller bottles under serum-reduced conditions (with

low bovine IgG FBS), the collected medium was centrifuged 10 min at 6500 g to remove cells and debris. The pH of the cleared supernatant was corrected to 7.4 with NaOH if necessary, filtered (0.2 μm) and immediately purified.

HiTrap protein G HP 1ml columns were from GE Healthcare.

Wash buffer: PBS, pH 7.4

Elution buffer: 0.1 M glycine, pH 3.0

Neutralization buffer: 1.0 M Tris, pH 8.8 (all solutions were filtered)

The column was washed with 5 column volumes (CV) of water before equilibration with 10 CV of washing buffer. Filtrated hybridoma culture supernatant was loaded at a flow rate of 0.4-0.5 ml/min, and then the column was extensively washed with wash buffer until the OD_{280} reached baseline. The IgG was eluted with 10 CV of elution buffer and the eluates of 1ml collected into tubes already containing 50 μl of 1 M Tris buffer (pH 8.8) for rapid neutralization.

The collected eluates were combined, then the buffer was exchanged to PBS and the samples concentrated by using Icon centrifugal filter devices with cutoff 9 kDa (Pierce).

Final concentrations of purified IgG in PBS were determined by absorbance A_{280} measurement (IgG factor: A_{280} of 1.35 = 1 mg/ml).

2.3.4 Isotyping of anti-H1-CRD Antibodies

Isotyping ELISA-Kit SBA Clonotyping sytem / HRP was from Southern Biotech.

A Nunc MaxiSorb 96-well Immunoplate was coated over night at 4°C with 3 $\mu\text{g/ml}$ H1-CRD in HBS+Ca²⁺ (1 row buffer only, for blank). The coating-solution was discarded, and the plate was tapped dry on several layers of tissue paper. The plate was incubated with 150 $\mu\text{l/well}$ of blocking buffer for 2 h at 4°C and then washed 3x with HBS+ Ca²⁺ (150 $\mu\text{l/well}$). The antibodies diluted to 5 $\mu\text{g/ml}$ in HBS+ Ca²⁺ were added to the wells (100 $\mu\text{l/well}$) in duplicates, and the plate was incubated 2 h in a humid chamber on the shaker at 100 rpm. Then 100 $\mu\text{l/well}$ of the isotyping antibodies diluted 1:500 in HBS+Ca²⁺ were added to the cells and incubated for 1.5 h. The plate was washed 4 times with HBS + Ca²⁺

(150 μ l/well) and tapped dry before detection. ABTS substrate (100 μ l/well) was added and color-development was stopped after 5 min by adding 100 μ l/well of stop-solution (2% oxalic acid). O.D. was measured at $\lambda = 415\text{nm}$.

2.3.5 Hepatoma Cell-lines Culture Conditions

Hepatoma cell lines were propagated in Dulbecco's modified Eagle's medium (DMEM) high-glucose, supplemented with 10% fetal bovine serum (FBS), 2 mM L-glutamine, 100 U/ml penicillin, and 100 μ g/ml streptomycin (complete medium). During the incubation steps of the cells outside the incubator, medium with a CO₂-independent buffer system was used to stabilize the pH during incubation (DMEM high-glucose, without phenol red and FBS, containing 25 mM HEPES).

2.3.6 Propagation of Hepatoma Cells

Collagen coating of T75-flasks

To prepare collagen-coated flasks the bottoms of T75-flasks were covered with 0.5-1 ml of a 0.25 mg/ml collagen-solution diluted from a 3 mg/ml stock of Collagen S (Roche) in sterile acetic acid (0.5 M, pH 2.8). The flasks were stored at 4°C and washed once with 5 ml of PBS before use.

Twice weekly, cells grown in 75cm² area cell culture flasks (T75) were washed first with DPBS detached with Trypsin/EDTA solution for 2-3 min at 37°C. Then the cells were suspended in an equal amount of DMEM and transferred to a 15 ml falcon tube. To propagate the cultures the cells were centrifuged at 1000 rpm for 5-10 min, the old medium was removed and the cells were resuspended in a defined amount of fresh medium. HepG2 cells were spitted by 1/5 or 1/10 into collagen-coated flasks and SK-Hep1 1/10 or 1/20 into untreated flasks containing 20 ml of complete medium.

2.3.7 Preparation of Cover Slips for Microscopy

Collagen coating of cover slips

The cover slips were cleaned from dust, degreased and disinfected before use. First, the cover slips were separated one from another and placed in a 500 ml

beaker filled with water. Then the water was exchanged and the beaker was sonicated in a water-bath for 30 min. This procedure was repeated twice, and then the water was substituted with 50% ethanol and sonicated again for 30 min. This step was repeated with increasing concentrations of ethanol (70% and 95%). Finally, the slips were stored in 95% ethanol until use.

The cleaned cover slips were dripped off excess ethanol, kept shortly over the flame of a Bunsen burner, and placed one per well in a 6-well (square slips) or 12-well plate (round slips) with the help of sterile tweezers. Then they were covered with 60 μ l of a diluted collagen solution (0.5 mg/ml in sterile-filtered 0.5 M acetic acid, pH 2.8) and incubated overnight at 4°C. On the next day, the wells were washed once with PBS to remove the acetic acid, then filled with 1 ml of PBS and kept at 4°C until use.

Preparation of cell-covered slips

The cells were detached and centrifuged as described above, then they were counted in a cell counting chamber (Neubauer improved hemocytometer). The viability of the cells was checked by trypan blue-exclusion. $2 \cdot 10^5$ cells in 1-2 ml of medium/well were seeded to the prepared 6-well or 12-well plates containing collagen coated cover-slips and incubated over night in an incubator at 37°C, 5%CO₂ (v/v in humidified air).

Fixation of the cells

Fixation buffer (3% paraformaldehyde in PBS):

Freshly before use, a mixture of 0.3 g Paraformaldehyde (PFA) and 8.8 ml H₂O containing 10 μ l NaOH (1M) was heated in a water-bath to 60°C in a closed 15ml-Falcon tube until the solution cleared up. After cooling down to room temperature, 1 ml of 10x PBS and 20 μ l of HCl 1M were added to adjust the pH between 7 and 7.5. The pH was checked using indicator paper, (pH-electrodes could be destroyed by the fixative).

After carefully washing the cells twice with PBS, they were fixed in fixation buffer for 30 min at room temperature or over night at 4°C.

Mounting of the slides

Mowiol mounting buffer:

20g of Mowiol were dissolved in 80 ml PBS, then 40 ml of glycerol and 0.75% of the antioxidant *N*-propyl-gallate (Fluka) as anti-fading agent were added and the solution was stirred for 8h. Undissolved particles were removed by centrifugation (15 minutes at 12'000 rpm) and the buffer was stored airtight at 4°C in the dark.

The fixed, cell-covered cover slips were mounted onto glass-slides with a drop of Mowiol-mounting buffer. The mounted slides had to dry for at least 30 minutes before microscopy. After 12 hours, the mounting buffer got solid and the slides could be stored in the dark at 4°C for up to six months.

2.4 Immunohistochemistry (IHC)

Performed at the University Hospital Basel in the Group of Prof. L. Terrachiano.

Different procedures for the tissue staining were tested: Sections of paraformaldehyde-fixed, paraffin-embedded human liver tissue were dewaxed and the antigen retrieved either by microwaving in citrate buffer (pH 6.0) at 98°C for 30 or 60 min, or by steaming in citrate buffer (pH 6.0, pH 1-2, pH 10-11) at 120°C for 5 min, by treatment with 3 drops / 5min proteinase K, by digest with 1 mg/ml pronase XIV at 37°C for 15 min, or at 4°C for 30 min, or by incubation with 1 mg/ml trypsin at RT for 30 min. Optionally endogenous avidin/biotin activity was blocked. Sections were dehydrated in methanol-peroxide for 30 min and blocked with murine serum for 30 min, followed by incubation with 0.5–6 µg/ml anti-H1-CRD IgG for 30 min. After capturing with avidin-labeled goat anti-mouse IgG for 30min and with biotin-labeled HRP for 30 min, sections were stained with DAB substrate and optionally counterstained with Harris' hematoxylin prior to mounting onto glass slides.

2.5 Immunocytochemistry

2.5.1 Immunofluorescence Staining

2.5.1.1 Indirect Staining of Cells

Fixed cells were washed with PBS 3-4 times during 10-20 min to get rid of the paraformaldehyde and then permeabilized for 15 minutes at room temperature with 1 ml of 0.1% Triton X-100 in PBS.

Aldehyde quenching

To reduce autofluorescence of the fixed cells, the slides were treated twice for 15 min with 1 ml of freshly prepared ice-cold sodium borohydride (10 mg/ml in PBS) on ice, then washed abundantly with PBS until all bubbles disappeared and kept in PBS at room temperature for about an hour. After this, the PBS was removed and the cover slips were covered with 80 μ l of the first antibody, diluted 1:50 in PBS and incubated for 2 hours at room temperature. After washing the cover slips twice with PBS for 5 min, they were incubated with 80 μ l of the secondary antibody diluted in PBS (Cy3[®]-antibody 1:3000, Alexa Fluor[®] 488-antibody 1:800) for one hour at room temperature in the dark (Figure 20). Then the cover slips were washed again and mounted with Mowiol-mounting buffer onto glass-slides as described in chapter 2.3.7.

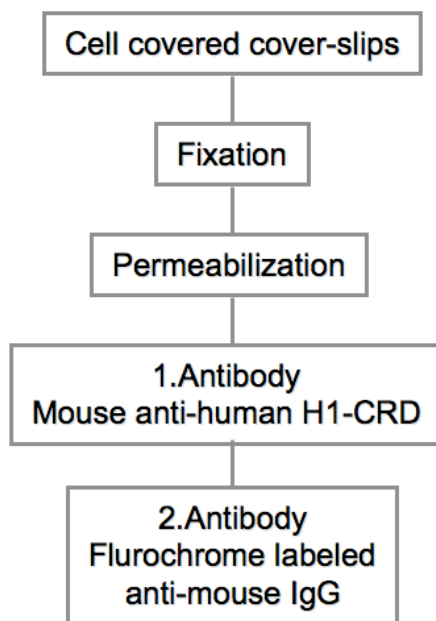


Figure 20. Indirect detection of antibody binding to the receptor

2.5.1.2 Direct Staining of Cells

Texas Red labeling of the antibodies and asialofetuin

The FluoReporter Texas Red X protein-labeling kit from Molecular Probes was used to label the antibodies and asialofetuin. The Texas-red X-dye provided in this kit has a succinimidyl-ester moiety, which reacts efficiently with primary amine groups of proteins (but also of glycine and Tris) to form stable dye-protein conjugates. The labeling was performed following the instructions of the manufacturer.

The buffer (100 mM glycine, Tris-buffered) of the purified monoclonal antibodies was changed to PBS by concentrating the antibody-solutions three times in Micronon YM 10 centrifugal devices (Millipore) and then the samples were diluted with PBS to a final volume of 250 μ l. Asialofetuin was dissolved in PBS. The antibody- or asialofetuin-solutions (200 μ l) were mixed for one hour with the calculated amount of fluorescent dye. The final concentration of the labeled material was estimated by calculating the employed amount of antibody or asialofetuin with the obtained volume after the purification step of the labeling procedure. The resulting conjugates were stored at 4°C and were stable for several months.

2.5.2 Receptor Specific Uptake of Ligands into HepG2 Cells

Receptor-mediated endocytosis experiments

Continuous receptor-mediated endocytosis (RME) was studied on living cells grown on collagen-coated cover-slips. Maintaining the physiological pH is essential to keep the cells healthy. Most media and buffers in cell culture use a carbonate buffer system and require a 5% carbon dioxide atmosphere to maintain the proper pH. To prevent pH changes whenever the plates were removed from the incubator, a HEPES buffered medium was used. The cells were carefully washed twice with 1-2 ml of serum-free HEPES-buffered DMEM medium to remove residual serum and antibiotics. Then they were serum-starved for 1h at 37°C. The medium was removed again and replaced by the unlabeled antibodies, Texas Red[®]-labeled asialofetuin (TR-ASF), or Texas Red[®] (TR)-labeled antibodies diluted in serum free medium. Then the plates were incubated for 20 minutes at 37°C in an incubator to allow internalization. Afterwards the cells were carefully washed twice with PBS and then fixed for 30 min at room temperature in the dark (flow chart depicted in Figure 22). If unlabeled antibody was used for the experiments, the cells were permeabilized after the fixation step as described in chapter 2.5.1.1 and incubated with a fluorochrome labeled 2. Antibody (flow chart depicted in Figure 21). After 3 additional washings with 1ml of PBS the slides were mounted onto glass slides with Mowiol mounting buffer and stored at 4°C in the dark until examination.

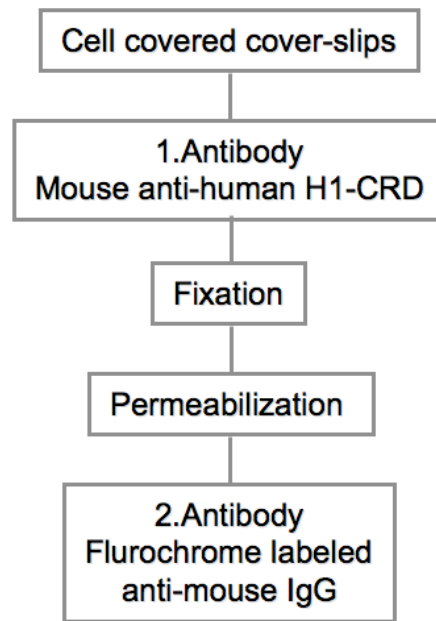


Figure 21. Indirect detection of internalized antibody

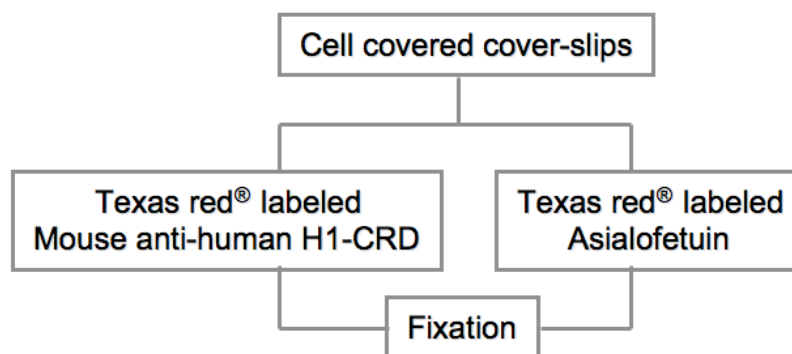


Figure 22. Direct detection of internalized antibody or ligand

Time dependency of Asialofetuin-uptake

Serum free medium (200 μ l) containing 5 or 10 μ g/ml Texas Red-labeled Asialofetuin (TR-ASF) were added to the previously serum-starved cells and incubated for 15, 30, 60 and 120 minutes at 37°C in the incubator. After the incubation, the cells were washed once with PBS and fixed at 37°C for 30 minutes. The cell-covered slips were then washed and mounted as described above.

The fluorescence-labeled cells were examined on a Zeiss Apofluorescence microscope with 100-times magnification using immersion oil. A selection of

slides was photographed with the camera featured by the microscope. The film used was a Kodak Elite 400 film for diapositives, up-speeded to 1600 ASA, which leads to shorter exposure times of the film and prevents excess photobleaching of the fluorochrome. The diapositives were then scanned with a Canon PI CS-U 4.1X flat bed scanner. Or the selective cellular uptake of the labeled compounds was visualized using a Zeiss Axiovert 135 microscope with a 63 x planapo objective (numerical aperture = 1.4, oil) with the appropriate filter set (450/490, FT 510, LP 520) equipped with a Zeiss AxioCam MRm CCD camera run by AxioVision 3.1 imaging software.

2.5.3 Extracellular Staining of Hepatic Cells by Flow Cytometry

FACS buffer: Ice-cold PBS, 0.5% BSA, 0.02% NaN₃ (sterile filtered)

Preparation of cells

HepG2 were grown in collagen-coated, SK-Hep1, Huh7, and clonal murine periportal Kupffer cells (a kind gift from the lab of Dr. R. Landmann, Division of Infectious Diseases, Department of Research, University Hospital, Basel, Switzerland) were grown in untreated 75 cm² tissue culture flasks.

The subconfluent cells were detached for 15 min on ice with 2 mM EDTA in cold PBS. All cells were collected and HepG2 cell-clumps were repeatedly pipetted up and down to obtain single cells. The cells were harvested by centrifugation at 1000 rpm (4°C) for 10 min, resuspended in complete medium to 1·10⁶ cells/ml and kept on ice until use.

Cells, 100 µl (1·10⁵ cells/well) and 100 µl of FACS buffer were distributed per well in a 96 U-well plate. The cells were pelleted by centrifugation of the plate at 1500 rpm for 2 min at 4°C and the supernatants were flicked off. Then the cell pellets were washed once by resuspension in 200 µl FACS-buffer and a repeated centrifugation step.

Surface staining

First, one well per cell-type was stained with 20 µl of the first antibodies, mouse anti-human H1-CRD C14.6 IgG2a, B01.4 IgG1, C09.1 IgG1, C11.1 IgG1 and C18.1 IgG1 at 10-20 µg/ml, the isotype controls for IgG2a (anti-human TCR-

BV11 C21, purified from hybridoma) at 20 µg/ml and IgG1 anti-human CD3 antibody TR66 (undiluted supernatant, both from the lab of Prof. G. De Libero) for 30 min on ice to prevent internalization of bound antibody. Then 200 µl of FACS-buffer per well were added, the cells were washed twice as described above and then they were resuspended in 20 µl of the 2nd antibody (goat-anti-mouse-IgG H+L chain) labeled with R-Phycoerythrin (RPE) (diluted 1:50 in FACS buffer) and incubated on ice in the dark for 20 min. After the addition of 200 µl FACS-buffer per well, the cells were washed twice by centrifugation. Viability of the cells was tested by propidium iodide (PI) exclusion (a 200 x-stock solution, 1 µg/ml was obtained from the lab of Prof. G. de Libero). Cells were resuspended in 200 µl ice-cold FACS buffer containing PI (5 µg/ml) before measurement. Surface staining of living cells was evaluated by comparing the shift of median fluorescence intensity (MFI) emitted at 580 nm between untreated cells (background fluorescence) and treated cells on a CyAN ADP flow cytometer (DakoCytomation) with Summit 4.1 software. The forward and side scatter gate 1 (R1) was set to count 50'000 living cells of each sample. In gate 2 (R2), the cells counted in gate 1 were gated for single cells. The median fluorescence intensity (MFI) shift of the staining was analyzed using GraphPad Prism 4 software.

2.6 Triantennary Gal/GalNAc Ligand Binding and Internalization

2.6.1 Fluorescence Microscopy

One day before the experiments, the cells were seeded at a density of $2 \cdot 10^5$ cells/well into 12-well plates containing-collagen coated glass cover slips. The cells were washed once with PBS, and then serum-starved for 30 min on ice in 1 ml of DMEM containing 25 mM HEPES. They were then incubated with 500 µl/well of the Alexa Fluor[®] 488-labeled compounds **6-8** (100 µM) in the same medium on ice for 1.5 h in the dark. After the binding step, the cells were washed carefully 4 times with cold PBS. Then fresh, prewarmed, complete DMEM medium (1 ml/well) was added and the cells were incubated for 40 min in an incubator at 37°C in a humidified CO₂ atmosphere (5%, v/v), leading to the internalization of the receptor-bound compounds into the cells. After the internalization step, the cells were washed twice with PBS and then fixed with

3% paraformaldehyde (PFA) in PBS for 30 min at 4°C. After fixation, the coverslips were washed abundantly with PBS and mounted upside down, in a Mowiol 4-88 mounting buffer containing *N*-propyl gallate, onto glass slides.

Selective cellular uptake of the Alexa Fluor[®] 488-labeled compounds was visualized using a Zeiss Axiovert 135 microscope with a 63 x planapo objective (numerical aperture = 1.4, oil) with the appropriate filter set (450/490, FT 510, LP 520) equipped with a Zeiss AxioCam MRm CCD camera run by AxioVision 3.1 imaging software.

2.6.2 Flow Cytometry

Cells were grown for 24 h in collagen coated (80 µg/ml) 24-well plates at a density of 3×10^5 cells/well or in 96-well plates at $1.5 \cdot 10^5$ cells/well.

The titration experiments were performed in 24-well plates, the cell-layers were first washed twice with cold PBS before incubation with compound **7** at concentrations ranging from 0.4 to 12.5 µM (1:2 serial dilutions) in 200 µl of DMEM without FBS for 40 min at 37°C. Then the cells were washed twice with cold PBS, detached and stripped from surface-bound compound by incubating them in a mixture containing 0.025% trypsin and 5 mM EDTA in PBS for 10 min on ice. Addition of complete medium quenched this process. The detached cells were collected and centrifuged at a speed of 1500 rpm for 3 min. Finally, the cells were fixed in 2% PFA in PBS for 15 min on ice followed by an aldehyde-quenching step with 100 mM lysine in PBS for 10 min. The fixed cells were then washed once with FACS buffer (PBS containing 0.5% BSA and 0.1% NaN₃) and resuspended in 200 µl of the same buffer for measuring. The competitive uptake experiments were performed with cells grown in 96-well plates. 20 µl of asialofetuin dilutions at concentrations ranging from 0.6 to 200 µM or GalNAc at 0.6 to 200 mM were added directly to the cells, immediately followed by the addition of 20 µl of compound **7** or **8** diluted to 20 µM in DMEM without FBS and then incubated for 60 min at 37°C in the incubator. The cells were washed, detached and fixed as described above.

Analyses were performed on a CyAn ADP flow cytometer with Summit 4.1 software (Dako Cytomation). The forward and side scatter gate 1 (R1) was set

to count 30'000 intact cells of each sample. In gate 2 (R2), the cells counted in gate 1 were gated for single cells. Uptake of compound into cells was evaluated by comparing the shift of median intensity of fluorescence (MFI) at 488 nm between untreated cells (background fluorescence) and treated cells.

Further analysis and IC₅₀ calculations were done with GraphPad Prism 4 software.

2.7 Molecular Cloning of Single Chain Antibodies

2.7.1 Vector Plasmids

2.7.1.1 The pAK Vector System

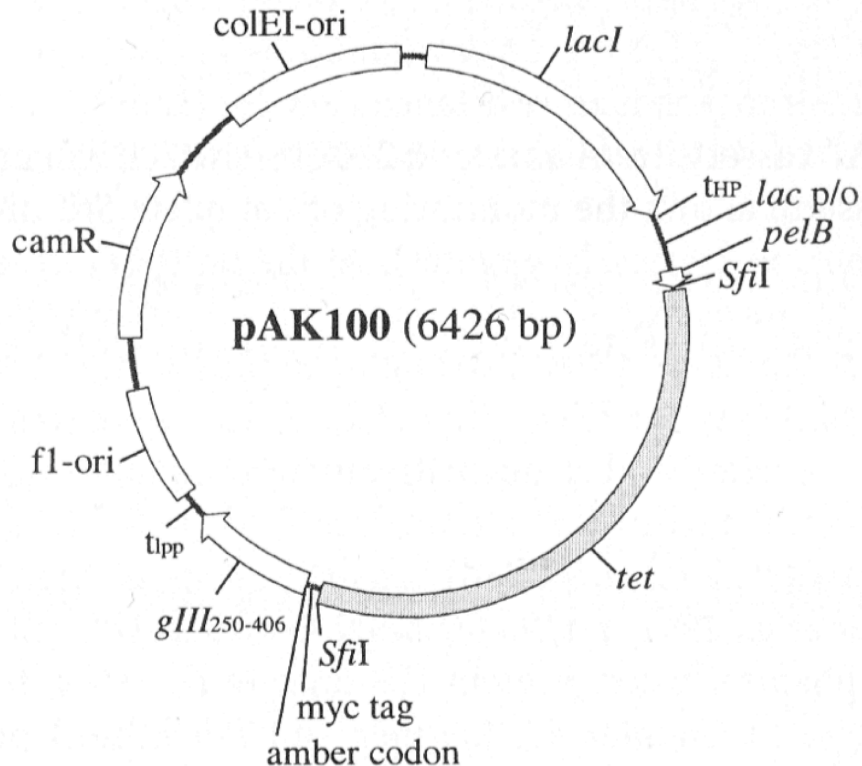


Figure 23. pAK100 phagemid vector map
pAK100 allows for phage-display of scFv antibody fragments.

pAK100 (Figure 23) is a phagemid vector used for phage display of murine scFv antibodies. The PCR-amplimer coding for the scFv fragment is cloned into the phagemid vector to be expressed as a fusion protein with a shortened form of the viral protein gpIII (gpIII₂₀₅₋₄₀₆) on the surface of the phage. The vector contains *Sfi* I restriction sites and codes for the c-myc tag¹⁴⁰. The sequence contains an amber stop-codon between the c-myc tag and the gpIII protein, which allows to express either soluble scFv or scFv-gpIII fusion proteins, depending on the *E. coli* expression host (suppressor, non-suppressor strain). An artificial Shine-Dalgarno sequence located near the LacZ-promotor allows only moderate translation of scFv-gpIII-fusion proteins that could be toxic to the expression host.

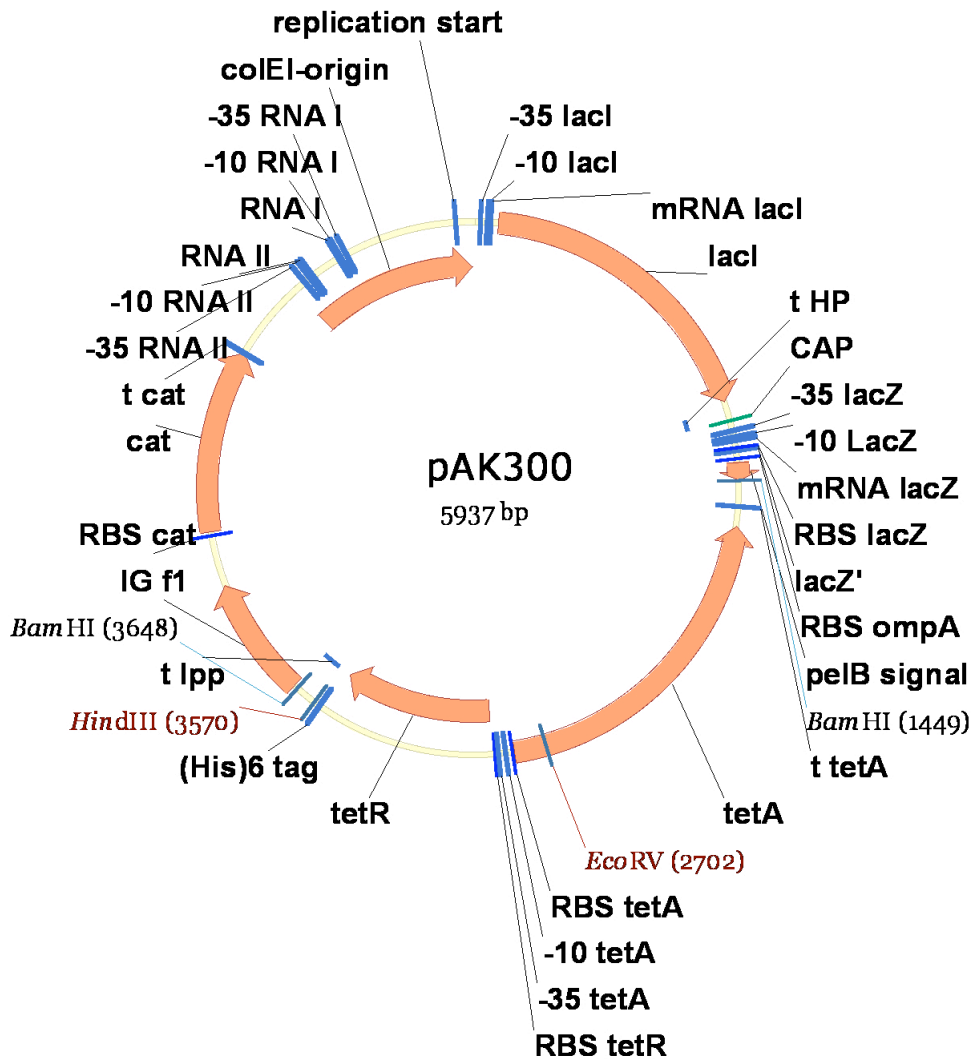


Figure 24. pAK300 expression vector map

The vector pAK300 (Figure 24) contains a *Sfi*I restricted tet-cassette for antibody cloning and an artificial Shine-Dalgarno sequence (SD_{art}), allowing only moderate protein expression after promoter activation. The plasmid is used for the soluble expression of scFv. An N-terminal His₆-tag allows the detection and purification of the scFvs¹⁴⁰.

2.7.1.2 The pHEN1 Phagemid Vector

The pHEN1 phagemid vector ¹⁵⁰ (Figure 25) is a derivative of pUC119 ¹⁷¹ allowing antibody genes to be cloned as *Sfi* I-*Not* I fragments for display on filamentous phage. It codes for a c-myc tag for detection ¹⁷². The amber codon allows choosing between expression of scFv_{III} fusion protein or soluble scFv, depending on the *E. coli* host.

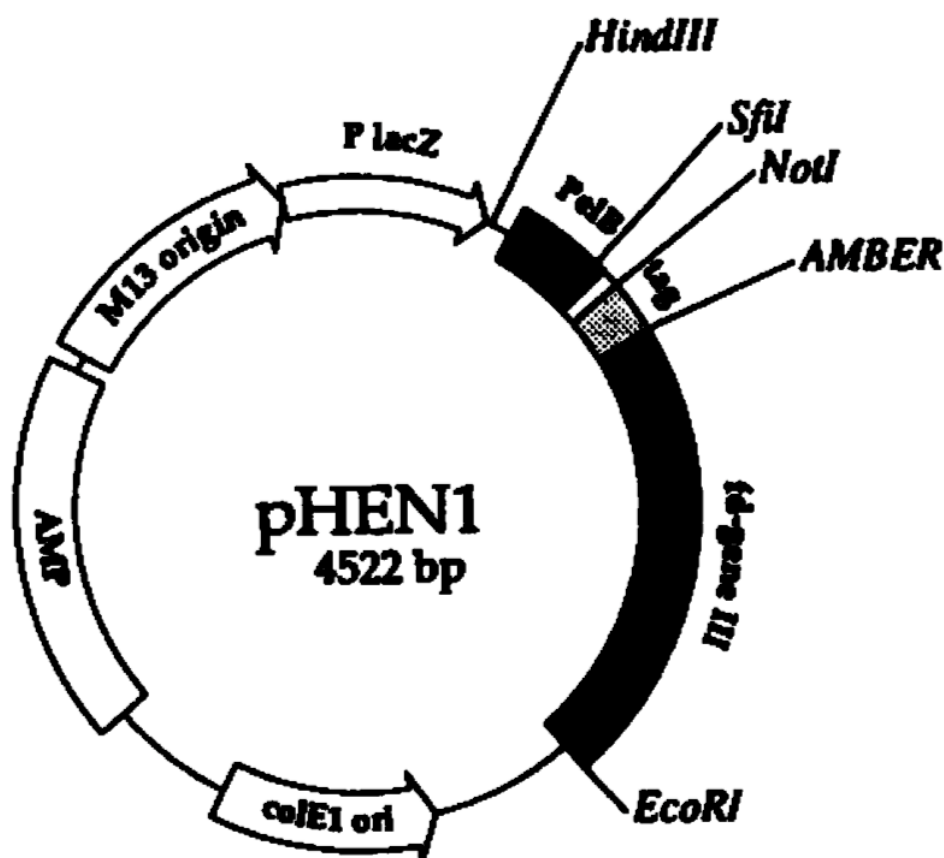


Figure 25. pHEN1 phagemid vector map
pHEN1 allows phage-display of scFv antibody fragments.

2.7.1.3 VCSM13 Helper Phage

VCSM13 interference-resistant helper phage was from Stratagene. VCSM13 interference-resistant helper phage (6 kb, single stranded) is derived from a M13 K07 mutant and carries the kanamycin-resistance gene in the IG region. It gives high phage rescue efficiencies with kanamycin selection.

2.7.2 Synthetic Oligonucleotides

2.7.2.1 Degenerate Primers for the Amplification of scFv

Mixtures of degenerate primers (Tables 3 to 6), which contain variable nucleotides at several positions in the sequence, were used to amplify the heavy and light chain of the antibodies variable domains ¹⁷³. The variable nucleotides are named according to the IUPAC/IUB rules:

R = A or G	S = C or G
K = G or T	B = C, G or T
H = A, C or T	M = A or C
D = A, G or T	W = A or T
Y = C or T	V = A, C or G

Preparation of primer mixes

Primers were reconstituted to 100 μ M in DEPC-treated water. Then the primers LB 1-17, LF 1-5, HB 1-19 and HF1-4 were mixed according to their degeneracy and stored at -20° C.

Table 3. V_LBACK-Primer mix

	Sequence (5' → 3')	Degeneracy	μ l
LB1	gccatggcggactacaaaGAYATCCAGCTGACTCAGCC	2	1
LB2	gccatggcggactacaaaGAYATTGTTCTCWCCCAGTC	4	2
LB3	gccatggcggactacaaaGAYATTGTGMTMACTCAGTC	12	5
LB4	gccatggcggactacaaaGAYATTGTGYTRACACAGTC	8	3.5
LB5	gccatggcggactacaaaGAYATTGTRATGACMCAGTC	8	4
LB6	gccatggcggactacaaaGAYATTMAGATRAMCCAGTC	16	7
LB7	gccatggcggactacaaaGAYATTCAGATGAYDCAGTC	12	6
LB8	gccatggcggactacaaaGAYATYCAGATGACACAGAC	4	1.5
LB9	gccatggcggactacaaaGAYATTGTTCTCAWCCAGTC	4	2
LB10	gccatggcggactacaaaGAYATTGWGCTSACCCAATC	8	3.5

LB11	gcatggcggactacaaaGAYATTSTRATGACCCARTC	16	8
LB12	gcatggcggactacaaaGAYRTTKTGATGACCCARAC	24	8
LB13	gcatggcggactacaaaGAYATTGTGATGACBCAGKC	12	6
LB14	gcatggcggactacaaaGAYATTGTGATAACYCAGGA	4	2
LB15	gcatggcggactacaaaGAYATTGTGATGACCCAGWT	4	2
LB16	gcatggcggactacaaaGAYATTGTGATGACACAACC	2	1
LB17	gcatggcggactacaaaGAYATTTTGCTGACTCAGTC	2	1

The capital letters in the sequence indicate the part that hybridizes with the FR1 region of the light chain variable domain. The underlined section codes for the shortened FLAG-tag.

Table 4. V_LFOR-Primer mix

	Sequence (5' → 3')	μl
LF1	ggagccgcccggcc(agaaccaccacc) ₂ ACGTTTGATTTCCAGCTTGG	1
LF2	ggagccgcccggcc(agaaccaccacc) ₂ ACGTTTTATTTCCAGCTTGG	1
LF4	ggagccgcccggcc(agaaccaccacc) ₂ ACGTTTTATTTCCAACCTTGG	1
LF5	ggagccgcccggcc(agaaccaccacc) ₂ ACGTTTCAGCTCCAGCTTGG	1

These primers contain a part of the Gly₄Ser linker. The third repetition, with a different codon usage to prevent mismatches in the SOE-PCR reaction, overlaps with the one in the V_HBACK-primers. The capital letters indicate the part that hybridizes at the transition region of the J- and C-Gen segment of the light chain.

Table 5. V_HBACK-Primer mix

	Sequence (5' → 3')	De-generacy	μl
HB1	ggcggcggcggctccggtggtggtgatccGAKGTRMAGCTTCAGGAGTC	8	4
HB2	ggcggcggcggctccggtggtggtgatccGAGGTBCAGCTBCAGCAGTC	9	4
HB3	ggcggcggcggctccggtggtggtgatccCAGGTGCAGCTGAAGSASTC	4	3
HB4	ggcggcggcggctccggtggtggtgatccGAGGTCCARCTGCAACARTC	8	4
HB5	ggcggcggcggctccggtggtggtgatccCAGGTYCAGCTBCAGCARTC	12	7
HB6	ggcggcggcggctccggtggtggtgatccCAGGTYCARCTGCAGCAGTC	4	2
HB7	ggcggcggcggctccggtggtggtgatccCAGGTCCACGTGAAGCAGTC	1	1
HB8	ggcggcggcggctccggtggtggtgatccGAGGTGAASSTGGTGGAAATC	4	2
HB9	ggcggcggcggctccggtggtggtgatccGAVGTGAWGYTGGTGGAGTC	12	5
HB10	ggcggcggcggctccggtggtggtgatccGAGGTGCAGSKGGTGGAGTC	4	2
HB11	ggcggcggcggctccggtggtggtgatccGAKGTGCAMCTGGTGGAGTC	4	2
HB12	ggcggcggcggctccggtggtggtgatccGAGGTGAAGCTGATGGARTC	2	2
HB13	ggcggcggcggctccggtggtggtgatccGAGGTGCARCTTGTTGAGTC	2	1
HB14	ggcggcggcggctccggtggtggtgatccGARGTRAAGCTTCTCGAGTC	4	2
HB15	ggcggcggcggctccggtggtggtgatccGAAGTGAARSTTGAGGAGTC	4	2
HB16	ggcggcggcggctccggtggtggtgatccCAGGTTACTCTRAAAGWGTSTG	8	5
HB17	ggcggcggcggctccggtggtggtgatccCAGGTCCAACVTCAGCARCC	6	3.5
HB18	ggcggcggcggctccggtggtggtgatccGATGTGAACTTGGAAAGTGTC	1	0.7
HB19	ggcggcggcggctccggtggtggtgatccGAGGTGAAGGTCATCGAGTC	1	0.7

These primers contain the rest of the linker sequence (in small letters). The capital letters indicate the part that hybridizes with the FR1 region of the heavy chain variable domain V_H.

Table 6. V_HFOR-Primer mix

	Sequence (5' → 3')	μl
HF1	ggaattc <u>ggccccc</u> gagggcCGAGGAAACGGTGACCGTGGT	1
HF2	ggaattc <u>ggccccc</u> gagggcCGAGGAGACTGTGAGAGTGGT	1
HF3	ggaattc <u>ggccccc</u> gagggcCGCAGAGACAGTGACCAGAGT	1
HF4	ggaattc <u>ggccccc</u> gagggcCGAGGAGACGGTGACTGAGGT	1

The capital letters indicate the part of the primers that hybridizes at the transition region of the J- and C-gene segment of the heavy chain. The primers contain the palindromic sequence recognized by *Sfi* I (underlined).

Table 7. SOE-PCR Primers

	Sequence (5' → 3')
scback	ttactcg <u>ggccc</u> cagcc <u>ggccat</u> ggcggactacaaaG
scfor	ggaattcggcccccgag

SOE-PCR primers were used to combine the V_H and the V_L to the scFv fragment. The 3' end of scback hybridizes with the 5' end of the V_LBACK primers. The *Sfi* I restriction site is underlined. scfor hybridizes with the V_HFOR primers.

2.7.2.2 Primers for Sequencing

Table 8. Primers for sequencing pAK300scFv

	Sequence (5'→ 3')	Properties
Rsp	AACAGCTATGACCATG	The Rsp-primer hybridizes with the sequence of the LacZ-promotor Starts 60 nt after the beginning of the His-tag sequence
scfor	GGAATTCGGCCCCCGAG	
Lsp	CACAATGTGCGCCATTTTTC	

Rsp: right sequencing primer, Lsp: left sequencing primer, designed with OligoPerfect™ Designer from Invitrogen.

Table 9. Primers for sequencing pHEN1scFv

	Sequence (5'→ 3')	Properties
fdseq1	GAATTTTCTGTATGAGG	Priming at the beginning of gIII ($T_m = 45.5^\circ\text{C}$)
DP47CDR2back	TACTACGCAGACTCCGTGAAG	Priming in the V_H germline gene, before the V_H CDR3 ($T_m = 59.8^\circ\text{C}$)

For sequencing the antibodies, these two primers are sufficient, since diversity is concentrated only in the CDR3 regions¹³³.

2.7.3 Construction of Murine scFv Expression Plasmids

2.7.3.1 mRNA Isolation from Hybridoma Cells

Illustra Quickprep mRNA purification kit was obtained from GE Healthcare.

Hybridoma cells in culture (RPMI 1640 + 15% FBS) or freshly thawed cells were centrifuged for 10 min at 1000 rpm. The pellets were washed once with serum-free medium to remove all DMSO and FCS. The cell pellet was processed as proposed by the manufacturer. The eluted mRNA was not quantified. The mRNA was precipitated by splitting the final elution in 2 aliquots of 0.32 ml, adding 10 μl of the glycogen, 32 μl of the potassium acetate solution (both provided in the kit) and a volume of 0.8 ml chilled absolute ethanol. The mixture was incubated for 30 min at -20°C . The mRNA extracted from hybridoma

clones B01.4, C14.6 and C11.1 and C23.8 (two vials each) was centrifuged for 30 min at 13'200 rpm and 4°C. The supernatant was discarded and the mRNA washed once in 1ml ice-cold ethanol, then stored in ethanol at -20°C.

2.7.4 PCR Reactions

All PCR reactions were carried out in 0.2 ml PCR tubes from BilaTec (Aldrich), in an icycler® thermo cycler from Bio-Rad.

2.7.4.1 First Strand cDNA Synthesis by RT-PCR

'Ready-To-Go You-Prime' First-Strand beads were from GE Healthcare, pd(N)₆-primers from Microsynth.

One vial of mRNA per clone was used for the cDNA synthesis. First strand cDNA synthesis was carried out according to the manual. One tube with rabbit globulin mRNA, also provided in the kit, was run with it as a control.

Ethanol was removed from the mRNA precipitate by tapping the tube upside down on clean tissue paper. The mRNA was then dissolved in 25 µl DEPC-treated water and inactivated by heating at 65°C for 10 min and cooling for 2 min on ice. cDNA synthesis was started by adding the mRNA to the 'Ready-To Go You-prime'- tubes. After 1 min, 1 µl pd(N)₆-primer (= 0,2 µg diluted in DEPC-water) was added and the synthesis was completed by incubating the tubes for 1h at 37°C and mixing at 400 rpm in a Thermomixer. The reaction was stopped by heating to 90°C for 2 min and the product was kept at -20°C until use.

2.7.4.2 Amplification of the Variable Antibody Domains V_H and V_L

Iproof[®] DNA-polymerase was from Bio-Rad, dNTPs were from Sigma.

Table 10. Reaction batch for variable antibody domain amplification

	Volume (μl)
cDNA template	5
iproof HF buffer (5x)	10
dNTP's (10 mM each)	1 (200 μM)
LB or HB primer mix	1 (100 μM)
LF or HF primer mix	1 (100 μM)
DEPC-H ₂ O	32
iproof DNA polymerase	1 (2 units)

Two tubes per antibody clone were used, one for V_L and one for V_H amplification.

Table 11. Cycling protocol for variable antibody domain amplification

Step	Temp. (°C)	Time	Number of cycles
Initial denaturation	98	3 min	1
			Addition of iproof DNA polymerase
Denaturation	98	10 s	7
Annealing	63	30 s	
	58	50 s	
Extension	72	30 s	23
Denaturation	92	30 s	
Annealing	63	1 min	
Extension	72	30 s	4
		Hold	

2.7.4.3 Assembly of the Variable Antibody Domains V_H and V_L

The so-called 'Splicing by overlap extension-PCR' (SOE-PCR) assembles the variable antibody domain genes with the linker sequence to scFv fragments. In the first two cycles of the PCR method, the two fragments are assembled via the complementary linker-sequence, then the primers scfor and scback were added to introduce the two *Sfi* I restriction sites.

Table 12. Reaction batch for SOE-PCR

	Amount
V _L DNA template	20 ng
V _H DNA template	20 ng
iproof HF buffer (5x)	10 µl
dNTP's 10 mM	1 µl (200 µM)
scfor 1:10	1 µl (100 pM)
scback 1:10	1 µl (100 pM)
DEPC-H ₂ O	ad 50 µl
iproof DNA Polymerase	1µl (2 units)

Table 13. Cycling protocol for SOE-PCR

Step	Temp (°C)	Time	Number of cycles
Initial denaturation	98	3 min	1
			Addition of iproof DNA polymerase
Denaturation	98	30 s	2
Annealing	63	30 s	
	58	50 s	
Extension	72	30 s	
Denaturation	98	30 s	7
Annealing	63	30 s	
	58	50 s	
Extension	72	30 s	
Denaturation	98	30 s	23
Annealing	63	30 s	
Extension	72	30 s	
Final extension	72	5 min	

The product was gel-purified using the Sigma GenElute gel-extraction kit, (Sigma).

2.7.5 Digestion and Cloning of murine scFv Genes

2.7.5.1 *Sfi* I Digest of the Vector and the scFv-DNA

Sfi I restriction enzyme was purchased from New England Biolabs (NEB).

To clone the scFv fragments into the pAK300-vector, fragments (Table 14) and vector (Table 15) were digested for 3-4 h at 50°C in with the restriction enzyme *Sfi* I.

Table 14. Reaction batch used for scFv digest

	Volume
NEB-Puffer 2 10x	2.0 μ l
BSA 100x	0.2 μ l
<i>Sfi</i> I (20 U/ μ l)	0.5 μ l
ddH ₂ O	2.3 μ l
scFv DNA	15.0 μ l

Table 15. Reaction batch used for vector digest

	Volume
NEB-Puffer 2 10x	10 μ l
BSA 100x	1 μ l
ddH ₂ O	33.4 μ l
<i>Sfi</i> I (20 U/ μ l)	5.6 μ l *
pAK300	50 μ l (= 11.3 μ g) *

*10 unit per 1 μ g vector in 100 μ l of volume were used

2.7.5.2 Ligation of scFv-DNA into pAK300-Vector

T4 ligase was from NEB.

Both, digested vector and scFv-fragments, were gel-purified and quantified before the ligation. The molar ratio vector to insert was 1.5:1, the ligation mixture was incubated overnight at 16°C (Table 16).

Table 16. Ligation mixture

	Amount
Vector DNA	200 ng
scFv gene fragment	20 ng
T4 ligase	1 unit
Ligase buffer with 10mM ATP (10x)	2 μ l
ddH ₂ O	20 μ l

2.7.5.3 Analytical Digest of Ligation Product

The ligation product was digested for 4 h at 50°C.

Table 17. Reaction batch for analytical digest

	Volume
NEB-Puffer 2 10x	2.0 µl
BSA 100x	0.2 µl
<i>Sfi</i> I (20 U/µl)	0.5 µl
ddH ₂ O	12.3 µl
pAK300scFv DNA	5.0 µl

2.7.6 DNA Sequencing

Sequencing was performed in house on an ABI 3100 Avant with 4 capillaries, using Big Dye 1.1 terminator sequencing kit from Applied Biosystems. Sodium acetate was from Fluka.

If the DNA purified by Miniprep was eluted with TE buffer, the EDTA had to be removed before sequencing. This was done using the gel purifying kit and elution of the plasmid with water.

Table 18. Reaction batch for sequencing PCR

	Volume
Miniprep sample as DNA template	5 µl
ddH ₂ O	1 µl
Primer (5µM)	1 µl
Terminator ready reaction mix	3 µl
Final volume	10 µl

Table 19. Cycling protocol for sequencing

	Cycles		°C	Time
Initial denaturation	1		96	1 min
Amplification	25	Denaturation	96	10 s
		Annealing	50	5 s
		Extension	60	4 min
Storage	1		4	∞

The product could be stored at 4°C overnight.

2.7.6.1 Purification of the Extension Products

Table 20. Ethanol precipitation of PCR-products

	Volume
PCR product	10 µl
ddH ₂ O	90 µl
Sodium acetate (3 M, pH 4.6)	10 µl
Ethanol abs.	250 µl

The samples were mixed by inversion and then incubated on ice in the dark for 15 min. Samples were then centrifuged for 10 min at 13'000 rpm at RT, and the supernatant was carefully removed with a fine Pasteur pipette. Then 350 µl of ethanol 70% were added to the pellets and the samples centrifuged again. After removing the supernatant, the pellets were air-dried for 30 min in the dark at RT. The dry pellets were submitted for sequencing.

2.7.7 Sequence Analysis

Sequences of the scFvs were compared using Codon Code Aligner version 2.1.

2.7.8 Agarose Gel Electrophoresis

Molecular biology-grade Agarose and Ethidium bromide solution 1% were purchased from Applichem. Boric acid and EDTA were from Fluka. DNA gel

loading buffer (10x) was from Eppendorf. DNA molecular weight markers were obtained from Invitrogen and NEB (Figure 26).

Agarose (0.8-2%, depending on the DNA fragment size) was suspended in 1x TBE (44.6 mM Tris, 44.6 mM Boric acid, 1 mM EDTA, pH 8) and heated for 1-2 min in the microwave until it fully dissolved. Per gel, 80 ml of the agarose-gel solution were poured in a beaker and left to cool down for 2-3 min to $\sim 50\text{ }^{\circ}\text{C}$, then 2 μl ethidium bromide 1% was added. The gel-solution was poured into a gel tray containing an appropriate comb. After formation of the gel the comb was removed and the gel was covered with TBE buffer. DNA samples were diluted with ddH₂O if necessary and an appropriate amount of loading buffer was added to the samples. DNA marker (2-5 μl) were included for size determination. The samples were loaded on the gel and an electric field was applied (80 V). The ethidium-stained DNA fragments were visualized under UV light and documented using Gel Doc XR and the software Quantity One 4.6.5.

For preparative use, the DNA fragments were purified from excised agarose gel-bands according to the manual (GenElute gel-extraction kit, Sigma).

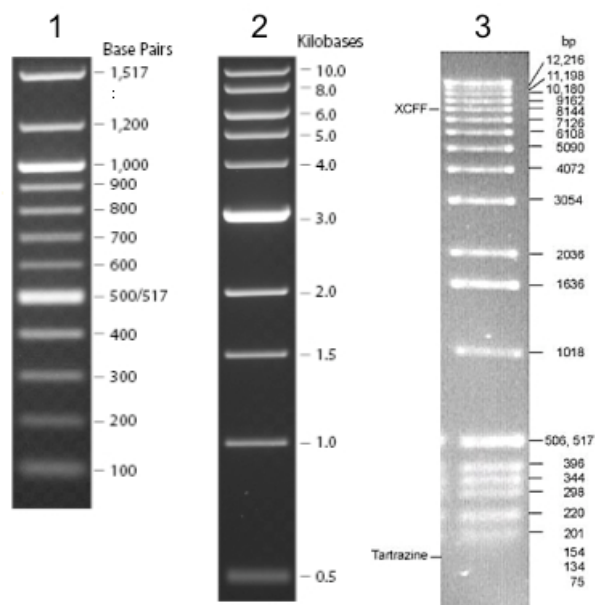


Figure 26. DNA Markers

(1) NEB 100 bp DNA ladder, (2) NEB 1 kb DNA ladder, (3) TrackIt 1kb DNA ladder

2.7.9 UV-Quantitation of DNA

OD values were measured in a BioRad spectrophotometer 3000 with a 100 μl -quartz cuvette. The dilution factor was usually 1:20.

The most common method for quantifying DNA samples is by conventional absorbance measurements; nucleic acids have an absorption maximum at $\lambda = 260$ nm. Most samples contain contaminants such as proteins and single stranded DNA/RNA that absorb maximally at $\lambda = 280$ nm. The equation for calculating DNA in the presence of contaminants is:

$$OD_{260}/OD_{280} = \text{pure dsDNA}$$

The higher the ratio, the purer the DNA sample. A ratio between 1.8 and 2.0 for a cuvette spectrophotometer is acceptable. With a conventional absorbance reading an OD_{260} of 1 corresponds to 50 $\mu\text{g/ml}$ dsDNA.

2.8 General Methods for Bacteria

2.8.1 Material

Bacto Tryptone, Bacto Yeast extract and Bacto agar were obtained from BD Becton Dickinson, IPTG and ampicillin sodium salt and glycerol 98% were from Applichem, chloramphenicol from Hanseler, tetracycline HCl from Sigma and kanamycine sulphate from Fluka. Petri-dishes 94 x 16 mm were from Greiner Bio-one, Petri-dishes for phage display 150 x 15 mm were from Falcon.

2.8.2 *E.coli* Strains

DH5 α was used for plasmid amplification. DH5 α increases insert stability and improves the quality of plasmid DNA prepared with mini-preps. The transformation efficacy in DH5 α is high and their background expression is minimal due to the lack of T7-RNA polymerase.

Genotype: F⁻ 80d*lacZ*M15 (*lacZYA-argF*) U169 *recA1 endA1 hsdR17*(r_k⁻, m_k⁺) *phoA supE44*⁻ *thi-1 gyrA96 relA1*

BL21(DE3) was used for scFv expression. It carries the lambda DE3 lysogen. Due to the protease deficiency (*lon* and *ompT*) the target protein should be more stable compared to other expression hosts.

Genotype: F⁻ *ompT hsdS_B*(r_B⁻m_B⁻) *gal dcm* (DE3)

AD494(DE3) was used for H1-CRD expression. It carries the lambda DE3 lysogen. AD494(DE3) favors the formation of cytoplasmic disulphide bonds.

Genotype: Δ ara-leu7697 Δ lacX74 Δ phoAPvull phoR Δ malF3 F'[lac+(lacIq)pro] trxB::kan(DE3)

XL1-Blue was used for phage display and scFv expression. The F' episome contains the tetracycline resistance gene. The production of the bacterial pili is essential for M13 phage infection.

Genotype: *recA1 endA1 gyrA96 thi-1 hsdR17 supE44 relA1 lac* [F'*proAB lacI^qZ* Δ M15 Tn10 (Tet^r)]

TG1 was used for phage display and scFv expression.

Genotype: *supE thi-1 Δ (lac-proAB) Δ (mcrB-hsdSM)5 (rK- mK-)* [F' traD36 proAB lacI^qZ Δ M15]

2.8.3 Bacterial Culture Media and Buffers

Tryptone and Yeast extract serve as a source of nitrogen, sulfur, and carbon, while Yeast extract also contains Vitamin B complex. Sodium chloride provides sodium ions for the membrane transport and maintains osmotic equilibrium of the medium.

All media ingredients were dissolved in dd H₂O. pH was adjusted before autoclaving at 120 °C.

LB broth (Lysogenic broth, or Luria-Bertani broth)

Bacto yeast extract 0.5%, Bacto Tryptone 1%, NaCl 1%, pH 7.5

2.8.3.1 Media and Buffer for Electro-competent Cells

SOB Broth

Bacto yeast extract 0.5%, Bacto Tryptone 2%, NaCl 0.05%, KCl 2.5 mM, MgCl₂ 5 mM, pH 7.5.

Glycerol solution

Glycerol 10% (v/v) in ddH₂O, sterile-filtered.

2.8.3.2 Media and Buffer for Chemo-competent Cells

SOC Broth

SOB Broth with addition of 20 mM glucose after autoclaving.

Psi Broth

Bacto yeast extract 0.5%, Bacto Tryptone 2%, MgSO₄ 5% (m/v). Adjusted to pH 7.6 with KOH.

Tfb 1 buffer

Potassium acetate 30 mM, RbCl 100 mM, CaCl₂ 10 mM, MnCl₂ 50 mM, glycerol 15% (v/v). Adjusted to pH 5.8 with dilute acetic acid.

Tfb 2 buffer

MOPS 10 mM, RbCl 10 mM, CaCl₂ 75 mM, glycerol 15% (v/v). Adjusted to pH 6.5 with dilute NaOH.

2.8.3.3 Expression Media

Terrific Broth (TB)

Terrific Broth is a highly enriched medium developed by Tartoff and Hobbs to improve yield in plasmid-bearing *E. coli*¹⁷⁴. Recombinant strains have an extended growth phase in the medium. Glycerol is used as the 'carbohydrate' source. Unlike glucose, glycerol is not fermented to acetic acid.

TB medium base: Bacto tryptone 1.2%, Bacto yeast extract 2.4%, glycerol 0.4% (v/v). Ad 900 ml with ddH₂O, sterilized by autoclaving, cooled to 60°C.

TB phosphate buffer: KH₂PO₄ 2.31 %, K₂HPO₄ 12.54 %, ad 100 ml, sterilized by autoclaving.

Prior to use, 900 ml TB medium base were combined with 100 ml TB phosphate buffer.

2xTY Broth¹⁷⁵

Bacto yeast extract 1%, Bacto tryptone 1.6%, NaCl 86 mM. Adjusted to pH 7.0 with NaOH.

Plasmids containing a lacZ promotor often show low expression of the proteins controlled by the promotor in the uninduced state. An addition of glucose to the growth medium is able suppress this basal expression¹⁷⁶.

2xTY-Repression medium

2xTY-medium with 1% glucose and appropriate antibiotics

2xTY-Expression medium

2xTY-medium with 0.1% glucose and appropriate antibiotics

IPTG (isopropyl- β -D-thiogalactopyranoside)

IPTG is a galactose derivate that triggers transcription of the lac operon. IPTG induces the transcription of the gene coding for beta-galactosidase, an enzyme that promotes lactose utilization, by binding and inhibiting the LacI repressor. In cloning experiments, the lacZ gene is replaced with the gene of interest and IPTG is then used to induce gene expression. Bacteria cannot hydrolyse it, preventing the cell from degrading the inductant.

Stock solution was 1 M in distilled water, sterile filtered. Aliquots (1 ml) were stored at -20°C. The final working concentration of IPTG is 1 mM for scFv expression and 0.4 mM for H1-CRD expression.

2.8.3.4 Agar Plates

For agar plates, Bacto agar was added to media to a final concentration of 1.5% (m/v) before autoclaving. After sterilization, the medium was cooled down to 50 °C and the appropriate antibiotics were added. The medium was poured into plates under laminar flow and allowed to solidify at room temperature. The plates were stored inverted at 4 °C in a sealed plastic bag.

2.8.3.5 Antibiotics for Selection

Chloramphenicol (Cam)

Chloramphenicol inhibits bacterial protein synthesis by blocking ribosomal peptidyl-transferase activity. It was used for selection of recombinant bacteria containing the pAK vectors.

1000x stock solution: 34 mg/ml in 100% ethanol; aliquots were stored at -20°C.

Kanamycin (Kan)

Kanamycin is a member of the aminoglycoside family of antibiotics and inhibits protein synthesis. It was used for selection of recombinant bacteria infected with

VCSM13 helper phage.

1000x stock solution: 25 mg/ml in distilled water, filter-sterilized (0.22 μ m).

Aliquots were stored at -20°C .

Tetracycline sulfate (Tet)

Tetracycline inhibits protein synthesis (elongation) by preventing binding of aminoacyl-tRNA to the 30S subunit. It was used for selective growth of XL1-Blue cells.

1000x stock solution: 12.5 mg/ml in distilled water, filter-sterilized. Aliquots were stored at -20°C in the dark.

Ampicillin, sodium salt (Amp)

Ampicillin inhibits the bacterial transpeptidase involved in peptidoglycan biosynthesis and thus inhibits cell wall synthesis. As such, ampicillin inhibits only log- phase bacteria. It was used for selection of recombinant bacteria containing the pHEN1 vector.

1000x stock solution was 100 mg/ml in distilled water, filter-sterilized. Aliquots were stored at -20°C .

2.8.4 Preparation of Competent Cells

Cells were cultivated in an Incubator shaker (Innova 4000, New Brunswick Scientific).

2.8.4.1 Rubidium Chloride Method for Chemo-competent *E.coli*

First, 1 ml of an overnight culture of DH5 α or XL1-Blue cells was inoculated in 100 ml Psi broth and grown at 37 $^{\circ}\text{C}$ with aeration to an OD_{600} = 0.5 and then put on ice for 15 min. The cells were pelleted in appropriate centrifuge tubes at 3-5000 x g for 5 min. The supernatant was discarded and the cells resuspended in 40 ml (0.4 x the original volume) Tfb 1 and incubated on ice for 15 min. Then the cells were pelleted again at 3-5000 g for 5 min. The supernatant was discarded and the cells resuspended in 4 ml (0.04 x volume) Tfb 2, kept on ice for 15 min and used directly for transformation or stored in aliquots of 200 μ l and shock frozen in liquid nitrogen prior to storage at -80°C . The cells were thawed on ice shortly before transformation ¹⁷⁷.

2.8.4.2 Cells for Electroporation

The *E. coli* strain was streaked out on LB-agar plates and incubated overnight at 37°C. Single colonies were picked and incubated overnight at 37°C in the incubator shaker in 5 ml SOB-medium without MgCl₂. Such overnight cultures were inoculated in 250 ml SOB-medium containing MgCl₂. During incubation, the optical density was measured at 600 nm (OD₆₀₀) every one to two hours. After reaching an OD₆₀₀ between 0.5 and 0.8, the cells were centrifuged at 5000 rpm and 4°C for 10 min. Cells were washed in cold 250 ml glycerol solution by re-suspension. Afterwards they were centrifuged again at 5000 rpm and 4°C for 10 min and resuspended in 50 ml cold glycerol solution. After an additional centrifugation step the cells were resuspended in 1 ml glycerol solution. Aliquots were immediately frozen in liquid nitrogen and stored at -80°C.

2.8.5 Transformation of *E. coli*

2.8.5.1 Heat-shock Transformation

Heat Shock Transformation for pAK Plasmid Amplification

Lyophilized pAK300 or pAK100 plasmid from 2 µl of a Midi-prep was obtained from the Plückthun lab. The plasmid was reconstituted in 10 µl of sterile TE buffer. Then 3 µl of the reconstituted pAK plasmids were mixed with 80 µl rubidium-competent DH5α cells and chilled on ice for 30 min. After a heat-shock at 42°C for 90s, the cells were put on ice for 2 min, then 400 µl of SOC medium was added and the cells incubated for 90 min at 37°C in the Thermomixer at 500 rpm. The cell suspension was split in two and spread on LB-Agar plates with Cam. The plates were then incubated over night at 37°C (Incubator Memmert). Single colonies were picked and inoculated in 2 ml LB-medium containing chloramphenicol. The cells were grown at 37°C under agitation at 250 rpm to reach an OD₆₀₀ of 2.5-3. Then 1.5 ml of the bacterial culture was harvested by centrifugation for 30s at 13'000 rpm. The supernatant was discarded and the pellet centrifuged again to remove residual supernatant and used for miniprep purification of the plasmids. Residual bacterial culture was used to prepare glycerol stocks.

Heat-shock Transformation of Competent BL21(DE3) Cells

Frozen rubidium chloride-chemocompetent BL21(DE3) cells were thawed on ice for some minutes. An aliquot of 80 μ l cells were mixed with 5 μ l of the Miniprep elutions of the plasmids pak300scFv and incubated on ice for 30min. After a heat-shock at 42°C for 90s the cells were put on ice for 2 min, then 400 μ l of SOC medium were added and the cells incubated for 90 min at 37°C in the Thermomixer at 500 rpm. This mixture was split in two and spread on LB-Agar plates with 34 μ g/ml chloramphenicol, and left in the laminar flow to dry. The plates were then incubated overnight at 37 °C (Incubator Memmert).

2.8.5.2 Electroporation

Desalting of Ligation Mixture

Prior to electroporation the ligase in the ligation reaction was first inactivated by heating to 65°C for 10 min, then the volume was supplemented to 50 μ l with ddH₂O and 500 μ l of 1-Butanol were added and the mixture vortexed for 10-20 s. The DNA was pelleted by centrifugation at 12'000 rpm for 15 min. The supernatant was discarded and the dried pellet was then resuspended in 10 μ l of ddH₂O¹⁷⁸.

Electroporation was performed using the Micro Pulser electroporation apparatus and Gene Pulser cuvettes 0.1 cm (Bio-Rad).

In 0.1 cm cuvettes, 50 μ l of electrocompetent cells were mixed with 5 μ l desalted ligation mixture. An electrical pulse with 1.80 kV was applied and immediately after the pulse 1 ml SOC medium was added to the cells. Afterwards, they were incubated at 37°C and 550 rpm on the thermomixer for 1.5 h. Subsequently, cell suspensions were streaked out on agar plates containing Cam.

2.8.6 Preparing Glycerol Stocks of Bacteria

For storage of transformed clones, 30 μ l of an overnight culture was inoculated in 3 ml LB-medium and incubated on a shaker for 4-5 hours, until the cells reached the exponential phase of growing. Then, 850 μ l culture were mixed with 150 μ l of sterile glycerol and directly shock-frozen in liquid nitrogen. Finally, the

aliquots were stored at -80°C .

2.8.7 Clone Picking and Plasmid Isolation (Mini-prep)

Isolation of plasmid DNA was performed using the GenElute plasmid Mini-prep kit from Sigma. Using a sterile pipette-tip, a single colony was picked and inoculated in 3 ml of LB-medium containing an appropriate antibiotic. The culture was grown on a shaking incubator (250 rpm, 37°C) until cells reached the stationary phase. Plasmid isolation was performed according to the supplier. The plasmid DNA out of 1.5 ml culture was finally eluted in 70 μl elution buffer.

2.9 Antibody Phage Display

All protocols were adapted from the manual of the 3rd Experimental Course in Antibody Phage Display Technologies¹⁵¹.

2.9.1.1 Exponential Growing Bacterial Cultures for Infection with Phage

Some microliters scratched of a frozen XL1 Blue bacterial stock were transferred into 3 ml of LB or 2xTY medium with Tet and grown over night at 37°C with shaking at 200 rpm. The next day the culture was diluted 1:100 (to OD 0.1) into fresh 2xTY medium and grown to OD 0.4-0.5 before infection with phage. The efficiency of infection is greatly reduced in cultures with an OD above 0.5.

2.9.1.2 Preparation of Helper Phage

First, 200 µl of *E. coli* XL1 Blue at OD 0.2 were infected with 10 µl of 1:100 serial dilutions of helper phage and mixed with 3 ml of H-top agar at 42°C, poured onto warm LB plates, and then incubated overnight at 30°C. A small, well separated plaque was picked and inoculated into 3-4 ml of an exponentially growing culture of XL1 Blue and grown for about 2 h and then inoculated into 500 ml of 2xTY, grown for 1 h and then supplemented with Kan to a final concentration of 70 µg/ml. The culture was grown another 16-20 h, then the supernatant was harvested by spinning down the bacteria at 7000 g for 30 min. Helper phage was immediately precipitated from the supernatant (see chapter 2.9.4). Aliquots in PBS with 10% glycerol were stored at -80°C.

2.9.2 Biopanning using Immunotubes

Nunc Maxisorp immunotubes were coated over night with 4 ml of a 20 µg/ml solution of human H1-CRD in HBS + 10 mM Ca²⁺, washed once with PBS and blocked with 3% BSA in PBS for 2 h at room temperature. The tube was rinsed 3 times with PBS, then 1 ml of library phage, 1 ml of PBS, and 2 ml of blocking solution were added and the tube sealed with parafilm. The phage were mixed and incubated with the H1-CRD by repeated inversion at RT for 30 min on a shaker, and then the phage was allowed to bind while the immunotube was standing upright at RT for 1.5 h. Unbound phage was discarded and the tube

washed 10 times with PBST (PBS with 0.1% Tween[®]20), and 10 times with PBS. Excess PBS was removed from the tube and the bound phage eluted by incubating 1 ml of a freshly prepared 100 mM triethylamine (Fluka) solution by repeated inversion for 5-10 min. The eluate was transferred to an Eppendorf-tube containing 0.5 ml Tris (1 M, pH 7.4) to neutralize the triethylamine.

2.9.3 Phage Amplification

For phage amplification, 10 ml of log-phase XL1 Blue cells (OD_{600} 0.4-0.5) were infected with the collected phage for 30-40 min at 37 °C and 70 rpm. To determine the titer of the phage, 10 μ l of the infected 10 ml XL1 Blue and a series of two 100-fold serial dilutions (titer = colonies $\times 10^3$, $\times 10^5$, and 10^7) in 2xTY using new pipette tips each time, were plated onto selective LB + glucose-agar. The titer plate was grown over night at 37°C. The remaining bacteria were spun down at 3300 g for 10 min, the pelleted bacteria resuspended in 0.5 ml 2xTY and spread on 2 big round agar plates of the appropriate selective 2xTY+1% glucose-agar and grown at 30°C. The plates were incubated until colonies were visible. Counting the colonies on the titer plate monitored the titer of the selection. The bacteria on the big agar plates were collected by gently loosen the bacteria with 5 ml 2xTY+15% glycerol with a glass spreader. Then, 50 ml of selective 2xTY+1% glucose were inoculated with enough bacterial suspension to yield an OD_{600} of 0.05-0.1. The remaining bacteria were stored at -80°C. The phage was rescued by growing the culture at 37°C to OD_{600} 0.4-0.5, infecting the cells with helper phage in a ratio of around 20:1 (phage : bacteria) for 30 min at 37°C. The infected bacteria were centrifuged at 3.300 g for 10 min and the pellet gently resuspended in 100 ml of selective 2xTY with Kan and grown overnight at 30 °C. Amplified phage was purified by PEG precipitation and stored in two separate 1 ml aliquots for further rounds of selection.

2.9.4 PEG precipitation of Phage

The phage was purified and concentrated by precipitation with PEG 8000 (Sigma).

PEG/NaCl solution 5x: 20% polyethylene glycol (PEG) 8000, 2.5 M NaCl in ddH₂O, sterile filtered.

Per 100 ml phage-containing supernatant 25 ml PEG/NaCl were added, mixed well and left for a minimum of 1 h at 4°C. This mixture was centrifuged at 3300 g for 30 min and the resulting pellet resuspended in 40 ml water, then 10 ml PEG/NaCl were added, mixed and left for a minimum of 20 min at 4°C. The mixture was centrifuged again and the supernatant discarded. An additional brief centrifugation step was included to remove remaining PEG/NaCl solution. The pellet was resuspended in 2 ml of PBS, and centrifuged for 2 min at 13'000 rpm to remove any residual bacterial cell debris. Long-term storage of the phage supernatant was in PBS with 10% glycerol at -80°C.

2.9.5 scFv Expression Screening ELISA

Goat anti-mouse IgG–HRP antibody and Sigma-fast OPD substrate were from Sigma, mouse anti c-myc antibody clone 9E10 was a kind gift of the Group of Prof. M.Hall, Biocenter Basel.

Individual colonies from the selection plates of phage-infected XL1 Blue after the second and fifth round of selection were picked using a toothpick, inoculated into 160 µl selective 2xTY with 0.1% glucose in 96-well U-bottom plates and grown for 3 h at 37°C in a shaking incubator. A replica plate was prepared by transferring 50 µl of bacterial supernatant into 50 µl 40% glycerol prior to induction. The replica glycerol plates were stored at -80°C. Then scFv expression was induced by the addition of 40 µl of a 5 mM IPTG solution to each well (final concentration 1 mM) and incubation of the plate in a shaking incubator at 30°C for 16 - 24 hours. The plate was centrifuged at 1800 g for 10 min to pellet bacteria, and then the supernatant containing the soluble scFv fragments was transferred to the prepared ELISA plate.

2.9.5.1 Preparation of ELISA Plate for scFv Expression Screening

H1-CRD, 5 µg/ml in HBS+10 mM Ca²⁺, was immobilized over night on a Nunc MaxiSorb 96 well Immunoplate. The coating solution was discarded and the plate was blocked with 200 µl PBS + 3% BSA for 2 h at room temperature. The plate was washed 3 times with PBS. Then, 90 µl of bacterial supernatant were transferred to the ELISA plate-wells and 20 µl of 5x mouse anti-c-myc antibody (1:1000) in PBS + 3% BSA were added. The plate was incubated for

2 h at room temperature in an orbital plate shaker at 200 rpm. The plate was washed again 3 times with PBS before adding 100 μ l goat anti-mouse IgG–HRP antibody (1:1000) in PBS + 1% BSA with incubation for 1 h at room temperature. The plate was washed 3 times with PB + 0.1% Tween followed by 3 times with PBS. Excess humidity was removed by tapping the plates upside down on tissue paper, and then 100 μ l of OPD substrate solution were added and incubated for about 5 min. The OD was determined at $\lambda = 450\text{nm}$ on a Spectramax 190 plate-reader.

2.9.6 Screening for murine scFv Clones by Colony Blotting

The HisDetector Nickel-AP kit was from KPL.

10% SDS in H₂O, adjusted to pH 7.2

Denaturing solution: 0.5 M NaOH, 1.5 M NaCl

Neutralization solution: 1.5 M NaCl, 0.5 M Tris, pH 7.4

20x SSC: 3 M NaCl, 0.3 M Sodium citrate, pH 7.0

Freshly transformed BL21(DE3)-cells were plated on LB agar plates with Cam and 0.5% glucose, and incubated over night at 37°C. First the plate-lids were slightly opened to let the condensation dry, then dry numbered nitrocellulose membranes were placed on the agar surface to get in contact with the colonies. The filters and agar were pierced asymmetrically with a syringe needle for later alignment. Then the membranes were removed and placed with the colony side up onto LB agar plates containing Cam, 0.5% glucose, and 250 μ M IPTG and incubated for 4 h at 37°C. (the colonies of the master plates were later re-grown for 4 h at 30°C).

A set of Petri dishes containing filter papers soaked with the following buffers were prepared and the nitrocellulose membranes placed with the colony side up on top of the filters incubated as indicated:

1.	10%SDS	10 min
2.	Denaturing solution	5 min
3.	Neutralization solution	5 min
4.	Neutralization solution	5 min
5.	2x SSC	15 min

The membranes were then further processed like western blots and all

incubation steps were performed on a shaker at RT. The membranes were washed twice for 10 min with TBS buffer, and then incubated for 1h in blocking buffer (1x Detector Block solution from the kit) at RT. Then they were washed twice for 10 min in TBST buffer, and once for 10 min in TBS buffer. The membranes were incubated for 1 h in 10ml HisDetector Nickel-AP conjugate solution (1:1000 diluted in Detector Block solution) at room temperature, and washed again twice for 10 min in TBST and once in TBS buffer. The membranes were soaked in 20 ml substrate buffer with 100 μ l of NBT/BCIP-substrate and incubated until a clearly visible signal appeared. Rinsing the membrane twice with water stopped the reaction.

2.9.7 Expression of soluble scFv in *E.coli*

2.9.8 Purification of murine scFv via His-tag

2.9.8.1 Periplasmic extraction

S-Buffer: 100 mM Tris, 0.5 M saccharose (Sigma), 1 mM EDTA, pH 8.0, sterile filtered.

When using pAK300 as expression vector in BL21(DE3) cells, scFv fragments should be enriched in the periplasmic space of the bacteria. To harvest the periplasmic fraction, the cell wall of the bacteria was destroyed by osmotic shock treatment.

The bacterial pellet of 500 ml culture was washed once in PBS, centrifuged at 7500 g for 20 min and 4°C. The washed pellet was resuspended in 20 ml of ice-cold S-Buffer and incubated for 30 min on ice with slow spinning and then centrifuged again. The supernatant (periplasmic fraction) was removed and kept on ice, while the pelleted spheroblasts were resuspended in 20 ml of a 5 mM MgSO₄ solution and incubated on ice for another 20 min. After a further centrifugation step, the supernatant (osmotic shock fraction) was removed and combined with the periplasmic fraction and dialyzed over night against loading buffer (PBS, 0.5 M NaCl, 20 mM imidazole, pH 7.4)

2.9.8.2 Downstream Protein Purification

Affinity chromatography of murine scFv

HisTrap FF crude columns (1ml) were from GE Healthcare, imidazole and NaCl from Fluka. PBS buffer (pH 7.4) was selfmade or from Invitrogen. Purification was carried out on a BioLogic FPLC system (Bio-Rad).

Loading: PBS, 0.5 M NaCl, 20 mM imidazole (pH 7.4)

Wash buffer: PBS, 0.5 M NaCl, 20 mM imidazole (pH 7.4), 0.05% Tween[®] 20

Elution buffer: PBS, 0.5 M NaCl, 100 mM imidazole (pH 7.4)

All purification steps were carried out at a flow-rate of 1 ml/min and at 4°C.

The column was equilibrated with 5 column volumes (CV) loading buffer. The combined, dialyzed periplasmic and osmotic shock fraction were loaded at 1ml/min, the column was washed with 30-40 CV of wash buffer and the bound protein eluted with 10 CV of elution buffer. The eluate was collected in 1-2 ml fractions and analyzed by SDS-PAGE and WB.

2.9.9 Purification of human scFv

Affinity chromatography using Protein A-Sepharose can be applied to purify antibody fragments encoded by V_H segments from the V_H3 family¹⁴⁰.

Protein A Sepharose column 5 ml was from Biovision

Wash buffer 1: PBS, 0.5 M NaCl, pH 7.4, 0.05% Tween 20

Wash buffer 2: PBS, 0.5 M NaCl, pH 7.4

Elution buffer: 0.2 M Glycine pH 3.0

Neutralization buffer: 1 M Tris, pH 8.0

All purification steps were carried out at a flow-rate of 1 ml/min at 4°C. The column was equilibrated with 3 CV of PBS, then it was loaded with filtered (0.45 µm) supernatant, firstly washed with 6 CV of wash buffer 1, then 5 CV of wash buffer 2. The protein was eluted with 2 CV of elution buffer and the 2-3 ml eluates were collected into tubes containing neutralization buffer for immediate pH correction to pH 7.4.

2.9.9.1 Buffer Exchange and Sample Concentration

Due to the known stability of antibodies in PBS, the buffer of the scFv samples was exchanged to PBS after purification. Additionally, the concentration was increased.

Buffer exchange and sample concentration of the combined fractions was carried out with centrifugal filter devices Vivaspin 4, cutoff 5 kDa (Sartorius). All centrifugation steps were performed at 4°C and 7'000 g. First, the filter device was washed twice with 4 ml of PBS to remove glycerol from the membrane. Then a maximum of 4 ml of sample was applied. The final concentrated sample was washed twice using 4 ml of PBS.

2.9.10 Analysis of Binding Properties of murine scFv in ELISA

The plate was prepared and the assay performed as described in chapter 2.2.1, with the exception that instead of a glycomimetic compound the purified C11.1scFv in a 1:2 dilution series from 100 to 6.5 µg/ml (50 µl/well) was distributed to the wells (n=8 per concentration). To half of the plate 50 µl of a preformed conjugate of biot. GalNAc–PAA with streptavidin-peroxidase, diluted to give a final concentration of 0.5 µg/ml of PAA-polymer and 1U/ml of Streptavidin-peroxidase were added, whereas the second half was incubated with scFv only. The plate was incubated for 2 hours at room temperature in a humid chamber on a laboratory shaker at 100 rpm. After the incubation, the plate was carefully washed twice with HBS + Ca²⁺ followed by the addition of ABTS–substrate to the half plate with the polymer (and stopping the colour development after 2 min) while adding HRP-Ni conjugate (KPL) diluted 1:500 in assay buffer to the second half of the plate and incubating another hour. After the incubation, the second half of the plate treated with HRP-Ni was carefully washed twice with HBS + Ca²⁺ followed by the addition of ABTS–substrate. Color was allowed to develop and then the reaction was stopped with 2% oxalic acid in H₂O. Bound GalNAc-PAA-complex and bound scFv detected with HRP-Ni was measured by determining the optical density (OD) of the occurring blue-green color at $\lambda = 415$ nm with a Spectramax 190 plate-reader (Molecular Devices).

2.9.11 Affinity Measurements

Affinity measurements were performed on a Biacore 3000 surface plasmon resonance based optical biosensor (Biacore AB, Sweden). CM5 Sensor chips, the amine coupling kit (including all reagents needed for the immobilization procedure (*N*-hydroxysuccinimide (NHS), 3-(*N,N*-dimethylamino) propyl-*N*-ethylcarbo-di-imide (EDC), ethanolamine HCl), maintenance supply and ready-to-use (degassed and filtered) standard buffers HBS-P (10 mM HEPES, 150 mM NaCl, pH 7.4 + 0.005% (v/v) Tween 20) and HBS-EP (HBS-P + 3 mM EDTA) were purchased from Biacore AB. Data processing and equilibrium binding constant determinations were accomplished with Scrubber (Version 2.0). Double referencing was applied to correct for bulk effects and other systematic artifacts¹⁷⁹.

Amine coupling

The immobilization of H1-CRD to a CM5–chip was optimized by D. Ricklin⁷⁵

Before use, the sensor chips were preconditioned by injecting a series of conditioning solutions. Twice a cycle of 20 µl of 50 mM NaOH followed by 10 mM HCl, 0.1% SDS and 100 mM H₃PO₄ was injected at a flow rate of 50 µl/min. After preconditioning the chip was used for immobilization within the next 2 hours.

The carboxy-groups on the chip were activated for 7 minutes with a 1:2 mixture of 0.1 M *N*-hydroxysuccinimide (NHS) and 0.1 M 3-(*N,N*-dimethylamino) propyl-*N*-ethylcarbo-di-imide (EDC) at a flow rate of 5 µl/min. The H1-CRD solution (730 µg/ml, batch 071115) was diluted to 300 µg/ml in HBS-EP. Of this solution, 20 µl were mixed with 80 µl of acetate buffer to pH 5.0. This mixture was then injected to flow over the activated surface at a flow rate of 5 µl/min for 30-35 s⁷⁵. Obtained densities were between 3600 to 4400 RU depending on the contact time. Afterwards the flow cell was blocked with a 7 min injection of 1 M ethanolamine, pH 8.0. A reference cell was treated the same way (activation-deactivation) without immobilization of protein.

2.9.12 Activity Testing of H1-CRD in SPR

A 100 mM stock solution of GalNAc was prepared in running buffer (HBS-P with

50mM Ca^{2+}). Activity testing of H1-CRD was performed by injecting randomized twofold serial dilutions between 5 mM and 5 μM . Each sample was injected for 30 s with an undisturbed dissociation phase of 20 s using the instruments kinject command at a flow rate of 50 $\mu\text{l}/\text{min}$. No regeneration or washing steps was applied. Five buffer blanks were injected at the beginning of the series and one at the end. Signals of the reference flow cell and averaged blank injections were subtracted from the sample sensorgrams. Since referenced sensorgrams showed negative SPR signals, they were mirrored by multiplication of each data point with -1. Mirrored steady state data were evaluated between 10 and 20 s of the injection period and were fitted to a single site-binding model using Scrubber software version 2.1.

2.9.13 Affinity Testing of scFv

The concentration of the purified scFv samples was estimated from SDS-PAGE (15% non-reducing) after changing the buffer to HBS-P+ 50 mM CaCl_2 using Vivaspin 6 (cutoff 10 kDa) centrifugal filtering devices (Sartorius).

In a first screening assay, each scFv was injected at a concentration of 9 nM for 10 min with a dissociation phase of 10 min at a flow rate of 25 $\mu\text{l}/\text{min}$. Finally, the surface was regenerated by HBS-EP injection during 10 min and a regeneration phase of 10 min with the running buffer HBS-P+50mM Ca^{2+} .

Affinity testing of scFv antibody 5B8 and 2E8 was conducted by injecting a twofold dilution series of 1.6 μM to 0.19 pM for 5B8 and 0.8 μM to 0.19 pM for 2E8. Samples were injected in a randomized order for 9 min at a flow rate of 25 $\mu\text{l}/\text{min}$. After a 10 min dissociation phase, the surface was regenerated by HBS-EP injection during 10 min at 25 $\mu\text{l}/\text{min}$ and a regeneration phase of 10 min with the running buffer HBS-P+50mM Ca^{2+} at 25 $\mu\text{l}/\text{min}$. Five buffer blanks were injected at the beginning of the series and one at the end. Signals of the reference flow cell and averaged blank injections were subtracted from the sample sensorgrams. Steady state data were evaluated between 10 and 20 s of the injection period and were fitted to a single site-binding model using Scrubber software version 2.1.

3. Results and Discussion

3.1 H1-CRD Production

The ability to test physiological and synthetic ligands on an isolated form of a receptor is a prerequisite for a deep understanding of molecular binding events. Since only the extracellular carbohydrate recognition domain of the human hepatic asialoglycoprotein receptor is involved in ligand binding and its activity is not influenced by posttranslational glycosylation, the lectin domain can be expressed in *E.coli*.

A truncated form of the H1 subunit of the ASGP receptor including the whole CRD domain (amino acid residues 147-291), the human hepatic asialoglycoprotein receptor H1-CRD, was produced in *E. coli* based on a published method^{73, 180}. Even though a protocol for the expression and purification already existed, the yields were rather low and the protein fraction contained several populations. The method was therefore further optimized by Rita Born, in order to increase both yield and purity¹⁶⁶. The H1-CRD production cycle is summarized in Figure 27.

Briefly, the protein was expressed as inclusion bodies in *E. coli* strain AD494(DE3) transformed with the plasmid pET3H1C⁷³. After IPTG (0.4 mM) induced expression in TB medium for 5 h at 37°C, the cells were harvested by centrifugation at 4°C and 5000 g for 10 minutes, resuspended in 20 mM Tris (pH 8.0) and lysed by sonication. The protein was denatured under reducing conditions and refolded by extent dialysis against Tris buffer. First, the correctly folded H1-CRD was purified by affinity chromatography using a Gal-Sepharose column connected to an FPLC-system (Bio-Rad)¹⁸¹.

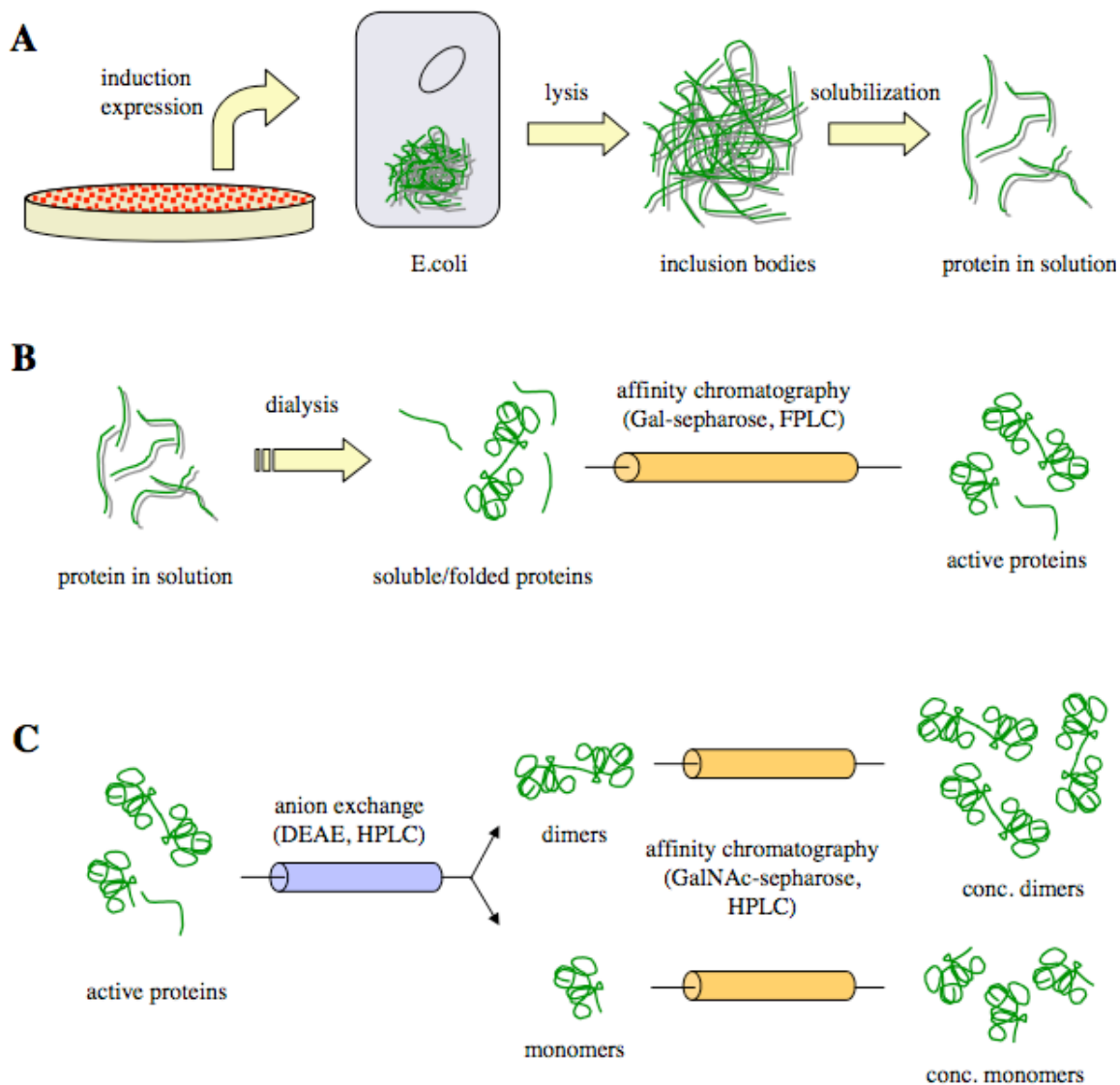


Figure 27. Simplified overview of the production cycle of H1-CRD (A) H1-CRD expression, (B) primary purification, and (C) monomer/dimer separation. Picture by courtesy of D.Ricklin

After a desalting step with a HiTrap Desalting column, the protein was separated into a monomer and dimer fraction by Ion exchange HPLC on a DEAE column.

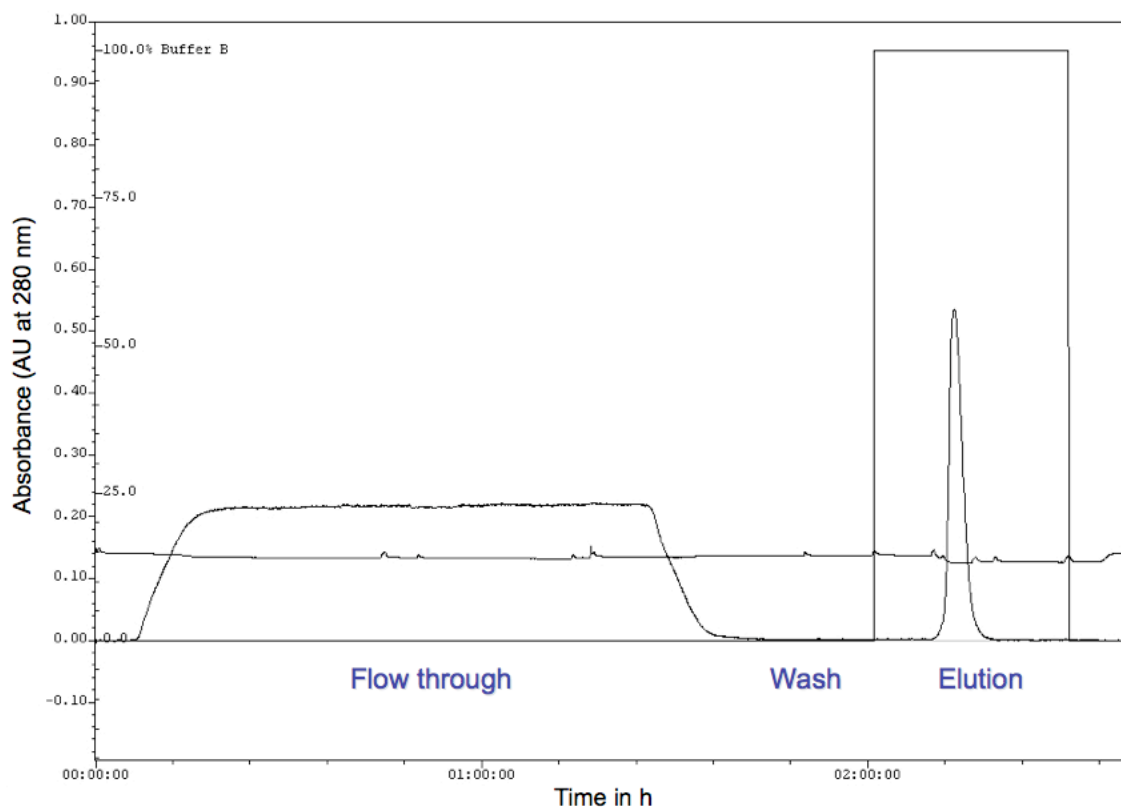


Figure 28. Affinity chromatography H1-CRD

After the loading (flow through) and washing step, a distinct peak can be seen during the elution, representing the H1-CRD.

Eluted fractions were analyzed by reducing SDS-PAGE (Figure 29). H1-CRD was predominately enriched in the eluates 3-4 (lane 8 and 9), corresponding to the elution peak in the chromatogram. H1-CRD could also be spotted in the flow through (lane 4), indicating either overloading of the column or alternatively misfolded protein.

Lane
 1 Marker
 2 Reference H1-CRD
 3 Loaded sample
 4 Flow through
 5 Wash
 6 Eluate 1
 7 Eluate 2
 8 Eluate 3
 9 Eluate 4
 10 Eluate 5

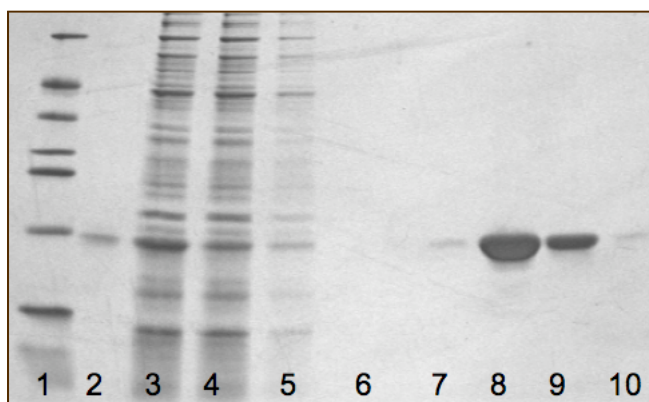


Figure 29. Analysis of collected affinity chromatography fractions of H1-CRD (Reducing 15% SDS-PAGE)

Analysis with non-reducing SDS-PAGE shows the occurrence of both

monomeric and dimeric H1-CRD (Figure 31, lane 2). No consistent ratio of the two species could be determined, as the fractions appeared to vary among different batches.

To separate the monomers and dimers, HPLC IEC was employed. Protein samples were loaded onto a DEAE column and eluted with a CaCl_2 gradient.

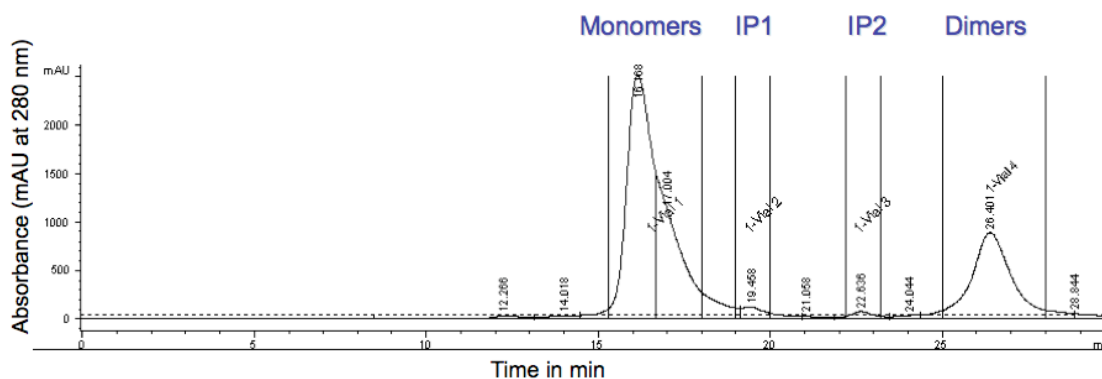


Figure 30. Separation of H1-CRD monomers and dimers by HPLC. IP1 and IP2 are minor impurities that are present in every batch of H1-CRD.

Monomeric H1-CRD, less charged than the dimeric form, was found to elute at a lower CaCl_2 concentration, while the dimers emerged at higher CaCl_2 concentration. Repeated injections of H1-CRD showed highly similar chromatograms, confirming the reproducibility of the method (data not shown). The monomers could be seen in the HPLC chromatogram as the first peak with a tailing shoulder (IP1). A small, unidentified impurity peak (IP2) was seen following the monomers and preceding the dimers. The final peak corresponds to dimers of H1-CRD (Figure 30).

- | | |
|------|----------------------|
| Lane | |
| 1 | Marker |
| 2 | H1-CRD, FPLC elution |
| 3 | Monomer fraction |
| 4 | Shoulder fraction |
| 5 | Impurity fraction |
| 6 | Dimer fraction |

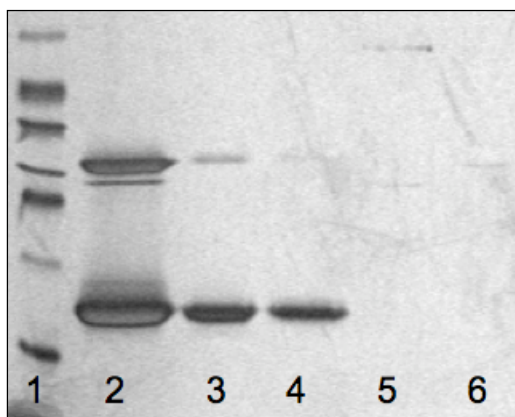


Figure 31. Analysis of fractions collected during HPLC IEC. Fractions (lane 3, 4 and 7) are clearly enriched in monomers, but also contain traces of dimers (15% Non-reducing SDS-PAGE).

The monomeric H1-CRD was concentrated by rebinding to a GalNAc-

Sepharose column (Figure 32) and the final protein concentration estimated by Bradford assay¹⁷⁰.

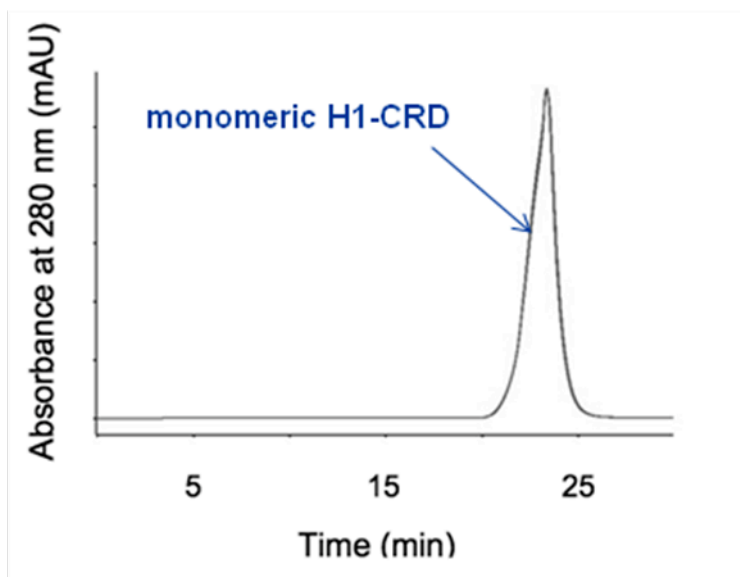


Figure 32. Final preparation of monomeric H1-CRD
Monomer fractions were pooled and purified by HPLC affinity chromatography using a GalNAc-Sepharose column.

From 4L of processed expression culture a total of 4.73 mg of monomeric H1-CRD and 1.30 mg of dimeric H1-CRD were purified.

3.1.1 Production of a Big Batch of H1-CRD

To be able to do all assay developments, SPR measurements, and NMR studies on the same batch of protein, a big batch of H1-CRD was produced starting from 41.7 g of wet pellet from *E.coli* AD494 (DE3) clone 4 cells containing pET3H1C produced in a 14 L fermentor at Roche and was processed in 3 batches according to the methods described in Chapter 0.

The eluted H1-CRD fractions were collected and each starting batch was concentrated separately using Icon concentrators (20ml, 9 kDa, Pierce). The samples were concentrated up to ca. 1/4 of the starting volume and Tris-buffer (25mM, pH 8) was supplemented to a final volume of ca. 12-13 ml. This step was repeated 4 times to reduce the salt load from the elution and change the buffer. After the HPLC separation of monomers and dimers on a DEAE-column, the samples were concentrated again with Icon concentrators and the protein concentration estimated by Bradford. This batch yielded in 14.51 mg of H1-CRD monomers. Aliquots of 500 μ l a 730 μ g/ml were shock frozen in liquid nitrogen.

and stored at -20°C . After thawing, the samples were kept at 4°C and were stable for several weeks.

3.1.1.1 Stability of the Protein

The protein of the first, smaller batch was stable for one year when stored at -20°C as shock-frozen aliquots of $500\ \mu\text{l}$ in HBS + 1mM CaCl_2 , then the binding activity of the protein decreased, also observed in the competitive solid phase assay. The activity of the protein could be stabilized by the addition of more calcium to the HBS buffer (data not shown). Although the absolute IC_{50} obtained with the long-storage protein where about a third lower than the IC_{50} obtained with fresh H1-CRD, this did not hamper the evaluation of new compounds, as the IC_{50} of all measured compounds decreased to the same extent, the relative IC_{50} 's, in comparison with GalNAc remained the same. The second, big batch of H1-CRD in a storage buffer with increased content of calcium, HBS with $10\ \text{mM CaCl}_2$ instead of the previous $1\ \text{mM CaCl}_2$, was still active after two years.

The protein dimerizes upon storage and was a $\sim 1:2$ mixture of monomers ($17\ \text{kDa}$) and dimers ($34\ \text{kDa}$) after 1 year of storage at -20°C (Figure 33).

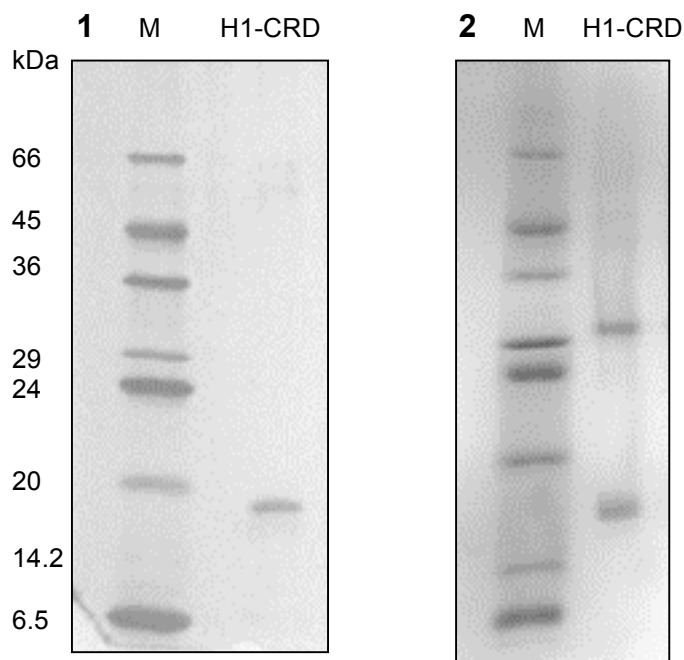


Figure 33. Purified H1-CRD monomers after 1 year of storage
(1) SDS-PAGE (15%) under reducing conditions (2) SDS-PAGE (15%) under non-reducing conditions

Conclusion

Although the purification procedure of H1-CRD was constantly optimized and simplified and lead to highly pure and active protein, the purification stayed tedious and time consuming, especially when larger amounts were produced to obtain a consistent batch of protein (e.g. due to the limited loading capacity of the column in the separation of monomers and dimers by HPLC). Using size exclusion chromatography (SEC) at this step seemed to be the obvious choice. D.Ricklin attempted using SEC for separation, but the protein could not be isolated in its monomeric form even when using a relatively long (60 cm) column for better resolution. In addition, the lectin domain was found to interact with the column material and the size exclusion method was therefore regarded as non-suitable for the separation of H1-CRD monomers and dimers.

A problem that occurred during production and could be omitted with the optimized procedure was the precipitation of protein during the refolding by dialysis step. It was also observed that in the desalting step with the Amersham desalting columns some protein was found in the wash solution, indicating an overload of the column. When the big batch of H1-CRD was produced, the protein was therefore desalted and concentrated by centrifugation using Icon concentrators. There the observation was made that when the protein is too concentrated (> 2 mg/ml) precipitates occur, which can also lead to a loss in the overall yield of protein.

The dimer content was not fully consistent from batch to batch and even after the HPLC separation of monomers and dimers, the occurrence of dimer formation could not be avoided. The reason for this was thought to be an odd cysteine in the H1-CRD structure, which contains 7 cysteines (further discussed in ²⁰²).

3.2 Heterogeneous Competitive Solid-phase Binding Assay

3.2.1 Selection of the Competitive Ligand and Buffer System

Some general criteria which influence the selection of a possible ligand-probe in a competitive binding assay are that it should bind to the same receptor site as the unlabelled ligands, it should be chemically stable and resistant to enzymatic and hydrolytic degradation and non-specific binding to plastic materials used must be minimal. Heterogeneity of natural glycoconjugates, in particular glycoproteins, complicates their use as tools for the study of carbohydrate-binding molecules, so the synthetic analogues of glycoconjugates play an important role in glycobiology research. Polyacrylamide, used as a high molecular weight carrier (M_r approx. 30 kDa), has a low non-specific sorption and is stable to chemical and proteolytic action.

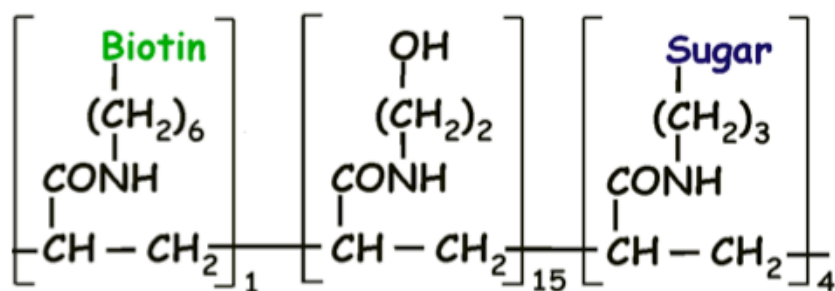


Figure 34. Constitution of a biotin labeled glyco-PAA-polymer

GalNAc-PAA-polymer was selected as competitive ligand due to the fact that of the natural sugar ligands Gal and GalNAc, the H1-CRD has a higher affinity for the latter (as shown in Table 22). In Rat, the affinity of RHL1 (rat hepatic lectin 1), which has a high homology to the human H1 subunit (80%), is reported to be even 50 times higher for GalNAc than for Gal⁶².

The PAA-polymer contains 20% mol of β -N-acetylgalactosamine-moieties and biotin (as 6-aminohexylamide) at 5% mol, which enables the detection of the polymer binding when conjugated with Streptavidin-Peroxidase. The polyacrylamide carrier forms a random coil of about 30 kDa with flexible distance between the attached β -N-acetylgalactosamine-moieties¹⁸². This flexibility allows the residues to adjust themselves to bind their target molecule H1-CRD. For more information on polyacrylamide type glycoconjugates see the

review by Bovin ¹⁸³.

Setup of the competitive solid-phase assay

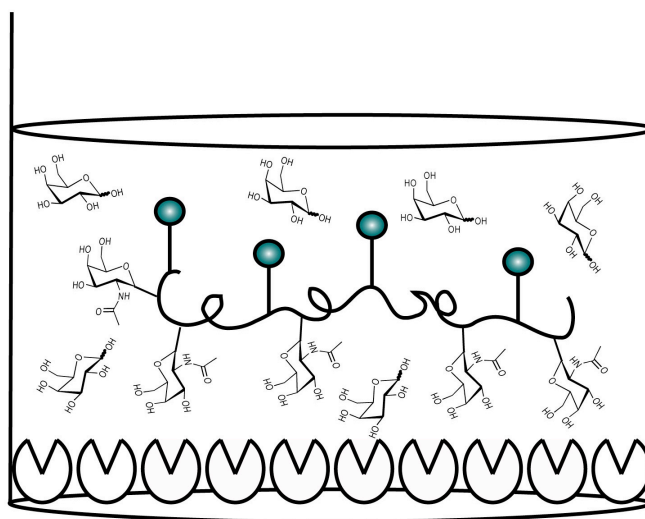


Figure 35. Setup of the competitive solid-phase binding assay
Setup of the competitive solid-phase binding assay for the screening of GalNAc-derivates. H1-CRD is adsorbed on the plastic surface of 96-well-plates and specifically interacts with the probe biot. GalNAc-PAA-polymer (pre-complexed with Streptavidin-Peroxidase). If the studied compound binds to the H1-CRD, a decrease in the color development of ABTS-substrate is registered.

Since it provides stable buffering in the physiological pH-range and allows the addition of calcium, which is not the case for PBS, in which calcium precipitates as calcium phosphate, the HEPES buffer system was selected for the assay buffer. A Tris buffer system could also be used, but it has the disadvantage of a temperature dependent pH. As the pH is important for the conformation of the protein and therefore the ligand binding to H1-CRD, Tris buffer was avoided.

3.2.2 Receptor / Ligand Probe Concentrations

Different concentrations of both the ligand probe and the protein were titrated against each other. To find the conditions to attain an optimal signal-to-noise ratio of binding to the immobilized H1-CRD of around 10, H1-CRD in the concentration of 0-5 $\mu\text{g/ml}$ was immobilized on the plate and incubated with different concentrations of the polymer (0.1, 0.5, 1 $\mu\text{g/ml}$) (see Figure 36).

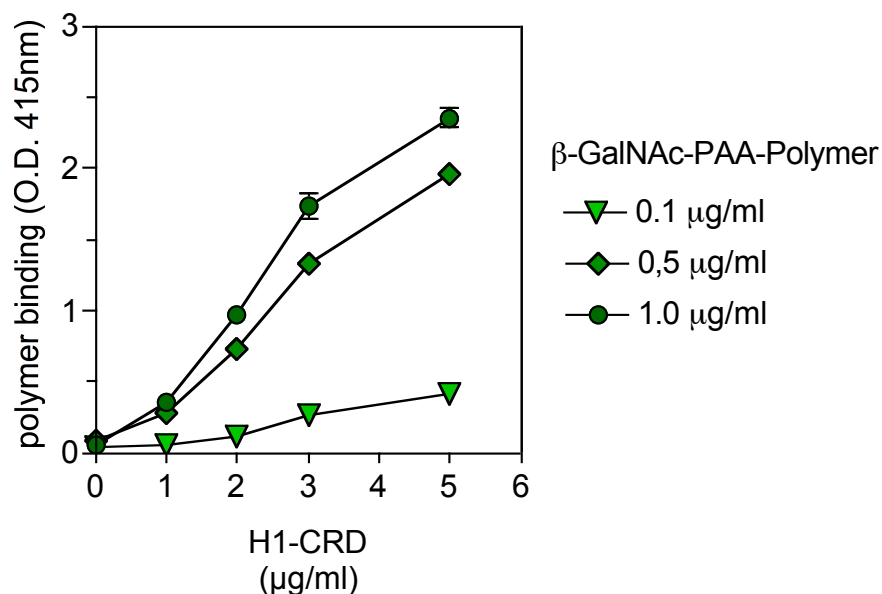


Figure 36. Optimization of H1-CRD and polymer concentrations
Mean of O.D. \pm S.D. (n=4)

The combination of 3 µg/ml of H1-CRD on the plate and 0.5 µg/ml biot. β -GalNAc-PAA-polymer for binding resulted in a good signal-to-noise ratio and stable assay conditions with a reasonable consumption of protein and polymer and was therefore introduced as standard for the assay.

3.2.3 Specificity of the Assay System

Because the H1-CRD is a C-type lectin domain, its binding of D-Galactose or D-GalNAc moieties is dependent on the presence of calcium. Therefore the effect of EDTA as a calcium-chelator was tested in concentrations from 0.01 to 3 mM. As shown in Figure 37, 1 mM EDTA completely abolished the binding of biot.GalNAc-PAA-polymer to the immobilized H1-CRD.

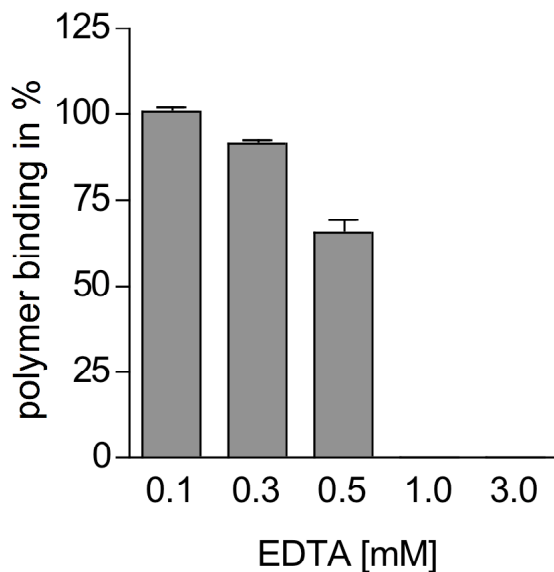


Figure 37. Calcium dependency of polymer binding
Mean \pm S.D. (n=4)

To further confirm the specificity of the binding, two other carbohydrate-PAA-polymers expected not to bind to the H1-CRD of the ASGP-R were tested as ligand-probes. Instead of 20%mol β -GalNAc, these glyco-PAA-polymers contain either 20%mol of β -D-Glucose or sLe^a residues.

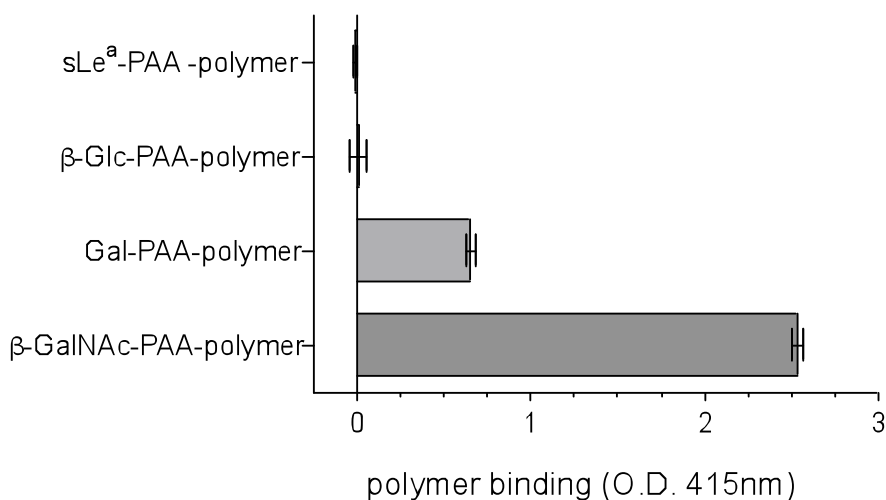


Figure 38. Binding of different glycopolymers to the H1-CRD
Mean \pm S.D. (n=4)

In the concentrations tested (0.5 μ g/ml), no specific binding of these polymers could be detected. This confirms the specificity of the binding of GalNAc-residues on the β -GalNAc-PAA-polymer to the H1-CRD (Figure 38). In the competitive solid-phase assay, binding of Gal-PAA-polymer to H1-CRD is about

4 times lower than of β -GalNAc-PAA-polymer, which corresponds to the results obtained in SPR experiments, where the K_D 's of monovalent β -GalNAc and D-Gal show a 10 times difference in affinity ⁷⁵ (see Table 22).

3.2.4 Variability of the Assay

The variability of the assay system was evaluated in 5 independent experiments (N=5). The OD-values for GalNAc-PAA-polymer binding to wells in absence of H1-CRD (unspecific or 0% binding) or in presence of H1-CRD-coating of the wells (specific or 100% binding) was acquired under standard assay conditions. Every experiment includes the measured OD values of 6 wells (n=6).

Table 21. Variability measurements

Unspecific binding (0%)	Experiments					Mean (N)
	1	2	3	4	5	
OD value means (of n=6)	0.212	0.127	0.138	0.075	0.116	0.134
SD	0.009	0.026	0.016	0.016	0.026	0.019
CV (%)	4.03	20.47	11.59	21.33	22.41	13.86

Specific binding (100%)	Experiments					Mean (N)
	1	2	3	4	5	
OD value means (of n=6)	1.668	1.720	1.611	1.507	1.964	1.694
SD	0.112	0.046	0.097	0.062	0.095	0.082
CV (%)	6.69	2.67	6.02	4.11	4.84	4.86

The assay evinces a low day-to-day variability below 15%, and the use of different preparations of GalNAc -PAA-polymer complexed with streptavidin-POD had no influence on the results.

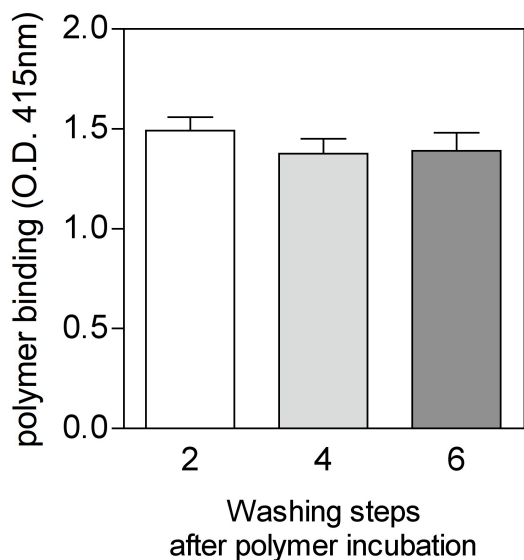


Figure 39. Washing steps after polymer incubation

The results depicted in Figure 39 reveal that polymer binding to H1-CRD is very stable. Even an increase of the last washing steps of the plate after polymer incubation from 2 to 6 did not influence the OD significantly.

3.2.4.1 Probing pH Dependence of Ligand Binding to H1-CRD

Ligand binding to the ASGP-R is pH dependent, as the receptor has to release its ligand upon fusion with endosomes. This mechanism is caused by a decrease of the endosomal pH to 5.4, which leads to a conformational change of the receptor followed by a release of the calcium ions and the ligand. In rat ASGP-R, charged amino acids in and next to the binding site were identified as a molecular 'switch', which initiates the ligand release. The key step in this mechanism is the protonation of His202 which corresponds to His256 in human H1-CRD¹⁸⁴. Therefore, ligand binding to the H1-CRD is expected to show a significant pH-dependency in a critical pH range below 6.5. In order to investigate the effect of pH on ligand binding to the H1-CRD, GalNAc-PAA-polymer diluted in buffer at various pH values was incubated with the protein on the plate, applying standard assay conditions. In addition, after polymer binding and washing of the plate, the pH in the wells was re-equilibrated to pH 7.4 with an incubation step of 10 min using the standard buffer. The buffer used during the incubation step of GalNAc-PAA-polymer on immobilized H1-CRD was HBS+1 mM Ca²⁺ adjusted to pH 4, 5, 6, 7, 7.4, and 8. Since some pH values

(pH 4, 5, 6) were below the buffer capacity range of HEPES (pKa = 7.55), the pH of the buffers was carefully controlled before and after the experiment.

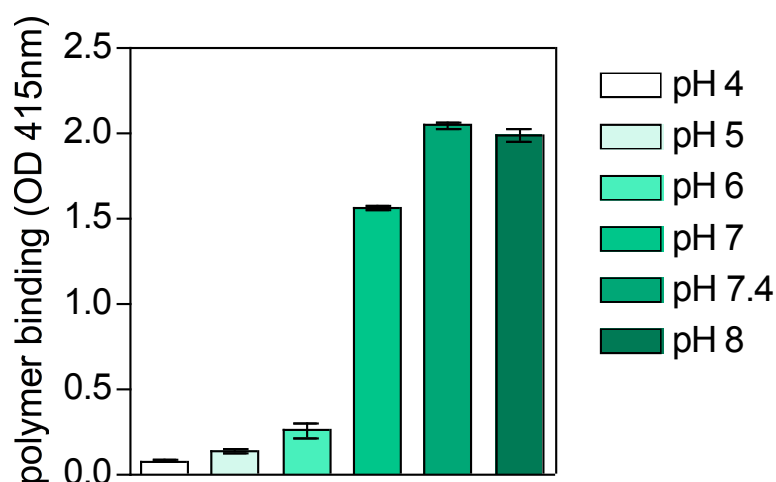


Figure 40. pH dependency of ligand binding to the H1-CRD

OD values for each pH were measured in quadruplicates. While a decrease of pH from 7.4 to 7 showed only a slight influence on binding, a significant activity drop was visible at pH 6.0. Finally, essentially no binding could be detected when lowering the buffer below pH 5 (Figure 40). The obtained results confirmed the pH-dependency of binding for β -GalNAc and D-Gal to H1-CRD observed by D.Ricklin in SPR⁷⁵, the results of the NMR experiments performed with the H1-CRD at our institute by Dr. B. Cutting, and are also in good agreement with the findings reported in literature. For rat ASGP-R, a rapid decrease of ligand binding was reported when lowering the pH from 8.8 to 4.8. The midpoint of ligand release was reported to be at pH 7.1 and almost all ligand was released at the endosomal pH of 5.4¹⁸⁴.

3.2.4.2 Amount of Calcium in Buffer

Initially the assay was set up with a buffer system containing a physiological amount of 1mM calcium, but experience showed that long term storage of the recombinantly produced H1-CRD in a buffer containing more calcium (10 mM instead 1mM) improved the stability and activity of the protein. Moreover the calcium content in the buffer for SPR experiments had to be increased to 50 mM to achieve stable binding. Hence, the influence of higher amounts of calcium in the buffer system on β -GalNAc-PAA-polymer binding to H1-CRD was

evaluated. For this purpose, H1-CRD was either coated to the plate over night in buffer containing 20 mM Ca^{2+} , or the 2 h- binding step of the polymer to the H1-CRD in the presence of of the competitor D-galactose (10, 3, 1 and 0.3 mM) was performed with buffer containing 20 mM Ca^{2+} , or this buffer was used in both steps (coating and binding). The IC_{50} s of galactose under these different conditions were compared to the results obtained with the buffer containing 1 mM Ca^{2+} during all incubation steps.

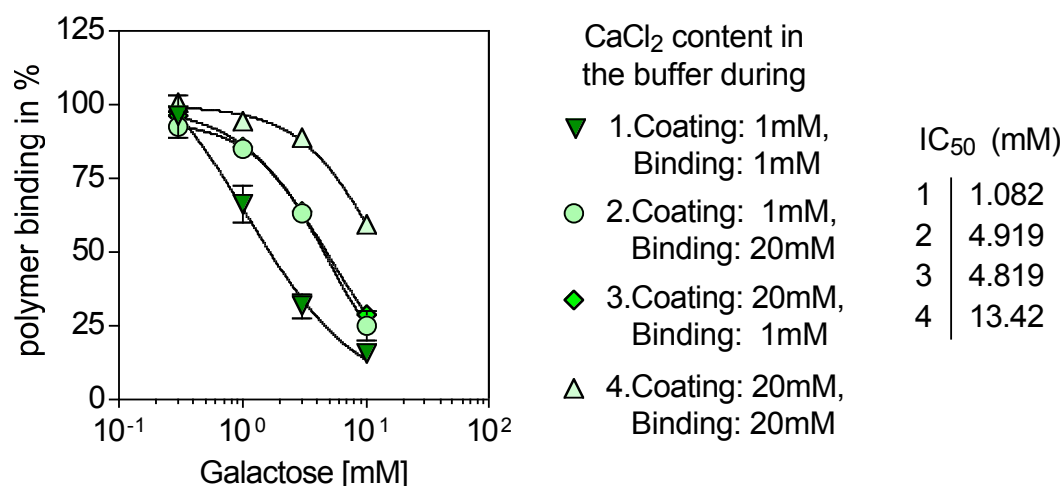


Figure 41. Influence of calcium concentration in the buffer on the IC_{50} of galactose

The increase of calcium in the HEPES-buffered saline (HBS) (20 mM instead of 1 mM) during any of the incubation steps lead indeed to a stonger binding of the β -GalNAc-PAA-polymer to the protein, and the increasing IC_{50} (Figure 41) indicate that this binding could hadly be inhibited by the tested competitor anymore. The assay with HBS containing 1 mM CaCl_2 gave IC_{50} values that were in the range of the K_D 's measured in SPR (see Table 22), this lead to the decision to maintain 1 mM Ca^{2+} as the standard calcium concentration in the assay buffer .

3.2.4.3 Incubation Temperature

The influence of the temperature during the two hours step of competitive binding of polymer and analyte on the obtained IC_{50} values was tested at 37°C, at room temperature (RT) and at 4°C while shaking on an orbital plate shaker.

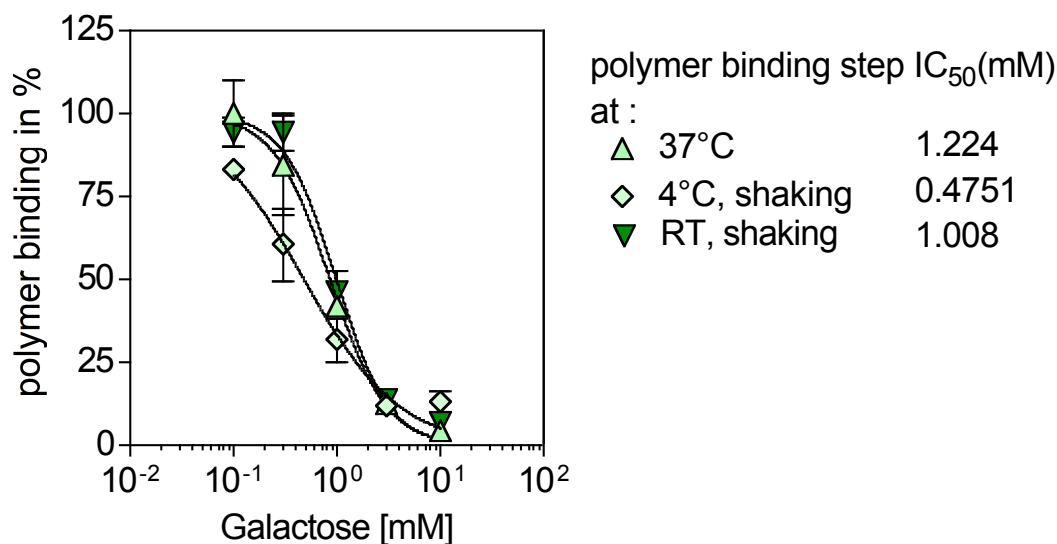


Figure 42. Influence of incubation temperature during the polymer-binding step

Incubating the plates at 37°C and at RT effectuated higher OD values than incubation at 4°C. Additionally, at RT the the obtained IC_{50} s were more stable and the standard deviations between the values of replicate wells were lower compared to those achieved when incubating at 37°C (Figure 42), probably mainly due to the homogenous mixing during incubation on the orbital shaker. Thus, room temperature with shaking was selected as standard condition for the competitive binding step.

3.2.4.4 DMSO Tolerance

The development and synthesis of novel carbohydrate mimics is often accompanied by a significant increase in their hydrophobicity. Therefore, organic modifiers have to be added to the solvent. DMSO is suited for most applications due to its miscibility with water, its nonvolatile character, and its biocompatibility. However, addition of DMSO nevertheless might influence protein activity or binding properties. Most of the tested compounds were readily soluble in assay buffer. DMSO was only used to prepare stock-solutions of higher substituted Gal/GalNAc mimics that were not soluble in buffer alone.

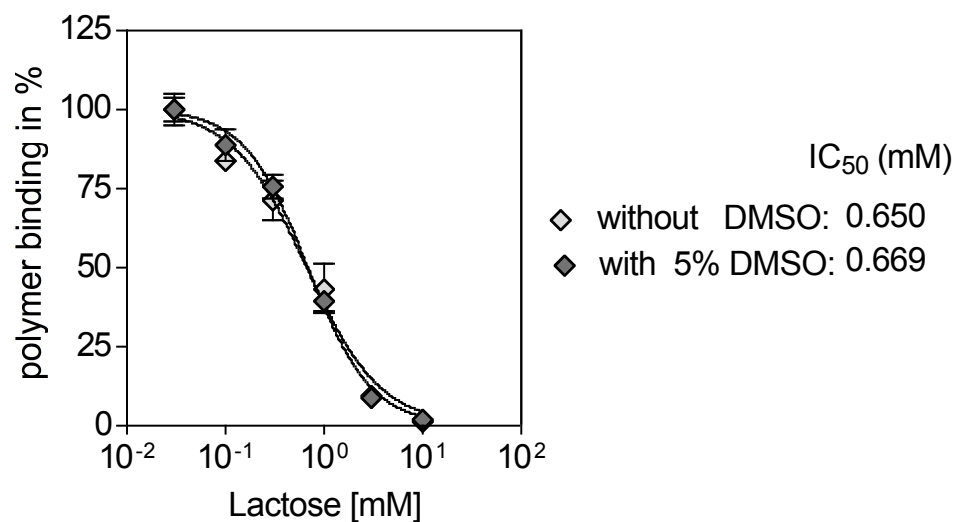


Figure 43. DMSO Tolerance of the competitive solid-phase binding assay

The influence of DMSO was tested up to a final concentration of 20% DMSO per well (data not shown). No influence on polymer binding and on IC_{50} values tested under standard conditions could be observed at DMSO concentrations up to 5% (Figure 43), confirming the suitability of the assay also for the screening of hydrophobic, drug-like substances.

3.2.5 Sensitivity of the Assay System, Testing of H1-CRD Ligands

The carbohydrate analytes were dissolved in assay buffer to 100 or 20 mM and then diluted in log-scale dilutions to 20, 6, 2, 0.6, 0.2, 0.06, 0.02 mM. After the blocking step the plates were washed and tapped dry. Directly after the addition of a volume of 50 μ l/well of the 2-fold-concentrated analyte-dilutions, 50 μ l of a 2-fold-concentrated polymer solution (1 μ g/ml) were added to the wells and then incubated at RT for 2 hours on a plate shaker. Washing of the plates and detection of the polymer binding were performed as described in Chapter 2.2.1.

Table 22. Comparison of results of a panel of carbohydrate analytes in the competitive solid-phase assay with surface plasmon resonance affinity measurements

Carbohydrate Analyte	Competitive solid-phase assay ^a		Surface plasmon resonance ^b		Literature values ^c	
	IC ₅₀ [μ M]	rIC ₅₀	K _D [μ M]	rK _D	IC ₅₀ [μ M]	rIC ₅₀
<i>N</i> -acetyl-D-galactosamine (GalNAc)	113 \pm 13	1	150 \pm 0.9	1	90	1
Galactose	1049 \pm 101	9.3	1460 \pm 10	9.7	1700	18.9
Lactose	1077 \pm 87	9.5	2090 \pm 50	13.9		
Methyl- β -D-galactopyranoside	1828 \pm 169	16	2200 \pm 40	14.7	1000	11.1
Methyl- α -D-galactopyranoside	2831 \pm 140	25	2760 \pm 60	18	1600	17.8
Glucose	>30000	n.d.	>10000	n.d.	60000	667
Asialofetuin	0.285 \pm 0.012	2.5 \times 10 ⁻³	0.119	1.2 \times 10 ⁻³	n.d.	-
Methyl- α -glucopyranoside	>30000	-	n.d.	-	n.d.	-
Methyl-acetyl-glucosamine	>30000	-	n.d.	-	n.d.	-

^a The IC₅₀s represented in the table were calculated using the datasets of a minimum of 3 independent experiments (measured on different plates, at different days using individually weighted compounds for each experiment). The curves represent the mean values \pm the standard deviation (SD). ^b The K_D values were obtained in Surface Plasmon Resonance (SPR) experiments with H1-CRD coated on the chip (performed by D. Ricklin⁷³). ^c Literature values are IC₅₀ from isolated rabbit ASGP-R lectin, the assays were performed with radioactively labeled ligands^{182, 183}. (n.d.= not determined)

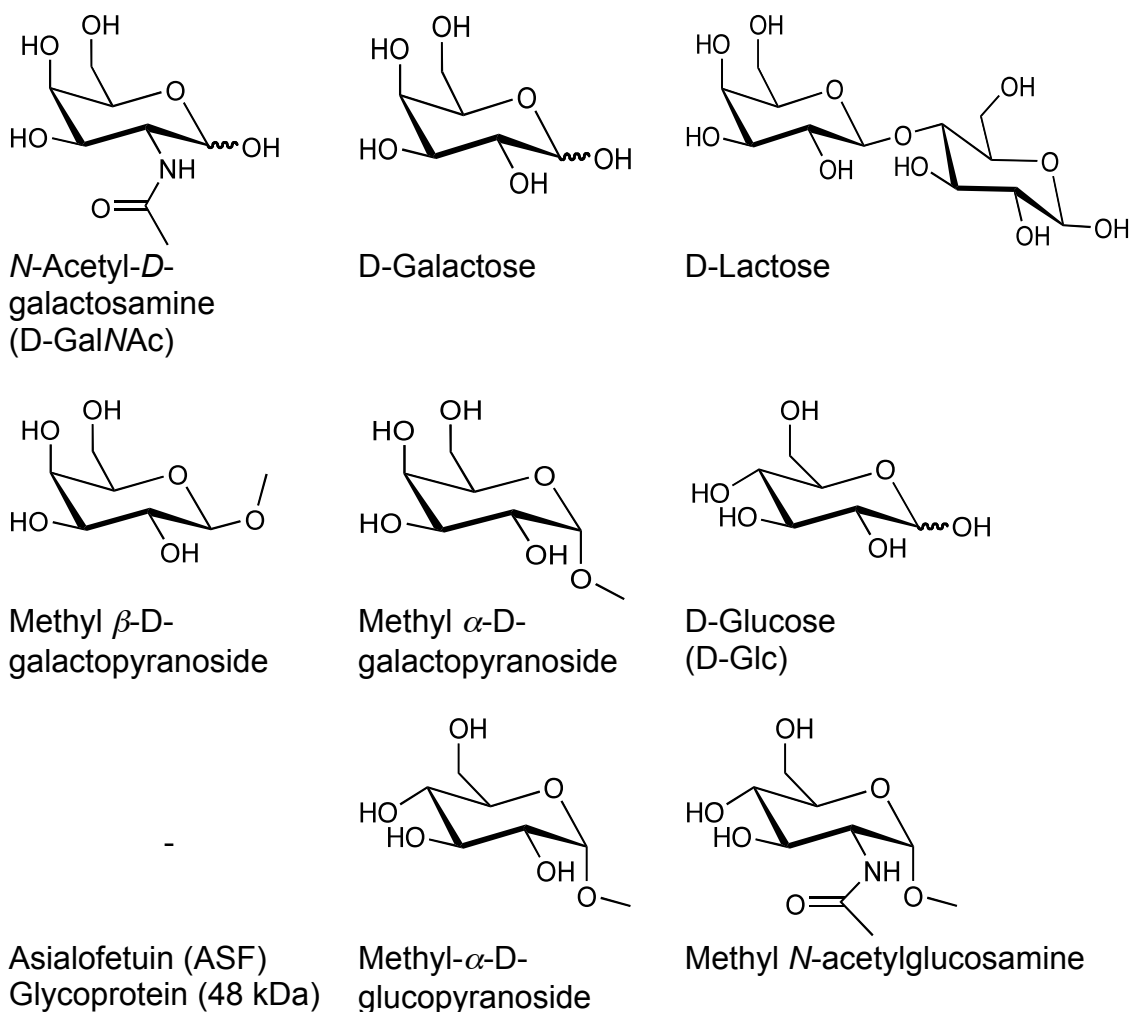


Figure 44. Structures of carbohydrate analytes used for the validation of the competitive solid-phase assay

3.2.6 Analysis of the Data

The IC_{50} values of the tested compounds were calculated with Prism GraphPad-program version 4. Two models for the calculation of the non-linear fit are feasible in this case, the 'one-site competitive binding' and the 'sigmoidal dose-response with variable slope'. Statistical comparison of the two models showed the 'sigmoidal dose-response (variable slope)' model to give superior fits (data not shown). The datasets were normalized to percentage of binding by setting background binding (non-specific GalNAc-PAA binding to wells without H1-CRD) as 0% and maximal specific binding (GalNAc-PAA binding to H1-CRD with addition of buffer instead of analyte dilution) as 100%. The nonlinear-fit of the normalized data was calculated with a four-parameter logistic equation: $y = \text{bottom} + (\text{top} - \text{bottom}) / (1 + 10^{((\log EC_{50} - x) * \text{Hillslope})})$, with x as the logarithm of

concentration, y the response, with the bottom of the curve constraint to zero and the top to 100. The IC_{50} defines the molar concentration of the test compound that reduces 50% of the maximal specific binding of GalNAc-PAA to H1-CRD. The relative IC_{50} (rIC_{50}) is the ratio of the test compound IC_{50} to the IC_{50} of GalNAc.

3.2.7 Adaptation of the Assay to the H2-CRD

The rationale of developing a competitive solid phase binding assay for H2-CRD in parallel to the one with H1-CRD is obvious. As the receptor in its native form is an oligomer consisting of H1 and H2 subunits, it would make sense to develop a drug-carrier that also addresses the H2 subunit of the receptor for tight and specific binding to the hepatic ASGP-R.

The H2-CRD used for the assay development was basically prepared in the same way as H1-CRD. Monomeric H2-CRD expressed as inclusion bodies in *E.coli*, purified by affinity chromatography on a Gal-Sepharose column, and separated from dimers by HPLC, was prepared at our institute by Dr. S. Rabbani. The binding of GalNAc- or Gal-PAA-polymer to the H2-CRD was tested under the same conditions applied with the H1-CRD (see page 2-48).

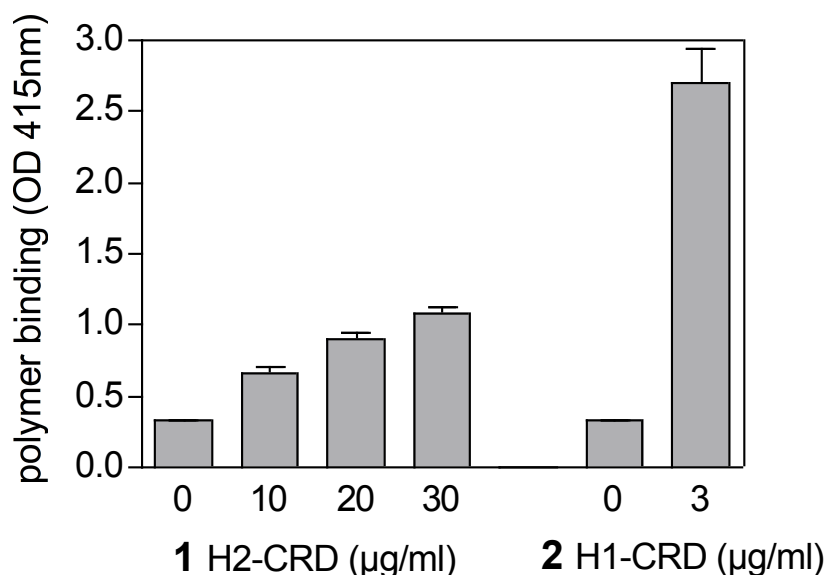


Figure 45. Adaptation of the assay to H2-CRD
GalNAc-PAA polymer binding to 1 H2-CRD in the concentration range from 10-30 µg/ml; 2 H1-CRD at the standard concentration of 3 µg/ml

Using the standard assay conditions with 0.5 µg/ml of GalNAc-PAA polymer for binding, H2-CRD immobilized on the plate at 10 to 30 µg/ml and even a

prolonged incubation time with ABTS-substrate of 10 min resulted in low OD values and only moderate specific binding of the GalNAc-PAA polymer to H2-CRD in comparison to the reference (H1-CRD) incubated on the same plate (Figure 45).

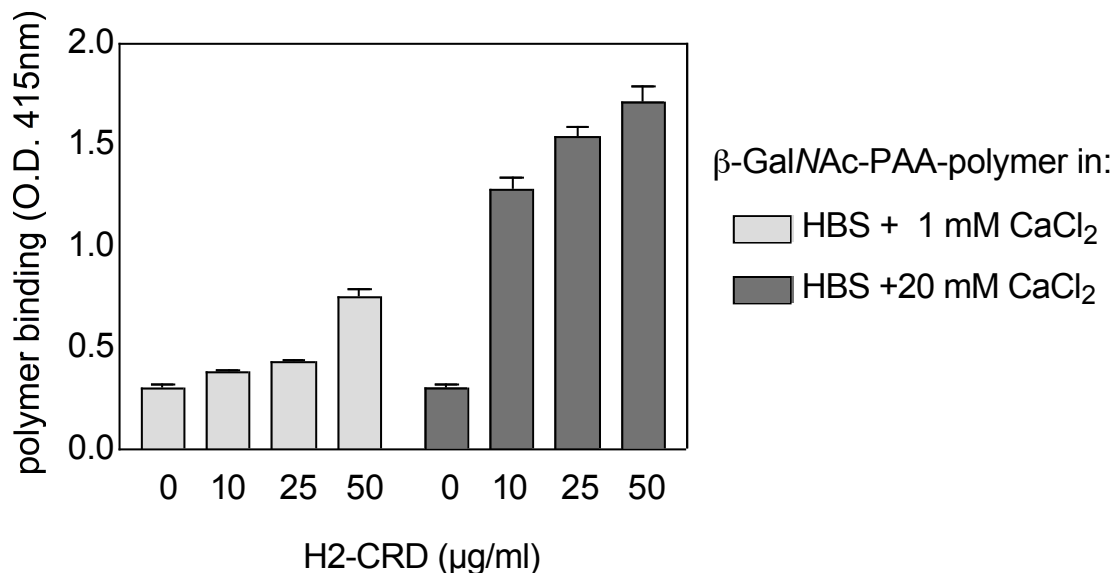


Figure 46. Comparison of the binding activity of H2-CRD (0-50 µg/ml) to GalNAc-PAA polymer (0.5 µg/ml) in buffer with 1 and 20 mM calcium, respectively.

Increasing the calcium content of the buffer from 1 mM to 20 mM improved the obtained OD values for specific binding of the GalNAc-PAA polymer (Figure 46).

The fact that H2-CRD can be purified over a Gal-Sepharose column but not a GalNAc-column (observation by Dr. S. Rabbani) lead to the assumption, that unlike H1-CRD, the H2-CRD might have a higher affinity for galactose than for GalNAc. Therefore a polyacrylamid-polymer bearing galactose instead of GalNAc was used as ligand probe (Figure 47).

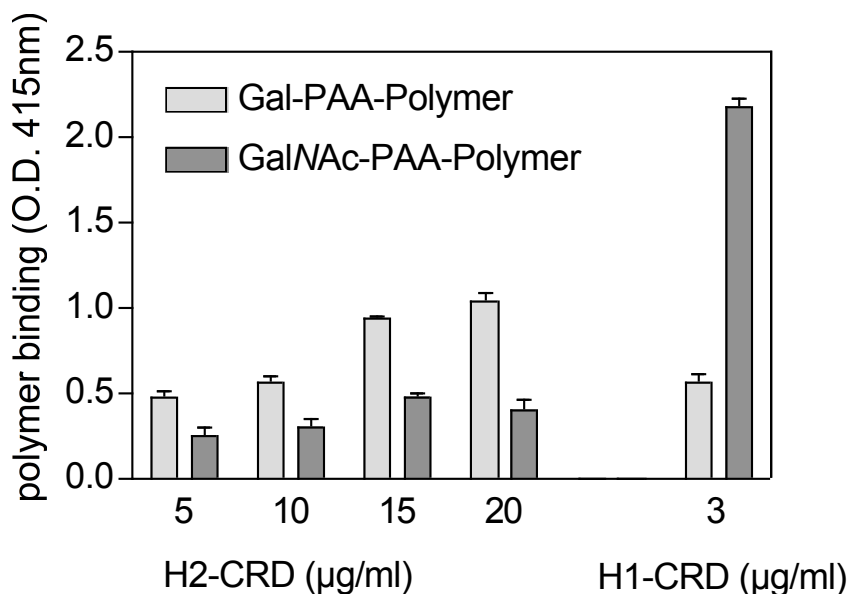


Figure 47. Comparison of Gal- and GalNAc-PAA-polymer (0.5 µg/ml) binding to H2-CRD immobilized at concentrations from 5 to 20 µg/ml of protein, to the standard H1-CRD concentration for the competitive solid phase binding assay in HBS with 20 mM Calcium (Individual backgrounds are removed)

The assay performed with monomeric H2-CRD showed a better signal-to-noise ratio with the Gal- than the GalNAc-PAA-polymer, albeit the ratio was not nearly as high as the one of GalNAc-PAA-polymer binding to H1-CRD. High amounts of protein were needed for immobilization to get a good signal-to-background ratio in the assay with H2-CRD. The amount of protein needed is the limiting factor in this case and to use the assay in this format for ligand testing is not applicable.

To date, the ligand specificity of the H2-CRD is still unclear. During her master thesis at our institute, D. Abgottspon screened a panel of more than 30 different sugars for binding to the H2-CRD in SPR, but none of them could be identified as high affinity ligand of the H2-CRD¹⁸⁷.

3.3 Evaluation of new Glycomimetic Ligands for the ASGP-R

In the approach to develop new glycomimetic ligands to be employed as binding moieties for a drug-carrier targeting the ASGP-R, several small, directed libraries were synthesized. The first ones, synthesized by Dr. C. Riva in the scope of her thesis, comprised about 50 compounds with modifications in the 2 and 6 position of galactose¹⁸⁸. Dr. O. Khorev synthesized a smaller library with modification in the 2 position of the Galatose scaffold¹⁸⁹. All components of the

libraries were evaluated in the competitive solid-phase binding assay by the author of this thesis and the affinity values (rIC_{50}) were compared to the lead compound GalNAc.

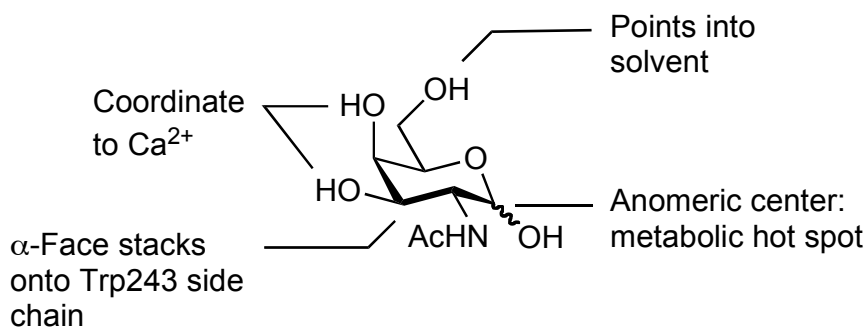


Figure 48. Lead compound *N*-acetylgalactosamine (GalNAc) showing important interactions with the binding site of the ASGP-R H1-CRD

Molecular modeling studies performed at our institute confirmed that, as also indicated by the crystal structure of H1-CRD, the 3-OH of the sugar moiety must be equatorial and the 4-OH must be axial for binding to occur. Further analysis of the crystal structure revealed also that the 2- and probably the 6-positions of the sugar ring might be modified. The substituent at the 2-position of Gal is directed towards the core of the protein, and in this region either H-bonds or hydrophobic interactions can be established between the ligand and the CRD (Tyr 272, His 256, Asn 264, Asp 266). The 6-position of Gal is pointing towards the surrounding water, but maybe extended to reach Trp 243, suggesting a hydrophobic interaction.

First generation

The aim of the work of Dr. Claudia Riva was to improve the understanding of the structural requirements for simple mono-galacto-derivatives for improved binding to the H1-CRD¹⁸⁸. All compounds were analyzed and ranked in the competitive solid-phase binding assay and some selected ones were further evaluated by SPR experiments, providing kinetic binding values for the synthetic small ligands to the H1-CRD.

Based on the crystal structure of the H1-CRD and SAR studies for similar receptors, four families of D-Galactose and D-Galactosamine derivatives and mimics thereof, modified at the 2- (**iii** and **iv**) or 6-position (**i** and **ii**), were

synthesized by Dr. Claudia Riva either in solution or on solid phase. Similar or improved affinities relative to GalNAc were obtained in the competitive solid-phase binding assay. Substituents in the 2-position (**iii** and **iv**) tightly interact with the receptor, while substituents in the 6-position (**i** and **ii**) could only modestly improve the affinity. However, with di-substituted monosaccharide mimics **v** the additive effects of substituents in the 2- and 6-position could not be confirmed.

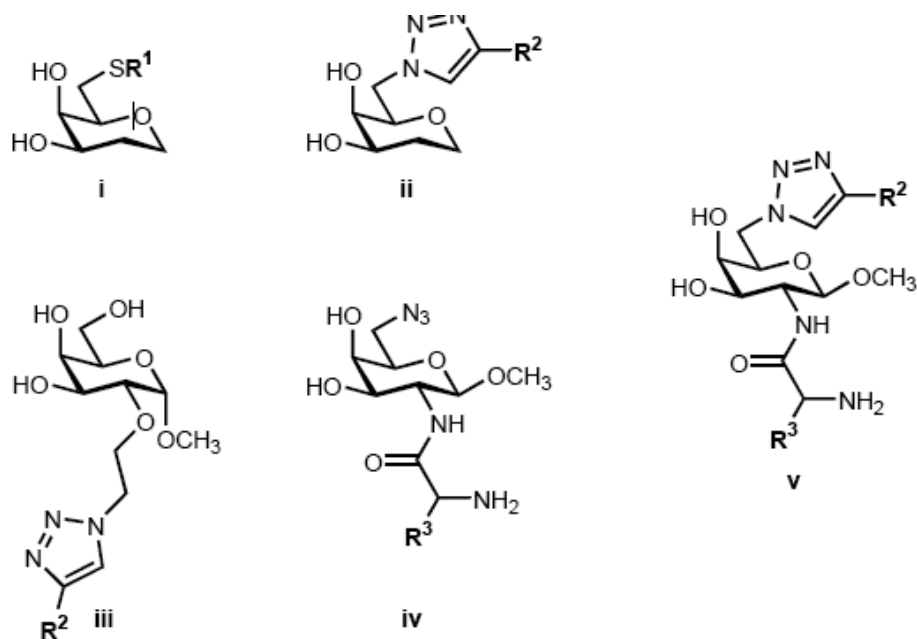


Figure 49. Summary on the 4 directed libraries produced by C.Riva
R1: hydrophobic groups, **R2**: hydrophobic or hydrophilic groups **R3**: H, CH₃, or CH(CH₃)₂

All compounds were tested in the competitive solid-phase assay by the author of this thesis, the obtained IC₅₀ values are represented in the thesis of Dr.C.Riva¹⁸⁸ and served together with the results of molecular modeling studies as the starting point for the design of the next generation of new glycomimetics.

Second Generation

To date, the highest affinity small molecular weight, monovalent ligand known for the ASGP-R is *N*-acetylgalactosamine (GalNAc). Its structure and physicochemical properties make it a poor candidate for therapeutic use. A high polarity, due to many hydrogen bond donors and acceptors, cause it to violate Lipinski's rules for good absorbance, and make it prone to fast elimination. In addition, GalNAc is susceptible to oxidation/reduction leading to a short plasma half-life due to its metabolically labile anomeric center.

In the scope of his thesis Oleg Khorev attempted to overcome these obstacles by the design and synthesis of a small, directed library of new glycomimetics based on the structure of GalNAc, by modifying in the 2-position of the sugar scaffold and by removing its anomeric center.

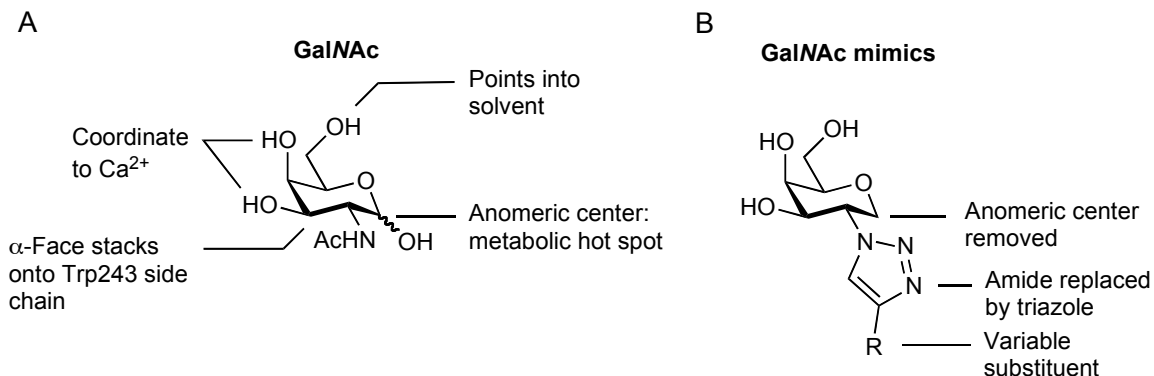


Figure 50. Starting point for the design of new glycomimetic ligands for the H1-CRD
(A) Lead compound GalNAc, showing important interactions with the binding site of the ASGP-R H1-CRD; **(B)** General structure of the compounds designed by Oleg Khorev.

The focus of this project was to design a GalNAc mimic, which would be more lipophilic, metabolically stable, and synthetically easily accessible and have a higher or similar affinity towards the ASGP-R when compared to GalNAc.

Oleg decided to remove the anomeric centre, which is not absolutely necessary for binding and acts as a metabolic hotspot, in order to increase the metabolic stability of the compounds. The 6-OH group pointing into the solvent showed to have enough space around it to accommodate a wide range of substituents (in-house modeling studies performed by Dr. M. Lill). Therefore, it could be removed altogether or replaced by a more lipophilic substituent in order to improve the Lipinski parameters. Alternatively, the 6-OH could also serve as an attachment point for conjugation to oligovalent carriers (Figure 55).

Binding studies published by other groups using galactose derivatives affirm the suggested theoretical binding mode of Gal/GalNAc to the ASGP-R^{63, 190}. Both, the acylation of the amino group of galactosamine with carboxylic acids featuring alkyl chains longer than 2 carbons, and the replacement of the *N*-acetyl group in GalNAc with a bulkier *N*-benzoyl group significantly decreased the affinity of the compounds to the rat hepatic lectin subunit 1 (RHL-1)^{60, 183, 188}.

Molecular modeling studies performed by Dr. M. Lill and the affinity data for ligands synthesized by Oleg Khorev (general structure depicted in Figure 52), reveal that the binding pocket surrounding the 2-position of GalNAc has presumably a dumbbell-shaped cavity (Figure 51). A direct steric clash with the protein surface due to this dumbbell-shaped binding pocket might explain the drop in affinity for compounds with bulky and /or long substituents in the 2-position¹⁹². But for all that the binding pocket offers still enough space for substituents seeking interactions at its sides by orienting themselves approximately 90° to the scaffold-triazole axis.

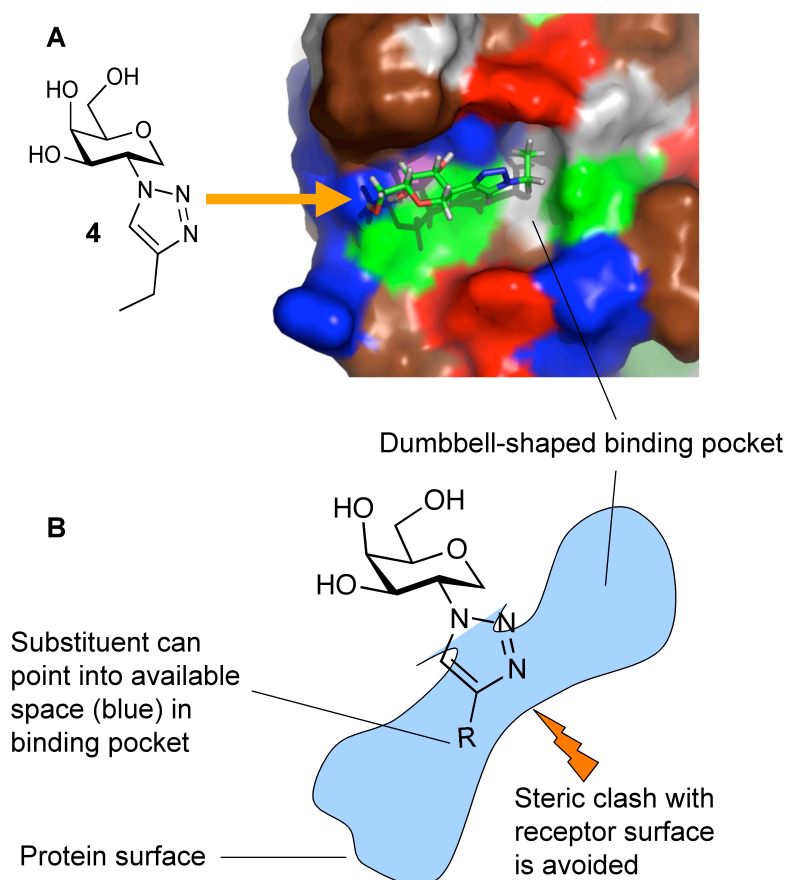


Figure 51. Docking study of hypothetical Ligand into H1-CRD

(A) A model of a hypothetical substituted triazole compound **4**, similar in structure to the compounds generated by O.Khorev, docked with the ASGP-R H1-CRD. Colors: red = positively charged amino acids; blue = negatively charged amino acids; purple = Ca^{2+} ; green = polar amino acids; brown = hydrophobic amino acids; grey = aromatic amino acids. (B) Schematic representation of the orientation of the 4-substituent of the triazole in the dumbbell-binding pocket. Picture courtesy of M.Lill and O.Khorev¹⁸⁹.

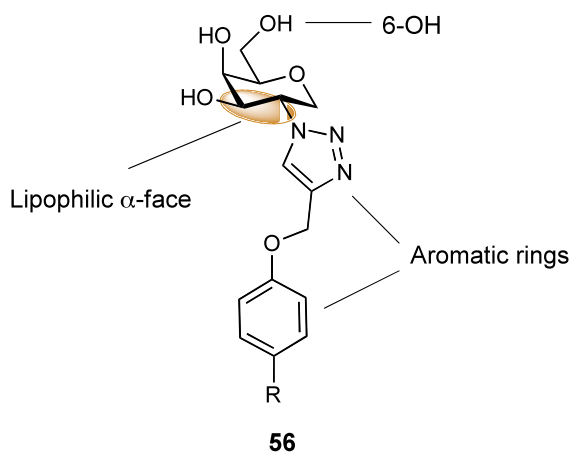
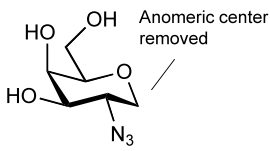
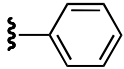
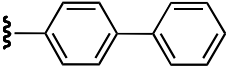
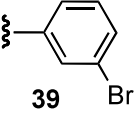
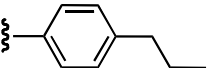
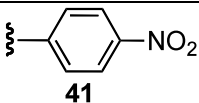
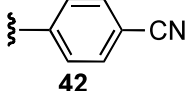
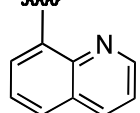
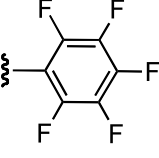
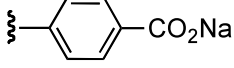
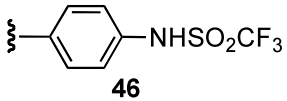
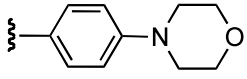
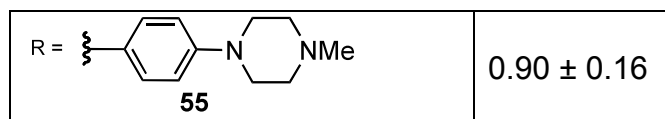


Figure 52. Compound **56** represents a general structure of the compounds synthesized in the directed library

The final compounds from the directed library were tested for their affinity towards the ASGP-R H1-CRD using the competitive solid-phase binding assay (Figure 53), and the results are summarised in Table 23.

Table 23. Summary of the competitive binding assay results for the directed library compounds

Compound	$rI_{C_{50}} \pm SD$
GalNAc	1.0
 Deprotected scaffold	13.7 ± 4.3
 49	1.1 ± 0.2
 38	n.d.
 39	n.d.
 40	n.d.
 41	0.8 ± 0.2
 42	0.5 ± 0.1
 43	n.d.
 44	2.6 ± 0.7
 45 Sodium salt	8.7
 46	n.d.
 52	n.d.



(n.d.: Stock-solution in DMSO, the compounds precipitated upon further dilution in HBS+Ca²⁺)

The major drawback of the final compounds was their poor aqueous solubility, which could perhaps be overcome by the addition of solubilizing groups.

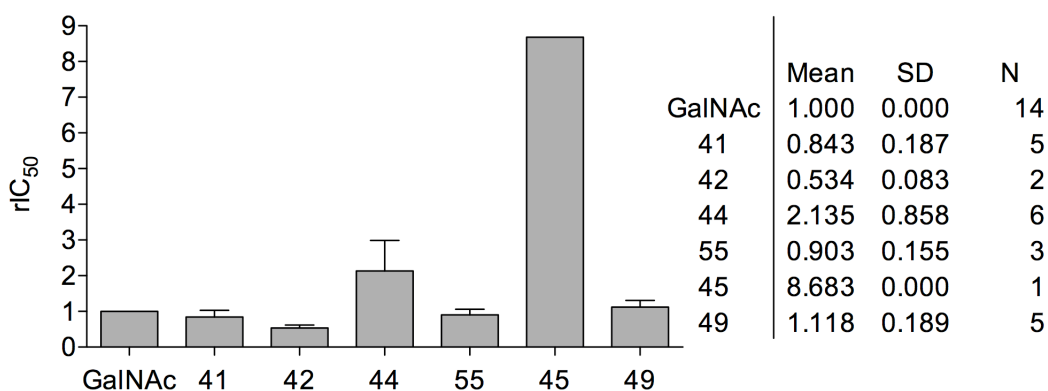


Figure 53. Relative IC₅₀ values measured in the competitive solid-phase H1-CRD assay in comparison with the lead compound GalNAc (N = number of experiments)

The assay results showed that two compounds (**49** and **55**, Table 23 with quite different structures bound to the H1-CRD with an affinity comparable to that of D-GalNAc - the best small molecular weight ligand for the ASGP-R so far – and that compound **42** bound twice as good as GalNAc. The latter suggests that the *p*-cyano group could make an important interaction with the surface of the binding site.

Comparing the structures of **49** and **55** (Figure 54), and assuming that both compounds have the same binding mode, suggest that there is ample room in the binding pocket for accommodating substituents in the *para*-position of the phenyl group. This further reinforces the “dumbbell-shaped binding pocket” hypothesis that was central to this strategy. Hence, after further molecular modelling studies, it would be worthwhile to generate compounds with other substituents in the *para*-position, to further optimize the interaction with the protein and improve the affinity even more.

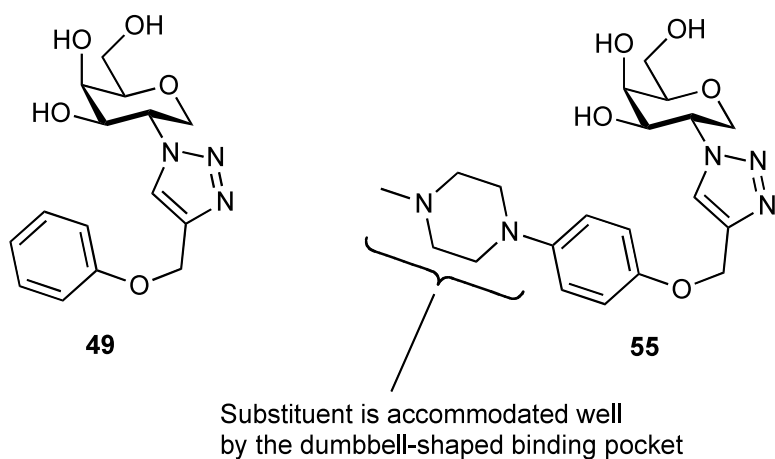


Figure 54. A comparison of the structures of the best binding drug-like ligands generated in the directed library by O. Khorev.

The binding affinity of compound **42** suggests that the *p*-cyano group could make an important interaction with the surface of the binding site,.

In addition, by replacing the Gal/GalNAc residues on multivalent ligands (**1**, Figure 55) with a higher affinity glycomimetic, a compound with even higher affinity would be generated, therefore improving the existing multivalent ligands intended for liver-specific drug delivery described in Chapter 3.8.

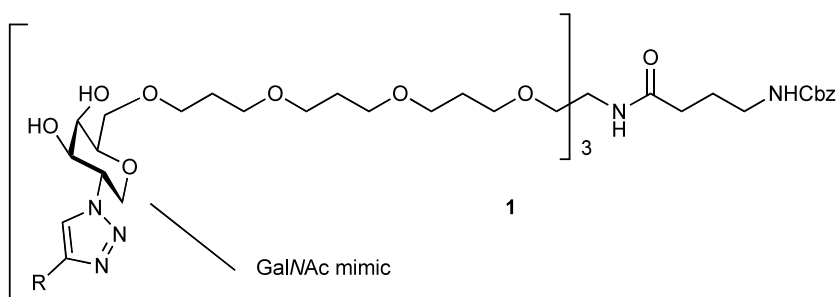


Figure 55. A hypothetical trivalent ligand (**1**) for the ASGP-R featuring a GalNAc mimic attached via the 6-position for use in liver-specific drug delivery. Picture by O.Khorev

3.4 Murine anti-H1-CRD Antibodies

For the investigation of the physiological function of the ASGP-R and for analytical and diagnostic applications, monoclonal antibodies directed against the H1-CRD are valuable tools. Dr. Rita Born produced in the scope of her thesis¹⁶⁵ monoclonal mouse anti-H1-CRD antibodies following the traditional procedure of Köhler and Milstein¹⁰³.

A selection of the obtained hybridoma clones was further characterized.

Their binding characteristics *in vitro*, their binding and internalization properties to different cell-lines and their binding to liver tissue sections as well as their epitope were investigated within our group.

3.4.1 Antibody Production

From these hybridoma clones five clones were selected for the production of new batches of purified antibodies.

To reduce costs of production, the hybridoma cells were adapted to grow in suspension in medium with a low concentration of serum.

During the adaptation of the cells to low serum medium as described in chapter 2.3.2.1, the hybridoma supernatants were monitored by ELISA and western blot against H1-CRD for their antibody production.

In general, the growth of hybridoma clones C11.1, C18.1, and C14.6 cells was very slow and their growth conditions had to be optimized. The cells of clone C23.8 died shortly after the thawing, even in medium supplemented with 20% FBS, and could no longer be propagated.

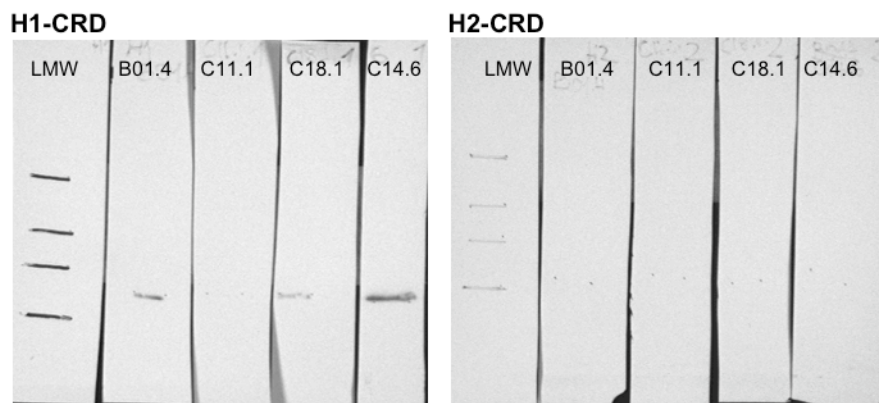


Figure 56. Western Blot analysis with hybridoma cell supernatants H1-CRD and H2-CRD (0.5 μ g/lane) on SDS-PAGE gel 12% under non-reducing conditions was transferred to nitrocellulose and immunostained with hybridoma supernatant from clone B01.4, C11.1, C18.1 and C14.6 followed by detection with AP-labelled goat anti-mouse IgG.

All mAb recognized H1-CRD in ELISA (data not shown) and western blot, but not H2-CRD (Figure 56). Variations in the intensity of bands,, e.g. the faint band visible for H1-CRD detected with C11.1- supernatant, is likely caused by low concentration of Abs in the supernatant due to unsatisfactory growth of these cells during the adaptation to low serum conditions.

Purification of Monoclonal Antibody

After establishing their stable growth in low-serum medium, the remaining 4 hybridoma clones were cultivated in roller bottles at 37°C. Only clone B01.4 could be adapted to grow with 3% low IgG FBS, all other clones were adapted to medium containing 6% low IgG FBS.

The hybridoma cells were kept in roller bottles under serum-reduced conditions for 3-6 weeks. The collected medium was centrifuged 10 min at 6500 g to remove cells and debris and the pH of the cleared supernatant was corrected to 7.4 with NaOH if necessary, then filtered (0.2 μ m) and immediately purified at 4°C.

Murine IgG usually show better binding to protein G than to protein A, but have to be eluted at lower pH, which sometimes causes loss of binding activity or aggregation of the eluted protein.

All supernatants were affinity purified using 1ml G-protein Sepharose columns (FPLC) as described in chapter 2.3.3.

Table 24. Productivity of hybridoma clones

Clone	Yield in mg/L
B01.4	17.8
C14.6	7.5
C11.1	16.1
C18.1	17.4

The purity of the purified antibodies was analyzed by 12% SDS-PAGE under reducing and non-reducing conditions. Subsequently, all eluates obtained of an individual antibody clone were combined and the final buffer exchange to PBS and concentration step was carried out using Vivaspin 6 centrifugal filter devices with cutoff 50 kDa (Sartorius).

Therafter, the final concentrations of the purified antibodies were determined by absorbance A_{280} measurements and their activity was tested in ELISA against H1-CRD with an HRP-labeled secondary antibody. Finally, the antibody samples were shock-frozen in aliquots of 0.5 ml in liquid nitrogen and stored at -20°C . Once thawed up, the antibody samples were stored at 4°C with the addition of 0.02% NaN_3 to avoid bacterial growth.

3.4.2 Immunohistochemistry (IHC)

The potential application of the anti human H1-CRD antibodies for diagnostic purposes in liver disease was evaluated in collaboration with Prof. L. Terracciano and L. Tornillo at the University Hospital in Basel.

Initially, the antibodies B01.4, C09.1, C11.1, C14.6 and C18.1 were tested for their use in IHC in normal liver tissue with different methods of antigen retrieval and staining. Only C14.6 was able to stain the receptor in fixed and paraffin-embedded healthy liver sections, confirming the findings by Rita Born, that this antibody preferentially binds to denatured H1-CRD protein¹⁶⁵.

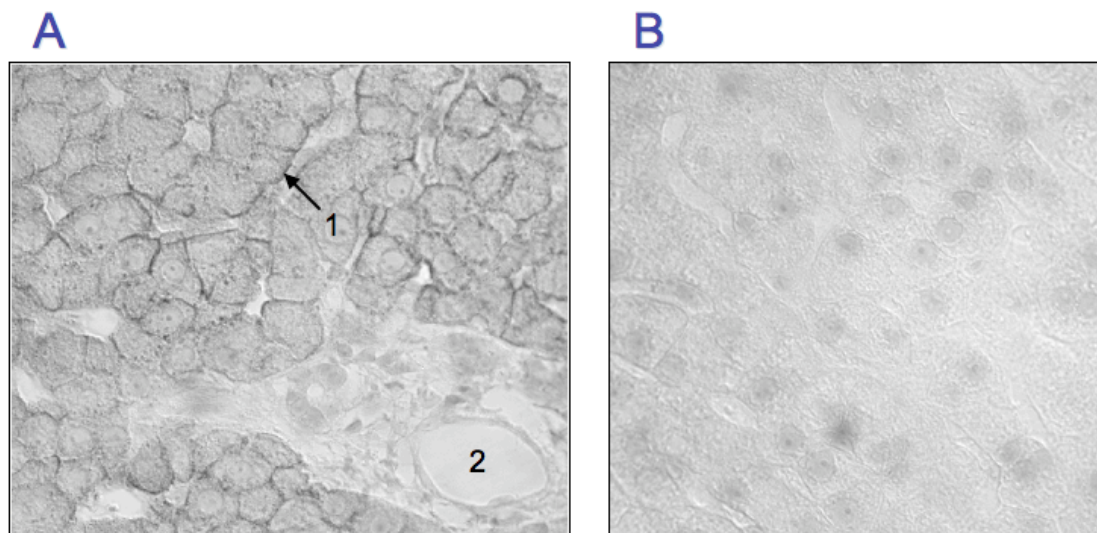


Figure 57. Immunohistochemistry staining of H1-CRD in human liver tissue. Normal paraffin-embedded human liver tissue section was (A) indirectly DAB-stained with 6 µg/ml C14.6 IgG2a or (B), incubated with PBS before adding the secondary antibody and after antigen retrieval by microwaving for 30 min at 98°C (control) (1) the arrow indicates the stained ASGP-R located on the sinusoidal surface of the hepatocytes. (2) No staining is visible along the blood vessels.

Because antibody C14.6 showed its use in staining normal liver tissue, it was also tested on tissue sections from liver biopsies obtained from patients suffering from various liver diseases.

Table 58. Visual interpretation of tissue staining (by Prof. Terracciano)

Disease	Number of patients	Intensity of staining with C14.6						
		Strong (3+)	Strong mediate (2+/3+)	Mediate (2+)	Mediate low (1+/2+)	Low (1+)	No (0)	Not evaluated
ALD	14	4	2	5	-	-	-	3
HCV	15	15	-	-	-	-	-	-
HBV	15	8	2	5	-	-	-	-
PBC	15	12	1	-	-	-	-	1
PSC	15	9	5	-	-	-	-	1
AIH ad.	3	-	-	-	1	2	-	-
AIH juv.	10	-	-	-	-	-	10	-

ALD is alcoholic liver disease, HCV and HBV are hepatitis C and B, PBC is primary biliary cirrhosis, PSC is primary sclerosing cholangitis, AIH is autoimmune hepatitis

In a preliminary experiment, the staining of paraffin-embedded liver tissue sections from patients with liver diseases with antibody C14.6 was evaluated. Two experts examined the slides under the microscope and rated the intensity of staining with the C14.6 antibody, hence this evaluation was qualitative only.

Interestingly, in liver tissue from children with AIH no staining and in adults only low intensity of staining with C14.6 was observed. For the pathologists these are promising findings, since there is no diagnostic tissue marker available for the disease so far.

Conclusion

The results show that antibody C14.6 is a promising candidate for a potential new diagnostic antibody in AIH.

There are still some questions to be answered:

Is the ASGP receptor masked by autoantibodies, or internalized and degraded?

Is it not or less expressed than in normal liver?

The juvenile AIH tissue slides were prepared in Napels and not in Basel. Is

there a difference in the fixation and paraffin-embedding procedure leading to a loss of the receptor? Most likely this not the case, as the tissue sections from adult AIH patients prepared in Basel also show a low staining intensity. The children on the other hand were treated with massive doses of immunosuppressiva (the biopsies were from transplantation patients), which could lead to lower expression of the receptor. To corroborate their findings, Prof. L. Terracciano and L. Tornillo are currently trying to get tissue samples from other institutes. It is also under discussion, if it would be worthwhile to test the other antibodies for their binding to H1-CRD on Cryostat tissue sections, therefore avoiding fixation and paraffin embedding.

3.5 Ligand Uptake in Hepatoma Cells

Choice of cell lines

The HepG2-cells originate from a human hepatocellular carcinoma. HepG2 is a highly differentiated cell line known to express the ASGP-R and is frequently used for *in vitro* assessment of drug- and gene delivery to the liver^{36, 193}. It displays approximately $2.25 \cdot 10^5$ ASGP-receptors per cell, which is about half the number found in primary hepatocytes¹⁹⁴. Although it is a reduced amount of receptors, it is still a large number for a hepatic tumor cell, which typically shows a low state of differentiation.

The human hepatocellular carcinoma cell line Huh7 is also well differentiated and expresses the ASGP-R although the receptor is expressed in lower numbers⁷⁰ when compared to HepG2.

The epithelial-like SK-Hep1 cells from human liver adenocarcinoma do not express the ASGP-receptor and represent therefore the ideal control cells to rule out unspecific binding or uptake of ligands and antibodies.

Fixation and background fluorescence

Fluorescence detection sensitivity is severely compromised by background signals, which may originate from the cell itself (referred to as autofluorescence) or from unbound or non-specifically bound probes (reagent background).

Although glutaraldehyde fixation is more suitable to keep the cytoskeleton structure of the cells intact, a fixation buffer of 3% paraformaldehyde in PBS

was used in order to avoid the increased autofluorescence of the cells when treated with glutaraldehyde.

3.6 Internalization Experiments

The methods for the internalization experiments were initially established using Texas red[®] labeled Asialofetuin (TR-ASF) and were adapted from Novikoff and Seow^{48 60}.

Preliminary tests with different concentration of TR-ASF (0.1 to 20 $\mu\text{g/ml}$) showed that from 1 $\mu\text{g/ml}$ up to 10 $\mu\text{g/ml}$ of TR-ASF the internalization of the ligand after 40 minutes could be observed under the microscope as bright red vesicles in HepG2-cells but not in SK- Hep1 (Figure 59). Using 20 $\mu\text{g/ml}$ of TR-ASF during incubation lead to non-specific uptake into SK-Hep1-cells and fluorescent precipitates in the medium. Hence concentrations of 5 and 10 $\mu\text{g/ml}$ of TR-ASF were used in experiments on time-dependent uptake of the ligand. The internalization-process of TR-ASF into HepG2-cells was stopped after 15, 30, 60 and 120 minutes. After 15 minutes, many small spots in the cells were observed. These spots or vesicles decreased in number over time, but grew bigger and brighter and were finally localized in close proximity to the nuclei of the cells.

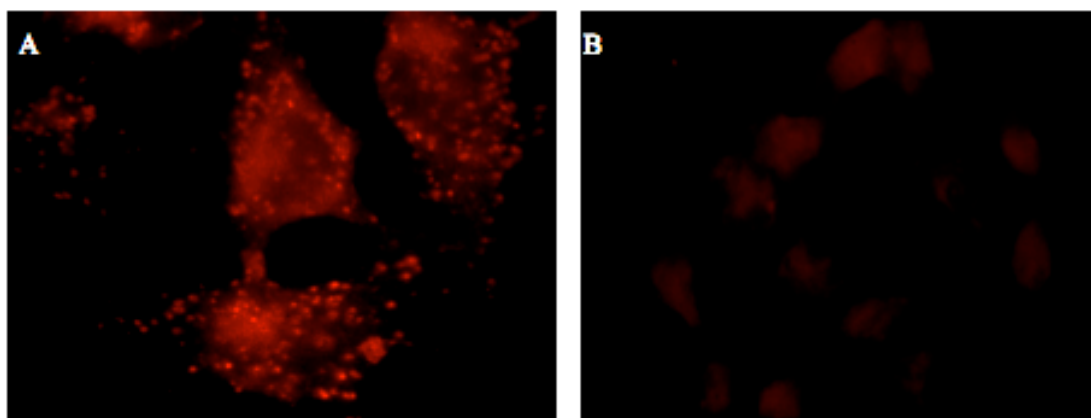
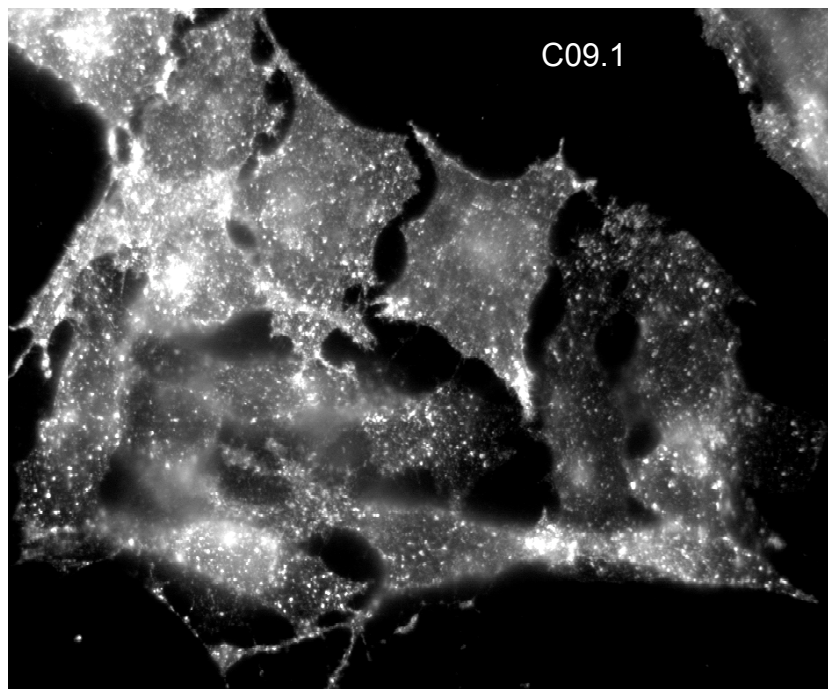
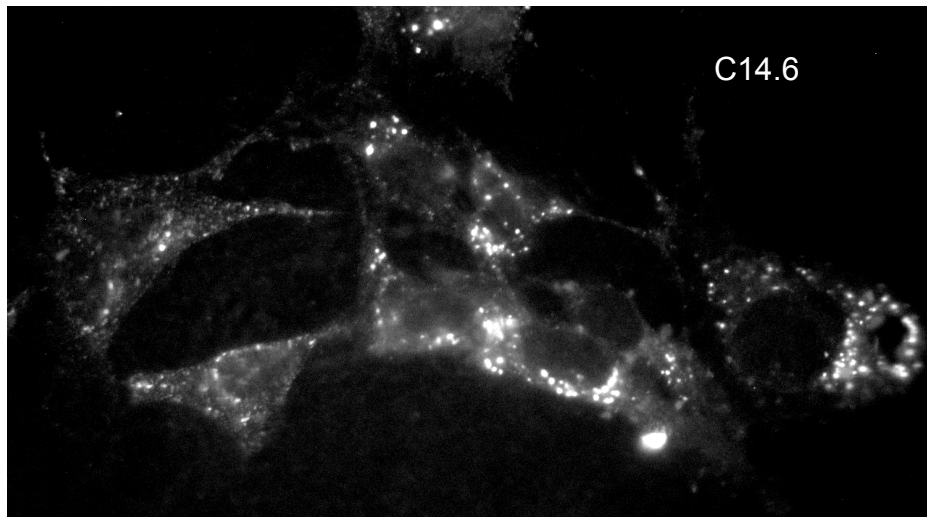


Figure 59. Internalization of Texas Red labeled Asialofetuin (10 $\mu\text{g/ml}$) into HepG2 cells (**A**) or SK-Hep1 (**B**). After 40 minutes of incubation with 10 $\mu\text{g/ml}$ TR-ASF, bright red vesicles of internalized TR-ASF could be observed in HepG2 and none in SK-Hep1-cells.

3.6.1 Immunofluorescence (IF)

Antibodies C11.1, B01.4, C09.1, C18.1 and C23.8 were tested for their potential to be actively internalized via the ASGP-receptor into living HepG2 cells. SK-Hep1 cells, which do not express the receptor, were treated likewise to rule out internalization via an unspecific endocytotic pathway.

Anti-H1-CRD antibodies were coupled to Texas red as described in chapter 2.5.1.2. The cell slides were prepared as described in chapter 2.3.7, and the cells were incubated to actively internalize the labeled antibodies as described in Methods chapter 2.5.2. The employed antibody concentration was 20 µg/ml.



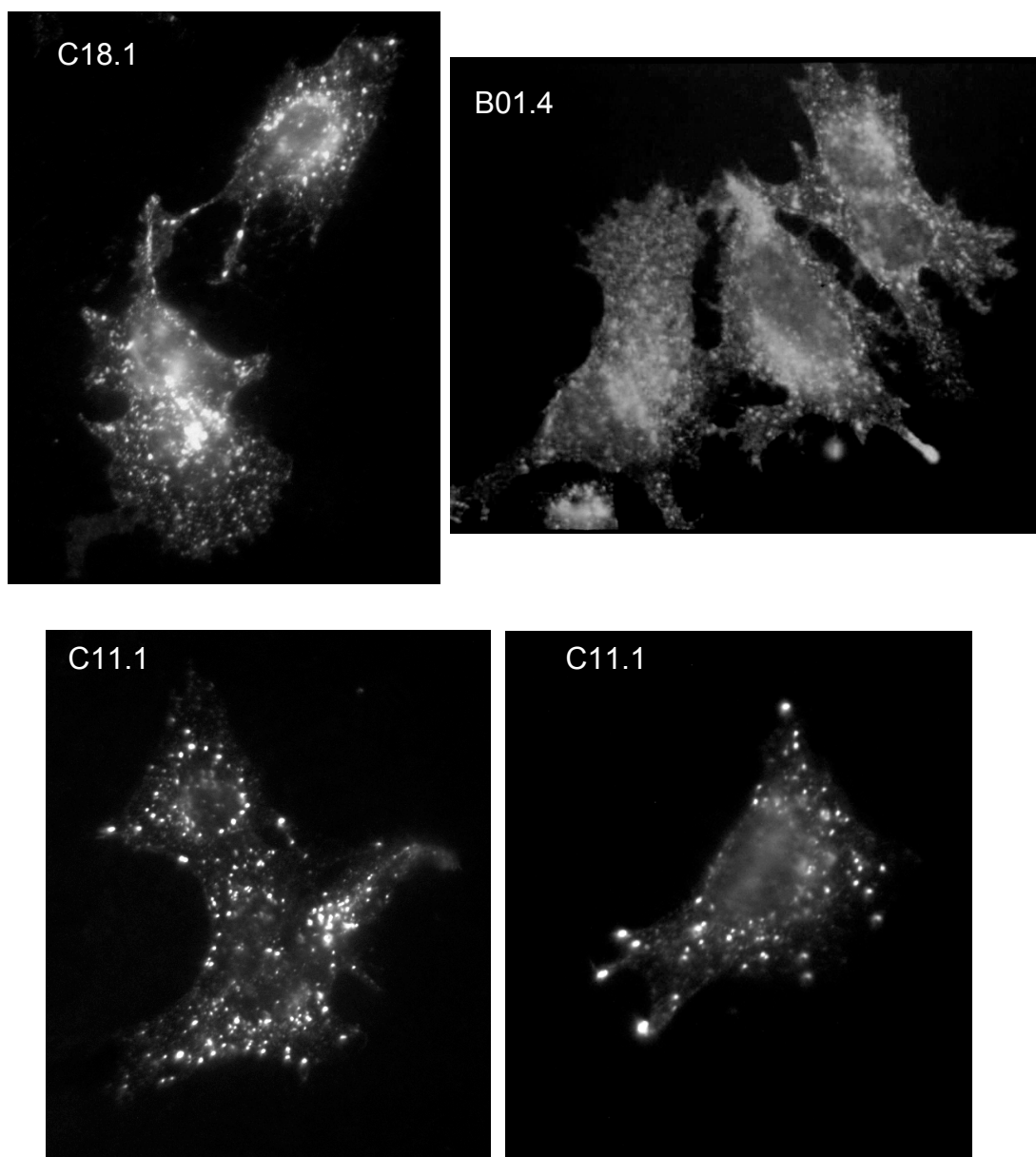


Figure 60. Internalization of ant human H1-CRD antibodies via the ASGP-R Direct Immunofluorescence staining of cells. HepG2 and SK-Hep1 cells were incubated with Texas Red[®]-labeled C14.6, C09.1, C18.1, B01.4, C11.1 (20 $\mu\text{g/ml}$) at 37°C to allow internalization of the labeled antibodies prior to cell fixation with paraformaldehyde. Mounted slides were examined with 630 times magnification (binocular 10x/20, objective 63x/1.25oil, Ph3plan-neofluor 440481) using red fluorescence filter (BP546, FT580, LP590)

All tested antibodies show good internalization properties in to HepG2 cells and no binding or uptake was visible in SK-Hep1 cells. Although the staining pattern is similar, some differences were observed. For example antibody C14.6 leads to an irregular staining pattern, probably due to its preference to bind to denatured H1-CRD. Antibody C11.1 lead to less but bigger and very bright accumulations in the cells. Western blots¹⁶⁵ and a very slow dissociation phase on dimeric H1-CRD in SPR⁷⁵ suggest, that C11.1 has a higher affinity towards

dimeric H1-CRD. This could explain the difference in the staining pattern, as only preorganized receptor in coated pits would be bound efficiently.

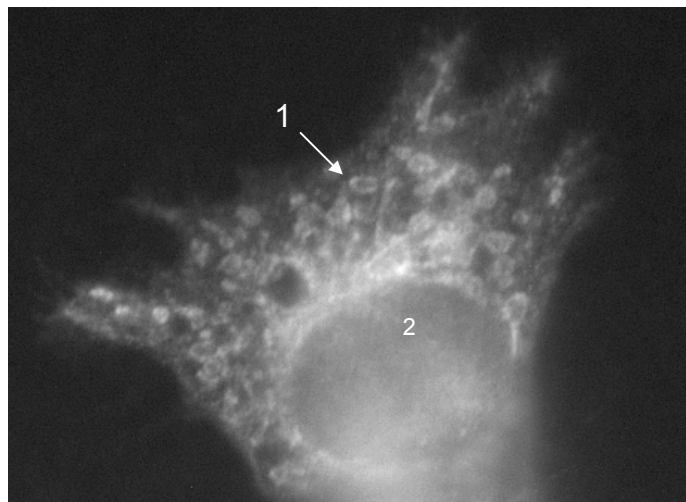


Figure 61. Storage of ASGP-R in fixed and permeabilized HepG2, stained with antibody C18.1. Arrows indicate a stained endosome (1) and the nucleus (2) of the cell.

HepG2 cells grown on collagen coated cover-slips were fixed for 20 min with 3% PFA at room temperature, then permeabilized using 0.5% Triton X in PBS for 20 min. after washing twice with PBS and a blocking step with 1.5% BSA in PBS for 2 h, the slips were washed again 4 times with PBS and incubated with 20 $\mu\text{g}/\text{ml}$ of TR-labeled C18.1 antibody. Round and oblong vesicles were stained in the HepG2-cells cytoplasm (Figure 61) but not in Sk-Hep1, suggesting the location of the ASGP-R in its storage vesicles.

3.7 Flow Cytometry with murine Antibodies

HepG2 cells were treated as described in chapter 2.5.3. The cells were detached with 2 mM EDTA in order to prevent the loss of surface-receptor by trypsination, . The cells were analyzed for cell-surface binding of the ASGP-R H1-CRD with the unlabeled antibodies C14.6, B01.4, C09.1, C11.1, and C18.1 at concentrations 12.5, 25 and 50 $\mu\text{g}/\text{ml}$ and matching isotype controls for 20 min on ice to prevent internalization. Antibody binding was detected with a secondary anti-mouse IgG antibody labeled with R-Phycoerythrin (RPE). Cells were analyzed by flowcytometry using PI exclusion to gate for living cells. Surface staining of living cells was evaluated by comparison of the shift of

median fluorescence intensity (MFI) emitted at 580 nm between untreated cells (background fluorescence) and treated cells on a CyAN ADP flow cytometer (DakoCytomation) with Summit 4.1 software

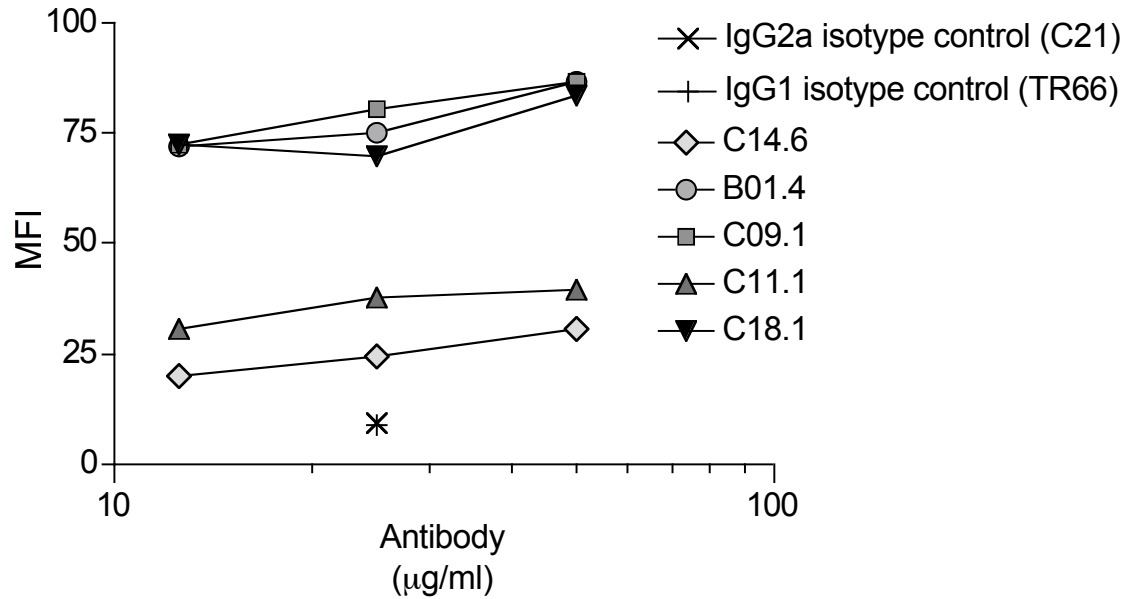


Figure 62. Titration of mouse anti-human H1-CRD antibodies
Surface staining of ASGP-R on detached HepG2 with anti-human H1-CRD antibodies, detection via 2nd Ab goat anti-mouse IgG (H+L) RPE, gated for living cells via PI-exclusion.

Additionally the antibodies were used to evaluate their binding to HepG2, Huh7 and SK-Hep1 (control) cells at 20 µg/ml for C14.6 and C11.1 and at 10 µg/ml for the remaining antibodies.

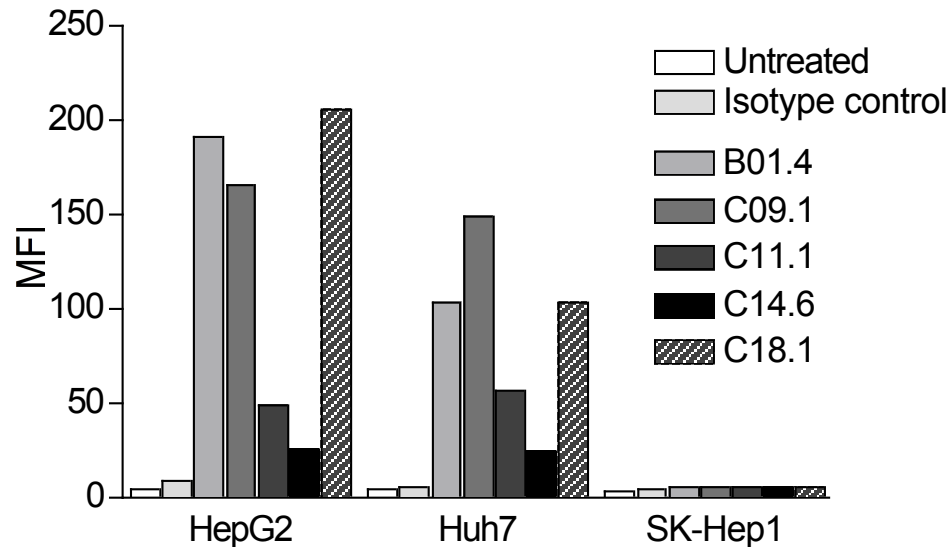


Figure 63. Mouse anti-human H1-CRD mAb binding to different hepatoma cell lines 1
Surface staining of ASGP-R on detached cells with anti H1-CRD antibodies B01.4, C09.1, C18.1 at 10 µg/ml, and C14.6, C11.1 at 20 µg/ml, detected via 2nd Ab goat anti-mouse IgG (H+L) RPE, gated for living cells via PI-exclusion.

Interestingly, antibodies C14.6, used in Immunohistochemistry (chapter 3.4.2), and C11.1, which showed calcium dependent binding and might preferentially bind dimeric H1-CRD (chapter 3.6.1), showed the lowest affinity to ASGP-R on the surface of detached cells. Huh7-hepatoma cells could also be used for ASGP-R-related experiments, they grow faster than HepG2-cells and are easier to handle, as they do not depend upon collagen-coated surfaces to grow in monolayers. The results of this experiment suggest that they present less ASGP-receptor on their surface than HepG2 cells.

In the last experiment the antibodies at 20 $\mu\text{g/ml}$ were incubated with the above-mentioned cells and, in addition, with mouse periportal Kupffer cells (KC) to exclude cross-reactivity with the Kupffer cell-receptor, which is homologous to the ASGP-R on parenchymal liver cells. The so-called Kupffer cell ASGP-R is not yet well characterized but it is suggested that this receptor primarily binds and internalizes particulate Gal- or Fucose-bearing ligands and might have a preference for O-glycosylated asialoglycoproteins¹⁹⁵, whereas the liver-cell ASGP-R preferentially binds N-glycosylated asialoglycoproteins.

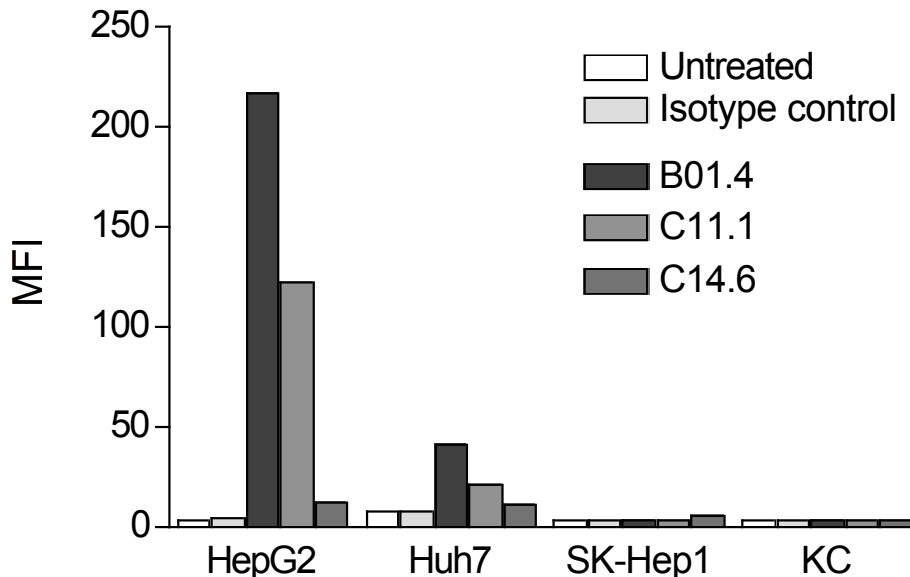


Figure 64. Mouse anti-human H1-CRD mAb binding to different hepatoma cell lines 2
Surface staining of ASGP-R on detached cells with anti-human H1-CRD antibodies B01.4, C14.6 and C11.1 (20 $\mu\text{g/ml}$), detected via 2nd Ab goat anti-mouse IgG (H+L) RPE, gated for living cells via PI-exclusion. KC are primary mouse Kupffer cells.

Kupffer cells are resident macrophages of the liver and play an important role in its normal physiology and homeostasis, and as a part of the reticuloendothelial

system (RES) of the immune system, they participate in the acute and chronic responses of the liver to toxic compounds.

The clonal primary murine periportal Kupffer cells (KC)¹⁹⁶ were obtained from the lab of Dr. R. Landmann (Division of Infectious Diseases, Department of Research, University Hospital, Basel, Switzerland). The murine KC display no binding of the tested anti-human H1-CRD antibodies, but one should be aware that the antibodies were raised in mice. Hence they probably do not react with a self-antigen from the same species. There is also no proof that the used cells actually still express the Kupffer cell-receptor, as there is no antibody available to verify its presence.

3.8 Endocytosis of Triantennary Galactose Compounds

In order to further exploit the ASGP-R for therapeutic purposes, trivalent ligands with pendant Gal or GalNAc residues connected by flexible spacers with appropriate lengths to a common branching point were synthesized. All these ligands incorporate 2-amino-2-hydroxymethyl-1,3-propanediol (Tris) as the branching point (Figure 65). Kempen *et al.*¹⁹⁷ synthesized the trivalent, Gal-terminated ligand **1**, where the carbohydrate moieties were directly linked to Tris. When **1** was labeled with cholesterol and incorporated into liposomes, they were mainly taken up by the Kupffer cells, via the Gal/Fuc-recognizing receptor, and not by the parenchymal liver cells via the ASGP-R.

Therefore, a new generation of ligands with optimal spacers was created. Biessen *et al.*^{77, 198} extended the distance between the Tris branching point and the Gal residues by using tetraethylene glycol spacers approximately 20 Å in length. This indeed led to ligands with improved affinities (see **2**, $K_i = 0.2 \mu\text{M}$, Figure 65) determined in a competition assay with ¹²⁵I-labeled asialoorosomucoid. In 1999, Sliedredt *et al.*¹⁹⁹ designed a second generation of cluster glycosides containing an essential modification (see **3**, $K_i = 93 \text{ nM}$, Figure 65). To enhance the chemical stability, the methylene acetal groups in **2**, which connect the spacers to Tris, were replaced by acid stable ether bonds. Furthermore, the spacers were no longer based on tetraethylene glycol to achieve the appropriate spacing between the Gal residues, but rather on a twelve atom fragment containing two amide bonds. Finally, Rensen *et al.*²⁰⁰ combined the various features from **2** and **3** to generate compound **4** ($K_i = 2 \text{ nM}$, Figure 65), which exploited the expected 50-fold higher affinity of GalNAc over Gal. To further improve the therapeutic profile of the previously reported ligands of the ASGP-R, we set out to synthesize an optimal trivalent linker with reduced synthetic complexity, high *in vivo* stability and improved spacer flexibility. The resultant intermediates **5a** and **5b** (Figure 65), which possess terminal Gal or GalNAc moieties, respectively, were then fluorescently labeled and tested for selective uptake by hepatocytes using fluorescence microscopy and flow cytometry. Moreover, since most of the previous research was done on rat^{76, 197-200} and mouse²⁰¹ liver cells, and the final aim of this research is liver-selective drug delivery in humans, all our biological assays were performed

using cell lines of human origin.

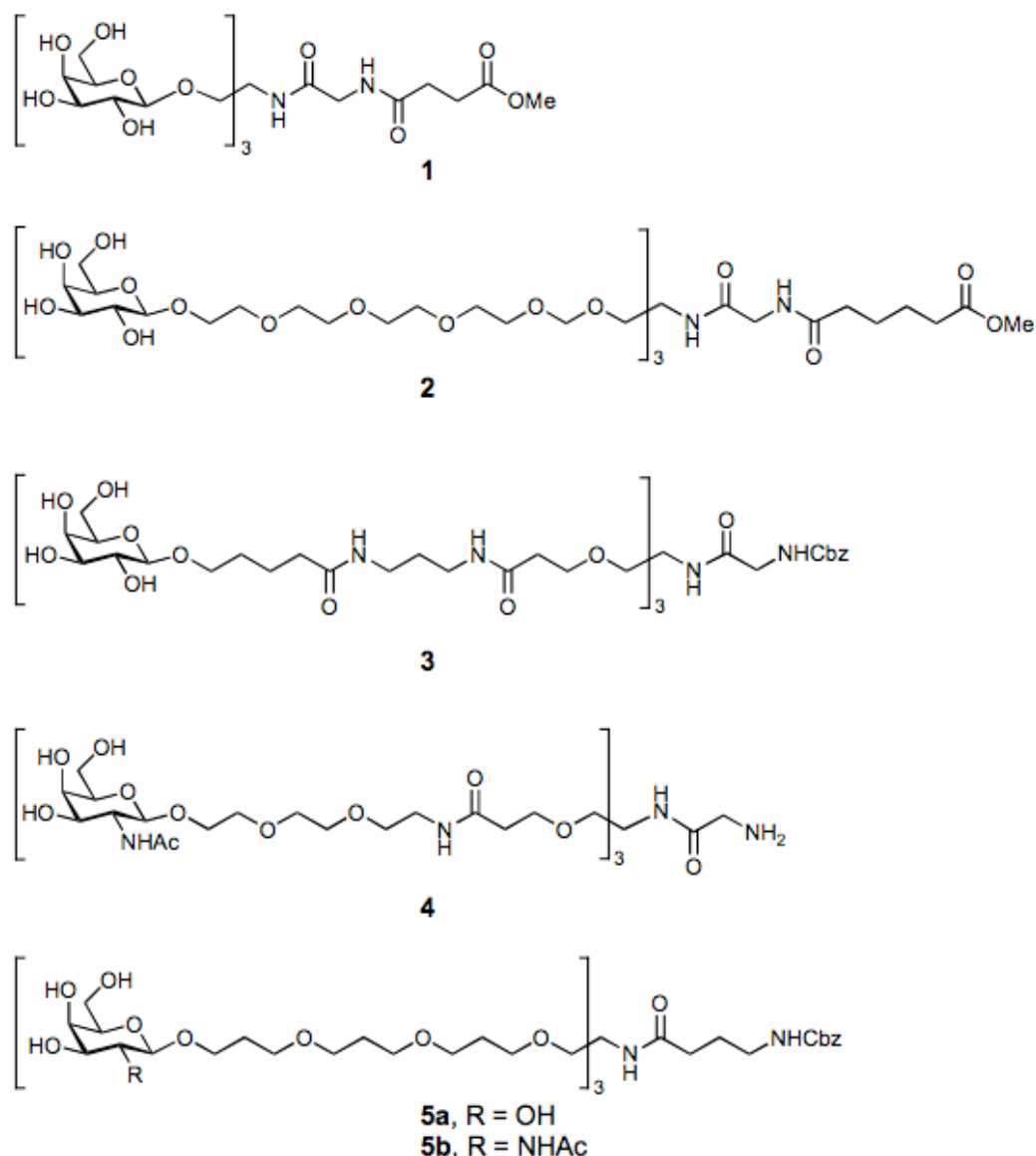


Figure 65. Triantennary compounds for the ASGP-R
1, **2**, **3** and **4** were specifically designed for, and tested on, the ASGP-R^{77, 197-200}. Compounds **5a** and **5b** are the trivalent, Cbz-protected intermediates introduced by Oleg Khorev¹⁵⁸.

The main structural features of the trivalent ASGP-R ligands **5a** and **5b** are as follows: (i) Tris is the central branching point, (ii) the spacers are based on polypropylene oxide, which combines flexibility with amphiphilicity, (iii) the linkage between Tris and the spacers is a hydrolytically stable ether bond and (iv) the length of the spacers can be easily varied (Figure 66).

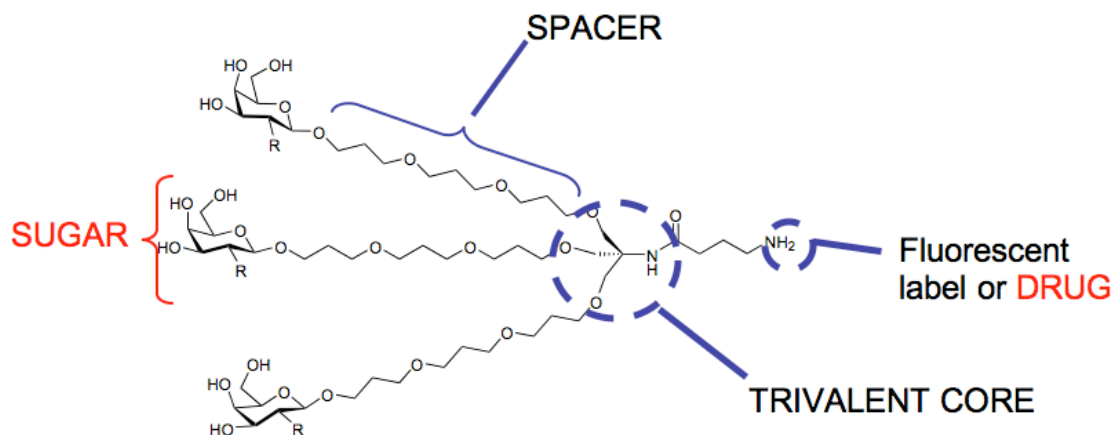


Figure 66. Summarized features of the trivalent drug carrier

The glycine acylating the amino group of Tris in **4** (Figure 65) has been replaced with Cbz-protected γ -aminobutyric acid, which upon deprotection furnishes a versatile primary amino group for the attachment of fluorescent labels and at a later stage therapeutic agent. For our studies, the amino group was coupled to Alexa Fluor[®] 488 fluorescent label (\rightarrow **6** and **7**, Figure 67), but in theory it could also be coupled to a therapeutic agent. As a negative control for the fluorescence microscopy studies, and especially to demonstrate the significance of the polypropylene oxide spacers featured in our final compounds **6** and **7**, we also synthesized compound **8** (Figure 67) The latter, in contrast to **6** and **7**, has only short spacers, and therefore does not fulfill the spatial requirements for trivalent binding to the ASGP-R.

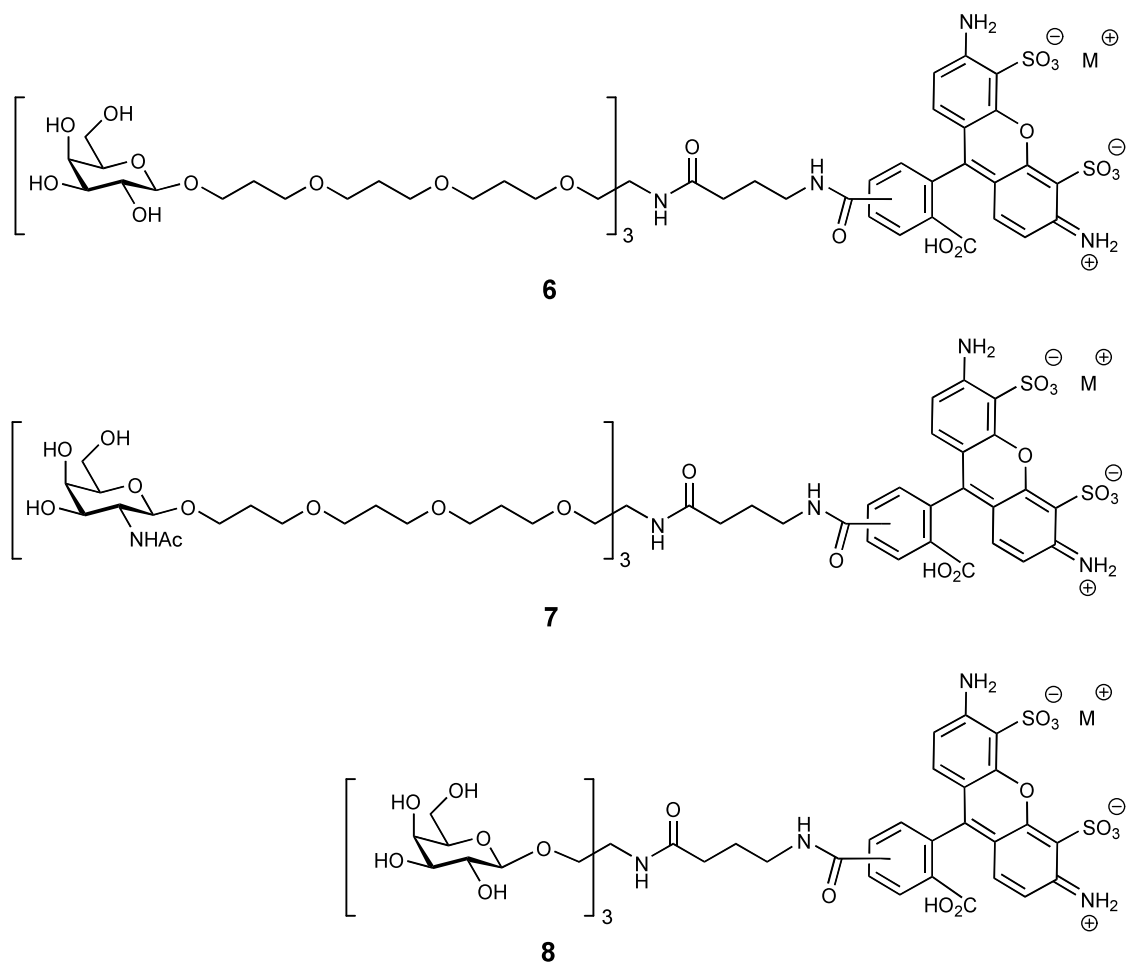


Figure 67. Fluorescent, trivalent compounds **6**, **7**, and control **8**; M^+ are variable counter ions.

Biological Evaluation

The trivalent ligands **6-8** were examined for their selective binding to, and internalization by the ASGP-R applying fluorescence microscopy and flow cytometry. Two different cell lines of hepatic origin were used: HepG2 cells derived from a human hepatocellular carcinoma expressing the ASGP-R, and the human more endothelial-like SK-Hep1 cells which lack the receptor.

Fluorescence Microscopy

The cells were incubated with the Alexa Fluor[®] 488-labeled compounds **6**, **7**, or **8** for 1.5 h on ice to allow binding of the compounds to the receptor while preventing unspecific uptake. In a washing step, unbound ligand was removed, and the cells were incubated for an additional 40 min at 37 °C to allow receptor-mediated endocytosis of bound compounds to take place. The specific uptake led to punctuate staining of the cells representing endosomes containing the

ligands, which were visualized by fluorescence microscopy. HepG2 cells showed specific uptake of **6** and **7**, and only negligible uptake of **8**. The fluorescent content of the endosomes can be distinctly seen (Figure 68, panels A and C) for compounds **6** and **7**, respectively. Because the cells were grown and incubated on glass cover slips, which were then mounted upside down for visualization, enriched fluorescence can only be observed in cytosolic areas that are not blocked by the nuclei. Panel E shows little or no such fluorescent vesicles, since control compound **8** was not internalized via the ASGP-R owing to insufficient spacer length. As expected, no internalization into SK-Hep1 cells (which do not express the ASGP-R) could be observed for compounds **6** and **7** (Figure 68, panels B and D). However, compound **8** showed a minor tendency to be internalized by this cell line in an ASGP-R-independent manner (Figure 68, panel F). Panels G and H show the autofluorescence of non-treated HepG2 and SK-Hep1 cells as controls.

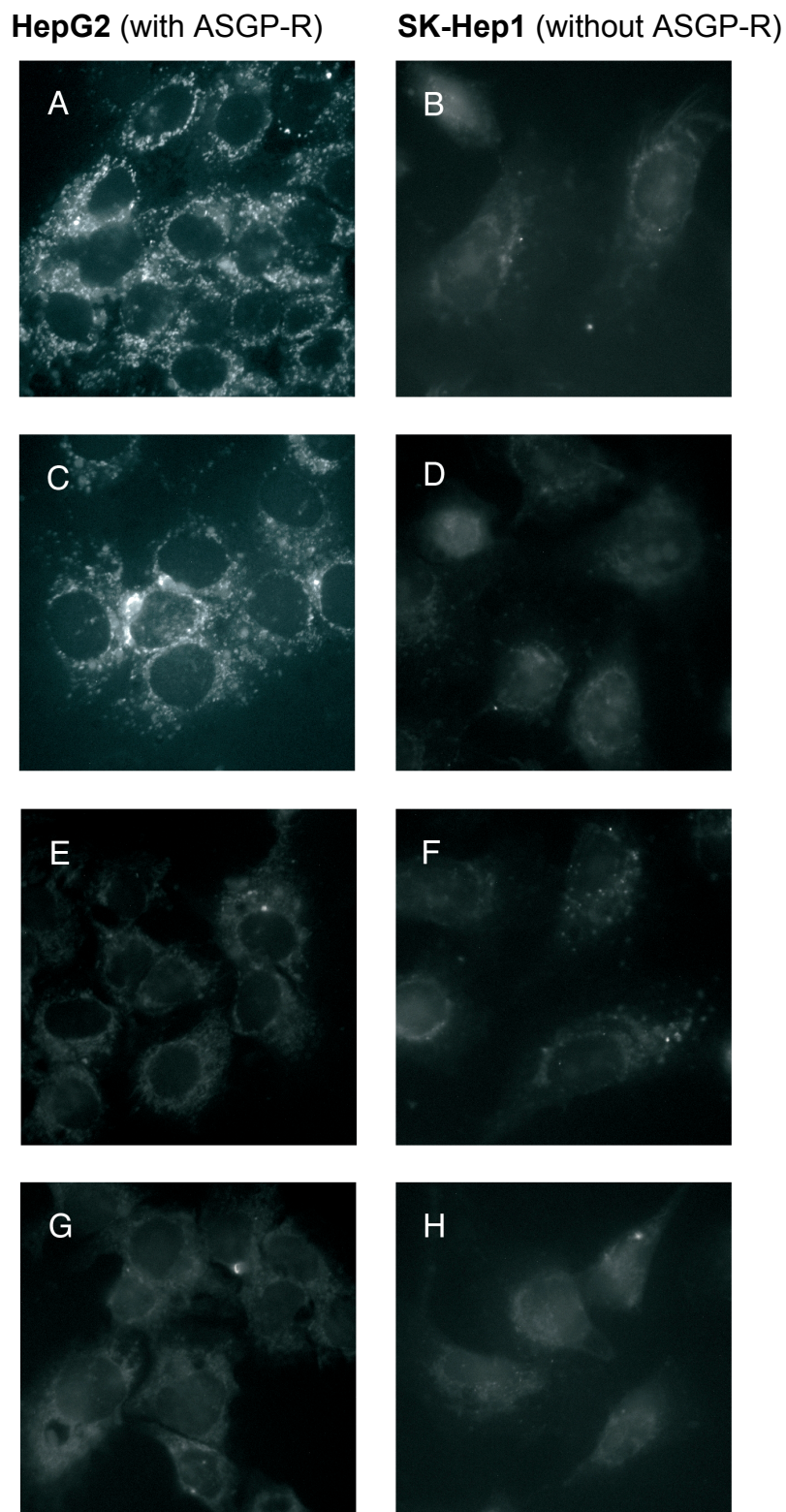


Figure 68, Fluorescent microscopy images depicting the ASGP-R-specific uptake of Alexa Fluor[®] 488-labeled compounds.

A) Compound **6** in HepG2 cells; B) Compound **6** with SK-Hep1 cells; C) Compound **7** in HepG2 cells; D) Compound **7** with SK-Hep1 cells; E) Compound **8** with HepG2 cells; F) Compound **8** with SK-Hep1 cells; G) Control HepG2 cells; H) Control SK-Hep1 cells.

Flow Cytometry

The ASGP-R-mediated uptake of compounds **7** and **8** (negative control) was quantitatively evaluated by flow cytometry. Instead of performing the previously described steps (prebinding on ice, removal of the excess and internalization of bound compound), the cells were continuously incubated with the test compounds at 37°C and analyzed as presented in Figure 69.

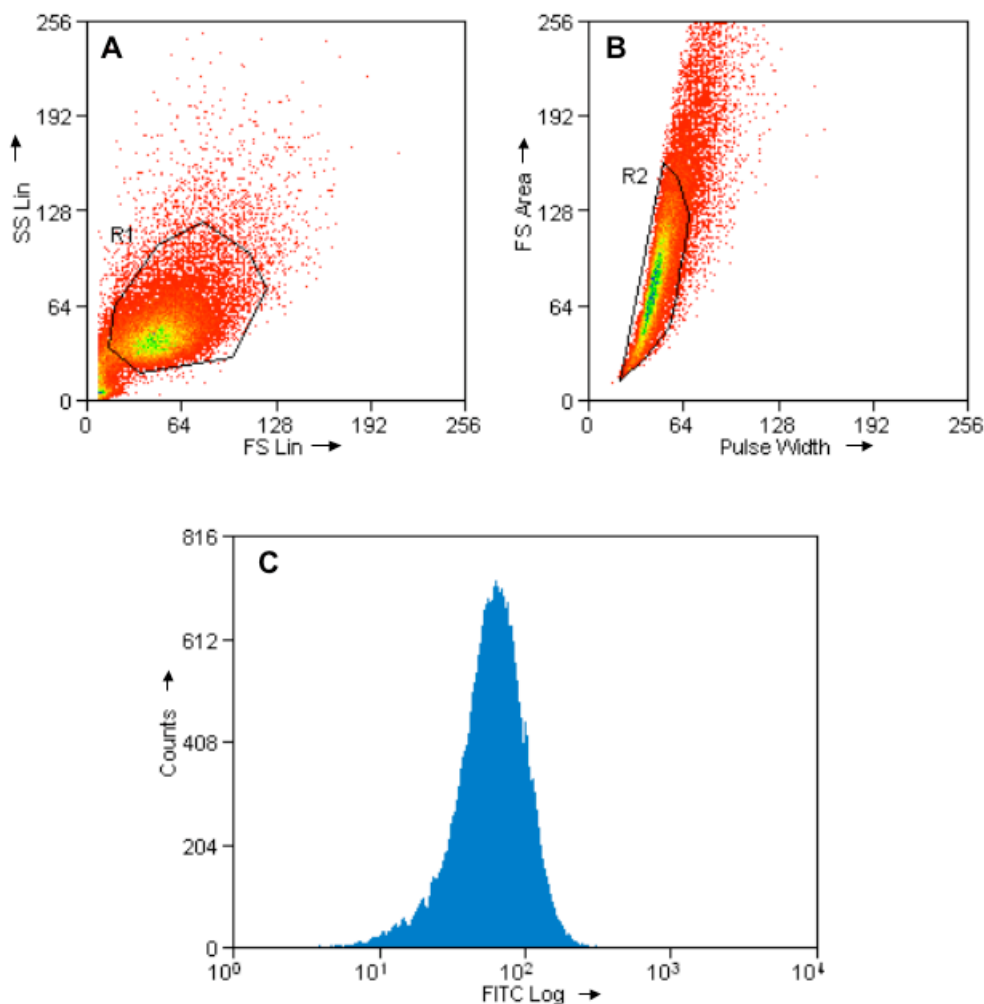


Figure 69. Example of flow cytometry analysis showing uptake of compound **7** into HepG2 cells. Dot plot (A) represents the HepG2 cell population gated for analysis (R1=30'000), plotted as a function of forward scatter (FS) and side scatter (SS). Dot blot (B) represents the population of R1 gated for single cells (R2) as a function of pulse-width and FS-area and histogram (C) depicts the log fluorescence intensity at 488 nm of the cells gated in R2. SK-Hep1 cells were analyzed in the same way, with a more compact population of cells and less debris in gate R1 and therefore smaller peaks due to less clumping of the cells (data not shown).

The median fluorescence intensity of cells incubated with compound **7** at concentrations ranging from 0.4 to 12.5 μM revealed low uptake of the compound into SK-Hep1 cells compared to HepG2 cells, in which the uptake

leads to a saturation hyperbola as it is typical for a receptor-mediated process (Figure 70).

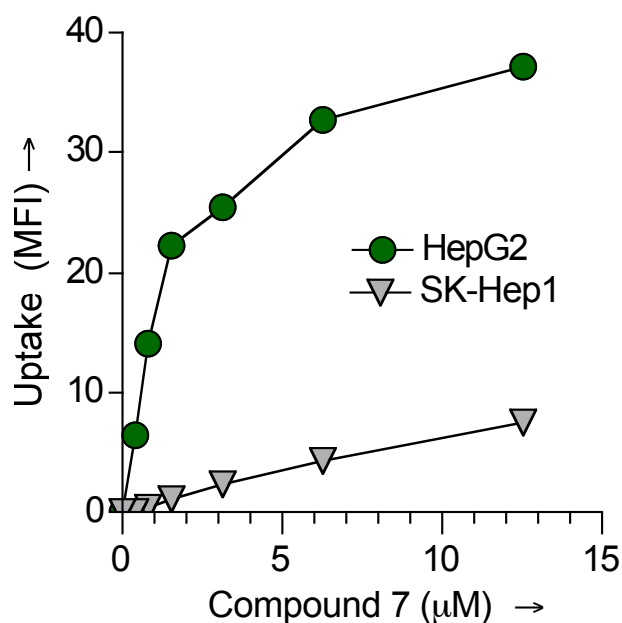


Figure 70. Titration of compound 7
Adherent HepG2 and SK-Hep1 cells were incubated with compound 7 at concentrations ranging from 0.4 to 12.5 μM for 40 min at 37°C. MFI is the shift in median fluorescence intensity from untreated to treated cells.

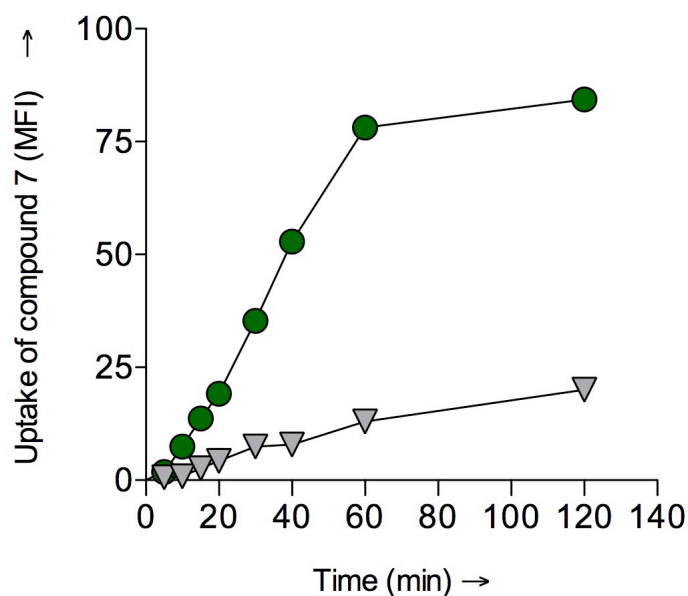


Figure 71. Time dependency of uptake of compound 7
Adherent HepG2 and SK-Hep1 cells were incubated with compound 7 at a concentration of 12.5 μM . after a prebinding step on ice (1h), continuous uptake of compound 7 during 0-120 min at 37°C was measured.

The internalization process of compound 7 at 12.5 μM was also clearly time

dependent and reached a plateau after 60 min (Figure 71).

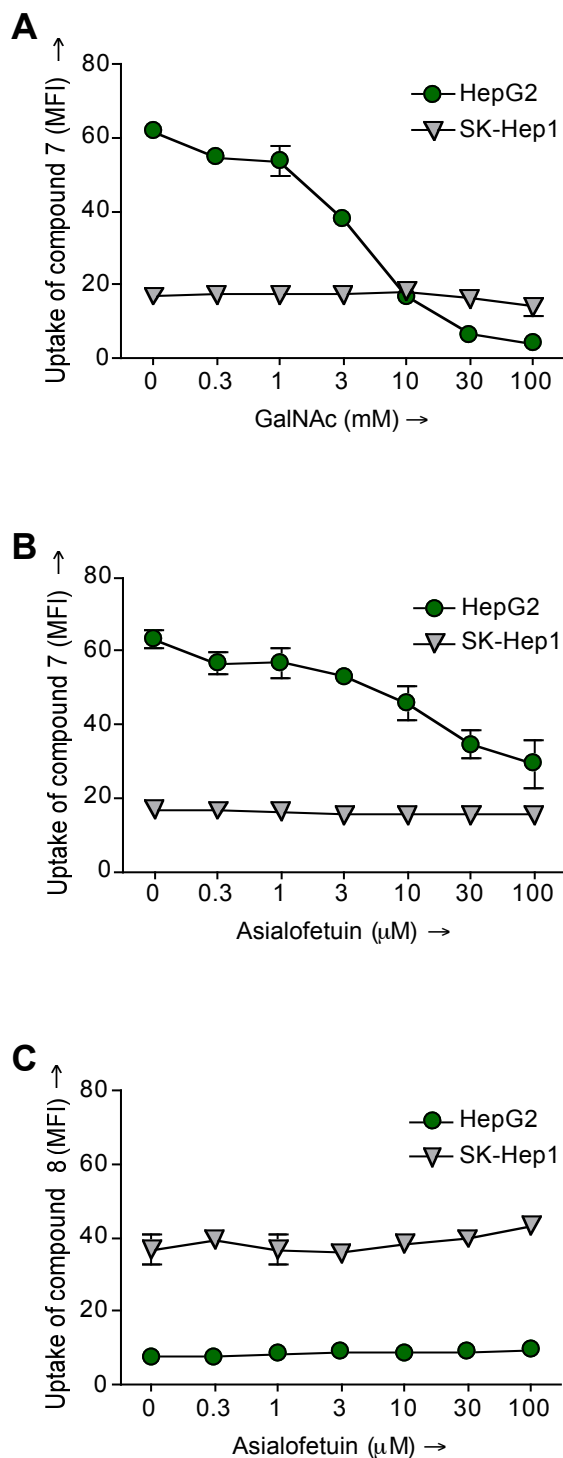


Figure 72. Competitive uptake of compound **7** at a concentration of 10 μ M in the presence of either GalNAc (0.3-100 mM) (**A**) or asialofetuin (0.3-100 μ M) (**B**). The graphs represent the mean of median fluorescence intensity (MFI) \pm SD of 3 independent experiments. (**C**) Uptake of control compound **8** at a concentration of 10 μ M in the presence of asialofetuin (0.3 –100 μ M) into HepG2 and ASGP-R-negative SK-Hep1 cells.

Uptake of compound **7** into HepG2 cells via the ASGP-R at a concentration of 10 μ M was competitively inhibited by the presence of monosaccharide ligands: GalNAc ($IC_{50} = 4.55 \pm 0.32$ mM) (Figure 72 A) and asialofetuin ($IC_{50} = 45.60 \pm 2.70$ μ M) (Figure 72 B), whereas the uptake into SK-Hep1 was low and not affected by the presence of asialofetuin.

In ASGP-R bearing HepG2 cells the uptake of control compound **8** was low and proved to be unspecific as it could not be inhibited by asialofetuin, a natural high affinity ligand of the receptor (Figure 72 C). ASGP-R-negative SK-Hep1 cells, on the other hand, evinced high uptake of compound **8**, unaffected by the presence of asialofetuin (Figure 72 C) which could be explained by their high endocytic activity that is usually associated with endothelial cells.

Conclusion

In this study, a set of novel, fluorescent, trivalent ligands for the ASGP-R (**6** and **7**, Figure 67) was evaluated. These compounds not only comply with the aforementioned optimal ASGP-R ligand criteria, but also are synthetically easily accessible and hydrolytically stable. Both criteria are a prerequisite for a therapeutic application at a later stage. Moreover, although similar compounds exist, these are the first trivalent synthetic ligands to be directly labeled with a fluorophore and tested on human liver cell lines.

Using fluorescence microscopy and flow cytometry, we have shown that compounds **6** and **7** exhibit selective uptake by the ASGP-R on HepG2 cells derived from human parenchymal liver cells – the major liver cell type. The formation of distinct endocytic vesicles could be clearly visualized. Furthermore, competition with asialofetuin, a naturally occurring serum glycoprotein and known ligand of the ASGP-R, and GalNAc confirmed the involvement of the ASGP-R in the uptake of **7**. Experiments using compound **8** have further re-enforced the generally accepted assumption that the sugar residues have to be in an optimal spatial arrangement in order to interact selectively and with high affinity with the native ASGP-R. In final analysis, we have demonstrated that compound **7** has a high potential for use in site-specific delivery of therapeutic agents (chemotherapeutics, DNA, etc.) to the liver.

3.8.1 Method Development - Lessons learned

Choice of the fluorescent label

Due to the high price of the Alexa[®] fluorochromes, a cheaper commonly used fluorochrome [5-(and 6)-carboxyfluorescein, succinimidyl ester] was used in a first approach to label the triantennary compounds;

Initially, the fluorescein-labeled compound **5a** and **5b** were tested on HepG2- (ASGPR positive) and SK-Hep1- (ASGPR negative) cells. Different incubation and cell treatment conditions were evaluated, e.g. duration of starving of the cells, incubation time and temperature. Preliminary results showed that the compound-uptake in to cells was visible as green vesicles, but it was difficult to discern the fluorescence of the compounds from to the auto-fluorescence of the cells (a problem especially in HepG2 cells, which sometimes show intense green and red vesicles when observed under the fluorescence microscope). Fluorescein is relatively cheap and can therefore be handled in higher amounts, which makes the labeling and purification of the compounds easier for the chemist. But fluorescein has some severe drawbacks, it is susceptible to photo-bleaching, has a relatively broad fluorescence spectrum and its fluorescence is pH-dependent ($pK_a \sim 6.4$) and significantly reduced below pH 7, which does not make it the ideal label for a substance that is delivered to the acidic environment of endosomes.

As the use of the fluorescein-labeled triantennary compounds **5a** and **5b** produced no convincing pictures of uptake into the hepatoma cells, Oleg Khorev switched to the brighter and more stable Alexa-Fluor[®]488 to label the compounds (resulting in compounds **6**, **7** and **8**). These 3 compounds were then used for the further development of internalization experiments.

Flow cytometry with the triantennary compounds

First experiments were performed with compound **7** at a concentration of 100 μ M on EDTA-detached HepG2, Huh7 and SK-Hep1 cells in suspension. This had the advantage that the cells could be incubated in a very small volume of liquid, which reduced the amount of consumed compounds. In addition, the cells could be further processed in 96-well U-bottom plates, which made their

handling easier. The cells were fixed in 3% PFA after the treatment, in order to keep them in the state they were after the internalization step.

Using these conditions, unlike expected, the SK-Hep1 showed higher uptake of compound **7** than the two ASGP-R positive cells.

When on the other hand cells adherent to the surface of tissue culture plates were incubated with compound **7** and the cells were detached after the internalization step, measured uptake into SK-Hep1 cells was negligible when compared to the ASGP-R positive cells. One of the factors clearly influencing the uptake of ASGP-R specific uptake of ligands into HepG2 and not SK-Hep1 cells is the physiological polarity of the hepatocytes. The ASGP-receptor is only present on the apical side of hepatocytes. Likewise SK-Hep1 cells that show more epithelial-cell-like features, benefit in suspension from an excess of surface available for uptake of compounds via ASGP-R-independent endocytosis when compared to their adherent state.

Consequently, to keep the cells in their physiological polarized condition, all further tests were performed while incubating the tested compounds on adherent cells.

3.8.2 Uptake of Ligands in Living Cells

These experiments were performed with cells in MaTek glass-bottom dishes coated with collagen. Initially Tyrode's solution, also used for live imaging of nerve cells, was used instead of normal medium during imaging in an attempt to lower the high autofluorescence of HepG2 cells, but the hepatoma cells started to detach from the bottom of the dishes. When phenol red-free medium was used during cell propagation and also during incubation with compounds and imaging, autofluorescence could detectably be reduced and the cells remained adherent.

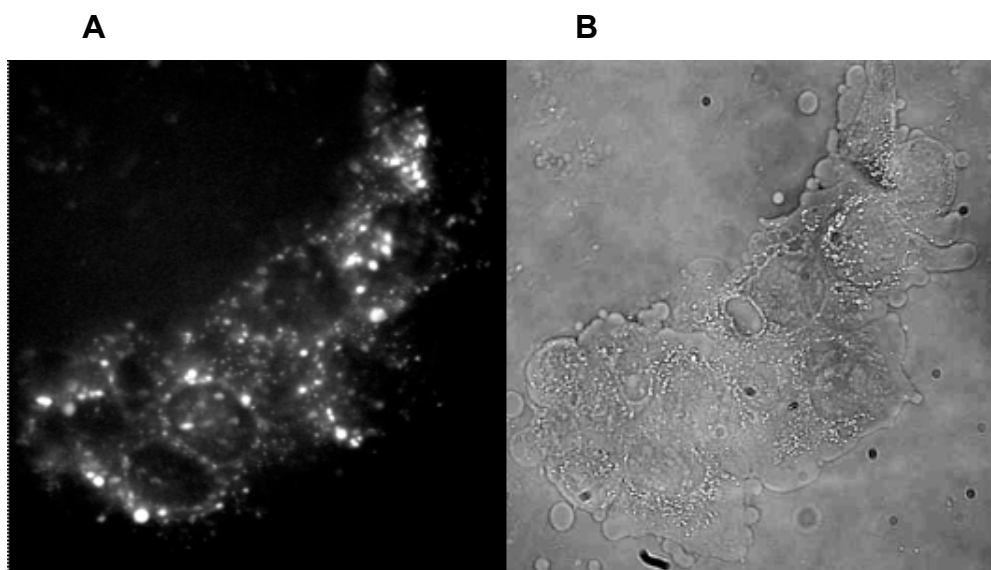


Figure 73. Uptake of compound **6** in HepG2 cells (live image)
(A) Fluorescence and (B) bright-field view

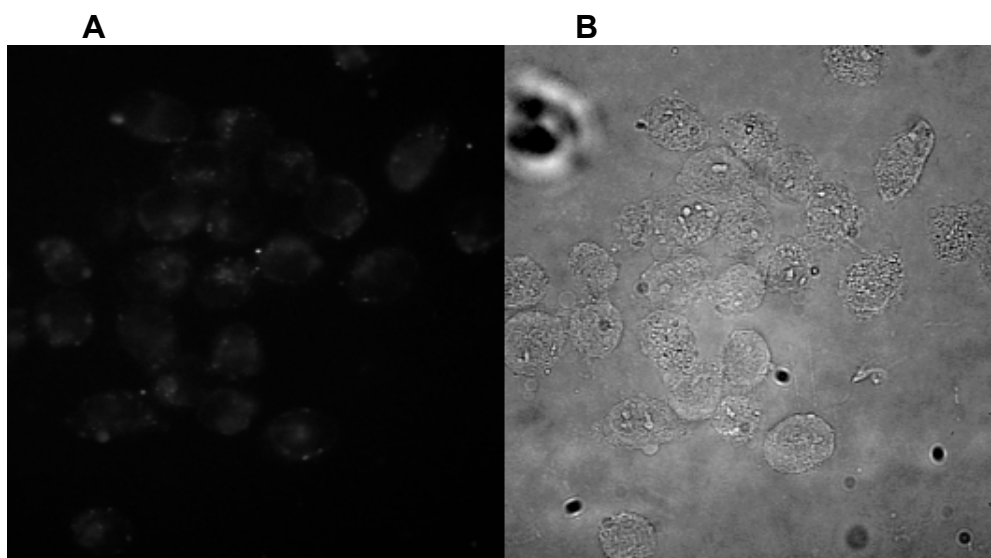


Figure 74. Uptake of compound **6** in SK-Hep1 cells (live image)
(A) Fluorescence and (B) bright-field view

Compound **6** at 100 μM was incubated with HepG2 and Sk-Hep1 cells in Ma-Tek glass-bottom dishes (Figure 73 and Figure 74). Binding was performed on ice for 1 hour and after the binding step the cells were washed with PBS, to allow only membrane bound compound to be internalized via receptor-mediated endocytosis. Excessive washes were necessary to prevent unspecific endocytosis of unbound compound **6** remaining in the medium by receptor-negative SK-Hep1 cells. Live imaging of uptake took place at 37°C in phenol red- and serum free medium and pictures were taken with a Leica inverted microscope featuring a digital camera. Uptake of compound **6** was clearly

restricted to the ASGP-R positive HepG2 cells, but the high auto-fluorescence of these cells made it difficult to distinguish between the signal of endosomes containing the compound and autofluorescent vesicles in the cells (Figure 75). SK-Hep1 cells displayed no uptake of compound **6** (Figure 74).

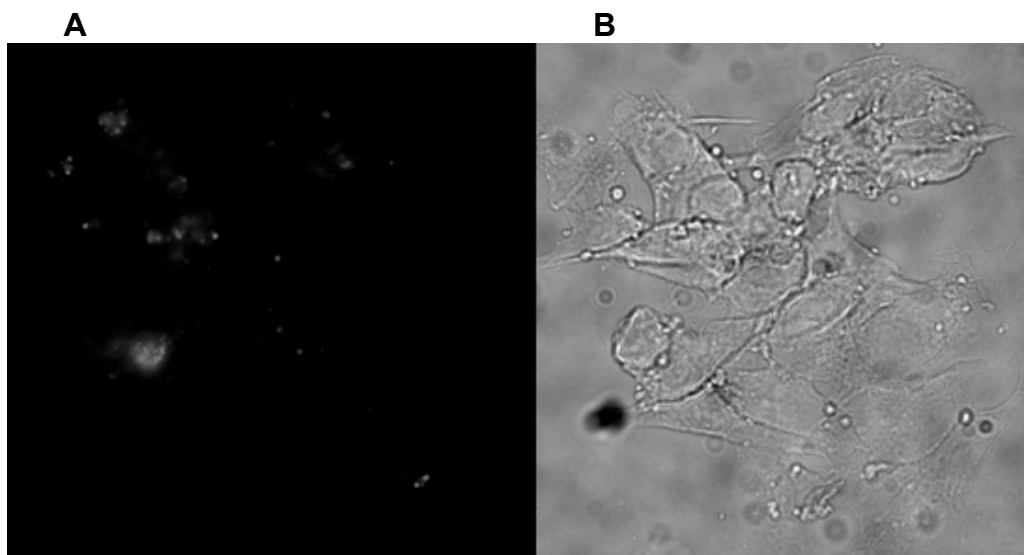


Figure 75. Autofluorescence of untreated HepG2 cells (Live image)
(A) Fluorescence and (B) bright-field view

For this kind of experiments the use of the fluorochrome Alexa fluor[®]488 was the appropriate choice, as it is stable and not susceptible to fast bleaching due to free radicals produced in living cells during illumination. The fast bleaching of the fluorescent label after less than 2 min of imaging impeded for example live imaging of Texas red[®]-labeled antibody uptake into HepG2 .

Filming the live uptake of the compound **6** into HepG2 cells and it's shuffling in endosomes was also attempted. But it was not possible to discern between the cells movement in the dish and the actual movement of the vesicles within the cells.

Preliminary experiments with fixed cells

Compounds **7** and **8** at 100 μ M were incubated on HepG2 and SK-Hep1 cells for one hour on ice to allow binding of the compounds and afterwards washed extensively with serum free medium. Then, the cells were placed for 10 min at 37°C to boost receptor mediated endocytosis. After a further wash with PBS, the cells were fixed with 3% PFA and mounted onto glass slides as described in chapter 2.3.7. A Zeiss Axiovert inversed microscope was employed for imaging.

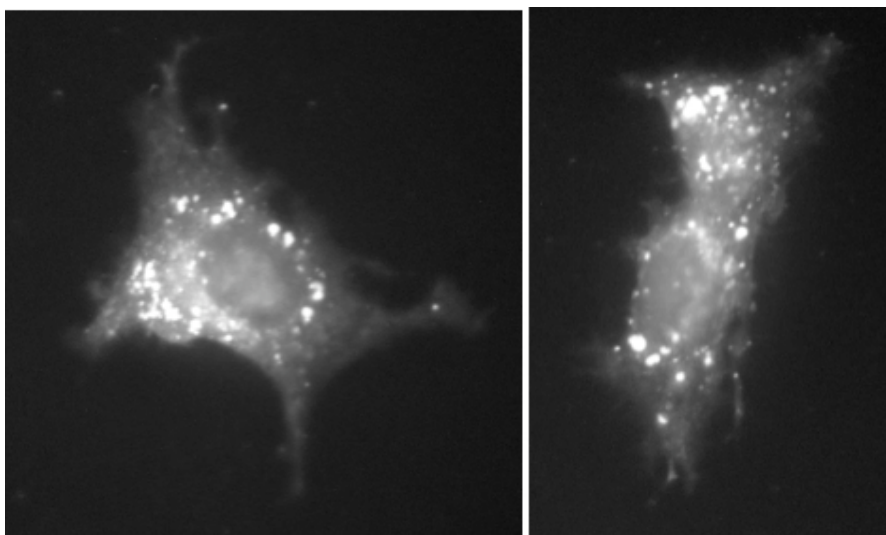


Figure 76. Uptake of compound **7** in single HepG2 cells after 10 min of internalization

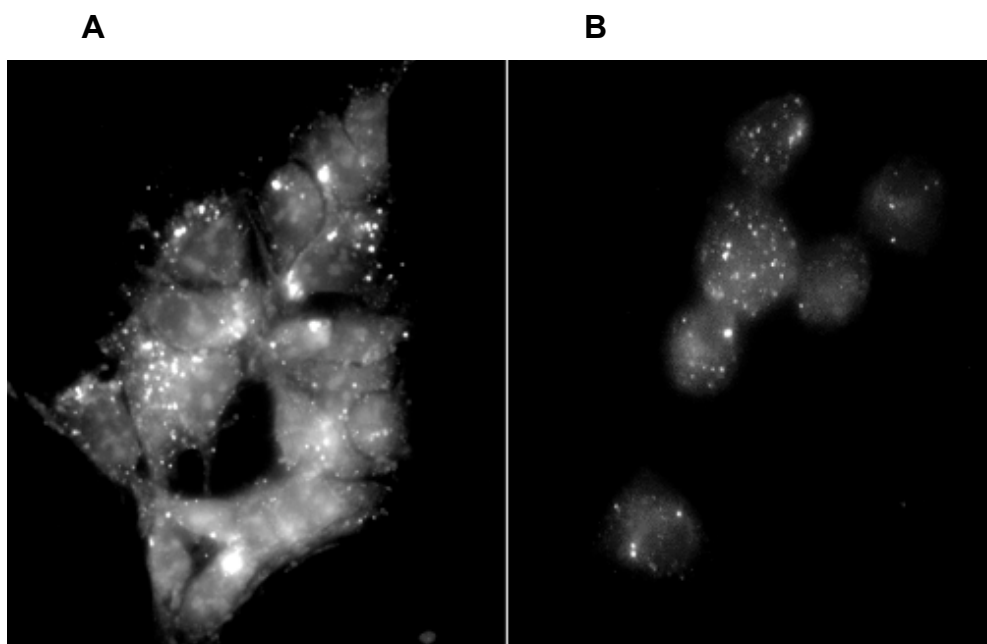


Figure 77. Uptake of compound **8** in (A) HepG2 and (B) in SK-Hep1 after 10 min of internalization

Triantennary GalNAc compound **7** was exclusively internalized into HepG2 cells (Figure 76), whereas compound **8**, with the shorter spacers, was internalized into HepG2 as well as SK-Hep1 cells (Figure 76).

3.9 Adaptation of mouse Antibodies to scFv

3.9.1 Source of mRNA

Both hybridoma and spleens are suitable sources of mRNA. Therefore, properly spliced antibody genes can be isolated from either mouse antibody producing hybridoma or spleen-derived B-lymphocytes. Since hybridoma cells express the heavy and light chain of one single antibody, they represent the most abundant and straightforward source from which antibody genes can be cloned.

Several well-characterized murine hybridoma clones producing antibodies against the truncated CRD of the human H1 subunit of the ASGP-R were available at our institute; four of them were selected as antibody gene source.

3.9.1.1 Selection of Antibodies for Adaption

The four clones were selected for their different binding characteristics (summarized in Table 25.).

Table 25. Characteristics of selected H1-CRD antibodies

	B01.4	C11.1	C14.6	C23.8
Isotype	IgG1 κ	IgG1 κ	IgG2a κ	IgG1 κ
K _D Biacore	308 pM	78 pM	n.d.	n.d.
Ca dependency of binding	-	+	-	++
IHC after fixation	-	-	+	-
Growth and Ab-production of the original clone	+++	++	+	-

B01.4 was selected for its good growth properties and high antibody yield in production. This antibody also showed good internalization properties into ASGP-R bearing cells and was already commonly used at our institute to detect H1-CRD in western blots. B01.4 showed no cross- reactivity in FC with other cells bearing galactose-receptors¹⁶⁵. C11.1 another interesting clone produces an antibody, with high affinity in SPR experiments, shows calcium dependent binding which indicates that the epitope it recognizes on the H1-CRD is in proximity to the sugar binding site, and it probably also preferentially binds to the dimeric form of H1-CRD. Clone C14.6 produces an antibody that

preferentially recognizes denatured H1-CRD, and is a potential candidate for diagnostic use in AIH (see chapter 3.4.2). C23.8 on the other hand produced an antibody with interesting properties by also displaying strong calcium dependent binding to the H1-CRD, but this unstable clone could no longer be propagated (see chapter 3.4.1). Hence C23.8 was selected for the adaptation to the scFv format in order to save this antibody whose properties would otherwise be lost.

3.9.1.2 Isotyping

The isotyping ELISA revealed that 3 of the selected hybridoma clones, B01.4, C11.1 and C23.8, produce antibodies from the isotype IgG1kappa and one, C14.6, from subtype IgG2a (Figure 78).

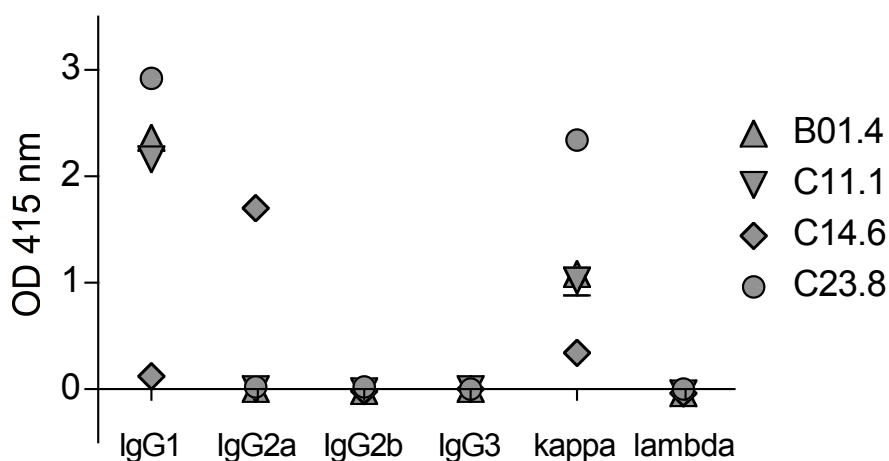


Figure 78. Antibody isotyping ELISA

3.9.1.3 mRNA Purification and First Strand cDNA Synthesis

One of the first steps in an antibody-engineering project is the isolation of the immunoglobulin heavy (V_H)- and light (V_L)-chain variable-region genes that encode the binding domains of the antibody.

The success of antibody cloning depends not only depend on the amount, but mainly on the purity of the mRNA. The use of total RNA is not recommended, since background product may also be amplified during PCR and would decrease the yield and purity of the desired PCR product.

The mRNA from hybridoma cells B01.4, C14.6, C11.1 and C23.8 was isolated

with the Illustra Quickprep mRNA purification kit obtained from GE Healthcare according to the protocol of the manufacturer. This method uses oligodT-cellulose spin columns, which take advantage of the polyA-tail that is common to eukaryotic mRNAs. The eluted sample was not quantified to prevent mRNA loss. The mRNA was then precipitated by splitting the final elution in 2 aliquots of 0.32 ml each, adding 10 μ l of glycogen, 32 μ l of the potassium acetate solution (both provided in the kit) and a volume of 0.8 ml ice-cold ethanol. The mixture was incubated for 30 min at -20°C . The precipitated mRNA from one aliquot was collected by centrifugation for 30 min at 16000 g at 4°C , followed by a wash in 1 ml 99% ethanol and then stored in Ethanol at -20°C . One vial of mRNA per clone was used for cDNA synthesis.

At first, the sample was centrifuged again for 30 min at 13'200 rpm and 4°C , the supernatant was discarded and the mRNA pellet washed once more in 1 ml ice-cold ethanol. Reverse transcriptase synthesizes first strand cDNA from mRNA primed with random hexamers. The use of random hexamers eliminates the need for immunoglobulin-specific primers or oligo(dT) primers which would require the synthesis of a long cDNA, encoding the heavy and light chain genes.

The cDNA synthesis didn't work the first time and was repeated. A possible reason was that the lyophilized reverse transcriptase in the 'Ready-to-use you prime'-kit was less efficient than the one in solution that is usually used. To ensure that there would be enough templates for the amplification of V_H and V_L , the remaining mRNA aliquot of each clone was resuspended in 50 μ l of DEPC- H_2O and split in two RT-PCR tubes for cDNA synthesis, which was then done according to the manufactures protocol. The two cDNA products were later combined for further processing.

3.9.1.4 Amplification of V_L and V_H - First Step in Assembly

Since the V_L and V_H genes represent only a very small fraction of the total cDNA, they must first be amplified to generate sufficient DNA for cloning.

For this purpose, a mixture of degenerate primers, which contain variable nucleotides at several positions in the sequence, designed to hybridize to opposite ends of the variable regions of each domain, was used to amplify the

heavy and light chain of the antibodies variable domains¹⁷³. During this step, the genes are not only amplified but part of the *Sfi* I restriction site, a FLAG-tag and also the linker sequence are introduced. The V_L BACK-primer mix introduces a shortened FLAG-tag (DYKD) the V_L FOR- primer mix contains a part of the Gly₄Ser-linker sequence of which the third repetition, with a different codon usage to prevent mismatches in the SOE-PCR reaction, overlaps with the one introduced by the V_H BACK-primers. The V_H FOR primer mix introduces a palindromic sequence as *Sfi*I restriction site to the V_H domain.

As the four selected hybridoma clones produce antibodies from the kappa subtype, no primers for lambda light chains were included in the mixture. These could otherwise amplify unwanted 'junk' lambda light chains sourcing from the myeloma fusion partner of the hybridoma cell. The V_L and V_H antibody genes were amplified in separate reactions using a proofreading DNA polymerase and premixed sets of forward and backward primers.

According to Plückthun et al.¹⁷³ the fragment size for the V_L domain is between 375 and 402 bp, and that of the V_H domain between 386 and 440 bp, depending on the CDR lengths of the corresponding antibodies. The amplified heavy and light chain fragments were purified separately by agarose gel electrophoresis to remove primers and extraneous amplification products. The bands were excised and the DNA fragments purified with the GenElute kit from Sigma.

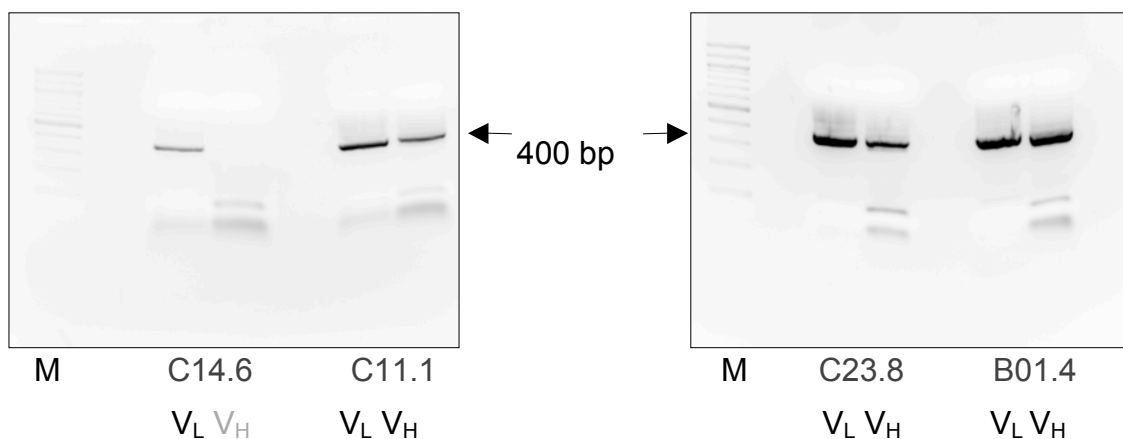


Figure 79. V_L and V_H amplification
(2% TBE Agarose gel)

The V_H fragment of C14.6 could not be amplified (Figure 79). Several attempts

with different DNA polymerases (Taq and Phusion from NEB instead of iproof) and varying annealing temperatures (45°C, 51.2°C, and 55°C) did not lead to success. C14.6 is the only one of the selected antibodies with IgG2a subtype, therefore it could be concluded that the used degenerated heavy chain primer set did not include a matching primer for this subtype or for this specific antibody gene. Another cause that cannot be excluded is that there was not enough of the template heavy chain cDNA of C14.6 or that the quality was not sufficient.

3.9.1.5 Assembly of the Heavy and Light Chains

The so-called 'Splicing by overlap extension-PCR' (SOE-PCR) assembles the variable antibody domain genes with the linker sequence to scFv fragments. In the first two cycles of the PCR method, the two fragments were assembled via the complementary linker-sequence, then the primers scfor and scback were added to introduce the second *Sfi* I restriction site to V_L (via scback) and to amplify the scFv genes.

The gel-purified heavy and light variable domain DNA products of the antibody clones B01.4, C11.1, and C23.8 were quantified by UV, so that the optimal amount of each could be used for the assembly reaction.

Equal amounts of the V_H and V_L fragment of the three remaining antibodies were used for the assembly reaction and the products were purified from the Agarose gel (Figure 80).

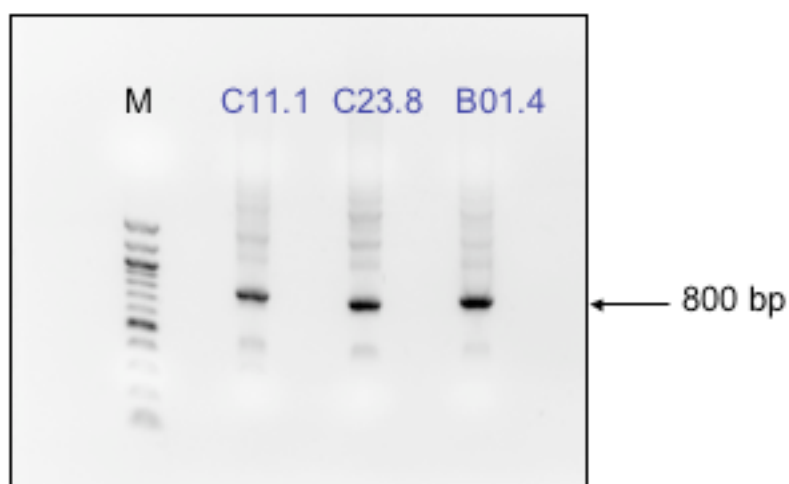


Figure 80. Assembly of scFv (V_L -linker (Gly₄Ser)₄- V_H) (2% TBE Agarose gel)

3.10 Cloning of the scFv Genes into pAK300

3.10.1 Digestion of pAK300 and the scFv Constructs

The plasmid for scFv expression, lyophilized pAK300 from 2 µl of a Midi-prep, was kindly provided by the lab of Prof. Plückthun, ETH Zurich. The plasmid was reconstituted in 10 µl of sterile TE buffer. Then, 2 µl of the reconstituted plasmid were heat-shock transformed into rubidium competent DH5α cells and purified by Miniprep from 3ml over night cultures of single colonies in TB medium with Cam. The purified plasmid was quantified by UV. To remove the tet-stuffer cassette and open the pAK300-plasmid for cloning of the scFv gene fragments, the plasmid and the fragments were digested with *Sfi*I for 3-4 h at 50°C.

The restriction enzyme *Sfi*I recognizes a rare palindromic sequence of 8 bases, interrupted by 5 non-recognized bases:

*Sfi*I restriction site

5' GGCCNNNN'NGGCC 3'

3' CCGGN'NNNNCCGG 5'

The base sequence of the *Sfi*I restriction site can be designed in many ways, because the five nucleotides inside the restriction site can be varied. As *Sfi*I preferentially cuts two sites simultaneously when two restriction sites are present either on the plasmid or on the gene constructs, nearly no single cut plasmid-intermediates occur.

The two distinct *Sfi*I restriction sites on the plasmid as well as on the scFv gene constructs omitt a double digest and prevent the plasmid from self-ligation

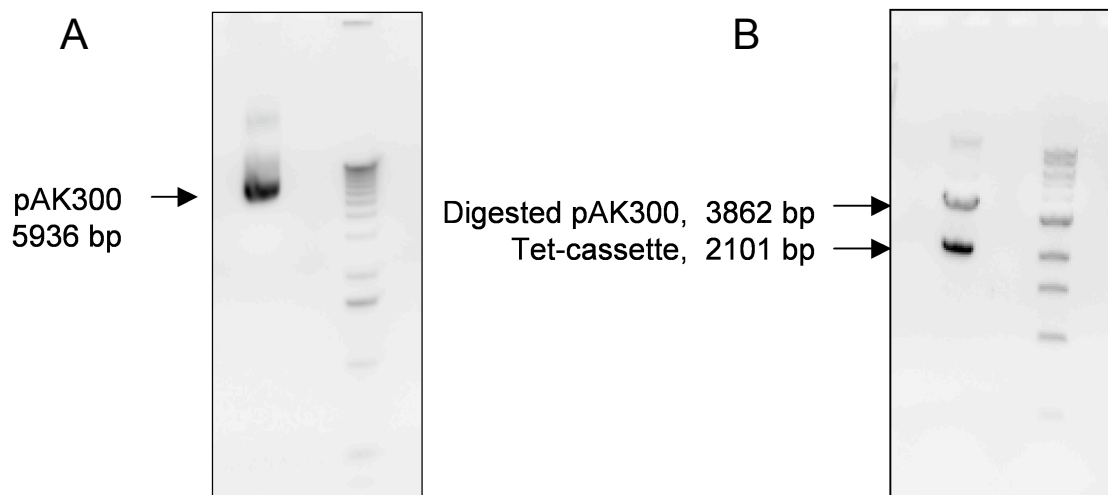


Figure 81. pAK300 digestion
(A) undigested, (B) *Sfi* I digested (1% TBE Agarose gel)

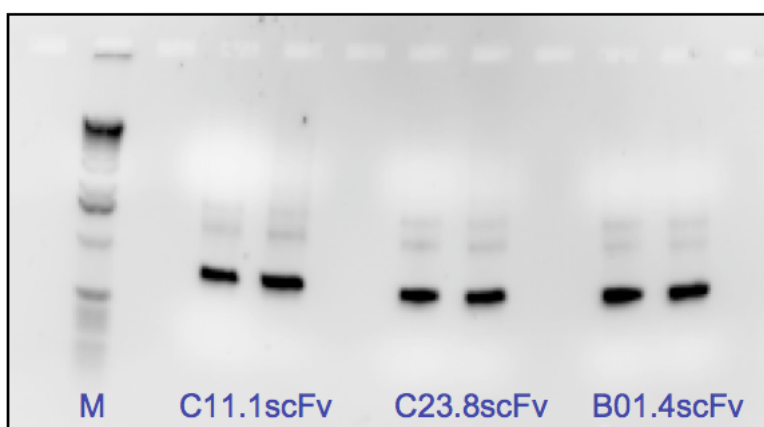


Figure 82. Digested scFv fragments
(1% TBE Agarose gel)

3.10.1.1 Ligation of the scFv Constructs into pAK300

Both, digested vector and scFv-fragments, were gel-purified (Figure 81 and 82) and quantified before ligation. The molar ratio vector to insert was 1.5:1 and the ligation mixture was incubated over night at 16°C with T4 ligase. The pAK300 introduces a C-terminal His₆-tag to simplify the purification of the scFv.

3.10.2 pAK300-scFv Plasmid Amplification

To amplify the pAK 300 plasmid with the scFv inserts, 5 µl of the gel-purified ligation reaction of pAK300scFvC11.1, C23.8 and B01.4 were transformed into RbCl-competent DH5α cells by heat-shock transformation. Clones were picked

and grown in 3 ml of TB medium with Cam over night and the plasmids were extracted by miniprep.

Agarose-gel electrophoresis and analytical digest with *Sfi*I of selected clones showed that a some did not contain the scFv insert, but the religated tet-cassette (Figure 83).

Table 26. Size of plasmid and insert (in bp)

Plasmid	Size digested	Size of insert	Size ligated
pAK300	3.9	2.1	6
pAK300scFv	3.9	0.8	4.7

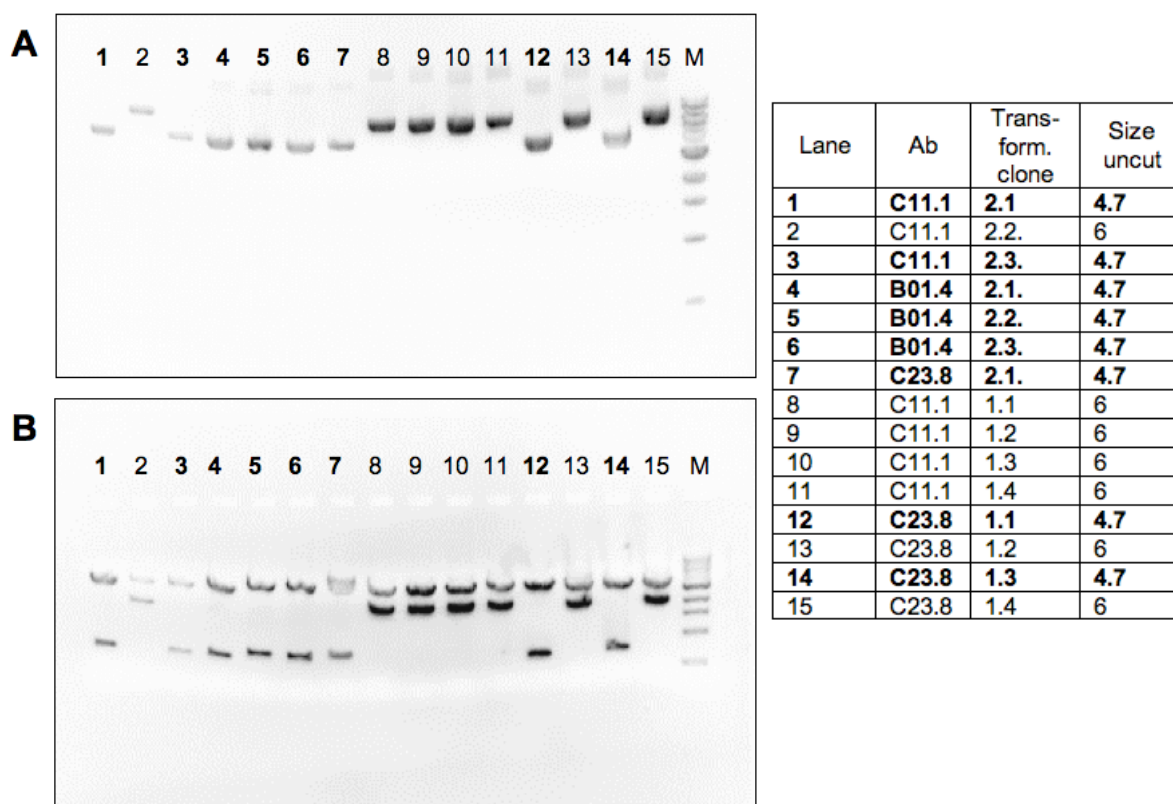


Figure 83. Agarose gel of selected pAKscFvs before (**A**) and after (**B**) analytical digest

The problem was partially solved by repeating the plasmid digestion and by running the preparative gel for a longer time to achieve a better separation of the digested plasmid and the tet-stuffer cassette.

To ensure that the selected clones contain the full scFv insert, some of them were selected and sequenced. The sequencing of the clones revealed the occurrence of many inserts without or with a shortened linker sequence, which

would be needed for correct folding of the antibody fragments. A reason for this problem could be that the used degenerate primers were of low quality, which is crucial for the correct amplification of the variable domains.

3.10.3 Production and Purification of murine scFv

3.10.3.1 Transformation of pAK300scFv into BL21(DE3) for Expression

One clone containing the full scFv per parental antibody was selected and was transformed into *E.coli* BL21(DE3) by electroporation. Transformed cells grew on Agar plates containing chloramphenicol (Cam).

Because the pAK300 vector contains a pelB signal sequence, bacterial expression of the scFv in *E.coli* BL21(DE3) should lead to soluble scFv secreted and enriched in the periplasma of the cells.

The obtained transformed cells were tested for scFv production by colony blotting using Ni-AP conjugate to detect the his-tag on the secreted scFvs (Figure 84).

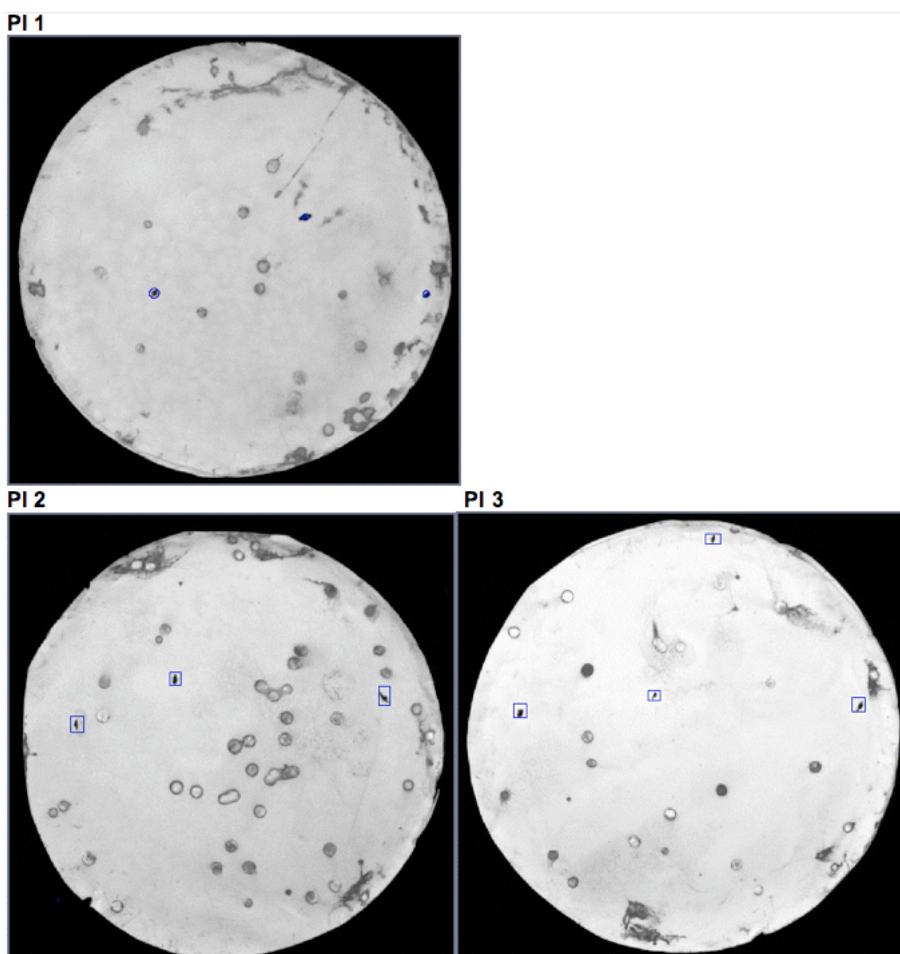


Figure 84. Colony blotting of transformed BL21(D3) pAk300scfv
(**PI1**) B01.4 (**PI2**) C11.1 (**PI3**) C23.8

Small positive colonies from the regrown master plates were picked and inoculated in 2 ml LB + Cam for minipreps and glycerol stocks.

3.10.4 Expression and Purification of murine scFv

Expression of C11.1scFv in 500ml scale to establish a purification protocol

An over night culture of BL21(DE3)pAK300scfvC11.1 cl 2.1,T4.1 with some μ l scratched from the glycerol stock in 20 ml SB with 1% glucose and 34 μ g/ml Cam (complete medium) was grown at 37°C with 200 rpm.

The cells from 10 ml of this culture were harvested by centrifugation at 1500 rpm and 5 min. The cells were resuspended in 10 ml complete SB medium and added to 500 ml SB expression medium with Cam and 0.1% glucose (expression medium) in a 1l Erlenmeyer flask. Cells were grown at 30°C and 200 rpm to an OD_{600} of 1.0 before induction with 1mM IPTG. Every hour a

sample was taken for OD₆₀₀ measurements to monitor cell growth.

After reaching the stationary phase of growth (5 h after induction, Figure 85), the cells and supernatant were harvested by spinning 20 min at 3300 g, 4°C. The supernatant was collected and filtered (0.22 µm) and stored at 4°C.

To harvest the scFv from the wet cell pellet, CeLytic B reagent from Sigma was used according to the producer's manual.

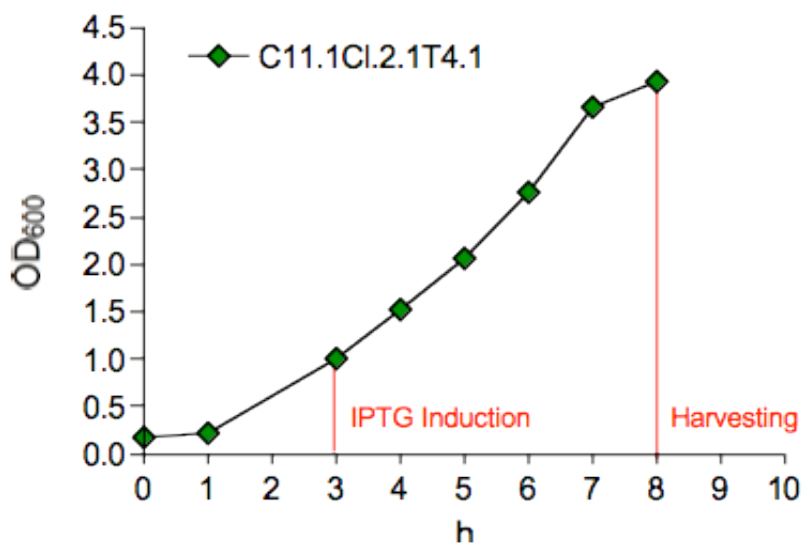


Figure 85. Growth of C11.1scFv, 500ml culture used to establish the purification strategy

Different purification strategies of the scFv via the his-tag using IMAC purification with HiTrap ff crude columns (1ml) were tested. The parameters that were varied were different concentrations of imidazole (0-20 mM) in the binding buffer and elution in one step and/or with increasing concentrations of imidazole (5-10 mM) in the last washing step before the elution with 100 mM imidazole in PBS.

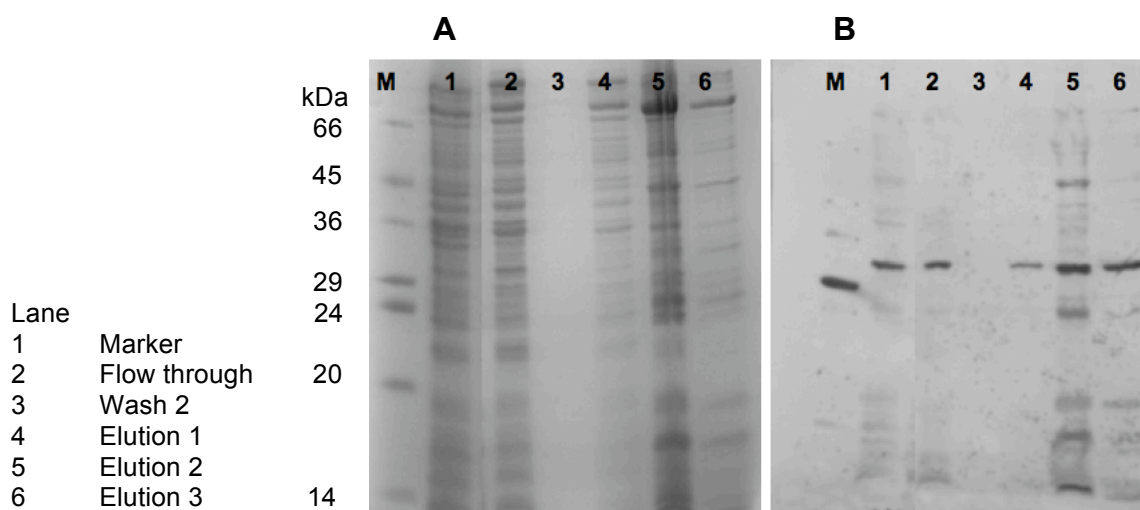


Figure 86. SDS-PAGE analysis of C11.1scFv purification via IMAC (A) non-reducing SDS-PAGE, (B) Western blot of the same samples detected with Ni-AP-conjugate

With all tested strategies the occurrence of substantial amounts of bacterial proteins together with the scFv in the elutate, could not be avoided. There were also still high amounts of scFv detected in the flow through (Figure 86). This could be due to an overload of the column or because the his-tag is partially buried in the structure of the scFv.

In order to solve the problem of contaminating bacterial protein, a 'one step 2-columns' purification procedure proposed by Plückthun et al.¹⁷³ was tried. This method uses a MHA buffer system (Mes (2-morpholinoethanesulfonic acid, HEPES, Sodium acetate), an elution step with a salt-free imidazole buffer and direct loading of the eluted protein from the Ni-NTA column to a S12 anion exchange chromatography column (Bio-Rad). This attempt was not successful and only very small amounts of protein could be eluted. Hence this method was not further employed.

Production of B01.4, C11.1 and C23.8scFv

Cultures (500 ml) for C11.1scFv, B01.4scFv and C23.8scFv were started, and scFv expression was induced as described above. To reduce the load of bacterial protein contaminants only the periplasmic and osmotic shock fraction of the collected cell pellets were harvested this time. For that purpose the cell wall of the bacteria was destroyed by osmotic shock treatment as described in

chapter 2.9.8.1. IMAC purification via his₆- tag was performed as described in chapter 2.9.8.

The purity could be increased but still only small amounts of protein could be purified from the dialyzed periplasmic and osmotic shock fraction (represented in the small peak in Figure 87 for B01.4 scFv).

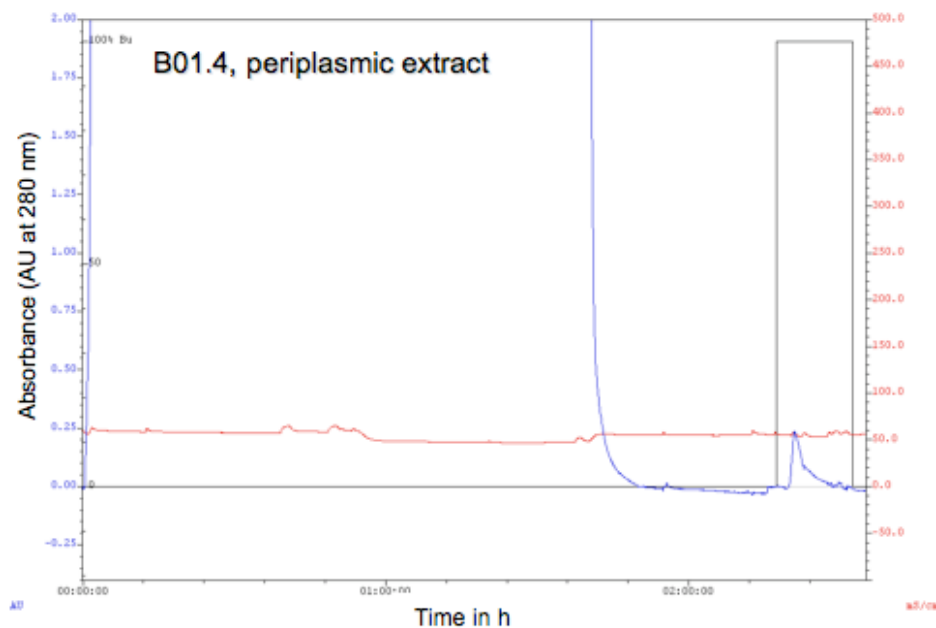


Figure 87. Example chromatogram of IMAC purification for B01.4scFv from periplasmic extract

The collected scFv elutions were concentrated and the buffer was changed to either PBS or HBS-P+ 50mM CaCl₂ for SPR screening.

H1-CRD was immobilized and its activity was evaluated as described in chapter 2.9.12. SPR screening was performed as described in chapter 2.9.13.

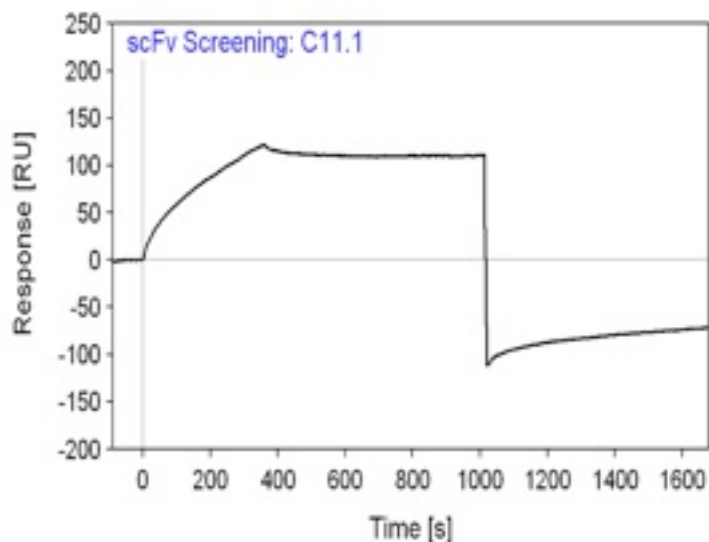


Figure 88. Sensorgram obtained from the screening of C11.1scFv in SPR

Of the tested scFvs only purified C11.1scFv was able to bind to immobilized H1-CRD (See Figure 88).

C11.1scFv was also tested for its binding to H1-CRD in ELISA, using HRP-Ni conjugate for detection, and in addition in the competitive solid-phase binding assay for its inhibition of GalNAc-PAA-polymer binding (See chapter 2.9.10.)

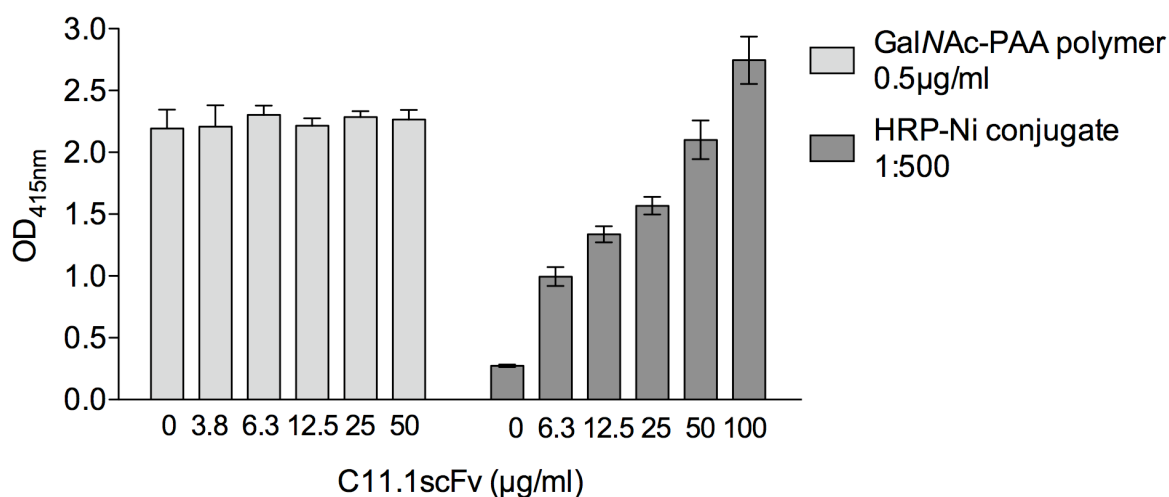


Figure 89. purified C11.1scFv tested for binding to H1-CRD in the competitive solid-phase binding assay (light grey), and in ELISA using a HRP-Ni conjugate for detection (dark grey)

The results depicted in Figure 89, show that C11.1scFv binds to the H1-CRD in a concentration dependent manner, but that it does not inhibit the binding of GalNAc-PAA-polymer to the H1-CRD and therefore does not block its sugar-binding site.

3.11 Phage Display of murine scFvs

Usually the application of phage display is the first step in the selection of a binding scFv constructed from hybridoma cells, but it's not essential. When phage display technology became available in our lab, the technique was also deployed to find a binding scFv-clone from the adapted murine antibodies.

3.11.1 Cloning of murine scFvs into Phagemid Vector pAK100

The SOE-PCRs of V_H and V_L gene fragments from the hybridoma clones C11.1, B01.4, C23.8 were repeated and the obtained scFv constructs were cloned into the digested pAK100 phagemid vector as described for pAK300.

The analytical digest of the ligation products confirmed the presence of the insert in all three pAK100scFv constructs (Figure 90).

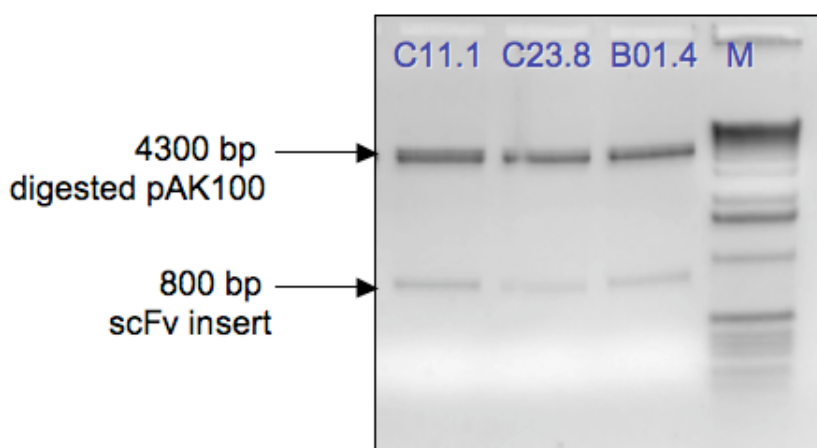


Figure 90. Analytical digest of pAK100scfv constructs

3.11.2 Preparation of mouse scFv Phage Libraries

The pAK100scFv constructs were transformed into *e.coli* XL1 Blue by electroporation. Three different phage display libraries in XL1 Blue (C11.1, B01.4, C23.8) were obtained. All clones were washed from the selection plates and transferred to 200 ml of 2xTY medium with 1% glucose and Cam and grown to an OD_{600} of 0.5. From these cultures 20 ml each were infected with 200 μ l VCSM helper phage for 30 min at 50 rpm, then 30 min at 200 rpm. Phage was amplified as described in chapter 2.9.3. Bacteria were pelleted at 3300 g for 10 min and 4 ml of phage solution were purified from the supernatant

of each of these libraries by PEG precipitation as described in chapter 2.9.4.

3.11.2.1 First Round of Phage Panning on Immuntubes

Immuntubes were coated over night at 4°C with 20 µg/ml of H1-CRD in HBS + 10 mM Ca²⁺, blocked for 2 h with 3% BSA in PBS, and incubated with 1ml of the purified phage library of each clone. Bound phage was eluted and log-phase XL1 Blue cells were infected with the eluted phage and then plated onto big selection plates. The plates were incubated over night at 30°C. No colonies appeared on the plates harboring XL1 Blue infected with pAK100scFvC23.8, 3 colonies on the pAK100scFvB01.4 plates, and 5 colonies were visible on the pAK100scFvC11.1 plates. The bacterial colonies were picked, grown over night in LB + Cam and 1% glucose and the phagemid vectors were purified from 1.5 ml by Miniprep and stored at -20°C.

3.11.2.2 Soluble scFv ELISA

The picked clones were grown in 5 ml cultures with Cam and 0.1% glucose, induced with 1mM IPTG at OD₆₀₀ 1.0 and scFv was expressed over night at 30°C and 200 rpm. A soluble scFv ELISA was carried out with 150 µl of the supernatants/well, as described in chapter 2.9.5.1.

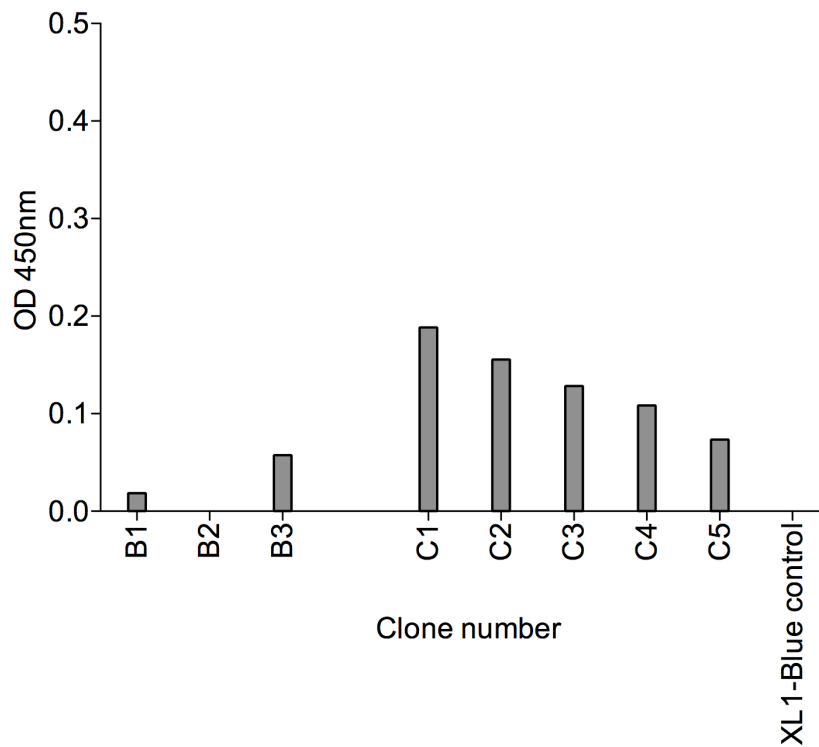


Figure 91. Soluble scFv ELISA of murine antibodies after the first panning round
B1-3 clones from pAK100 B01.4sFv, C1-5 from pAK100C11.1.4sFv, XL1-Blue control is medium from uninfected XL-1 Blue cells

The ELISA results are displayed in Figure 91. The obtained OD values were relatively low. In the scope of this thesis, the work on the murine phage display using pAK100 phagemid vector was stopped at this point.

3.12 Phage Display human scFv

The first 2 rounds of phage panning on human H1-CRD were conducted during the practical part of the course on Phage display technology organized by Prof. D.Neri at the ETH Zurich. A frozen 5 ml glycerol-stock of bacteria from a big selection agar plate after the first panning round obtained after the course was used for further rounds of panning.

3.12.1.1 ETH-2-Gold Phage Sub-library Rescue after First Panning

TG1 bacterial library glycerol stock (ca. 5ml) from the big agar plate was inoculated into 200 ml of 2xTY+Amp + 1% glucose to reach an $OD_{600} = 0.1-0.2$ and grown to $OD_{600} 0.4-0.5$ at 37°C. Then 10 ml of this culture were infected with helper phage in a ratio of around 20:1 (phage: bacteria) for 30 min at 37 °C. The infected bacteria were pelleted at 3300 g for 10 min, gently resuspended in 100 ml of 2xTY-Amp-Kan and incubated at 30°C overnight, shaking. Then, the culture was spun again at 3300 g for 10 min and the phage was immediately PEG precipitated from the supernatant. The obtained phage sub-library was stored in 2 aliquots at -20°C.

3.12.1.2 Biopanning using Immunotubes

The panning on immunotubes was conducted as described in chapter 2.9.2. After each round of panning the bacteria were harvested from the big selection plates and the phage rescued as described in chapter 2.9.3. The rescued phage was split in two aliquots of which one was stored for backup at -80°C and the other one used for the next round of panning.

H1-CRD was coated to the immunotubes using its normal storage buffer HBS + 10 mM $CaCl_2$ to provide the protein with the necessary calcium for its active conformation. All further steps were carried out in PBS, as there was no previous experience with using HBS buffer during panning.

Reducing the density of the antigen H1-CRD immobilized to the immunotubes and increasing the washing steps after the pannings increased the stringency of selection. The first two rounds of panning were carried out during the Antibody phage display course with 100 µg/ml of H1-CRD as antigen. The blocking agent

for the tubes during these first two rounds was 2% milk powder. Because milk powder contains galactose that could serve as a ligand of the H1-CRD and hence block its binding site, all further rounds of panning were carried out using 3% BSA for blocking of the tubes.

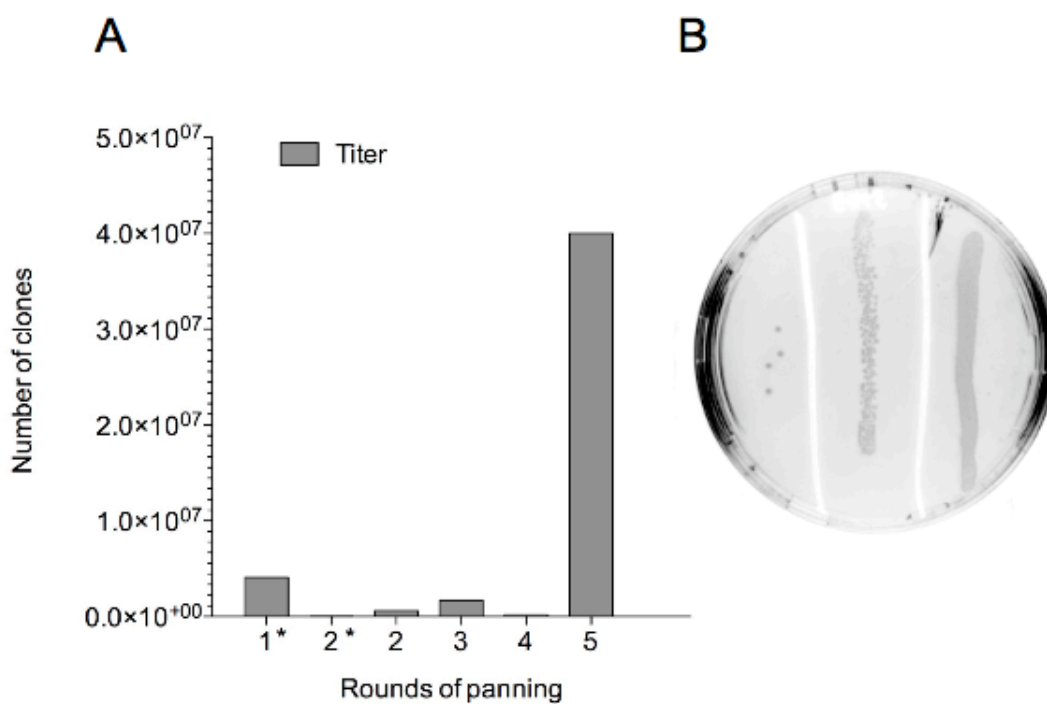


Figure 92. Titer after panning rounds on immunotubes (A) 1* and 2* panning round during the course with 2% milk powder, panning rounds 2-5 with 3% BSA as blocking agent (B) Titer Agar plate ETH2 gold after panning round 5

The titer after the first round of panning on 100 µg/ml H1-CRD was 4.1×10^6 cfu (colony forming units)/ml. After the second round in the course the titer was low (8.8×10^3 cfu/ml) (1* and 2*, Figure 92) and only 44 clones could be picked from the big selection plate to control the selection with a soluble scFv ELISA. One of these clones was detected positive for binding to 100 µg/ml of H1-CRD in ELISA. In panning round 2 and 3, carried out in our lab on 20 µg/ml of immobilized H1-CRD, the titer was $6 \cdot 10^5$ and 1.7×10^6 cfu/ml, respectively. Panning rounds 4 and 5 were carried out using 10 µg/ml of H1-CRD and resulted in titers of $2 \cdot 10^5$ and finally 4×10^7 cfu/ml.

3.12.1.3 Screening scFv Expression by ELISA

After some rounds of panning, it is usually good practice to monitor the progress of the selection by ELISA, either with soluble scFv, or by using the scFv displayed on phage. This means that either colonies of bacteria infected with

phage from the desired round of panning are picked individually and induced to express soluble antibodies into the supernatant or that the clones are infected with helper phage to produce and secrete scFv-gpIII-phage particles in bacterial supernatants, both can be tested in ELISA to screen for antigen binding scFvs. *E.coli* suppressor strains such as XL1 Blue or TG1 allow regulated expression of scFv-gpIII fusion protein as well as soluble recombinant scFv because *E.coli* supE44 strains only partially suppress the amber stop codon TAG in the reading frame between scFv and gpIII. To screen the infected bacteria in ELISA for their expression of soluble scFv has the advantage to detect clones that not only produce scFv that bind the antigen but are also able to express sufficient amounts of scFv to be detected in one step.

XL1-Blue clones picked from round 2 and of round 5 plus the positive TG1 clone identified in the first ELISA during the Phage display course were tested for soluble scFv expression in ELISA.

Cells were grown and induced in U-well plates as described in chapter 2.9.5. After 16 h of induction, the plate was spun down to pellet the bacteria and the supernatants containing the soluble scFvs were transferred to the prepared ELISA plate coated with 5 µg/ml of H1-CRD and blocked with 3% BSA. The plates were incubated over night at 4°C in a humid chamber and processed as described in chapter 2.9.5.1. After color development with OPD-substrate the OD was measured at $\lambda=450$ nm. The results are depicted in Figure 93.

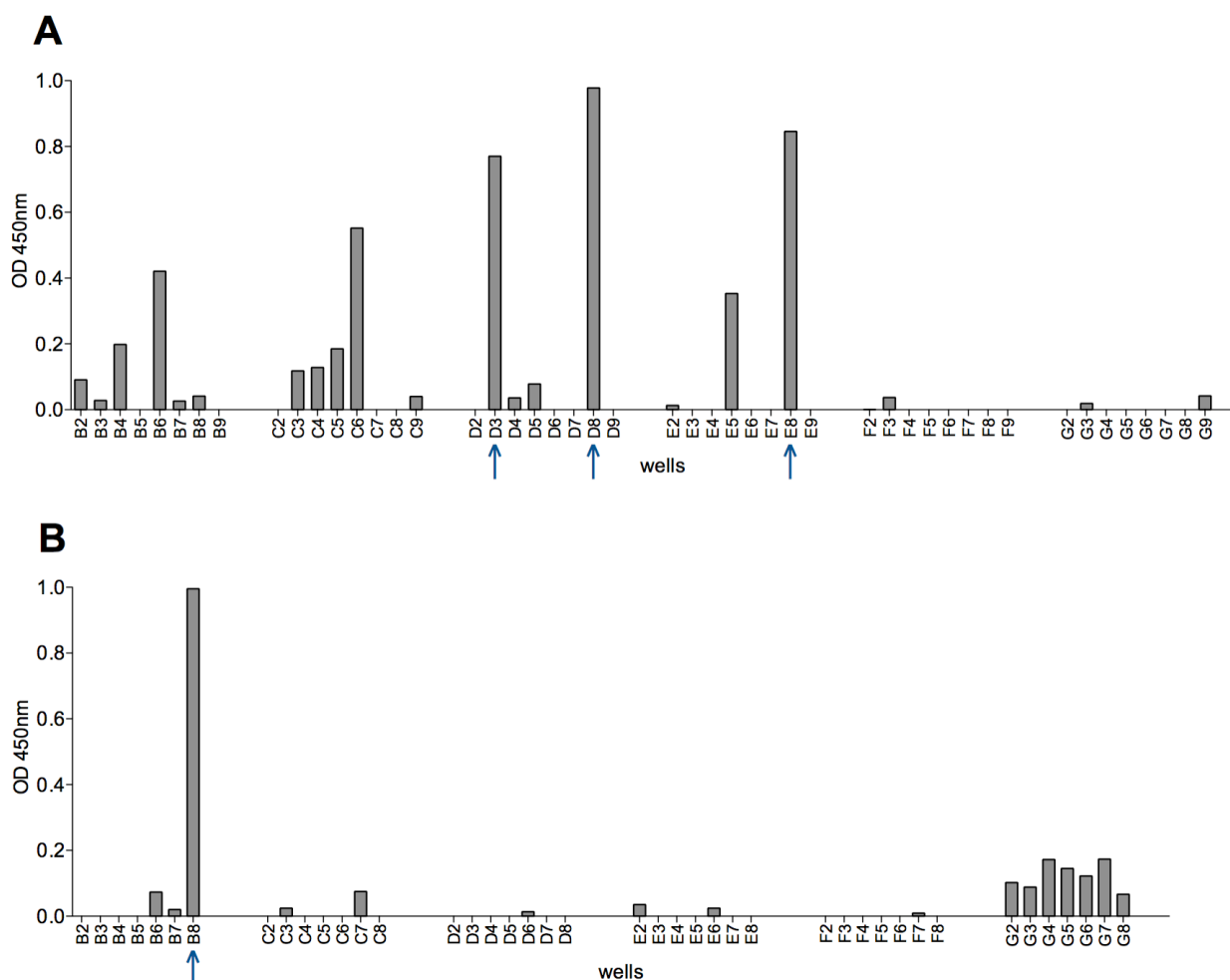


Figure 93. Soluble scFv ELISA from ETH-2-Gold clones (A) after panning round 2, (B) after panning round 5. Arrows indicate clones selected for small-scale expression of scFv

Plate 2 contained several positive clones and plate 5 only one, the positive one previously selected during the course.

Remarks:

More positive clones were expected from panning round 5, as the titer in this round was the highest (4×10^7 cfu/ml). Here scFv production was probably impaired because the lid of the U-well plate 2 harboring the selected clones from round 5 was not fully closed and some medium evaporated during the induction step. Hence, it would be worthwhile to repeat the ELISA with the cells from round 5.

Small-scale production of scFv was carried out with 3 of the positive clones from plate 2 and the positive clone from plate 5.

3.12.1.4 Small Scale Production of human scFv

Some μ l of cells from clones 5B8, 2D3, 2D8, and 2E8 were scratched from the backup plate and inoculated into 3 ml 2xTY medium with Kan and 1% glucose and grown over night at 37°C with shaking at 200 rpm. The next day the cultures were diluted into 100 ml of fresh 2xTY medium with Kan and 0.1% glucose and grown at 37°C to OD₆₀₀ 1.0 before induction with 1mM IPTG. Induction was carried out for 16 h at 25°C and 200 rpm. Then the cells were harvested and the supernatant filtered (0.45 μ m).

The filtered supernatants were purified by affinity chromatography over a protein A column as described in chapter 2.9.9.

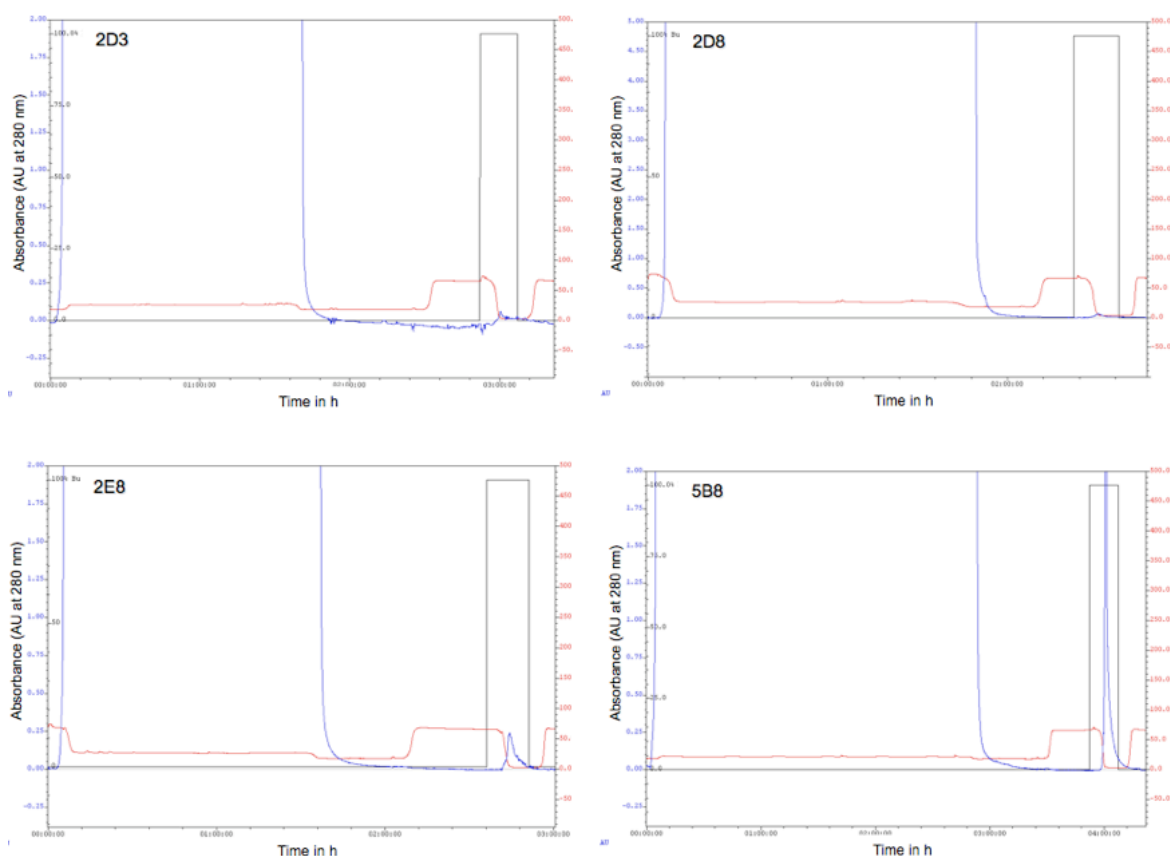


Figure 94. Chromatograms of the affinity purification of selected scFvs 2D3, 2D8, 2E8 and 5B8 from 100ml of supernatant of each clone using a Protein A column

The chromatograms in Figure 94 show that only clone 5B8 secretes high amounts of scFv to the supernatant. This clone was also used to express scFv in a 500 ml production batch induced for 18 h at 25 °C and 220 rpm from which the scFvs were purified in the same way.

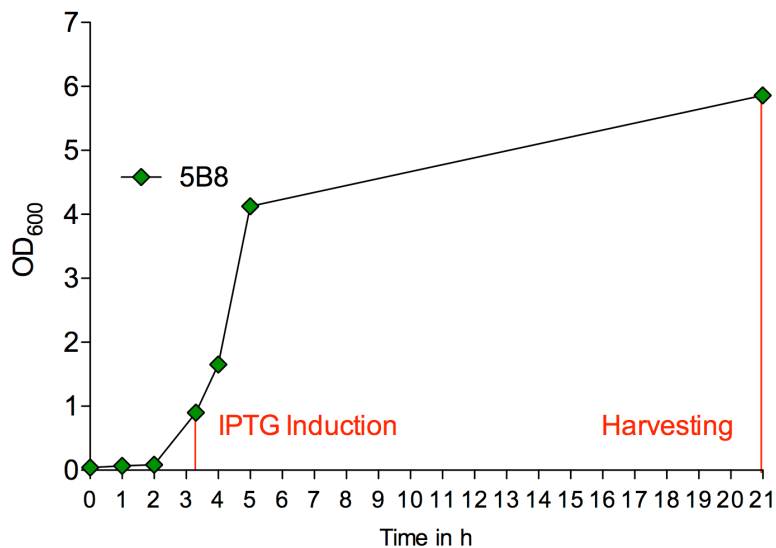


Figure 95. Growth curve of clone 5B8, 500ml culture the supernatant was harvested after 18h induction at 25°C.

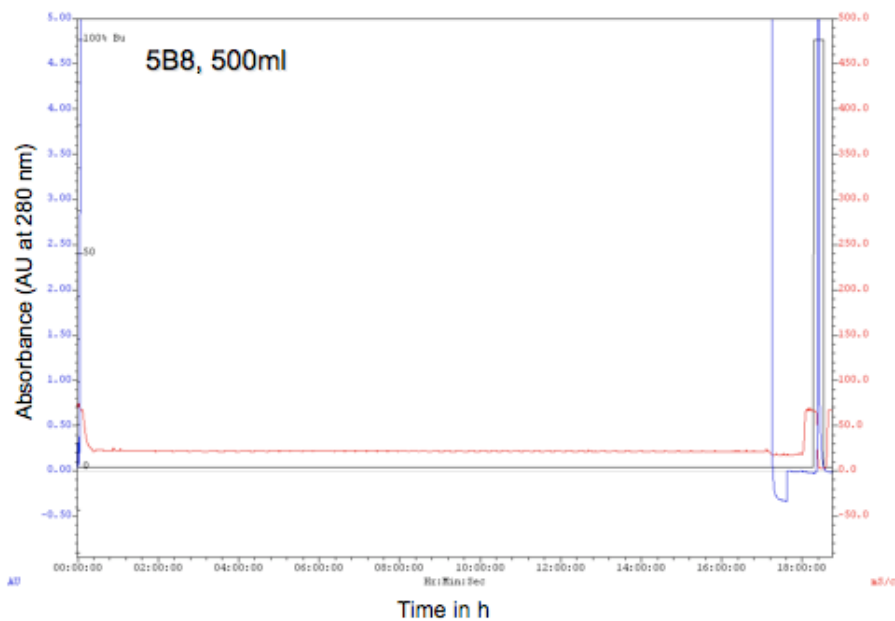


Figure 96. Chromatogram of the affinity purification of scFv 5B8 from 500 ml supernatant

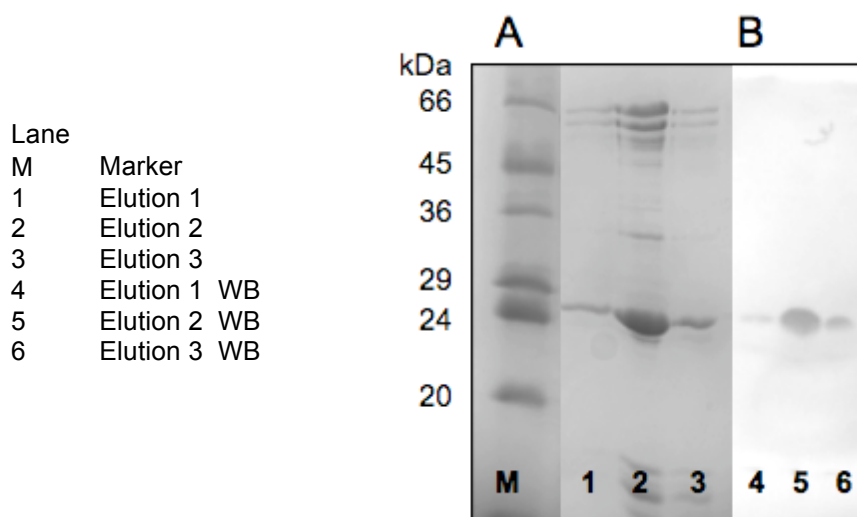


Figure 97. Analysis of scFv 5B8 purified from supernatant over Protein A
(A) SDS-Page 15% non-reducing (B) Western blot (detection with c-myc Ab)

SDS page analysis reveals the occurrence of bacterial contaminants in the eluted samples. Size exclusion chromatography was applied to remove these impurities, but technical problems with the column Bio Prep SE 100/17 (Bio-Rad) impeded further polishing. The samples were therefore used in the state they were except for 5B8 where at least high molecular weight contaminants could be removed by filtrating the sample trough a centrifugal filter device with a cutoff of 50 kDa and from which then the flow through was used for SPR. ScFv concentration was determined from SDS-PAGE using BSA as standard.

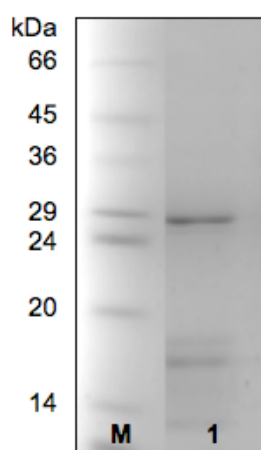


Figure 98. 5B8 scFv sample for SPR analysis
(1) After filtration through a centrifugal filtering device with cutoff 50kDa

3.13 Affinity Evaluation of scFvs

Protein immobilization is a crucial step in a SPR experiment. Loss of partial or entire target activity changes in ligand affinity, and many other artifacts are directly related to unfavorable immobilization. The standard CM5 sensor chip from Biacore contains a glass slide with a thin gold layer (50 nm) that is covered with a carboxymethylated dextran with a dimension of 100 nm under physiological conditions. Introduced carboxy groups on the dextran chains allow covalent immobilization of proteins, oligosaccharides, nucleotides, or small molecules.

H1-CRD was immobilized by amine coupling as described in chapter 2.9.11

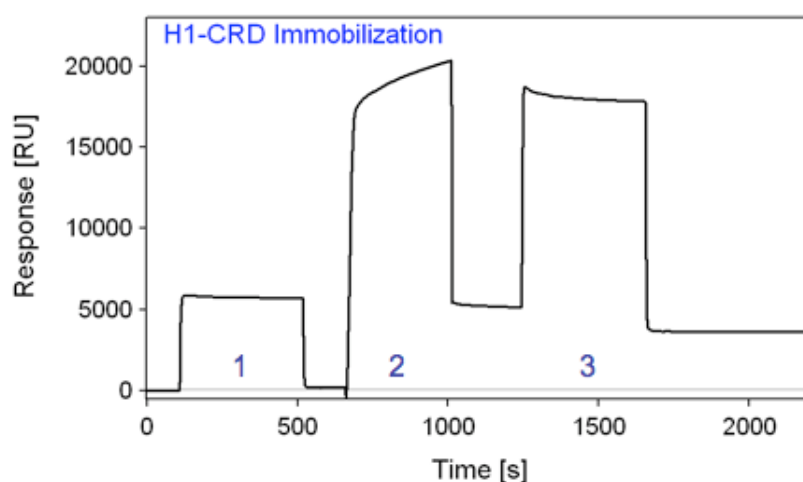


Figure 99. Immobilization of H1-CRD on a CM5 sensor chip. (1) Surface activation with NHS/ EDC, (2) amine coupling of H1-CRD, (3) deactivation with ethanolamine.

3.13.1 Activity Testing of H1-CRD

To demonstrate that the immobilized H1-CRD was in its active conformation and able to bind GalNAc (see also chapter 3.1.1.1) activity testing on the H1-CRD was performed as described in chapter 2.9.12.

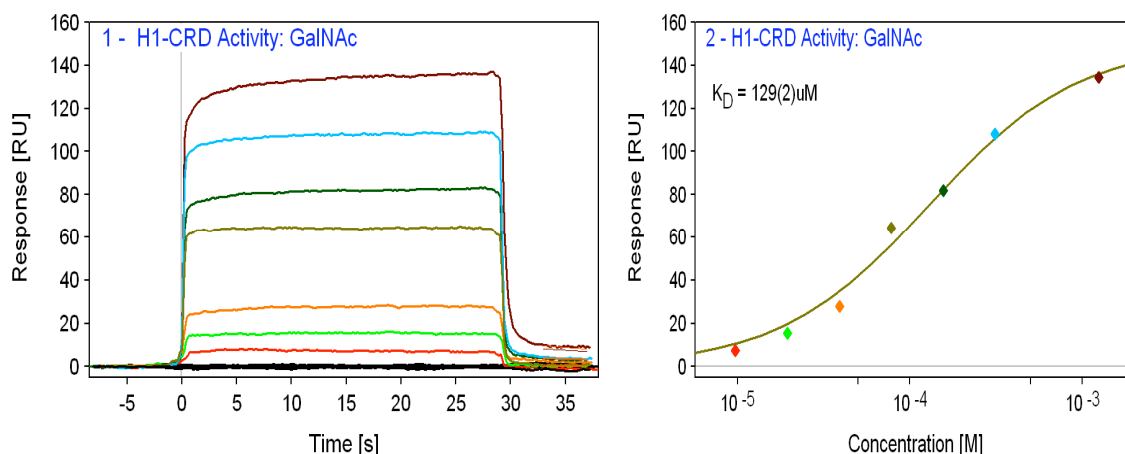


Figure 100. Sensorgram of H1-CRD activity testing with GalNAc

The obtained K_D for GalNAc was 129 μM and in the range obtained in previous tests (see Table 22), confirming that the protein was still active after 2 years of storage at -20°C .

3.13.2 Screening of human scFv in SPR

The buffer of the purified scFv antibodies 2E8 and 5B8 from the ETH-2-Gold library was changed to the SPR-buffer HBS-P + 50 mM CaCl_2 using Vivaspin 6 concentrators (cutoff 10kDa). The amounts purified from supernatants of clones 2D3 and 2D8 were not sufficient for testing. Screening was conducted as described in chapter 2.9.13.

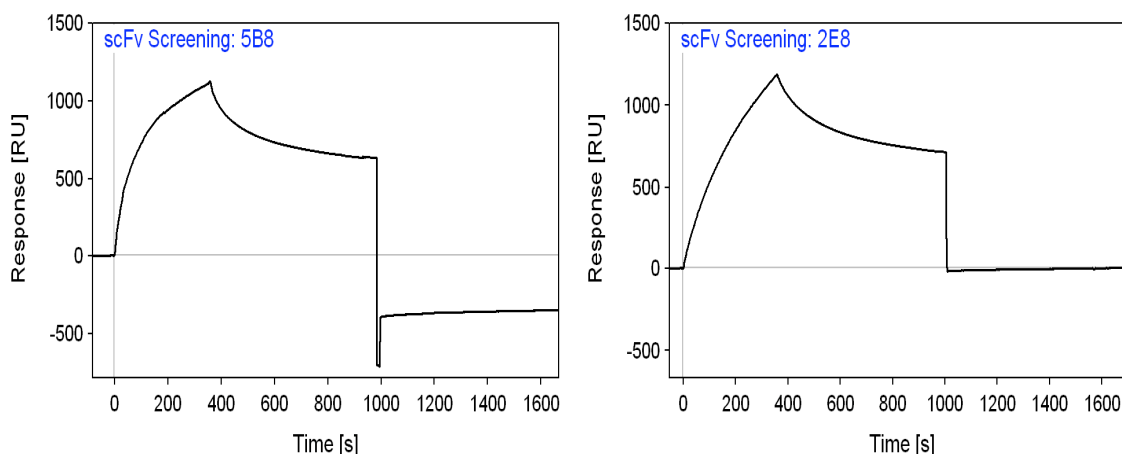


Figure 101. Screening of human ETH-2-Gold derived scFvs

The screening of the two scFv preparations reveal specific binding of the scFv to the H1-CRD immobilized on the chip (Figure 101).

3.13.3 Affinity Determinations of human scFv

For affinity determinations the scFv antibodies were injected in a random series of concentrations ranging from 1.6 μM to 0.19 pM for 5B8 and 0.8 μM to 0.19 pM for 2E8 as described in chapter 2.9.13.

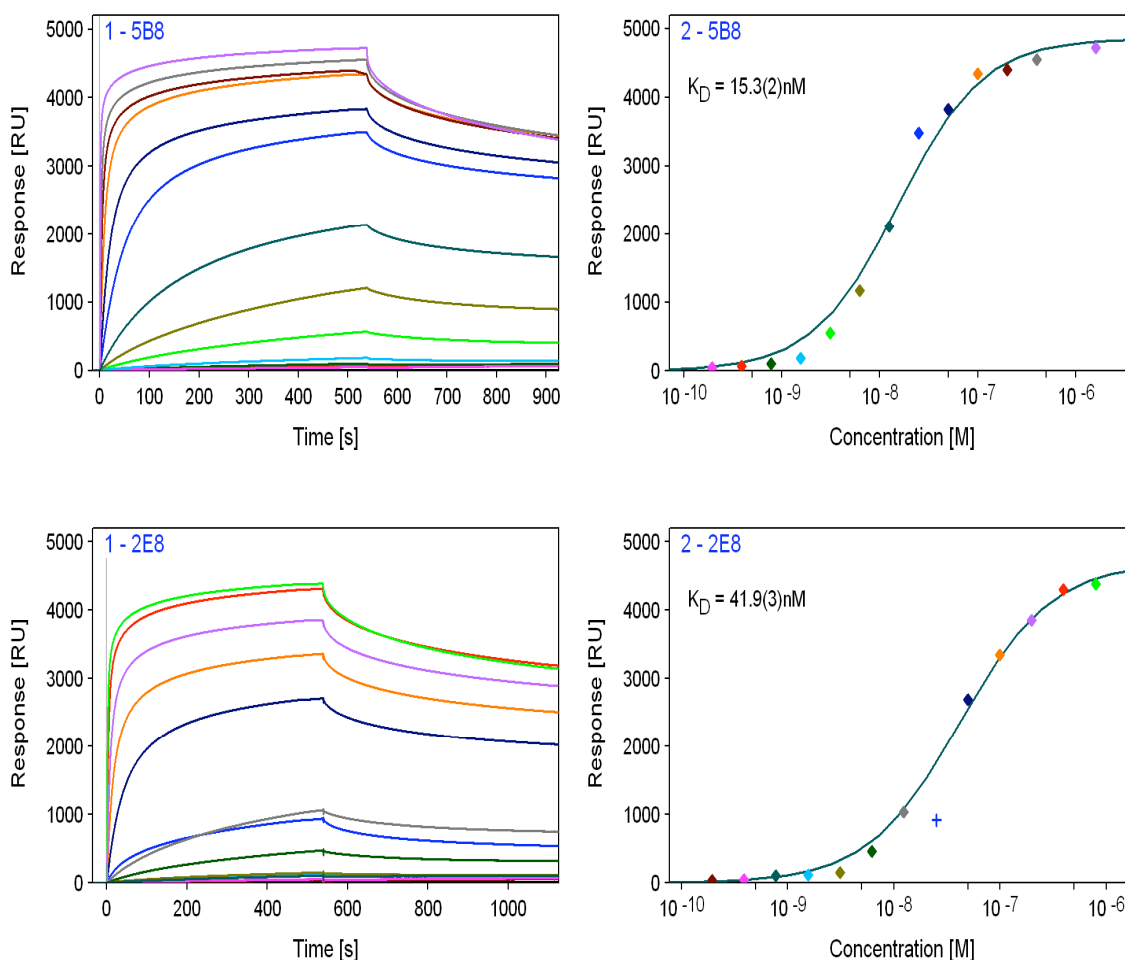


Figure 102. Preliminary affinity measurements of human scFv 5B8 and 2E8

The apparent K_D measured for the purified sample of scFv 5D8 was around 16 nM and that of 2E8 42 nM. Kinetic values could not be determined from these curves, as it would be necessary to conduct the measurements on a low immobilization H1-CRD surface as described on the Biacore homepage²⁰². Kinetic analysis would determine the rate of complex formation and dissociation. Reliable determination of kinetic constants would require the adaptation of the immobilization protocol, as the amount of immobilized H1-CRD should give an R-value in the range of 100-400 RU.

4. General Discussion and Outlook

4.1 ASGP-R Carbohydrate Recognition Domains H1- and H2-CRD

At our institute we are now able to prepare both H1-CRD and H2-CRD in amounts needed for ongoing research on the ASGP-R. With the H1-CRD we were able to establish a reliable competitive solid-phase binding assay, a SPR assay and substantial work on the binding mode of H1-CRD has been done by or NMR team.

In case of the H2-CRD we still don't know its binding specificities and it would be interesting to start a collaboration with a laboratory working with glyco-microarray, as described by Coombs et al.²⁰³ in order reveal its ligand preferences.

4.2 Competitive Solid-phase Binding Assay

The new competitive solid-phase binding assay for the H1-CRD developed in this thesis is a simple, yet effective assay for the purpose of ranking newly developed small glycomimetic ligands to the H1 subunit of the ASGP-R. Its use allows the iterative improvement of the developed compounds and the reagents required to for the assay are readily accessible.

With this assay we were able to monitor the activity of H1-CRD protein during the development of the purification and refolding procedure and to compare the activity of the resulting protein batches. Likewise, the influence of mutations in the cysteines in the H1-CRD on the correct folding and binding activity of the protein were evaluated with this assay, the results are to be found in the thesis of Dr. K. Johansson²⁰⁴. Unlike in an ELISA, where an antibody not necessarily needs to bind the active conformation of the protein, GalNAc-PAA polymer interaction with the protein is solely dependent on the occurrence of correctly folded protein representing an active binding site.

The assay could not be adapted to the H2-CRD in a competitive format needed for ligand testing. Nonetheless, the results confirmed that the affinity of the protein in regard to Gal and GalNAc is very low. We could also show that the H2-CRD has, in contrast to H1-CRD, a higher affinity towards Gal than GalNAc.

Finally, these results reflect the lack of information on the sugar-binding specificity of the H2 subunit of the ASGP-R in literature. Although both subunits contain a CRD, it is believed that high affinity binding of ligands by Gal/GalNAc recognition occurs only via the H1 subunit and that H2 serves to generate the functional native receptor, since both subunits are necessary for efficient ligand binding and internalization by hepatocytes⁴⁴.

This assay format can readily be adapted to be used for other medically interesting lectin CRDs to achieve assays to e.g. evaluate the binding activity of protein after recombinant production and purification, assess binding specificities of endogenous ligands and to rank new glycomimetic compounds produced by our chemists. This is currently done at our Institute for the lectins FimH, DC-Sign, E- P- and L-selectin.

4.3 New Glycomimetic Ligands for the human H1-CRD

More than 50 new potential glycomimetic ligands for the H1-CRD were tested in the competitive solid-phase binding assay for the H1-CRD. From those we were able to identify several new ligands for the ASGP-R evincing more drug-like properties than the natural ligand GalNAc while having a similar or even better affinity to the H1 subunit of the receptor.

To achieve the aim of our group, which is to develop a high affinity drug-carrier for hepatotropic drug delivery via the Asialoglycoprotein-receptor, it will now be necessary to couple these ligands to the triantennary drug carrier that was presented in this work, and to evaluate in a first step their binding specificities to human hepatocytes with the methods developed in the scope of this thesis. The evaluation of the specificity of binding and internalization into other cells will show if the newly developed drug carriers obey the rules of a good site-specific targeting vehicle, which is its high specificity for the targeted site, the ASGP-R on human parenchymal liver cells.

4.4 Antibodies against the ASGP-R for Drug Targeting

Although there is much interest in the use of the ASGP-R for hepatotropic drug delivery, no attempt has been made to address the receptor using antibodies instead of the usual sugar-based delivery systems²⁰⁵. There are reports about

polyclonal and partially characterized monoclonal antibody directed against the ASGP-R^{37, 61, 206-209}, but to date no drug targeting attempts have been made.

The initial idea to use a H1-CRD specific antibody fragment for targeting of siRNA came from the publication of Song *et al.*²¹⁰ The authors could show that it's possible to use antibody fragments expressed as truncated protamine fusion proteins, to bind, protect and target siRNA into cells via receptor-mediated endocytosis. The process of uptake and endosomal escape of the siRNA molecules is still discussed^{211, 212}. This approach could be interesting to silence cancer related genes in HCC or viral genes in viral Hepatitis with specific siRNA molecules targeted to the ASGP-R via scFvs fused to protamine (or another cationic tail).

4.4.1 Mouse anti-human H1-CRD Antibodies

The mouse anti-human H1-CRD antibodies that were produced at our Institute by Dr R. Born¹⁶⁵ and that were characterized by her in collaboration with Dr.D.Ricklin⁷⁵ and the author of this thesis, show interesting binding characteristics.

They are valuable research tools, and especially the antibodies C11.1, B01.4, C09.1 and C18.1 could be from interest in a proof of concept model to target drugs or siRNA to hepatocytes, as they not only bind, but also are efficiently internalized into hepatocellular carcinoma cells via the ASGP-R. Antibody C14.6 can be applied in Immunohistochemistry and is a promising candidate for a histological diagnostic tool in AIH.

Because of their mouse origin, the use of these antibodies for drug targeting in humans is limited. If they could be used in a mouse model is questionable, they were generated in mice and can therefore not be expected to react with the mouse hepatic lectin 1 (MHL-1), even if it has a high sequence homology to the human H1- subunit (79%).

4.4.2 Murine scFv Adaptation

In the scope of this thesis it was attempted to adapt four of the mouse antibodies to the scFv format. Those were the clones C11.1, B01.4, C14.6 and C23.8, an instable hybridoma clone that could no longer be propagated. The

effort only worked for clone C11.1, whose scFv fragment still binds to the H1-CRD. The attempt to speed up the selection of a efficient binder clone from the produced scFv constructs by applying phage display in parallel was not successful within the scope of this thesis and likely impeded by the use of an unsuitable *E.coli* host for soluble scFv production (as will be discussed in chapter 4.4.3).

The production and especially the purification procedure will have to be optimized to get highly pure scFv in sufficient amounts for further tests. The purification strategy for the murine scFvs using IMAC by taking advantage of the encoded his-tag showed to be unsuitable. The eluates contained substantial amounts of co-purified bacterial proteins and there was also still scFv detectable in the flow trough. The best strategy in this case would be to apply affinity chromatography using a H1-CRD column, which would only bind correctly folded and active scFvs.

4.4.3 Selection of human scFv against the H1-CRD

From the ETH-2-gold library one human scFv that binds specifically to the H1-CRD could already be selected within the scope of this thesis.

The detection of additional binders was probably impeded by the use of an inappropriate *E.coli* host for soluble scFv expression. The scFv_{gIII} fusion protein expression in *E.coli* XL1 Blue is most likely not as leaky as in TG1; hence this strain is not suitable to combine phage display with antibody production as it is feasible when using *E.coli* TG1. The further strategy to select more H1-CRD specific binders could be either to infect TG1 with the purified phage from round 5 and to repeat the soluble scFv ELISA (this has the advantage that the selected clones can be directly employed for scFv production), or to carry out a phage ELISA instead of the soluble scFv ELISA, and to infect another suitable *E.coli* strain with the ELISA-positive phage particles for soluble scFv production.

The selected human scFv 5B8 was perceived to be an antibody fragment with high affinity to the H1-CRD but further evaluation of its binding properties will be needed. Kinetic SPR affinity measurements could not be performed in the scope of this thesis, because the method for immobilization of the H1-CRD

would have to be adapted to give a 'low immobilization' surface and presumably the regeneration strategy would need to be modified also (i.e. using HCl instead of EDTA).

The scFv purification procedure will have to be optimized to get highly pure scFv in sufficient amounts for further tests. Purification via affinity chromatography on Protein A alone is not sufficient as some bacterial contaminants remain. In this case, Size exclusion chromatography (SEC) with a new column should be sufficient for polishing.

If the selected scFv antibodies' kinetic affinity or stability is not high enough, affinity maturation could be used to achieve an improvement in these properties. There are several methods described in literature e.g. the affinity maturation concept described by Pini et al.¹³⁷ that was successfully applied on an scFv clone derived from the ETH-2-Gold library.

In a further step, the selected scFv should be tested for its ability to be internalized efficiently into hepatocytes, which is essential if the scFv is intended to be used for delivering drugs or genes to hepatocytes.

Even if the selected scFv shows high affinity to the H1-CRD, it cannot automatically be assumed that it is internalized as efficiently by the ASGP-R on cells as the murine anti-H1-CRD antibodies. The full IgGs possess an important feature that scFvs lack, they have two binding sites and are therefore able to crosslink two H1 subunits, which very likely helps to trigger their internalization.

The methods for the evaluation of these properties and to exclude cross-reactivity with similar receptors on other cells were established in the scope of this thesis. The scFv could either be labeled directly with a fluorochrome for detection, e.g. with one of the Alexa Fluor® series (labeling kits for antibodies are commercially available) or indirectly detected after internalization with a labeled secondary antibody directed against the heavy or light variable domains or the C-myc tag on the scFvs in permeabilized cells and analyzed in fluorescence microscopy and/or flow cytometry.

Alternatively, methods for panning of phage on cellular surface antigen on living cells and for selection of internalizing phage have also been described but are difficult to implement^{213 214}.

The next step could then be to apply the ETH-2-Gold library by phage display for the selection of an scFv fragment specific to the H2-CRD of the human ASGP-R. If antibodies against both subunits could be generated, it would be interesting to couple them to form a drug carrier addressing both the H1 and the H2-subunit of the ASGP-R at once. Combining the two binding specificities in one molecule could lead to a highly specific drug-carrier. Dual specificity is probably also beneficial in regard to uptake efficiency, as both ASGP-R subunits are necessary for efficient internalization.

A strategy to increase the avidity to efficiently address the ASGP-R for drug targeting is the engineering of a multivalent structure by fusion of scFv fragments to coiled-coil structures as described by Charles *et al.*²¹⁵, Kipriyanov *et al.*²¹⁶ and Plückthun *et al.*²¹⁷

5. Appendices

5.1 Sequences of scFv

Human scFv from ETH-2-Gold Clone 5B8 Protein Sequence

EVQLLESGGGLVQPGGSLRLSCAASGFTFSSYAMSWVRQAPGKGLEWVSAI
SGSGGSTYYADSVKGRFTISRDNSKNTLYLQMNSLRAEDTAVYYCAKDQIPFD
YWGQGTLVTVSSGGGGSGGGGSGGGGSSELTQDPAVSVALGQTVRITCQSL
RSYYASWYQQKPGQAPVLVIYGKNNRPSGIPDRFSGSSSGNTASLTITGAQE
DEADYYCNSSPTHHVPVVFGGGTKLTVLGAAAEQKLISEEDLNGAA*

V_H DP47

Linker G₄SG₄SG₄

c-myc tag

V_λ DPL16

Appended random loops

5B8 Nucleotide Sequence

GAGGTGCAGCTGTTGGAGTCTGGGGGAGGCTTGGTACAGCCTGGGGGGT
 CCCTGAGACTCTCCTGTGCAGCCTCTGGATTCACCTTTAGCAGCTATGCCA
 TGAGCTGGGTCCGCCAGGCTCCAGGGAAGGGGCTGGAGTGGGTCTCAGC
 TATTAGTGGTAGTGGTGGTAGCACATACTACGCAGACTCCGTGAAGGGCC
 GGTTACCATCTCCAGAGACAATTCCAAGAACACGCTGTATCTGCAAATGA
 ACAGCCTGAGAGCCGAGGACACGGCCGTATATTACTGTGCGAAAGATCAG
 ATTCCGTTTGACTACTGGGGCCAGGGAACCCTGGTCACCGTCTCGAGTGG
 TGGAGGCGGTTCAGGCGGAGGTGGCTCTGGCGGTGGCGGATCTTCTGAG
 CTGACTCAGGACCCTGCTGTGTCTGTGGCCTTGGGACAGACAGTCAGGAT
 CACATGCCAAGGAGACAGCCTCAGAAGCTATTATGCAAGCTGGTACCAGC
 AGAAGCCAGGACAGGCCCTGTACTTGTCTATGGTAAAAACAACCGG
 CCCTCAGGGATCCCAGACCGATTCTCTGGCTCCAGCTCAGGAAACACAGC
 TTCCTTGACCATCACTGGGGCTCAGGCGGAAGATGAGGCTGACTATTACT
 GTAACCTCTCCTACGCATCATGTTCCCGTGGTATTCGGCGGAGGGACC
 AAGCTGACCGTCCTAGGCGCGGCCGCAGAACAAAACTCATCTCAGAAGA
 GGATCTGAATGGGGCCGCAT

Deduced Protein Sequence of the scFv Fragment from mouse anti-human H1-CRD Antibody C11.1, Clone 2.1

DYKDIVMTQSPASLAVSLGQRATISYRASKSVSTSGYSYMHWNQQKPGQPPR
 LLIYLVSNLESGVPARFSGSGSGTDFLNIHPVEEEDAATYYCQQXXGGAYTF
 GGGTKLEIKRGGGSGGGGSGGGGSGGGGQQVQLQQSGAELVKPGASVKL
 SCKTSGYTFTSYWIQWVKQRPGQGLGWIGEIFPGTGTSYYNENFKGKATLTID
 TSSSTAYMQPSSLTSEDSAVYFCARTNNYRSYALDYWGQGTNYRS

V_K

Linker (G₄S)₄

V_H

Shortened FLAG- tag

C11.1 scFv Clone 2.1 Nucleotide Sequence

AGACTACAAAGATATTGTGATGACCCAGTCTCCTGCTTCCTTAGCTGTATCT
 CTGGGGCAGAGGGCCACCATCTCATACAGGGCCAGCAAAGGTGTCAGTAC
 ATCTGGCTATAGTTATATGCACTGGAACCAACAGAAACCAGGACAGCCACC
 CAGACTCCTCATCTATCTTGTATCCAACCTAGAATCTGGGGTCCCTGCCAG
 GTTCAGTGGCAGTGGGTCTGGGACAGACTTCACCCTCAACATCCATCCTG
 TGGAGGAGGAGGATGCTGCAACCTATTACTGTCAGCAGNAGNTAGGGGGA
 GCTTACACGTTCCGAGGGGGGACCAAGCTGGAAATAAAACGTGGTGGTG
 GTGGTTCTGGTGGTGGTGGTTCTGGCGGCGGCGGCTCCGGTGGTGGTGG
 ATCCCAGGTGCAGCTGCAGCAGTCTGGAGCTGAGCTGGTGAAGCCTGGG
 GCTTCAGTGAAGCTGTCCTGCAAGACTTCTGGCTACACCTTCACCAGCTAC
 TGGATTCAGTGGGTAAAACAGAGGCCTGGACAGGGCCTTGGGTGGATTGG
 AGAGATATTTCTGGAAGTGGCACTTCTTACTACAATGAGAAGTTCAGGG
 CAAGGCCACACTGACTATAGACACATCCTCCAGCACAGCCTACATGCAGC
 CCAGCAGCCTGACCTCTGAGGACTCTGCTGTCTATTTCTGTGCAAGAACTA
 ATA ACTATAGGTCCTATGCTTTGGACTACTGGGGTCAAGGAACTAATTACC
 GTTCC

5.2 Curriculum Vitae

Daniela Stokmaier

Address Käppelgasse 3, CH-4125 Riehen

Nationality Swiss

Date of Birth 5th of May 1972

Professional Experience

02.2009-present	Clinical Research Scientist , Actelion Pharmaceuticals Ltd., Allschwil, Switzerland
12.2004-11.2008	PhD Student and Teaching Assistant at the Institute of Molecular Pharmacy, University of Basel, Switzerland Organization and tutoring of undergraduate's practical course in 'Modern Drug Design' (2004-2008) Supervising tutor of 3 Master theses (2005-2006) Training of new PhD students in cell culture and assay development
9.2002-1.2005	Pharmacist , part-time (20%), CityRing Apotheke, Basel, Switzerland
9.2001-9.2002	Assistant Pharmacist Internship in a public pharmacy, CityRing Apotheke, Basel, Switzerland
3.1998-3.2002	Person in charge , part time (20-30%) at a shelter for the homeless, Caritas and Staatliche Notschlafstelle für Frauen und Männer Basel-Stadt, Switzerland
4.1996-3.1998	Research Associate , part-time (50%) Core Technology Applications, Biomolecules Production, Novartis Pharma AG, Basel, Switzerland
5.1991-3.1996	Research Associate Preclinical Research, Transplantation and Autoimmune Research, Sandoz Pharma AG, Basel, Switzerland Training of new coworkers and supervision of laboratory technician-apprentices during their practical year, responsible for laboratory infrastructure
2.1990-2.1991	Internship Preclinical Research, Sandoz Pharma AG, Basel, Switzerland

Education

12.2004-11.2008	PhD in Natural Sciences 'Targeting Hepatocytes via the Asialoglycoprotein-Receptor' Institute of Molecular Pharmacy, University of Basel, Supervisor: Prof. Beat Ernst
10.1999-11.2004	Pharmacist (Master of Science in Pharmacy / Staatsexamen Pharmazie), University of Basel, Switzerland
1.2004-7.2004	Master thesis 'Receptor-mediated Endocytosis in human Hepatocytes' Institute of Molecular Pharmacy, University of Basel, Switzerland
4.1996-9.1999	Eidgenössische Matura Typ B , University entrance diploma Maturitätsvorbereitungs-Schule für Erwachsene Minerva, Basel, Switzerland

3.1988-3.1991 **Laboratory Technician** specialized in Biology and Pharmacology, Schule für Biogelaboranten Sandoz-Wander, Bern, Switzerland

Vocational Training

Essentials in Drug Development and Clinical Trials, theoretical course with a case study, Swiss Tropical Institute, Basel, Switzerland (2008)

Venture Challenge, practical course on entrepreneurship, organized by IFJ Institut für Jungunternehmen, St. Gallen, Switzerland (2008, one semester)

Scientific Writing, training on medical and scientific writing by Dr. Silvia M. Rogers, MediWrite GmbH, University of Basel, Switzerland (2008, one semester)

3rd Experimental Course in Antibody Phage Technology, Hands-on course and seminar series on phage display technologies organized by Prof. Dario Neri, ETH Zurich, Switzerland (2008)

Pharma-Business, Marketing and Communication, Practical and theoretical course, ETH Zurich, Switzerland (2007)

Novartis European Biotechnology Leadership Camp, with selected students from all over Europe. Basel, Switzerland (2007)

Monoclonal Antibodies Workshop, part of the Pharmaceutical Sciences World Congress (PSWC), Seminar series on new developments in antibody therapeutics and on regulatory issues. Amsterdam, the Netherlands (2007)

Writing Efficiency, scientific writing workshop, Advanced Study Center, University of Basel, Switzerland (2007)

Mentoring program WIN – Woman into Industry, joint project of the University of Basel and Novartis Pharma AG, Switzerland (2006-2007)

Introduction into Project Management, University of Basel, Switzerland (2006)

Key Issues in Drug Discovery & Development, Practical and theoretical postgraduate course, University of Basel and ETH Zurich, Switzerland (2005)

Scientific Qualifications

Publications	<p>Stokmaier D, Khorev O, Cutting B, Born R, Ricklin D, Ernst TO, Böni F, Schwingruber K, Gentner M, Wittwer M, Spreafico M, Vedani A, Rabbani S, Schwardt O, Ernst B. (2009) Design, synthesis and evaluation of monovalent ligands for the asialoglycoprotein receptor (ASGP-R), Bioorg Med Chem. Oct 15;17(20):7254-64.</p> <p>Khorev O., Stokmaier D., Schwardt O., Cutting B., Ernst B., (2008) Trivalent, Gal/GalNAc-containing Ligands Designed for the Asialoglycoprotein Receptor, Bioorg Med Chem 16(9), 5216-31</p> <p>Weitz-Schmidt G., Stokmaier D., Scheel G., Nifant'ev N. E., Tuzikov A. B., and Bovin N. V. (1996). An E-selectin binding assay based on a polyacrylamide-type glycoconjugate. Anal Biochem 23, 184-190</p>
Oral Presentations	<p>Stokmaier D., Khorev O., Johansson K., Ricklin D., Ernst B., Targeting Hepatocytes via the Asialoglycoprotein Receptor, Fall Meeting of the Swiss Chemical Society 2006, Zurich</p>

Language Skills

German	Native language
English	Fluent, written and spoken
French	Basic knowledge

Additional Activities

2005 – 2008	Member of the board, Association of the Teaching Assistants, University of Basel, Switzerland
2000 – 2004	Students representative in the committee planning the new learning objectives in Pharmaceutical Sciences, Department of Pharmaceutical Sciences, University of Basel, Switzerland
Interests	Hiking, Pilates and yoga, photography, reading, traveling, movies and music

References

Prof. Beat Ernst, Head of the Department of Pharmaceutical Sciences, Institute of Molecular Pharmacy, Klingelbergstr. 50, CH-4056 Basel, Tel: +41 61 267 15 51, Beat.Ernst@unibas.ch

Dr. Gabriele Weitz-Schmidt, Senior Research Investigator in Autoimmunity and Transplantation, Novartis Institutes for BioMedical Research, Novartis Pharma AG, CH-4056 Basel, 4053 Basel, Tel: +41 61 324 92 52, Gabriele.Weitz@novartis.com

Dr. Beate Kleuser, Head of Cell Biology/Biotech Process Development, Merck Serono SA, Zone Industrielle B, CH-1809 Fenil-sur-Corsier, Tel: +41 21 923 24 21, Beate.Kleuser@merckserono.net

6. Bibliography

1. http://www.conatuspharma.com/liverfacts/images/IMG_liver_fig01.jpg,
2. <http://www.meddean.luc.edu/lumen/MedEd/Histo/HistoImages/hl9-07.jpg>.
3. Spiess, M. The asialoglycoprotein receptor: a model for endocytic transport receptors. *Biochemistry* **29**, 10009-18 (1990).
4. Winau, F. et al. Ito Cells Are Liver-Resident Antigen-Presenting Cells for Activating T Cell Responses. *Immunity* **26**, 117-129 (2007).
5. Sookian, S. Hepatitis B virus and pregnancy, *Hep B Annual*, **4**, 12-23, (2007)
6. Keeffe, E.B., Dieterich, D.T., Han, S.b., Jacobson, I.B. A treatment algorithm for the management of chronic hepatitis B virus infection in the United States, *Clinical Gastroenterology and Hepatology*, **2**, 87-106 (2004)
7. Strader, D.B., Wright, T., Thomas, D.L. & Seeff, L.B. Diagnosis, management, and treatment of hepatitis C. *Hepatology* **39**, 1147-71 (2004).
8. Manns, M.P. et al. Peginterferon alfa-2b plus ribavirin compared with interferon alfa-2b plus ribavirin for initial treatment of chronic hepatitis C: a randomised trial. *Lancet* **358**, 958-65 (2001).
9. Manns, M.P. & Vogel, A. Autoimmune hepatitis, from mechanisms to therapy. *Hepatology* **43**, S132-44 (2006).
10. Czaja, A.J. The variant forms of autoimmune hepatitis. *Ann Intern Med* **125**, 588-98 (1996).
11. Parkin, D.M., Bray, F., Ferlay, J. & Pisani, P. Estimating the world cancer burden: Globocan 2000. *Int J Cancer* **94**, 153-6 (2001).
12. Llovet, J.M., Burroughs, A. & Bruix, J. Hepatocellular carcinoma. *Lancet* **362**, 1907-17 (2003).
13. El-Serag, H.B. & Mason, A.C. Rising incidence of hepatocellular carcinoma in the United States. *N Engl J Med* **340**, 745-50 (1999).
14. Sangiovanni, A. et al. Increased survival of cirrhotic patients with a hepatocellular carcinoma detected during surveillance. *Gastroenterology* **126**, 1005-14 (2004).
15. Llovet, J.M. & Beaugrand, M. Hepatocellular carcinoma: present status and future prospects. *J Hepatol* **38 Suppl 1**, S136-49 (2003).
16. Llovet, J.M. & Bruix, J. Systematic review of randomized trials for unresectable hepatocellular carcinoma: Chemoembolization improves survival. *Hepatology* **37**, 429-42 (2003).
17. Thorgeirsson, S.S. & Grisham, J.W. Molecular pathogenesis of human hepatocellular carcinoma. *Nat Genet* **31**, 339-46 (2002).
18. Edamoto Y., T.L., Cathomas G., Disruption of retinoid-regulated Wnt signaling pathway in HCC. *J Hepatology* **42**, 106 (2005).
19. Beaugrand, M., N'Kontchou, G., Seror, O., Ganne, N. & Trinchet, J.C. Local/regional and systemic treatments of hepatocellular carcinoma. *Semin Liver Dis* **25**, 201-11 (2005).
20. Beaugrand, M. & Trinchet, J.C. [Non-surgical treatment of hepatocellular carcinoma. An overview]. *Cancer Radiother* **9**, 464-9 (2005).
21. Varela, M. et al. Chemoembolization of hepatocellular carcinoma with drug eluting beads: efficacy and doxorubicin pharmacokinetics. *J Hepatol* **46**, 474-81 (2007).
22. Bruix, J., Sala, M. & Llovet, J.M. Chemoembolization for hepatocellular carcinoma. *Gastroenterology* **127**, S179-88 (2004).
23. Forner, A., Real, M.I., Varela, M. & Bruix, J. Transarterial chemoembolization for patients with hepatocellular carcinoma. *Hepatol Res* **37 Suppl 2**, S230-7 (2007).
24. Trere, D. et al. The asialoglycoprotein receptor in human hepatocellular carcinomas: its expression on proliferating cells. *Br J Cancer* **81**, 404-8 (1999).

25. Fiume, L. et al. Doxorubicin coupled to lactosaminated albumin inhibits the growth of hepatocellular carcinomas induced in rats by diethylnitrosamine. *J Hepatol* **43**, 645-52 (2005).
26. Di Stefano, G. et al. Doxorubicin coupled to lactosaminated albumin: Effects on rats with liver fibrosis and cirrhosis. *Dig Liver Dis* **38**, 404-8 (2006).
27. Di Stefano, G., Busi, C., Fiume, L., Chieco, P. & Pariali, M. Doxorubicin coupled to lactosaminated albumin: enhanced drug levels in rat hepatocarcinomas. *Dig Liver Dis* **38**, 284-5 (2006).
28. Fiume, L., Baglioni, M., Bolondi, L., Farina, C. & Di Stefano, G. Doxorubicin coupled to lactosaminated human albumin: a hepatocellular carcinoma targeted drug. *Drug Discov Today* (2008).
29. Di Stefano, G. et al. Doxorubicin coupled to lactosaminated albumin: effect of heterogeneity in drug load on conjugate disposition and hepatocellular carcinoma uptake in rats. *Eur J Pharm Sci* **33**, 191-8 (2008).
30. Morell, A.G., Gregoriadis, G., Scheinberg, I.H., Hickman, J. & Ashwell, G. The role of sialic acid in determining the survival of glycoproteins in the circulation. *J Biol Chem* **246**, 1461-7 (1971).
31. Hudgin, R.L., Pricer, W.E., Jr., Ashwell, G., Stockert, R.J. & Morell, A.G. The isolation and properties of a rabbit liver binding protein specific for asialoglycoproteins. *J Biol Chem* **249**, 5536-43 (1974).
32. Pricer, W.E., Jr., Hudgin, R.L., Ashwell, G., Stockert, R.J. & Morell, A.G. A membrane receptor protein for asialoglycoproteins. *Methods Enzymol* **34**, 688-91 (1974).
33. Ashwell, G. & Morell, A.G. The role of surface carbohydrates in the hepatic recognition and transport of circulating glycoproteins. *Adv Enzymol Relat Areas Mol Biol* **41**, 99-128 (1974).
34. Drickamer, K. Membrane receptors that mediate glycoprotein endocytosis: structure and biosynthesis. *Kidney Int Suppl* **23**, S167-83 (1987).
35. Weigel, P.H. & Yik, J.H. Glycans as endocytosis signals: the cases of the asialoglycoprotein and hyaluronan/chondroitin sulfate receptors. *Biochim Biophys Acta* **1572**, 341-63 (2002).
36. Wu, J., Nantz, M.H. & Zern, M.A. Targeting hepatocytes for drug and gene delivery: emerging novel approaches and applications. *Front Biosci* **7**, d717-25 (2002).
37. Bischoff, J. & Lodish, H.F. Two asialoglycoprotein receptor polypeptides in human hepatoma cells. *J Biol Chem* **262**, 11825-32 (1987).
38. Drickamer, K. Two distinct classes of carbohydrate-recognition domains in animal lectins. *J Biol Chem* **263**, 9557-60 (1988).
39. Heilker, R., Spiess, M. & Crottet, P. Recognition of sorting signals by clathrin adaptors. *Bioessays* **21**, 558-67 (1999).
40. Bider, M.D., Wahlberg, J.M., Kammerer, R.A. & Spiess, M. The oligomerization domain of the asialoglycoprotein receptor preferentially forms 2:2 heterotetramers in vitro. *J Biol Chem* **271**, 31996-2001 (1996).
41. Yik, J.H., Saxena, A. & Weigel, P.H. The minor subunit splice variants, H2b and H2c, of the human asialoglycoprotein receptor are present with the major subunit H1 in different hetero-oligomeric receptor complexes. *J Biol Chem* **277**, 23076-83 (2002).
42. Henis, Y.I., Katzir, Z., Shia, M.A. & Lodish, H.F. Oligomeric structure of the human asialoglycoprotein receptor: nature and stoichiometry of mutual complexes containing H1 and H2 polypeptides assessed by fluorescence photobleaching recovery. *J Cell Biol* **111**, 1409-18 (1990).
43. Bider, M.D., Cescato, R., Jenö, P. & Spiess, M. High-affinity ligand binding to subunit H1 of the asialoglycoprotein receptor in the absence of subunit H2. *Eur J Biochem* **230**, 207-12 (1995).
44. Geuze, H.J. et al. Intracellular receptor sorting during endocytosis: comparative

- immunoelectron microscopy of multiple receptors in rat liver. *Cell* **37**, 195-204 (1984).
45. Wolkoff, A.W., Klausner, R.D., Ashwell, G. & Harford, J. Intracellular segregation of asialoglycoproteins and their receptor: a prelysosomal event subsequent to dissociation of the ligand-receptor complex. *J Cell Biol* **98**, 375-81 (1984).
46. Tycko, B., Keith, C.H. & Maxfield, F.R. Rapid acidification of endocytic vesicles containing asialoglycoprotein in cells of a human hepatoma line. *J Cell Biol* **97**, 1762-76 (1983).
47. Bananis, E., Murray, J.W., Stockert, R.J., Satir, P. & Wolkoff, A.W. Regulation of early endocytic vesicle motility and fission in a reconstituted system. *J Cell Sci* **116**, 2749-61 (2003).
48. Novikoff, P.M. et al. Three-dimensional organization of rat hepatocyte cytoskeleton: relation to the asialoglycoprotein endocytosis pathway. *J Cell Sci* **109 (Pt 1)**, 21-32 (1996).
49. Schwartz, A.L., Fridovich, S.E. & Lodish, H.F. Kinetics of internalization and recycling of the asialoglycoprotein receptor in a hepatoma cell line. *J Biol Chem* **257**, 4230-7 (1982).
50. Tozawa, R. et al. Asialoglycoprotein receptor deficiency in mice lacking the major receptor subunit. Its obligate requirement for the stable expression of oligomeric receptor. *J Biol Chem* **276**, 12624-8 (2001).
51. Windler, E. et al. The human asialoglycoprotein receptor is a possible binding site for low-density lipoproteins and chylomicron remnants. *Biochem J* **276 (Pt 1)**, 79-87 (1991).
52. Rotundo, R.F., Rebres, R.A., McKeown-Longo, P.J., Blumenstock, F.A. & Saba, T.M. Circulating cellular fibronectin may be a natural ligand for the hepatic asialoglycoprotein receptor: possible pathway for fibronectin deposition and turnover in the rat liver. *Hepatology* **28**, 475-85 (1998).
53. Rifai, A., Fadden, K., Morrison, S.L. & Chintalacheruvu, K.R. The N-glycans determine the differential blood clearance and hepatic uptake of human immunoglobulin (Ig)A1 and IgA2 isotypes. *J Exp Med* **191**, 2171-82 (2000).
54. McVicker, B.L. et al. The effect of ethanol on asialoglycoprotein receptor-mediated phagocytosis of apoptotic cells by rat hepatocytes. *Hepatology* **36**, 1478-87 (2002).
55. Hardy, M.R., Townsend, R.R., Parkhurst, S.M. & Lee, Y.C. Different modes of ligand binding to the hepatic galactose/N-acetylgalactosamine lectin on the surface of rabbit hepatocytes. *Biochemistry* **24**, 22-8 (1985).
56. Ili, M., Kurata, H., Itoh, N., Yamashina, I. & Kawasaki, T. Molecular cloning and sequence analysis of cDNA encoding the macrophage lectin specific for galactose and N-acetylgalactosamine. *J Biol Chem* **265**, 11295-8 (1990).
57. Mu, J.Z., Gordon, M., Shao, J.S. & Alpers, D.H. Apical expression of functional asialoglycoprotein receptor in the human intestinal cell line HT-29. *Gastroenterology* **113**, 1501-9 (1997).
58. Goluboff, E.T., Mertz, J.R., Tres, L.L. & Kierszenbaum, A.L. Galactosyl receptor in human testis and sperm is antigenically related to the minor C-type (Ca²⁺-dependent) lectin variant of human and rat liver. *Mol Reprod Dev* **40**, 460-6 (1995).
59. Pacifico, F. et al. The RHL-1 subunit of the asialoglycoprotein receptor of thyroid cells: cellular localization and its role in thyroglobulin endocytosis. *Mol Cell Endocrinol* **208**, 51-9 (2003).
60. Seow, Y.Y., Tan, M.G. & Woo, K.T. Expression of a functional asialoglycoprotein receptor in human renal proximal tubular epithelial cells. *Nephron* **91**, 431-8 (2002).
61. Park, J.H., Cho, E.W., Shin, S.Y., Lee, Y.J. & Kim, K.L. Detection of the asialoglycoprotein receptor on cell lines of extrahepatic origin. *Biochem Biophys Res Commun* **244**, 304-11 (1998).

62. Iobst, S.T. & Drickamer, K. Selective sugar binding to the carbohydrate recognition domains of the rat hepatic and macrophage asialoglycoprotein receptors. *J Biol Chem* **271**, 6686-93 (1996).
63. Treichel, U. et al. Demographics of anti-asialoglycoprotein receptor autoantibodies in autoimmune hepatitis. *Gastroenterology* **107**, 799-804 (1994).
64. Czaja, A.J., Pfeifer, K.D., Decker, R.H. & Vallari, A.S. Frequency and significance of antibodies to asialoglycoprotein receptor in type 1 autoimmune hepatitis. *Dig Dis Sci* **41**, 1733-40 (1996).
65. Dalekos, G.N., Zachou, K., Liaskos, C. & Gatselis, N. Autoantibodies and defined target autoantigens in autoimmune hepatitis: an overview. *Eur J Intern Med* **13**, 293-303 (2002).
66. Strassburg, C.P. & Manns, M.P. Autoantibodies and autoantigens in autoimmune hepatitis. *Semin Liver Dis* **22**, 339-52 (2002).
67. McFarlane, B.M., Sipos, J., Gove, C.D., McFarlane, I.G. & Williams, R. Antibodies against the hepatic asialoglycoprotein receptor perfused in situ preferentially attach to periportal liver cells in the rat. *Hepatology* **11**, 408-15 (1990).
68. Treichel, U. et al. Autoantibodies against the human asialoglycoprotein receptor: effects of therapy in autoimmune and virus-induced chronic active hepatitis. *J Hepatol* **19**, 55-63 (1993).
69. Yoshioka, M. et al. Anti-asialoglycoprotein receptor autoantibodies, detected by a capture-immunoassay, are associated with autoimmune liver diseases. *Acta Med Okayama* **56**, 99-105 (2002).
70. Treichel, U., Meyer zum Buschenfelde, K.H., Stockert, R.J., Poralla, T. & Gerken, G. The asialoglycoprotein receptor mediates hepatic binding and uptake of natural hepatitis B virus particles derived from viraemic carriers. *J Gen Virol* **75** (Pt 11), 3021-9 (1994).
71. Becker, S., Spiess, M. & Klenk, H.D. The asialoglycoprotein receptor is a potential liver-specific receptor for Marburg virus. *J Gen Virol* **76** (Pt 2), 393-9 (1995).
72. Cocquerel, L., Voisset, C. & Dubuisson, J. Hepatitis C virus entry: potential receptors and their biological functions. *J Gen Virol* **87**, 1075-84 (2006).
73. Meier, M., Bider, M.D., Malashkevich, V.N., Spiess, M. & Burkhard, P. Crystal structure of the carbohydrate recognition domain of the H1 subunit of the asialoglycoprotein receptor. *J Mol Biol* **300**, 857-65 (2000).
74. Kolatkar, A.R. & Weis, W.I. Structural basis of galactose recognition by C-type animal lectins. *J Biol Chem* **271**, 6679-85 (1996).
75. Ricklin, D. in *Institute of Molecular Pharmacy* (University of Basel, Basel, 2005).
76. Lee, Y.C. et al. Binding of synthetic oligosaccharides to the hepatic Gal/GalNAc lectin. Dependence on fine structural features. *J Biol Chem* **258**, 199-202 (1983).
77. Biessen, E.A. et al. Synthesis of cluster galactosides with high affinity for the hepatic asialoglycoprotein receptor. *J Med Chem* **38**, 1538-46 (1995).
78. Rensen, P.C. et al. Determination of the upper size limit for uptake and processing of ligands by the asialoglycoprotein receptor on hepatocytes in vitro and in vivo. *J Biol Chem* **276**, 37577-84 (2001).
79. Baenziger, J.U. & Fiete, D. Galactose and N-acetylgalactosamine-specific endocytosis of glycopeptides by isolated rat hepatocytes. *Cell* **22**, 611-20 (1980).
80. Mathai Mammen, S.-K.C., George M. Whitesides, . Polyvalent Interactions in Biological Systems: Implications for Design and Use of Multivalent Ligands and Inhibitors. *Angewandte Chemie International Edition* **37**, 2754-2794 (1998).
81. Lee, Y.C., Lee, R. T. in *Carbohydrates in Chemistry and Biology* (ed. B. Ernst, G.W.H., P. Sinaÿ) 549-561 (Wiley-WCH, , Weinheim, **2000**).
82. Bock, K., Arnarp, J. & Lonngren, J. The Preferred Conformation of Oligosaccharides Derived from the Complex-Type Carbohydrate Portions of

- Glycoproteins. *European Journal of Biochemistry* **129**, 171-178 (1982).
83. Nishikawa, M. Development of cell-specific targeting systems for drugs and genes. *Biological & Pharmaceutical Bulletin* **28**, 195-200 (2005).
 84. Grossman, M. et al. Successful Ex-Vivo Gene-Therapy Directed to Liver in a Patient with Familial Hypercholesterolemia. *Nature Genetics* **6**, 335-341 (1994).
 85. Wu, G.Y., Walton, C.M. & Wu, C.H. Targeted polynucleotides for inhibition of hepatitis B and C viruses. *Croat Med J* **42**, 463-6 (2001).
 86. Hara, T., Aramaki, Y., Takada, S., Koike, K. & Tsuchiya, S. Receptor-mediated transfer of pSV2CAT DNA to a human hepatoblastoma cell line HepG2 using asialofetuin-labeled cationic liposomes. *Gene* **159**, 167-74 (1995).
 87. Kawakami, S., Munakata, C., Fumoto, S., Yamashita, F. & Hashida, M. Novel galactosylated liposomes for hepatocyte-selective targeting of lipophilic drugs. *J Pharm Sci* **90**, 105-13 (2001).
 88. Wagner, S.D. & Neuberger, M.S. Somatic hypermutation of immunoglobulin genes. *Annu Rev Immunol* **14**, 441-57 (1996).
 89. Alberts, B. *Molecular Biology of the Cell* (Taylor & Francis, 1994).
 90. Burnet, F.M. A modification of Jerne's theory of antibody production using the concept of clonal selection. *CA Cancer J Clin* **26**, 119-21 (1976).
 91. Burnet, F.M. The immunological significance of the thymus: an extension of the clonal selection theory of immunity. *Australas Ann Med* **11**, 79-91 (1962).
 92. Alt, F.W., Blackwell, T.K. & Yancopoulos, G.D. Development of the primary antibody repertoire. *Science* **238**, 1079-87 (1987).
 93. Milstein, C. From antibody structure to immunological diversification of immune response. *Science* **231**, 1261-8 (1986).
 94. Tonegawa, S. Somatic generation of antibody diversity. *Nature* **302**, 575-81 (1983).
 95. Tomlinson, I.M. et al. A complete map of the human immunoglobulin VH locus. *Ann N Y Acad Sci* **764**, 43-6 (1995).
 96. Ermert, K., Mitlohner, H., Schempp, W. & Zachau, H.G. The immunoglobulin kappa locus of primates. *Genomics* **25**, 623-9 (1995).
 97. Agrawal, A., Eastman, Q.M. & Schatz, D.G. Transposition mediated by RAG1 and RAG2 and its implications for the evolution of the immune system. *Nature* **394**, 744-51 (1998).
 98. Kirschbaum, T., Jaenichen, R. & Zachau, H.G. The mouse immunoglobulin kappa locus contains about 140 variable gene segments. *Eur J Immunol* **26**, 1613-20 (1996).
 99. Theakston, R.D., Warrell, D.A., Griffiths, E. Report of a WHO workshop on the standardization and control of antivenoms. *Toxicon* **41** (5), 541-57 (2003).
 100. Kuby, J. *Engineered Monoclonal Antibodies* (W.H. Freeman and Company, New York, 1997).
 101. Davies, J. & Riechmann, L. Affinity improvement of single antibody VH domains: residues in all three hypervariable regions affect antigen binding. *Immunotechnology* **2**, 169-79 (1996).
 102. Theakston, R.D., Warrell, D.A., Griffiths, E. Report of a WHO workshop on the standardization and control of antivenoms. *Toxicon* **41** (5), 541-57 (2003).
 103. Kohler, G. & Milstein, C. Continuous cultures of fused cells secreting antibody of predefined specificity. *Nature* **256**, 495-7 (1975).
 104. Courtenay-Luck, N.S. et al. Development of primary and secondary immune responses to mouse monoclonal antibodies used in the diagnosis and therapy of malignant neoplasms. *Cancer Res* **46**, 6489-93 (1986).
 105. Boulianne, G.L., Hozumi, N. & Shulman, M.J. Production of functional chimaeric mouse/human antibody. *Nature* **312**, 643-6 (1984).
 106. Bruggemann, M. et al. A repertoire of monoclonal antibodies with human heavy chains from transgenic mice. *Proc Natl Acad Sci U S A* **86**, 6709-13 (1989).
 107. Neuberger, M.S. et al. A hapten-specific chimaeric IgE antibody with human

- physiological effector function. *Nature* **314**, 268-70 (1985).
108. Jones, P.T., Dear, P.H., Foote, J., Neuberger, M.S. & Winter, G. Replacing the complementarity-determining regions in a human antibody with those from a mouse. *Nature* **321**, 522-5 (1986).
 109. Ainaï, A. et al. Renewal of EBV-hybridoma method: efficient generation of recombinant fully human neutralizing IgG antibodies specific for tetanus toxin by use of tetroma cells. *Hum Antibodies* **15**, 139-54 (2006).
 110. Bruggemann, M. & Taussig, M.J. Production of human antibody repertoires in transgenic mice. *Curr Opin Biotechnol* **8**, 455-8 (1997).
 111. Vaisbourd, M., Ignatovich, O., Dremucheva, A., Karpas, A. & Winter, G. Molecular characterization of human monoclonal antibodies derived from fusions of tonsil lymphocytes with a human myeloma cell line. *Hybrid Hybridomics* **20**, 287-92 (2001).
 112. Karpas, A., Dremucheva, A. & Czepulkowski, B.H. A human myeloma cell line suitable for the generation of human monoclonal antibodies. *Proc Natl Acad Sci U S A* **98**, 1799-804 (2001).
 113. Li, J. et al. Human antibodies for immunotherapy development generated via a human B cell hybridoma technology. *Proc Natl Acad Sci U S A* **103**, 3557-62 (2006).
 114. Porter, R.R. The hydrolysis of rabbit γ -globulin and antibodies with crystalline papain. *Biochem J* **73**, 119-26 (1959).
 115. Hoogenboom, H.R. Selecting and screening recombinant antibody libraries. *Nat Biotechnol* **23**, 1105-16 (2005).
 116. McCafferty, J., Griffiths, A.D., Winter, G. & Chiswell, D.J. Phage antibodies: filamentous phage displaying antibody variable domains. *Nature* **348**, 552-4 (1990).
 117. Huston, J.S. et al. Medical applications of single-chain antibodies. *Int Rev Immunol* **10**, 195-217 (1993).
 118. Adams, G.P. et al. Highly specific in vivo tumor targeting by monovalent and divalent forms of 741F8 anti-c-erbB-2 single-chain Fv. *Cancer Res* **53**, 4026-34 (1993).
 119. Worn, A. & Pluckthun, A. Mutual stabilization of VL and VH in single-chain antibody fragments, investigated with mutants engineered for stability. *Biochemistry* **37**, 13120-7 (1998).
 120. Bird, R.E. et al. Single-chain antigen-binding proteins. *Science* **242**, 423-6 (1988).
 121. Wu, A.M. & Senter, P.D. Arming antibodies: prospects and challenges for immunoconjugates. *Nature Biotechnology* **23**, 1137-1146 (2005).
 122. Song, E.W. et al. RNA interference targeting Fas protects mice from fulminant hepatitis. *Nature Medicine* **9**, 347-351 (2003).
 123. Skerra, A. & Pluckthun, A. Assembly of a functional immunoglobulin Fv fragment in *Escherichia coli*. *Science* **240**, 1038-41 (1988).
 124. Jost, C.R. et al. Mammalian expression and secretion of functional single-chain Fv molecules. *J Biol Chem* **269**, 26267-73 (1994).
 125. Bei, R., Schlom, J. & Kashmiri, S.V. Baculovirus expression of a functional single-chain immunoglobulin and its IL-2 fusion protein. *J Immunol Methods* **186**, 245-55 (1995).
 126. Davis, G.T., Bedzyk, W.D., Voss, E.W. & Jacobs, T.W. Single chain antibody (SCA) encoding genes: one-step construction and expression in eukaryotic cells. *Biotechnology (N Y)* **9**, 165-9 (1991).
 127. Whitelam, G.C., Cockburn, W. & Owen, M.R. Antibody production in transgenic plants. *Biochem Soc Trans* **22**, 940-4 (1994).
 128. Nicholls, P.J., Johnson, V.G., Blanford, M.D. & Andrew, S.M. An improved method for generating single-chain antibodies from hybridomas. *J Immunol Methods* **165**, 81-91 (1993).

129. Ferenci, T. & Silhavy, T.J. Sequence information required for protein translocation from the cytoplasm. *J Bacteriol* **169**, 5339-42 (1987).
130. Winter, G., Griffiths, A.D., Hawkins, R.E. & Hoogenboom, H.R. Making antibodies by phage display technology. *Annu Rev Immunol* **12**, 433-55 (1994).
131. Vaughan, T.J. et al. Human antibodies with sub-nanomolar affinities isolated from a large non-immunized phage display library. *Nat Biotechnol* **14**, 309-14 (1996).
132. Knappik, A. et al. Fully synthetic human combinatorial antibody libraries (HuCAL) based on modular consensus frameworks and CDRs randomized with trinucleotides. *Journal of Molecular Biology* **296**, 57-86 (2000).
133. Webster, D.M., Pedersen, J., Staunton, D., Jones, A. & Rees, A.R. Antibody-Combining Sites - Extending the Natural Limits. *Applied Biochemistry and Biotechnology* **47**, 119-134 (1994).
134. Pluckthun, A., Glockshuber, R., Pfitzinger, I., Skerra, A. & Stadlmuller, J. Engineering of antibodies with a known three-dimensional structure. *Cold Spring Harb Symp Quant Biol* **52**, 105-12 (1987).
135. Braden, B.C., Goldman, E.R., Mariuzza, R.A. & Poljak, R.J. Anatomy of an antibody molecule: structure, kinetics, thermodynamics and mutational studies of the antilysozyme antibody D1.3. *Immunol Rev* **163**, 45-57 (1998).
136. Schier, R. & Marks, J.D. Efficient in vitro affinity maturation of phage antibodies using BIAcore guided selections. *Hum Antibodies Hybridomas* **7**, 97-105 (1996).
137. Pini, A., Spreafico, A., Botti, R., Neri, D. & Neri, P. Hierarchical affinity maturation of a phage library derived antibody for the selective removal of cytomegalovirus from plasma. *J Immunol Methods* **206**, 171-82 (1997).
138. Steipe, B., Schiller, B., Pluckthun, A. & Steinbacher, S. Sequence statistics reliably predict stabilizing mutations in a protein domain. *J Mol Biol* **240**, 188-92 (1994).
139. Hoogenboom, H.R. et al. Antibody phage display technology and its applications. *Immunotechnology* **4**, 1-20 (1998).
140. Krebber, A. et al. Reliable cloning of functional antibody variable domains from hybridomas and spleen cell repertoires employing a reengineered phage display system. *J Immunol Methods* **201**, 35-55 (1997).
141. Marks, J.D. et al. By-passing immunization. Human antibodies from V-gene libraries displayed on phage. *J Mol Biol* **222**, 581-97 (1991).
142. Marks, C. & Marks, J.D. Phage libraries--a new route to clinically useful antibodies. *N Engl J Med* **335**, 730-3 (1996).
143. Hoogenboom, H.R. & Winter, G. By-passing immunisation. Human antibodies from synthetic repertoires of germline VH gene segments rearranged in vitro. *J Mol Biol* **227**, 381-8 (1992).
144. Barbas, C.F., 3rd, Bain, J.D., Hoekstra, D.M. & Lerner, R.A. Semisynthetic combinatorial antibody libraries: a chemical solution to the diversity problem. *Proc Natl Acad Sci U S A* **89**, 4457-61 (1992).
145. Silacci, M. et al. Design, construction, and characterization of a large synthetic human antibody phage display library. *Proteomics* **5**, 2340-50 (2005).
146. de Wildt, R.M., Mundy, C.R., Gorick, B.D. & Tomlinson, I.M. Antibody arrays for high-throughput screening of antibody-antigen interactions. *Nat Biotechnol* **18**, 989-94 (2000).
147. Tomlinson, I.M. et al. The imprint of somatic hypermutation on the repertoire of human germline V genes. *J Mol Biol* **256**, 813-17 (1996).
148. Chothia, C. & Lesk, A.M. Canonical structures for the hypervariable regions of immunoglobulins. *J Mol Biol* **196**, 901-17 (1987).
149. Ewert, S., Huber, T., Honegger, A. & Pluckthun, A. Biophysical properties of human antibody variable domains. *J Mol Biol* **325**, 531-53 (2003).
150. Hoogenboom, H.R. et al. Multi-subunit proteins on the surface of filamentous

- phage: methodologies for displaying antibody (Fab) heavy and light chains. *Nucleic Acids Res* **19**, 4133-7 (1991).
151. Neri, D. 3rd Experimental Course in Antibody Phage Display. *Course Material* (2008).
 152. Crevat-Pisano, P., Hariton, C., Rolland, P.H. & Cano, J.P. Fundamental aspects of radioreceptor assays. *J Pharm Biomed Anal* **4**, 697-716 (1986).
 153. Quesenberry, M.S. & Drickamer, K. Determination of the minimum carbohydrate-recognition domain in two C-type animal lectins. *Glycobiology* **1**, 615-21 (1991).
 154. Park, E.I., Manzella, S.M. & Baenziger, J.U. Rapid clearance of sialylated glycoproteins by the asialoglycoprotein receptor. *J Biol Chem* **278**, 4597-602 (2003).
 155. Iobst, S.T. & Drickamer, K. Binding of sugar ligands to Ca(2+)-dependent animal lectins. II. Generation of high-affinity galactose binding by site-directed mutagenesis. *J Biol Chem* **269**, 15512-9 (1994).
 156. Lee, R.T. Binding site of the rabbit liver lectin specific for galactose/N-acetylgalactosamine. *Biochemistry* **21**, 1045-50 (1982).
 157. Zhu, A., Wang, B., White, J.O. & Drickamer, H.G. The effect of high pressure and controlled stretching on the intramolecular twist of p-N-N-dirnethylaminobenzylidenemalononitrile in polyvinylacetate and polyvinylchloride. *Chemical Physics Letters* **321**, 394-398 (2000).
 158. Khorev, O., Stokmaier, D., Schwardt, O., Cutting, B. & Ernst, B. Trivalent, Gal/GalNAc-containing ligands designed for the asialoglycoprotein receptor. *Bioorg Med Chem* (2008).
 159. Liedberg, B., Nylander, C. & Lundstrom, I. Biosensing with surface plasmon resonance--how it all started. *Biosens Bioelectron* **10**, i-ix (1995).
 160. Karlsson, R. & Larsson, A. Affinity measurement using surface plasmon resonance. *Methods Mol Biol* **248**, 389-415 (2004).
 161. Cooper, M.A. Label-free screening of bio-molecular interactions. *Anal Bioanal Chem* **377**, 834-42 (2003).
 162. Johnsson, B. et al. Comparison of methods for immobilization to carboxymethyl dextran sensor surfaces by analysis of the specific activity of monoclonal antibodies. *J Mol Recognit* **8**, 125-31 (1995).
 163. Kortt, A.A., Oddie, G.W., Iliades, P., Gruen, L.C. & Hudson, P.J. Nonspecific amine immobilization of ligand can be a potential source of error in BIAcore binding experiments and may reduce binding affinities. *Anal Biochem* **253**, 103-11 (1997).
 164. Johnsson, B., Lofas, S. & Lindquist, G. Immobilization of proteins to a carboxymethyl-dextran-modified gold surface for biospecific interaction analysis in surface plasmon resonance sensors. *Anal Biochem* **198**, 268-77 (1991).
 165. Maniatis, T., Fritsch, E.F., Sambrook, J. *Molecular Cloning: A Laboratory Manual*. Cold Spring Harbour Laboratory Press. Cold Spring Harbour, New York (1982).
 166. Born, R. in *Institute of Molecular Pharmacy* (University of Basel, Basel, Switzerland, 2005).
 167. Laemmli, U.K. Cleavage of structural proteins during the assembly of the head of bacteriophage T4. *Nature* **227**, 680-5 (1970).
 168. Kang, D., Gho, Y.S., Suh, M., Kang, Ch. Highly Sensitive and Fast Protein Detection with Coomassie Brilliant Blue in Sodium Dodecyl Sulfate-Polyacrylamide Gel Electrophoresis. *Bulletin of the Korean Society of Chemistry* **23**, 1511-1512 (2002).
 169. Towbin, H., Staehelin, T. & Gordon, J. Electrophoretic transfer of proteins from polyacrylamide gels to nitrocellulose sheets: procedure and some applications. *Proc Natl Acad Sci U S A* **76**, 4350-4 (1979).
 170. Bradford, M.M. A rapid and sensitive method for the quantitation of microgram

- quantities of protein utilizing the principle of protein-dye binding. *Anal Biochem* **72**, 248-54 (1976).
171. Taylor, J.W., Ott, J. & Eckstein, F. The rapid generation of oligonucleotide-directed mutations at high frequency using phosphorothioate-modified DNA. *Nucleic Acids Res* **13**, 8765-85 (1985).
 172. Ward, E.S., Gussow, D., Griffiths, A.D., Jones, P.T. & Winter, G. Binding activities of a repertoire of single immunoglobulin variable domains secreted from *Escherichia coli*. *Nature* **341**, 544-6 (1989).
 173. Plückthun, A. et al. in *Antibody Engineering* (eds. McCafferty, J., Hoogenboom, H.R. & Chriswell, D.J.) 203-252 (IRL Press, Oxford, 1996).
 174. Tartoff, K.D., Hobbs, C.A. . Improved Media for Growing Plasmid and Cosmid Clones. *Bethesda. Res. Lab. Focus* **9** (1987).
 175. Miller, J.H.E.i.M.G.C.S.H.L., Cold Spring Harbor Laboratory, New York, 466 pp. *Experiments in Molecular Genetics* (Cold Spring Harbor Laboratory, Cold Spring Harbor, New York, 1972).
 176. De Bellis, D. & Schwartz, I. Regulated expression of foreign genes fused to lac: control by glucose levels in growth medium. *Nucleic Acids Res* **18**, 1311 (1990).
 177. Qiagen. (Qiagen, www.qiagen.com).
 178. Thomas, M.R. Simple, effective cleanup of DNA ligation reactions prior to electro-transformation of *E. coli*. *Biotechniques* **16**, 988-90 (1994).
 179. Rich, R.L. & Myszka, D.G. Advances in surface plasmon resonance biosensor analysis. *Curr Opin Biotechnol* **11**, 54-61 (2000).
 180. Bider, M.D. Expression, characterization, and crystallization of the carbohydrate recognition domain of subunit H1 of the asialoglycoprotein receptor. *unpublished manuscript*.
 181. Fornstedt, N. & Porath, J. Characterization studies on a new lectin found in seeds of *Vicia ervilia*. *FEBS Lett* **57**, 187-91 (1975).
 182. Bovin, N.V. et al. Synthesis of polymeric neoglycoconjugates based on N-substituted polyacrylamides. *Glycoconj J* **10**, 142-51 (1993).
 183. Bovin, N.V. Polyacrylamide-based glycoconjugates as tools in glycobiology. *Glycoconj J* **15**, 431-46 (1998).
 184. Wragg, S. & Drickamer, K. Identification of amino acid residues that determine pH dependence of ligand binding to the asialoglycoprotein receptor during endocytosis. *J Biol Chem* **274**, 35400-6 (1999).
 185. Connolly, D.T., Townsend, R.R., Kawaguchi, K., Bell, W.R. & Lee, Y.C. Binding and endocytosis of cluster glycosides by rabbit hepatocytes. Evidence for a short-circuit pathway that does not lead to degradation. *J Biol Chem* **257**, 939-45 (1982).
 186. Lee, R.T., Myers, R.W. & Lee, Y.C. Further studies on the binding characteristics of rabbit liver galactose/N-acetylgalactosamine-specific lectin. *Biochemistry* **21**, 6292-8 (1982).
 187. Abgottsporn, D. in *Institute of Molecular Pharmacy* (University of Basel, Basel, 2007).
 188. Riva, C. thesis at the Institute of Molecular Pharmacy (University of Basel, Basel, 2006).
 189. Khorev, O. thesis at the Institute of Molecular Pharmacy (University of Basel, Basel, 2007).
 190. Wong, T.C., Townsend, R.R. & Lee, Y.C. Synthesis of D-galactosamine derivatives and binding studies using isolated rat hepatocytes. *Carbohydr Res* **170**, 27-46 (1987).
 191. Yi, D. et al. Substructural specificity and polyvalent carbohydrate recognition by the *Entamoeba histolytica* and rat hepatic N-acetylgalactosamine/galactose lectins. *Glycobiology* **8**, 1037-43 (1998).
 192. Kolatkar, A.R. et al. Mechanism of N-acetylgalactosamine binding to a C-type animal lectin carbohydrate-recognition domain. *J Biol Chem* **273**, 19502-8

- (1998).
193. Aramaki, Y. et al. Efficient gene transfer to hepatoblastoma cells through asialoglycoprotein receptor and expression under the control of the cyclin A promoter. *Biol Pharm Bull* **26**, 357-60 (2003).
 194. Schwartz, A.L., Fridovich, S.E., Knowles, B.B. & Lodish, H.F. Characterization of the asialoglycoprotein receptor in a continuous hepatoma line. *J Biol Chem* **256**, 8878-81 (1981).
 195. Stefanich, E.G. et al. Evidence for an asialoglycoprotein receptor on nonparenchymal cells for O-linked glycoproteins. *J Pharmacol Exp Ther* **327**, 308-15 (2008).
 196. Dory, D. et al. Generation and functional characterization of a clonal murine periportal Kupffer cell line from H-2Kb -tsA58 mice. *J Leukoc Biol* **74**, 49-59 (2003).
 197. Kempen, H.J. et al. A water-soluble cholesteryl-containing trisgalactoside: synthesis, properties, and use in directing lipid-containing particles to the liver. *J Med Chem* **27**, 1306-12 (1984).
 198. Biessen, E.A., Broxterman, H., van Boom, J.H. & van Berkel, T.J. The cholesterol derivative of a triantennary galactoside with high affinity for hepatic asialoglycoprotein receptor: a potent cholesterol lowering agent. *J Med Chem* **38**, 1846-52 (1995).
 199. Sliedregt, L.A. et al. Design and synthesis of novel amphiphilic dendritic galactosides for selective targeting of liposomes to the hepatic asialoglycoprotein receptor. *J Med Chem* **42**, 609-18 (1999).
 200. Rensen, P.C., van Leeuwen, S.H., Sliedregt, L.A., van Berkel, T.J. & Biessen, E.A. Design and synthesis of novel N-acetylgalactosamine-terminated glycolipids for targeting of lipoproteins to the hepatic asialoglycoprotein receptor. *J Med Chem* **47**, 5798-808 (2004).
 201. Rensen, P.C.N. et al. Determination of the upper size limit for uptake and processing of ligands by the asialoglycoprotein receptor on hepatocytes in vitro and in vivo. *Journal of Biological Chemistry* **276**, 37577-37584 (2001).
 202. Biacore. (www.biacore.com).
 203. Coombs, P.J., Taylor, M.E. & Drickamer, K. Two categories of mammalian galactose-binding receptors distinguished by glycan array profiling. *Glycobiology* **16**, 1c-7c (2006).
 204. Johansson, A.K. in Institut of Molecular Pharmacy (University of Basel, Basel, 2007).
 205. Hashida, M., Nishikawa, M., Yamashita, F. & Takakura, Y. Cell-specific delivery of genes with glycosylated carriers. *Adv Drug Deliv Rev* **52**, 187-96 (2001).
 206. Bider, M.D. & Spiess, M. Ligand-induced endocytosis of the asialoglycoprotein receptor: evidence for heterogeneity in subunit oligomerization. *FEBS Lett* **434**, 37-41 (1998).
 207. Park, J.H., Kim, K.L. & Cho, E.W. Detection of surface asialoglycoprotein receptor expression in hepatic and extra-hepatic cells using a novel monoclonal antibody. *Biotechnol Lett* **28**, 1061-9 (2006).
 208. Schwartz, A.L. & Rup, D. Biosynthesis of the human asialoglycoprotein receptor. *J Biol Chem* **258**, 11249-55 (1983).
 209. Kohgo, Y. et al. Production and characterization of specific asialoglycoprotein receptor antibodies. *Hybridoma* **12**, 591-8 (1993).
 210. Song, E. et al. Antibody mediated in vivo delivery of small interfering RNAs via cell-surface receptors. *Nat Biotechnol* **23**, 709-17 (2005).
 211. Vornlocher, H.P. Antibody-directed cell-type-specific delivery of siRNA. *Trends Mol Med* **12**, 1-3 (2006).
 212. Sioud, M. RNAi therapy: antibodies guide the way. *Gene Ther* **13**, 194-5 (2006).
 213. Mutuberria, R., Hoogenboom, H.R., van der Linden, E., de Bruine, A.P. & Roovers, R.C. Model systems to study the parameters determining the success

- of phage antibody selections on complex antigens. *J Immunol Methods* **231**, 65-81 (1999).
214. Poul, M.A., Becerril, B., Nielsen, U.B., Morisson, P. & Marks, J.D. Selection of tumor-specific internalizing human antibodies from phage libraries. *J Mol Biol* **301**, 1149-61 (2000).
215. Charles, C.H. et al. Prevention of human rhinovirus infection by multivalent fab molecules directed against ICAM-1. *Antimicrob Agents Chemother* **47**, 1503-8 (2003).
216. Kipriyanov, S.M. et al. Affinity enhancement of a recombinant antibody: formation of complexes with multiple valency by a single-chain Fv fragment-core streptavidin fusion. *Protein Eng* **9**, 203-11 (1996).
217. Pluckthun, A. & Pack, P. New protein engineering approaches to multivalent and bispecific antibody fragments. *Immunotechnology* **3**, 83-105 (1997).